Electronic Supplementary Material (ESI) for CrystEngComm.

Table of contents:

1. Production of single crystals and single-crystal X-ray structure determination (Tables S1.1 and S1.2)

For most of the unknown cocrystal phases we managed to grow single crystals from solution. Experimental details of solution crystallization experiments are summarized in Table S1.1.

The structures of the **1:2 S-nprx/Lpro**, **1:1 S-nprx/DL-pro**, **1:2 S-nprx/DL-pro pol I**, **1:1 RS-nprx/D-pro pol I**, **1:1 RS-nprx/D-pro/MeOH**, and **1:1 RS-nprx/DL-pro** were solved from the single-crystal X-ray diffraction data collected using an Oxford Diffraction Gemini Ultra R diffractometer (Cu*K*α radiation). The data were integrated using the CrysAlisPro[1] software. The multi-scan absorption correction procedure implemented in the CrysAlisPro software was applied. The structures were solved by direct methods using the SHELXS-97[2] or by the dual-space algorithm implemented in SHELXT[3] program and refined by full-matrix least squares on $|F|^2$ using SHELXL-2016/4 or SHELXL-2014/7[4] and the shelXLe[5] shell. Non-hydrogen atoms were refined anisotropically; and hydrogen atoms were located from the difference Fourier map but placed on calculated positions in riding mode with equivalent isotropic temperature factors fixed at 1.2 times U_{eq} of the parent atoms and 1.5 times U_{eq} for methyl groups.

The structure of the **S-nprx/EtOH** solvate was solved from the single-crystal X-ray diffraction data collected on a MAR345 image plate detector using MoKα radiation (Rigaku UltraX 18 rotation anode, Xenocs Fox3D focusing multilayer mirror) at 150 K. The structure turned out to be unstable at room temperature. Data treatment and structure solution were the same as for the aforementioned structures.

The structure of the **2:3 S-nprx/L-pro** was solved from the single-crystal synchrotron X-ray diffraction data collected at the PROXIMA 1 beamline of the SOLEIL (Paris, France) synchrotron radiation facility, using a PILATUS 6M hybrid pixel detector. Data treatment and structure solution were the same as for the aforementioned structures.

The crystal data, data collection, and refinement details are summarized in Table S1.2.

The figures were generated using the Mercury program[6]; cif files were finalized using the Encifer[7] program.

All our attempts to obtain single crystals of the following cocrystals from solution under various conditions, including slow evaporation, failed: **1:1 S-nprx/L-pro pol II**, **1:1 RS-nprx/L-pro pol II**, **1:1 RS-nprx/L-pro pol III**, **1:1 RS/DL pol II**, **1:2 RS-nprx/L-pro**, and **1:1 S/DL/H_2O**. Hence, the structures of those cocrystals were solved from powder X-ray diffraction data.

Table S1.1 Experimental conditions of solution crystallization experiments for single crystal growth

Obtained cocrystal	Experimental conditions
1:2 S-nprx/L-pro	single crystals were obtained from ethanol solution upon cooling (35.3 mg of S-naproxen and 55.2 mg of L-proline were dissolved at ~50-60°C in 5 mL of solvent and cooled to 9 °C)
2:3 S-nprx/L-pro	single crystals were obtained from ethanol solution upon cooling (55 mg of S-naproxen and 25.2 mg of L-proline were dissolved at ~50-60°C in 5 mL of solvent and cooled to room temperature)
1:1 S-nprx/DL-pro	single crystals were obtained from methanol solution upon cooling (35.2 mg of S-naproxen and 55.2 mg of DL-proline were dissolved at ~50-60°C in 5 mL of solvent and cooled to -15 °C)
1:2 S-nprx/DL-pro	single crystals were obtained from ethanol solution upon cooling (35.2 mg of S-naproxen and 55.1 mg of DL-proline were dissolved at ~50-60°C in 5 mL of solvent and cooled to room temperature)
1:1 RS-nprx/D-pro pol I	single crystals were obtained from ethanol solution upon cooling (65 mg of RS-naproxen and 15.3 mg of D-proline were dissolved at ~50-60°C in 5 mL of solvent and cooled to 9 °C)
1:1 RS-nprx/D-pro/MeOH	single crystals were obtained from methanol solution upon cooling (45.4 mg of RS-naproxen and 35.3 mg of D-proline were dissolved at ~50-60°C in 5 mL of solvent and cooled to -10 °C)
1:1 RS-nprx/DL-pro	single crystals were obtained from ethanol solution upon cooling (19.70 mg of 1:1 RS-nprx/DL-pro powder obtained after ACN-LAG was dissolved in 1.5 mL of solvent at ~50-60°C and cooled to room temperature)
S-nprx/EtOH	single crystals were crystallized from ethanol solution upon cooling (22.96 mg of S-nprx were dissolved at ~50-60°C in 1.5 mL of solution and cooled to room temperature); crystals are unstable and decompose very quickly when taken out of solution

Table S1.2 Crystal data, data collection, and refinement details

	1:1 S/L pol II	1:2 S/L	2:3 S/L
Crystal data			
Chemical formula	$2(C_{14}H_{14}O_3)\cdot 2(C_5H_9NO_2)$	$C_{14}H_{14}O_3\cdot 2(C_5H_9NO_2)$	$2(C_{14}H_{14}O_3)\cdot 3(C_5H_9NO_2)$
M_r	690.77	460.51	805.90
Crystal system, space group	Monoclinic, $P2_1$	Orthorhombic, $P2_12_12_1$	Orthorhombic, $P2_12_12_1$
Temperature (K)	295	295	100
a, *b*, *c* (Å)	16.2991(7), 5.8654(3), 18.6876(9)	5.88160(7), 8.79809(10), 45.4679(5)	5.7018(1), 18.8609(3), 37.2392 (5)
α, β, γ (°)	90, 100.052(4), 90	90, 90, 90	90, 90, 90
V (Å^3)	1759.12(14)	2352.82(5)	4004.74(11)
Z	2	4	4
D_x (Mg m^{-3})	1.304	1.300	1.337
Melting point (K)	n/a	n/a	n/a
Radiation type	Synchrotron, λ = 0.776188 Å	Cu *K*α	Synchrotron, λ = 0.82656 Å
Specimen shape, size (mm)	Capillary, 4 × 0.5	0.43 × 0.10 × 0.06	0.21 × 0.01 × 0.01
Data collection			
Diffractometer	Mythen II	Oxford Diffraction Gemini Ultra R	Pilatus 6M
Method	powder	single-crystal	single-crystal
No. of measured, independent and observed reflections		23068, 4165, 4025	18663, 5419, 3761
R_{int}	–	0.049	0.130
θ values (°)	$2\theta_{min}$ = 2.149, $2\theta_{max}$ = 33.001, $2\theta_{step}$ = 0.004	θ_{min} = 3.9, θ_{max} = 67.2	θ_{max} = 28.7, θ_{min} = 1.8
Refinement			
R factors (%) and goodness of fit	R_p = 7.433, R_{wp} = 8.797, R_{exp} = 0.394, R_{Bragg} = 16.66, χ^2 = 497.290	$R[F^2 > 2\sigma(F^2)]$ = 4.0, $wR(F^2)$ = 11.1, S = 1.03	$R[F^2 > 2\sigma(F^2)]$ = 6.4, $wR(F^2)$ = 17.3, S = 0.95
CCDC number	1861026	1861017	1861028

Table S1.2 (continue) Crystal data, data collection, and refinement details

	1:1 S/DL	1:2 S/DL	1:1 S/DL/H_2O	1:1 RS/D pol I
Crystal data				
Chemical formula	$2(C_{14}H_{14}O_3)\cdot 2(C_5H_9NO_2)$	$C_{14}H_{14}O_3\cdot 2(C_5H_9NO_2)$	$2(C_{14}H_{14}O_3)\cdot 2(C_5H_9NO_2)\cdot 2(H_2O)$	$2(C_{14}H_{14}O_3)\cdot 2(C_5H_9NO_2)$
M_r	690.77	460.51	726.80	690.77
Crystal system, space group	Monoclinic, $P2_1$	Orthorhombic, $P2_12_12_1$	Orthorhombic, $P2_12_12_1$	Monoclinic, $P2_1$
Temperature (K)	295	295	295	295
a, *b*, *c* (Å)	8.84337(19), 5.83510(15), 33.6766(7)	5.8836(7), 9.0952(18), 44.047 (10)	6.06468(13), 12.2629(3), 50.6290(15)	12.1578(5), 5.8278(2), 25.6828(14)
α, β, γ (°)	90, 91.9839(19), 90	90, 90, 90	90, 90, 90	90, 98.762(5), 90
V (Å^3)	1736.74(7)	2357.1(8)	3765.29(17)	1798.45(14)
Z	2	4	4	2
D_x (Mg m^{-3})	1.321	1.298	1.282	1.330
Melting point K)	n/a	455(1)	n/a	435(1)
Radiation type	Cu *K*α	Cu *K*α	Synchrotron, λ = 0.798 Å	Cu *K*α
Specimen shape, size (mm)	0.17 × 0.07 × 0.01	0.17 × 0.03 × 0.02	Capillary, 4 × 0.5	0.19 × 0.16 × 0.03
Data collection				
Diffractometer	Oxford Diffraction Gemini Ultra R	Oxford Diffraction Gemini Ultra R	PILATUS@SNBL	Oxford Diffraction Gemini Ultra R
Method	single-crystal	single-crystal	powder	single-crystal
No. of measured, independent and observed reflections	10460, 4868, 4427	5139, 3125, 1899		11150, 5055, 4166
R_{int}	0.040	0.056		–
θ values (°)	θ_{min} = 2.6, θ_{max} = 67.20	θ_{min} = 4.0, θ_{max} = 62.7,	$2\theta_{min}$ = 1.37503, $2\theta_{max}$ = 34.99581, $2\theta_{step}$ = 0.01	θ_{min} = 3.5, θ_{max} = 67.2,
Refinement				
R factors (%) and goodness of fit	$R[F^2 > 2\sigma(F^2)]$ = 4.7, $wR(F^2)$ = 13.4, S = 1.03	$R[F^2 > 2\sigma(F^2)]$ = 6.1, $wR(F^2)$ = 14.8, S = 0.98	R_p = 2.45, R_{wp} = 3.63, R_{exp} = 0.16, R_{Bragg} = 2.59, χ^2 = 513.929*	$R[F^2 > 2\sigma(F^2)]$ = 6.4, $wR(F^2)$ = 19.6, S = 1.06
CCDC number	1861018	1861016	1861022	1861020

Table S1.2 (continue) Crystal data, data collection, and refinement details

	1:1 RS/D pol II	1:1 RS/L pol III	1:1 RS/D/MeOH	1:2 RS/L
Crystal data				
Chemical formula	$2(C_{14}H_{14}O_3)\cdot 2(C_5H_9NO_2)$	$2(C_{14}H_{14}O_3)\cdot 2(C_5H_9NO_2$	$2(C_{14}H_{14}O_3)\cdot 2(C_5H_9NO_2)\cdot CH_4O$	$C_{14}H_{14}O_3\cdot 2(C_5H_9NO_2)$
M_r	690.76	359.39	722.81	460.52
Crystal system, space group	Orthorhombic, $P2_12_12_1$	Monoclinic, $P2_1$	Monoclinic, $P2_1$	Orthorhombic, $P2_12_12_1$
Temperature (K)	295	402	295	407
a, *b*, *c* (Å)	12.5901(6), 5.7587(3), 51.425(3)	12.705(2), 5.7631(8), 25.000(5)	12.9532(4), 5.76337(15), 25.2764(6)	5.84172(9), 8.98394(13), 45.6816 (8)
α, β, γ (°)	90, 90, 90	90, 95.041(11), 90	90, 93.984(3), 90	90, 90, 90
V (Å^3)	3728.4(3)	1823.4(6)	1882.42(9)	2397.45(6)
Z	4	2	2	4
D_x (Mg m^{-3})	1.231	1.259	1.275	1.276
Melting point (K)	432(1)	n/a	n/a	444(1)
Radiation type	Synchrotron, λ = 1.0007 Å	Synchrotron, λ = 0.78487 Å	Cu *K*α	Synchrotron, λ = 0.708 Å
Specimen shape, size (mm)	Capillary, 4 × 0.5	Capillary, 4 × 0.5	0.49 × 0.06 × 0.05	Capillary, 4 × 0.5
Data collection				
Diffractometer	Mythen II	PILATUS@SNBL	Oxford Diffraction Gemini Ultra R	Mythen II
Method	powder	powder	single-crystal	powder
No. of measured, independent and observed reflections			11648, 5615, 4791	
R_{int}	–	–	0.030	–
θ values (°)	$2\theta_{min}$ = 1.800, $2\theta_{max}$ = 34.999, $2\theta_{step}$ = 0.004	$2\theta_{min}$ = 1.295, $2\theta_{max}$ = 37.002, $2\theta_{step}$ = 0.0155	θ_{max} = 67.2, θ_{min} = 3.4	$2\theta_{min}$ = 1.300, $2\theta_{max}$ = 33.001, $2\theta_{step}$ = 0.004
Refinement				
R factors (%) and goodness of fit	R_p = 5.72, R_{wp} = 6.275, R_{exp} = 0.170, R_{Bragg} = 12.489, χ^2 = 1367.520	R_p = 4.939, R_{wp} = 6.851, R_{exp} = 0.110, R_{Bragg} = 7.117, χ^2 = 3903.750*	$R[F^2 > 2\sigma(F^2)]$ = 5.1, $wR(F^2)$ = 15.3, S = 1.04	R_p = 1.865, R_{wp} = 2.188, R_{exp} = 0.531, R_{Bragg} = 4.288, χ^2 = 16.974
CCDC number	1861025	1861027	1861019	1861023

Table S1.2 (continue) Crystal data, data collection, and refinement details

	1:1 RS/DL pol I	1:1 RS/DL pol II	S-nprx/EtOH
Crystal data			
Chemical formula	$C_{14}H_{14}O_3 \cdot C_5H_9NO_2$	$C_{14}H_{14}O_3 \cdot C_5H_9NO_2$	$C_{14}H_{14}O_3 \cdot C_2H_6O$
M_r	345.38	345.38	276.32
Crystal system, space group	Orthorhombic, *Pbca*	Orthorhombic, $Pna2_1$	Orthorhombic, $P2_12_12_1$
Temperature (K)	295	428	150
a, *b*, *c* (Å)	9.9964(3), 9.0958(4), 39.9654(15)	34.537(4), 9.0077(8), 5.7183 (5)	5.9273 (2), 8.7713 (5), 28.0747 (15)
α, β, γ (°)	90, 90, 90	90, 90, 90	90, 90, 90
V (Å^3)	3633.8(2)	1779.0(3)	1459.61(13)
Z	8	4	4
D_x (Mg m^{-3})	1.263	1.290	1.257
Melting point (K)	425(1)	n/a	n/a
Radiation type	Cu *K*α	Synchrotron, λ = 0.78487 Å	Mo *K*α
Specimen shape, size (mm)	0.29 × 0.06 × 0.01	Capillary, 4 × 0.5	0.40 × 0.25 × 0.20
Data collection			
Diffractometer	Oxford Diffraction Gemini Ultra R	PILATUS@SNBL	MAR345 image plate
Method	single-crystal	powder	single-crystal
No. of measured, independent and observed reflections	18470, 3224, 2429		9659, 2620, 2291
R_{int}	0.048	–	0.042
θ values (°)	θ_{min} = 6.3, θ_{max} = 67.3	$2\theta_{min}$ = 2.13192, $2\theta_{max}$ = 33.99443, $2\theta_{step}$ = 0.00155	θ_{max} = 25.6, θ_{min} = 3.2
Refinement			
R factors and goodness of fit	$R[F^2 > 2\sigma(F^2)]$ = 4.0, $wR(F^2)$ = 10.7, *S* = 1.06	R_p = 5.13, R_{wp} = 7.78, R_{exp} = 0.11, R_{Bragg} = 8.76, χ^2 = 5251.901*	$R[F^2 > 2\sigma(F^2)]$ = 4.2, $wR(F^2)$ = 11.0, *S* = 1.10
CCDC number	1861021	1861024	1861015

'*' the χ^2 values for the structures determined from the X-ray diffraction data collected at SNBL (Grenoble, France) are high which is explained by the following. The data were collected using a 2D detector which means that the *esd* values are smaller than in the case of a linear or a point detector because the integration of the data from a 2D detector accounts for many pixels. *Esd* values are included into the calculation of the weights, which in their turn are used to calculate the χ^2 value. Hence, smaller *esd* values systematically lead to higher χ^2 factors as compared with point or linear detectors.[8]

2. Powder X-ray diffraction structure determination (Figs. S2.1-S2.9)

The structures of the **1:1 S-nprx/L-pro pol II**, **1:1 RS-nprx/L-pro pol II**, **1:1 RS-nprx/L-pro pol III**, **1:1 RS/DL pol II**, and **1:2 RS-nprx/L-pro** were determined from powder synchrotron X-ray diffraction data collected at the Swiss Light Source (SLS, PSI, Switzerland) at MS-X04SA beam line equipped with a 1D microstrip detector MYTHEN II (first two structures) and at the Swiss-Norwegian beamline BM1A at the European Synchrotron Radiation Facility (ESRF) (Grenoble, France), using a PILATUS 2M hybrid pixel detector (the last three structures). The crystal data, data collection, and refinement details are given in Table S1.2.

Indexing and Le Bail fit were performed using the FOX program[9]. The structures were found by global optimization in direct space (Monte Carlo/parallel tempering algorithm) using again the FOX program[9] and further refined by the Rietveld method in the TOPAS V5[10] software, text based input files prepared in the jedit editor were used[11]. Profile parameters were found from Pawley refinement and then fixed in further Rietveld refinement. The background was described manually using 25 points. The molecules were described as rigid body object; the following functional groups were kept rigid, for which only rotation was allowed: carboxylate, carboxyl group, and benzene rings. Bond distances and angles were fixed, whereas certain torsion angles were refined. Position and orientation of the molecules were refined as well. The torsion angles and the orientation of each molecule in the asymmetric unit were refined separately in an iterative manner and then fixed in the final refinement cycle. The equivalent isotropic temperature factors for hydrogen atoms were set at 1.2 times of those of parent atoms in a particular molecule. The equivalent isotropic temperature factors for non-hydrogen atoms in proline molecules were fixed to 15 if in the refinement they tended to exceed this value. Rietveld refinement plots are shown in Figs. S2.1-S2.5.

The Rietveld refinement of some of the structures is poor due to following reasons. The intensity values are highly sensitive to even slight changes in the orientations of the molecules or molecular conformations. From our previous experience when working with proline, the latter is conformationally flexible, which may cause disorder. This fact causes difficulty in finding the optimal orientation and conformation of the proline molecules from powder X-ray diffraction data. We tried to introduce disorder for proline in the refinement but it did not significantly improve the structural models and only made fit less stable, so we decided to omit it. In order to keep the structural correctness and integrity from the chemical point of view we had to find a compromise between a good Rietveld fit and a good structural chemical model. In the cases, where the Rietveld fit was poor, we think that the positions of the molecules were more or less reliably determined, but the orientations and conformations were not probably the optimal. However, all our attempts to improve the models failed.

In the **1:2 RS-nprx/L-pro** cocrystal, according to the found unit cell parameters and the volume of the unit cell, two of the naproxen enantiomers must be occupying the same position, in a manner similar to the 2:1 R-flurbiprofen/DL-proline cocrystal (CCDC 1537411[12]), in which **D-** and **L-proline** molecules shared the same position. One molecule of naproxen occupies volume of ~300 Å^3, one molecule of proline ~150 Å^3; therefore, an elementary unit with the 1:2 (**nprx** : **pro**) stoichiometry should have a volume of ~600 Å^3. For the **1:2 RS-nprx/L-pro** cocrystal, the volume of the unit cell was found to be around 2400 Å^3 and the space group was identified as $P2_12_12_1$, which has minimal $Z = 4$; therefore the volume of the asymmetric unit must also be around 600 Å^3. This means that we cannot put more than one naproxen molecule into the asymmetric unit and thus two enantiomers must share the same position. Since the diffraction pattern looked almost exactly as the one for the **1:2 S/L** (Fig S2.7), we suggested that it would seem reasonable if only the –CH3 and –H groups at the asymmetric carbon were disordered with the occupancies of 0.5 between the two positions that correspond to the S- and R-enantiomers, respectively. Thus, we introduced this kind of disorder into the **1:2 S/L** structure and performed Rietveld refinement, refining the unit cell parameters, the orientation and the coordinates of the molecules, without touching the torsion angles. The resultant structure fitted nicely the experimental X-ray powder

diffraction data; the Rietveld refinement plot is given in Fig. S2.3; the structure of the **1:2 RS/L** is presented in Fig. S2.8. The profile parameters were found from the Pawley fit in the same manner as for the previous structures and fixed in the Rietveld refinement.

In the case of the **1:1 S/DL/H_2O** cocrystal hydrate, the ratio of the initial components was assumed from the found unit cell volume. As was mentioned above, one molecule of naproxen occupies ~300 Å^3 and one molecule of proline ~150 Å^3. The total volume was found ~3800 Å^3 in the orthorhombic space group (most likely $P2_12_12_1$, which has minimal Z = 4), which means that one structural unit should have a volume of ~950 Å^3. Such a volume corresponds to 2 molecules of S-nprx, 1 molecule of L-pro, 1 molecule of D-pro. We suggested that the left volume of ~50 Å^3 is occupied by water. The number of water molecules per unit cell was determined from the TGA data (Fig. S9.3.6) (the weight lost during the first step corresponded to 2 molecules). For the indexing procedure and structure determination we collected synchrotron PXRD data (λ = 0.798 Å) at the Swiss-Norwegian beamline BM1A at the European Synchrotron Radiation Facility (ESRF) (Grenoble, France), using a PILATUS 2M hybrid pixel detector. The Pawley refinement plot is given in Fig. S2.6. The structure of **1:1 S/DL/H_2O** was found using the structure of **1:1 RS/DL/H_2O**: unit cell parameters of the former were very close to those of the latter, as well as the diffraction patterns of both cocrystals were very similar (see Fig. S2.9). Thus, we suggested that the structures should be similar. As **D-** and **L-pro** are present in both the **1:1 RS/DL/H_2O** and **1:1 S/DL/H_2O** and both structures contain two molecules of water in the asymmetric unit, we fixed **D-**, **L-pro** and both water molecules, changed **R-nprx** for **S-nprx**, and using the FOX program, optimized the position of only two **S-nprx** molecules in the asymmetric unit. This procedure gave a very good model which was further refined using TOPAS V5[10] software (only the coordinates of all the molecules taken as a whole were refined, along with the profile and unit cell parameters). The Rietveld refinement plot is given in Fig. S2.6.

Cif files were finalized using the Encifer[7] and the Platon[13] programs.

Figure S2.1. Rietveld refinement plot for the **1:1 S/L pol II** cocrystal, determined from synchrotron X-ray powder data collected at room temperature for the S-nprx/L-pro sample obtained by 1 : 1 ACN-LAG: λ = 0.776188 Å, T = 295 K, sample *13* in Table S4.1. Red and blue patterns represent calculated and experimental data, respectively; grey line corresponds to the difference profile; blue marks below the difference profile represent Bragg positions.

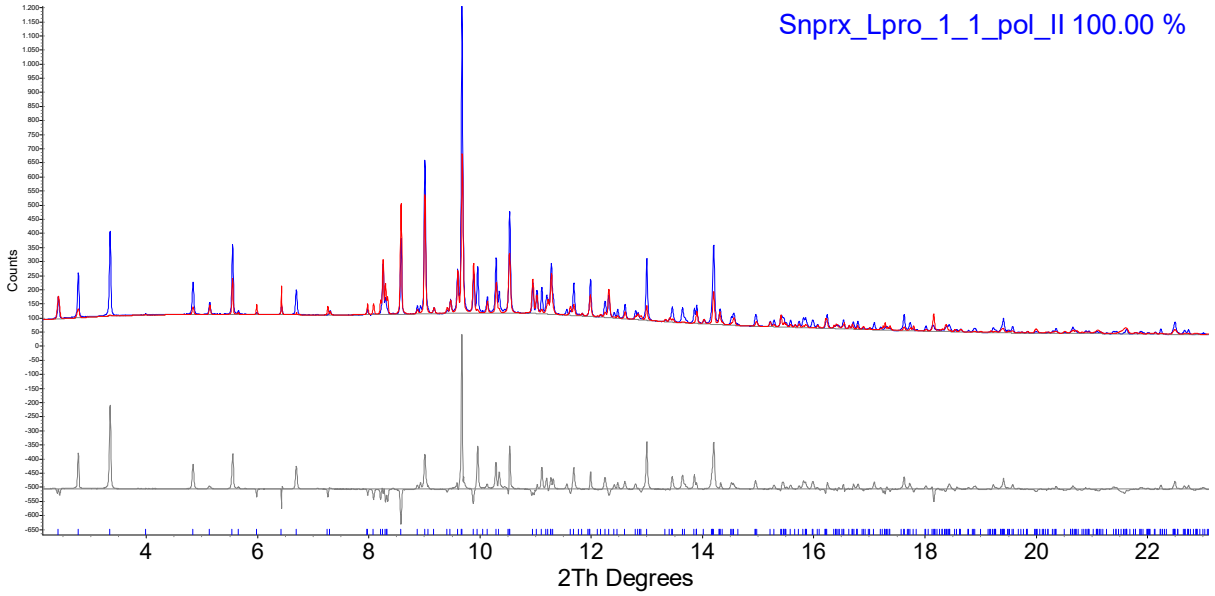

Figure S2.2. Rietveld refinement plot for the **1:1 RS/D pol II** cocrystal, determined from synchrotron X-ray powder data collected at room temperature for the RS-nprx/D-pro sample obtained by 1 : 1 ACN-LAG: λ = 1.0007 Å, *T* = 295 K, sample *13* in Table S6.1. Red and blue patterns represent calculated and experimental data, respectively; grey line corresponds to the difference profile; blue marks below the difference profile represent Bragg positions.

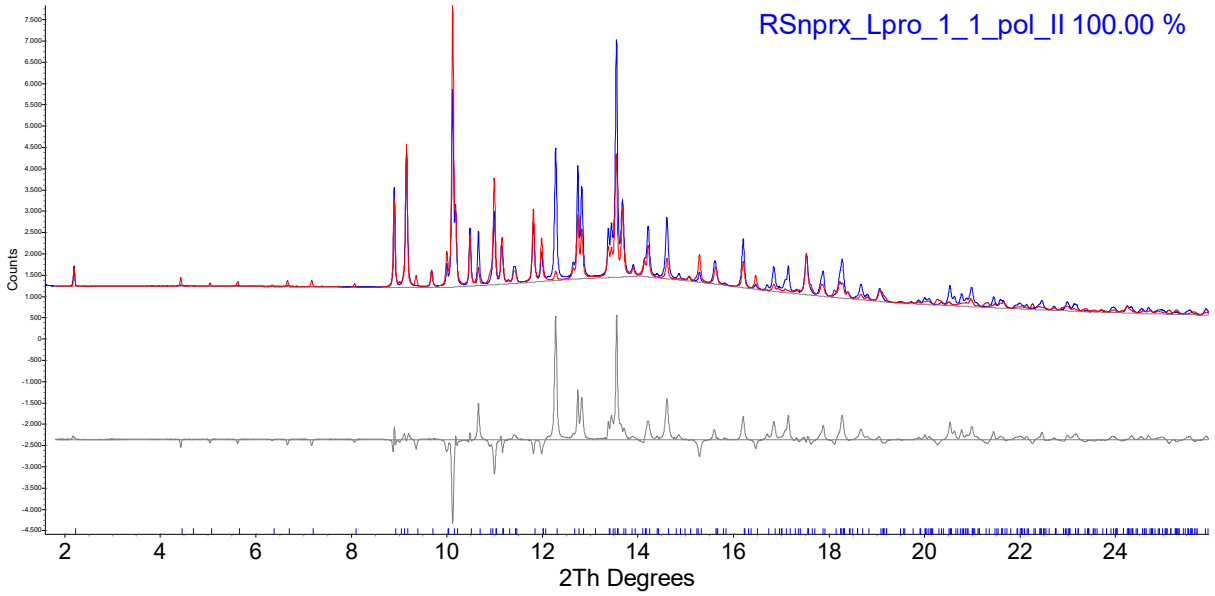

Figure S2.3. Rietveld refinement plot for the **1:2 RS/L** cocrystal, determined from synchrotron X-ray powder data collected upon heating for the RS-nprx/L-pro sample obtained by 1 : 2 ISPN-LAG: λ = 0.708 Å, *T* = 407 K, sample *10* in Table S7.1. Red and blue patterns represent calculated and experimental data, respectively; grey line corresponds to the difference profile; blue marks below the difference profile represent Bragg positions.

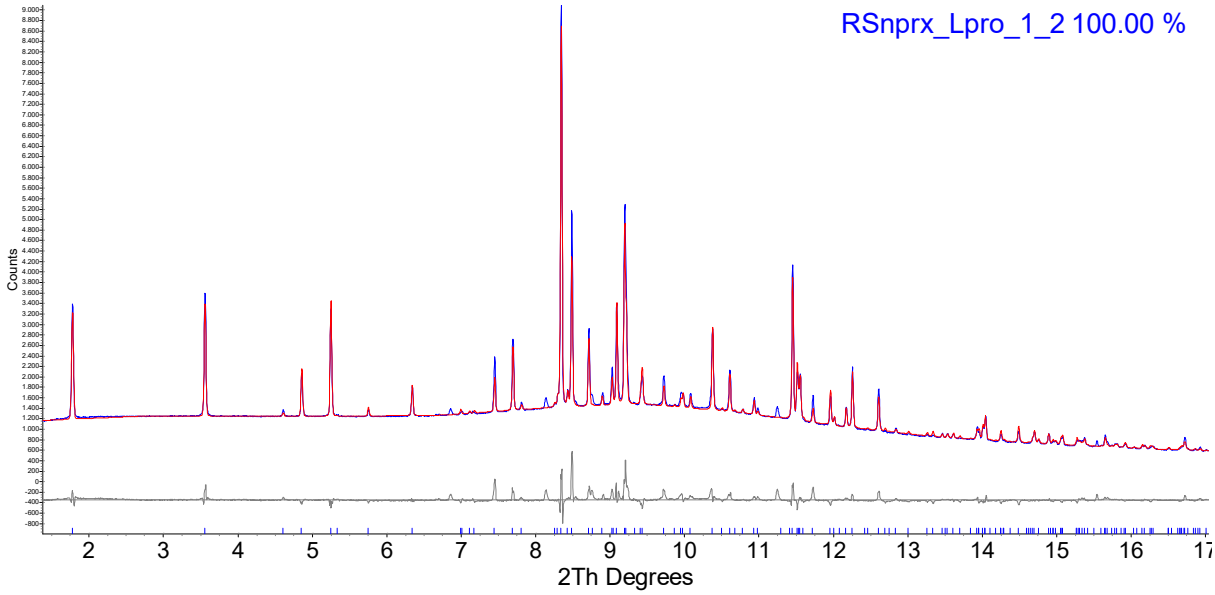

Figure S2.4. Rietveld refinement plot for the **1:1 RS/L pol III** cocrystal, determined from synchrotron X-ray powder data collected upon heating for the RS-nprx/L-pro sample obtained by 1 : 1 water-LAG: λ = 0.78487 Å, *T* = 402 K, sample *17* in Table S7.1. Red and blue patterns represent calculated and experimental data, respectively; grey line corresponds to the difference profile; blue marks below the difference profile represent Bragg positions.

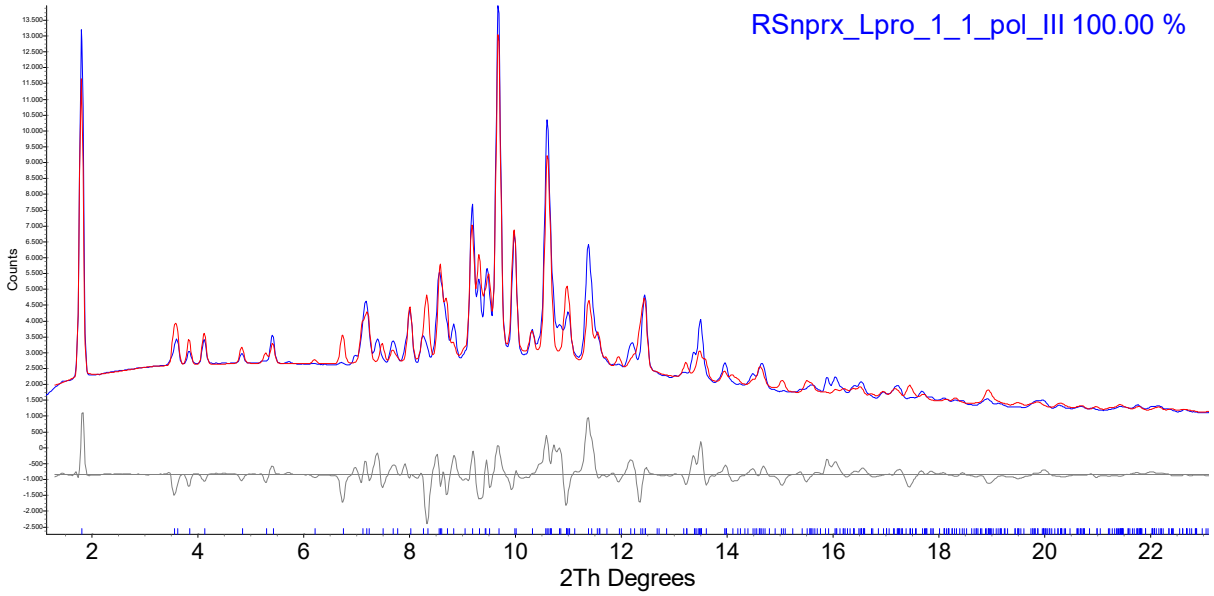

Figure S2.5. Rietveld refinement plot for the **1:1 RS/DL pol II** cocrystal, determined from synchrotron X-ray powder data collected upon heating for the RS-nprx/DL-pro sample obtained by 1 : 1 water-LAG: λ = 0.78487 Å, *T* = 428 K, sample *17* in Table S8.1. Red and blue patterns represent calculated and experimental data, respectively; grey line corresponds to the difference profile; blue marks below the difference profile represent Bragg positions.

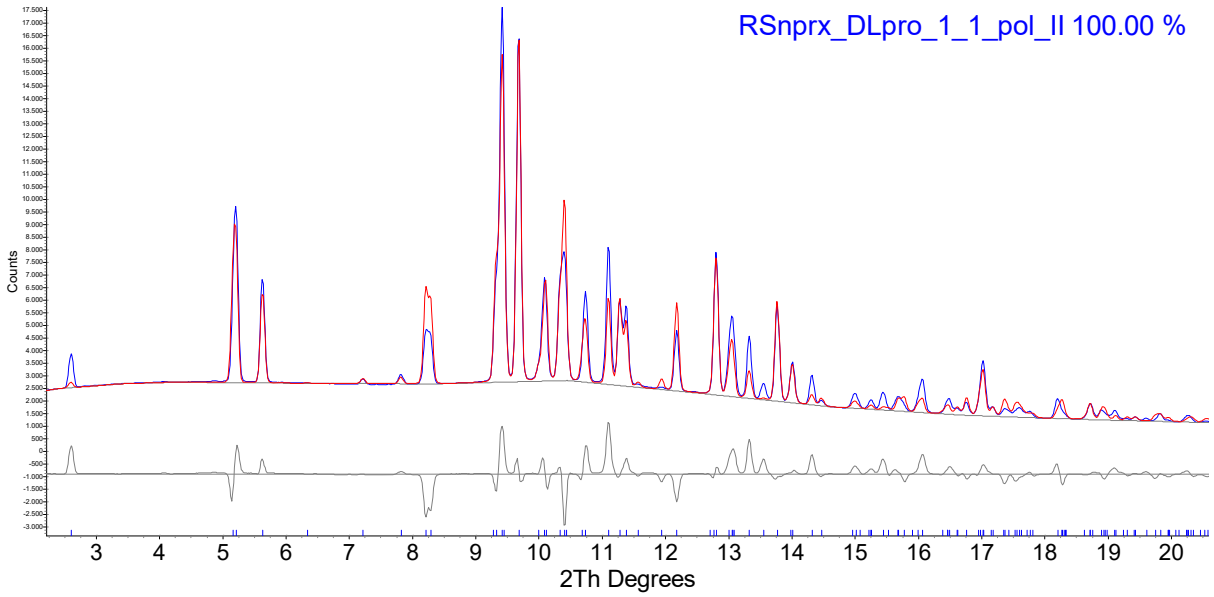

Figure S2.6. Rietveld refinement plot for the **1:1 S/DL/H_2O** cocrystal, determined from synchrotron X-ray powder data collected at room temperature for the S-nprx/DL-pro sample obtained by 1 : 1 water-LAG: λ = 0.798 Å, *T* = 298 K, sample *17* in Table S9.1. Red and blue patterns represent calculated and experimental data, respectively; grey line corresponds to the difference profile; blue marks below the difference profile represent Bragg positions. Not accounted peaks at ~3 and ~10° belong to S-nprx.

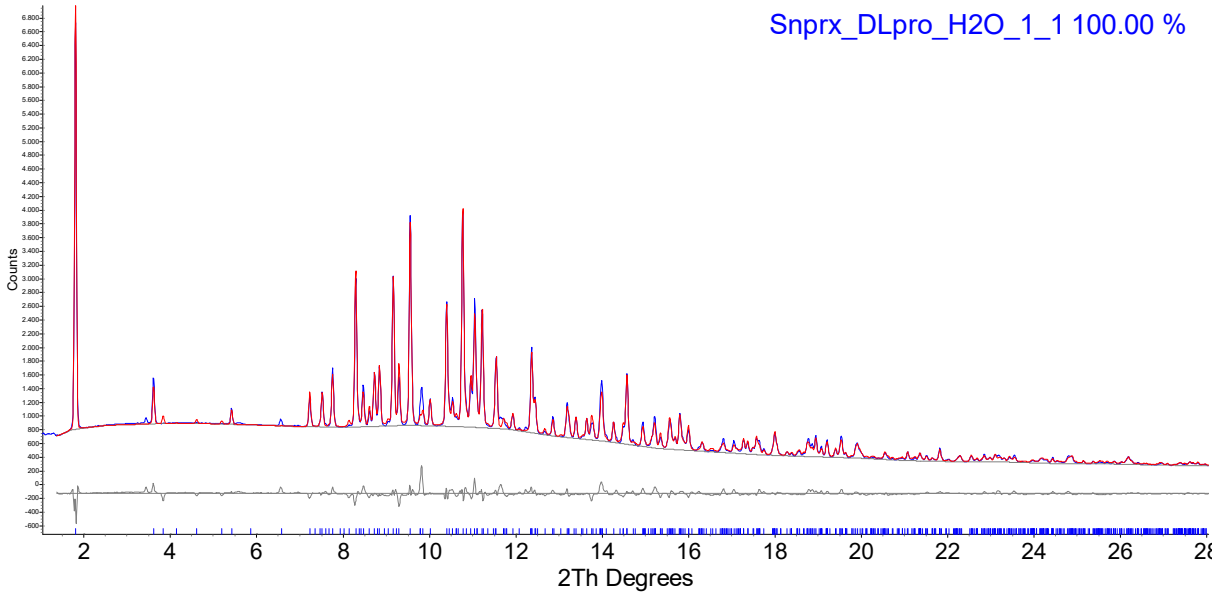

Figure S2.7. Comparison of the experimental diffraction pattern of the **1:2 RS/L** cocrystal (measured at 134 °C) and the simulated diffraction pattern of the **1:2 S/L** cocrystal (room temperature). Peaks are slightly shifted due to the difference in temperature of the diffraction patterns.

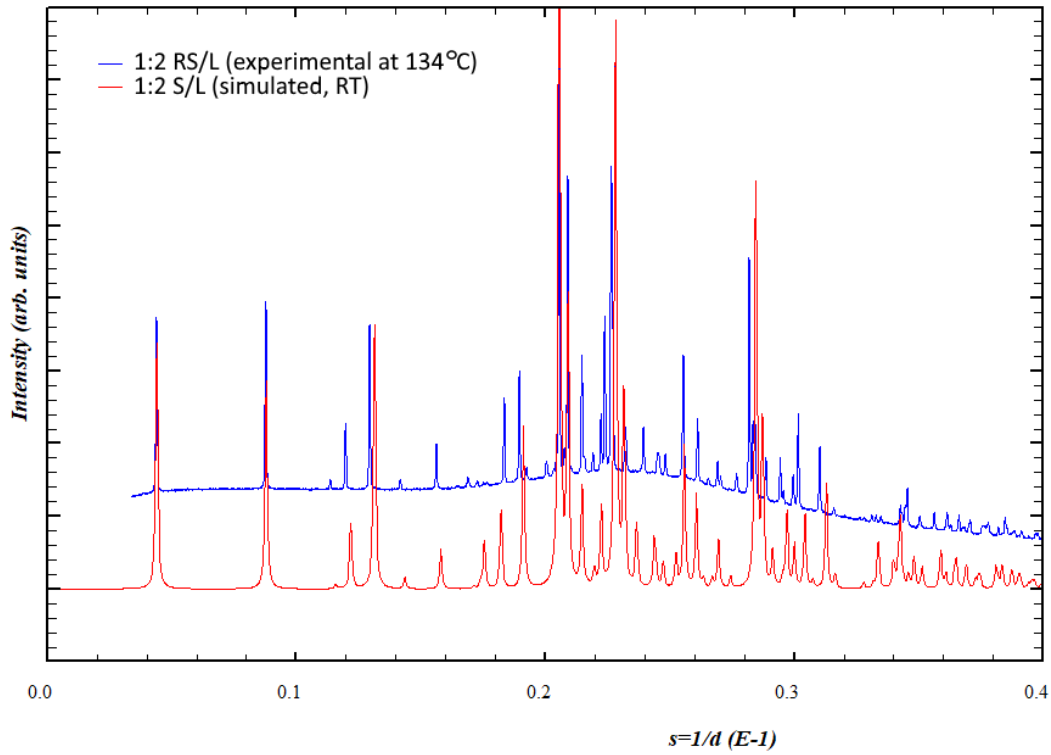

Figure S2.8. Structure of the **1:2 RS/L** cocrystal. **S-nprx** and **R-nprx** share the same position (the –CH3 and –H groups belonging to different enantiomers are colored in blue and green)

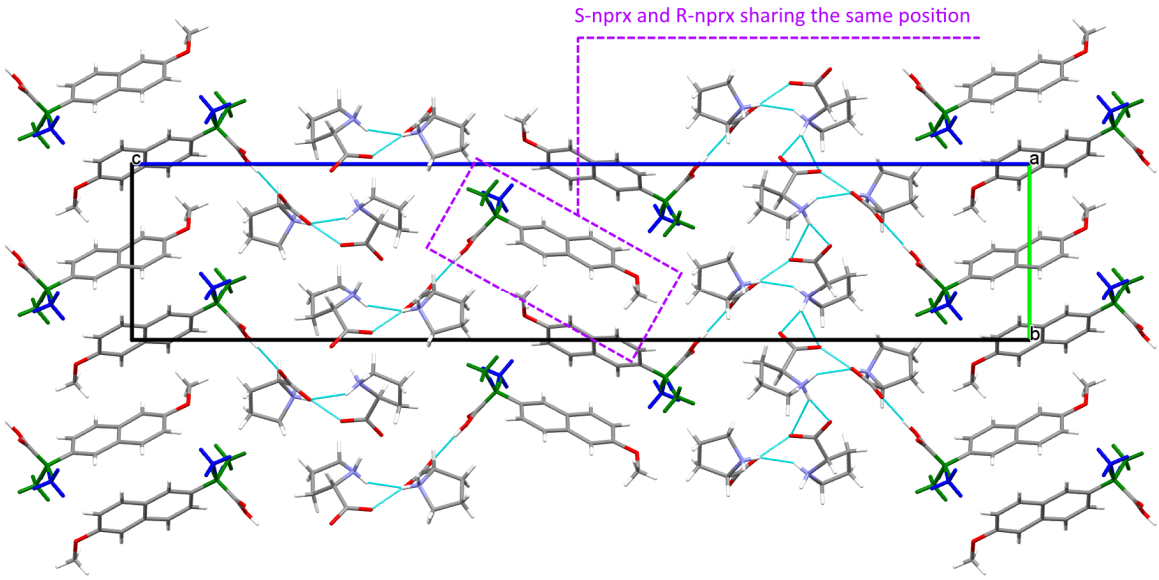

Figure S2.9. Comparison of the experimental diffraction pattern of the **1:1 S/DL/H_2O** cocrystal hydrate and the simulated diffraction pattern of the **1:1 RS/DL/H_2O** cocrystal hydrate (both are at room temperature).

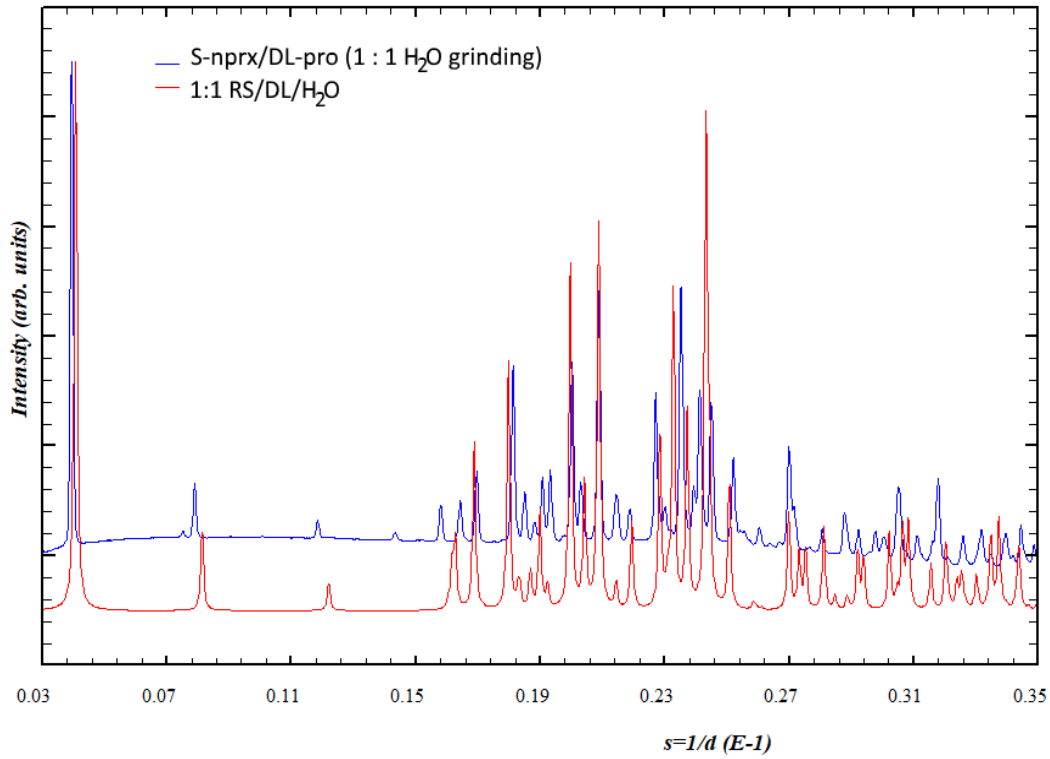

3. In situ ball-milling (Table S3.1)

Table S3.1. Experimental details of *in-situ* ball-milling experiments

#	Sample	m(Nprx), mg	m(Pro), mg	Molar ratio Nprx/Pro	Solvent	Amount of solvent	Grinding duration	Resultant powder
1	S-nprx + L-pro	575.94	288.15	1 : 1	Methanol	200 µL	25 min	1:1 S/L pol II (**Fig. S3.1.1**)
2	S-nprx + L-pro	565.33	282.93	1 : 1	Ethanol	200 µL	25 min	1:1 S/L pol II (**Fig. S3.1.2**)
3	S-nprx + L-pro	571.69	286.09	1 : 1	Isopropanol	200 µL	25 min	1:1 S/L pol II (**Fig. S3.1.3**)
4	S-nprx + L-pro	564.07	282.34	1 : 1	Acetonitrile	200 µL	25 min	1:1 S/L pol II (**Fig. S3.1.4**)
5	S-nprx + DL-pro	574.41	287.24	1 : 1	Methanol	200 µL	25 min	1:1 S/DL + 1:2 S/DL (**Fig. S3.1.15-S3.1.17**)
6	S-nprx + DL-pro	582.05	292.69	1 : 1	Ethanol	200 µL	25 min	1:1 S/DL + 1:2 S/DL (**Fig. S3.1.16-S3.1.17**)
7	S-nprx + DL-pro	757.85	379.05	1 : 1	Isopropanol	200 µL	25 min	1:1 S/DL + 1:2 S/DL(**Fig. S3.1.17**)
8	S-nprx + DL-pro	560.98	280.67	1 : 1	Acetonitrile	200 µL	25 min	1:1 S/DL + 1:2 S/DL (**Fig. S3.1.17**)
9	RS-nprx + L-pro	580.73	290.44	1 : 1	Methanol	200 µL	25 min	1:1 RS/L pol I (**Fig. S3.1.5** and **S3.1.11**)
10	RS-nprx + L-pro	586.82	293.66	1 : 1	Ethanol	200 µL	25 min	1:1 RS/L pol I (**Fig. S3.1.6** and **S3.1.11**)
11	RS-nprx + L-pro	581.41	290.75	1 : 1	Isopropanol	200 µL	25 min	1:1 RS/L pol I (**Fig. S3.1.7** and **S3.1.11**)
12	RS-nprx + L-pro	592.02	296.22	1 : 1	Acetonitrile	200 µL	25 min	1:1 RS/L pol I (**Fig. S3.1.8** and **S3.1.11**)
13	RS-nprx + L-pro	426.32	425.24	1 : 2	Isopropanol	250 µL	11 min*	1:2 RS/L + 1:1 RS/L pol I + L-proline monohydrate (**Fig. S3.1.9** and **S3.1.18** for the entire dataset)
14	RS-nprx + L-pro†	463.84	463.93	1 : 2	Methanol	200 µL	30 min	1:1 RS/L pol I + L-pro monohydrate (**Fig. S3.1.10**)
15	RS-nprx + DL-pro	634.34	316.97	1 : 1	Methanol	200 µL	30 min	1:1 RS/DL pol I (**Fig. S3.1.12**)
16	RS-nprx + DL-pro	660.19	329.67	1 : 1	Isopropanol	200 µL	30 min	1:1 RS/DL pol I
17	RS-nprx + DL-pro	407.38	406.45	1 : 2	Methanol	200 µL	30 min	1:1 RS/DL pol I + (1: S/DL + 1:2 R/DL) (**Fig. S3.1.13**)
18	RS-nprx + DL-pro	449.0	447.88	1 : 2	Isopropanol	200 µL	30 min	(1: S/DL + 1:2 R/DL) (**Fig. S3.1.14**)

'*' the jar broke during the experiment

'†' *in-situ* PXRD ball-milling data are of very poor quality and do not allow any reliable conclusions (only the diffraction pattern of the final sample is available)

3.1 In situ ball-milling (Figs. S3.1.1-S3.1.18)

Figure S3.1.1. Selected diffraction patterns from the *in-situ* ball-milling experiment for the **S/L** sample, 1 : 1 MeOH-LAG (sample *1* in Table S3.1); the diffraction patterns of the pure phases were simulated from the structures, except the PXRD pattern **1:1 S/L pol II** was taken as measured (sample *13* in Table S4.1). (*a*) –first frame measured within 30 seconds as reaction started; (*b*) – at the 3^{d} minute of reaction; (*c*) – at the 15th minute of reaction

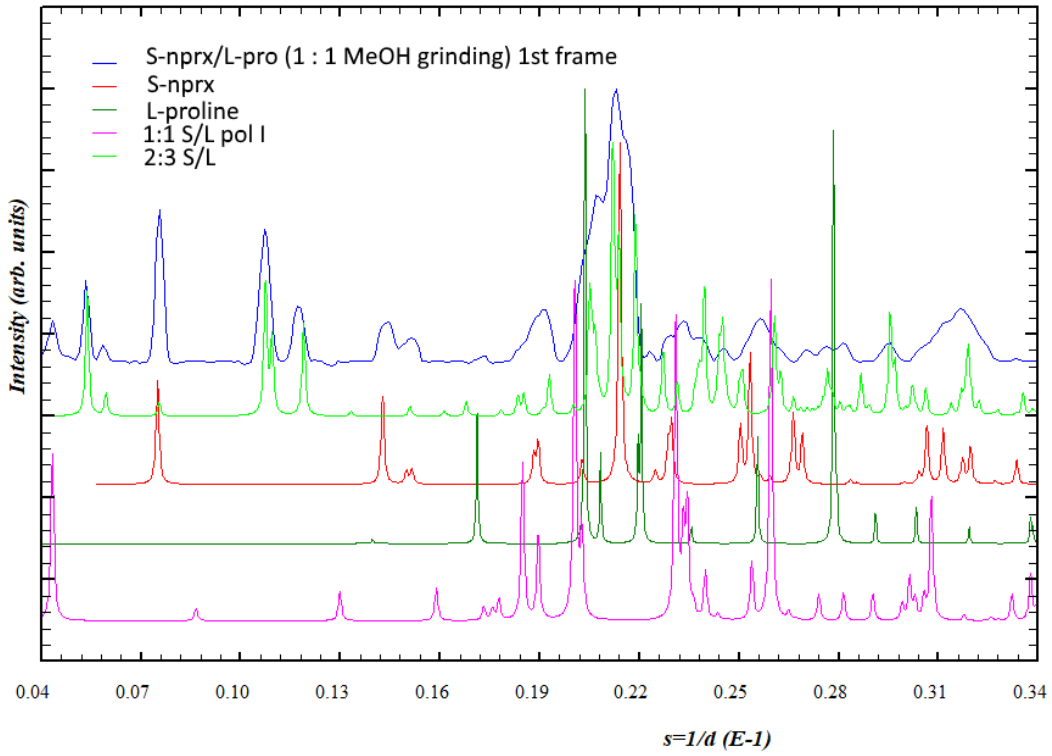

(*a*)

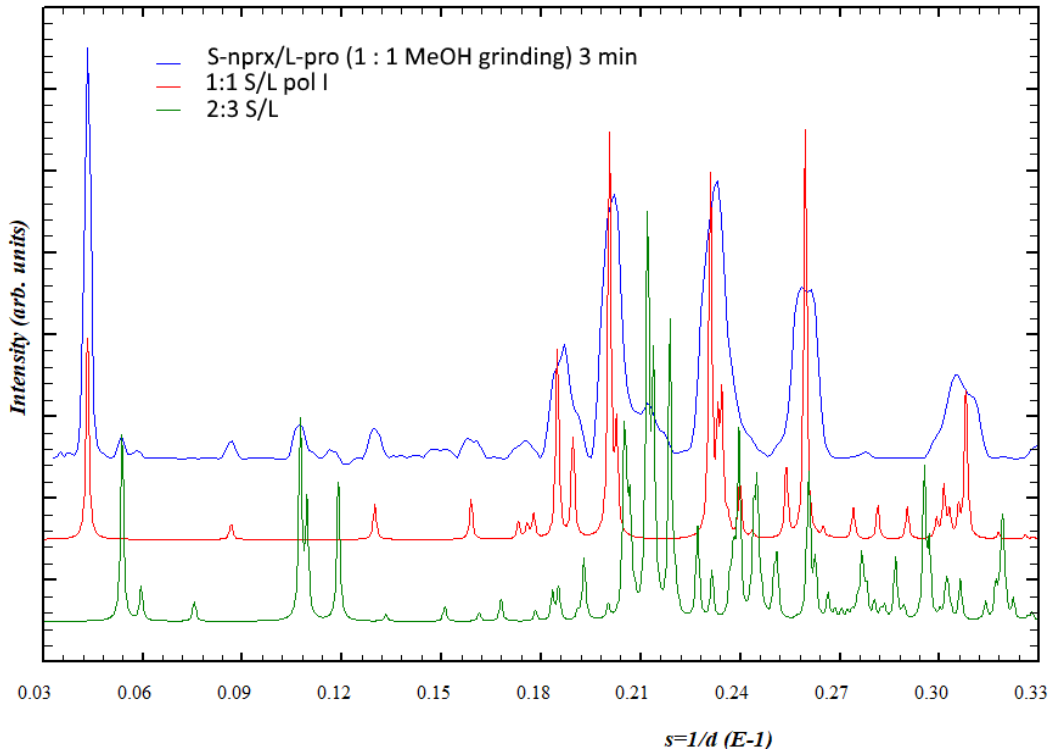

(*b*)

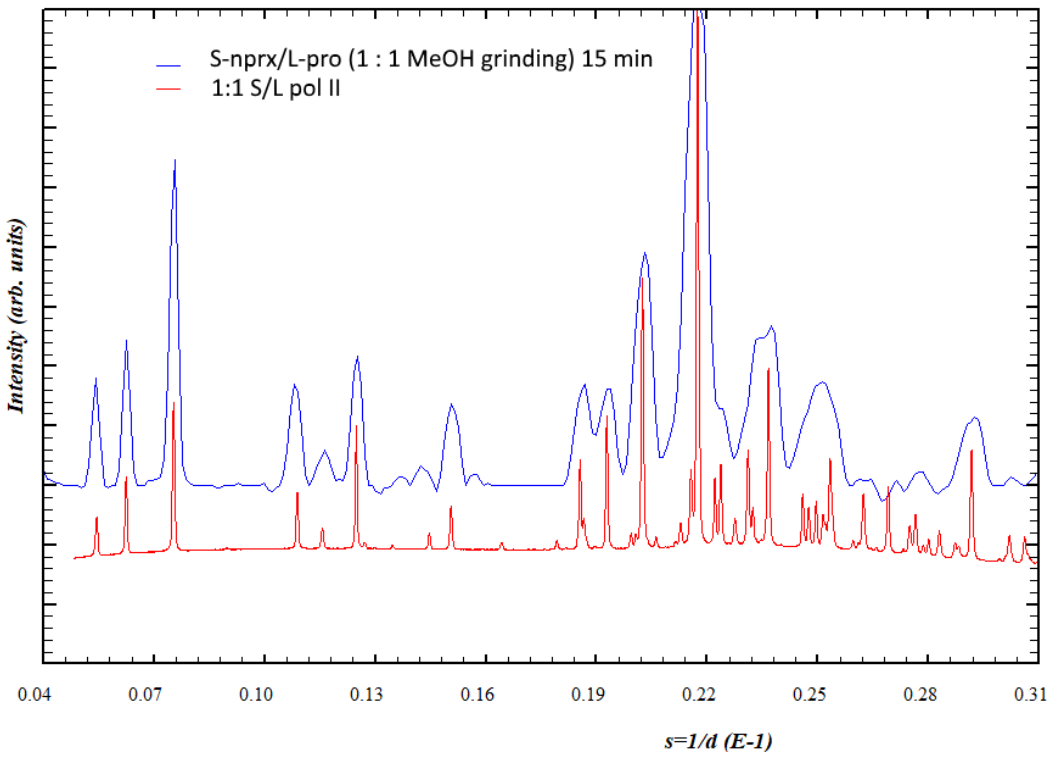

(*c*)

Figure S3.1.2. Selected diffraction patterns from the *in-situ* ball-milling experiment for the **S/L** sample, 1 : 1 EtOH-LAG (sample *2* in Table S3.1); the diffraction patterns of the pure phases were simulated from the structures, except the PXRD pattern **1:1 S/L pol II** was taken as measured (sample *13* in Table S4.1). (*a*) –first frame measured within 30 seconds as reaction started; (*b*) – at the 3^{d} minute of reaction; (*c*) – at the 15th minute of reaction

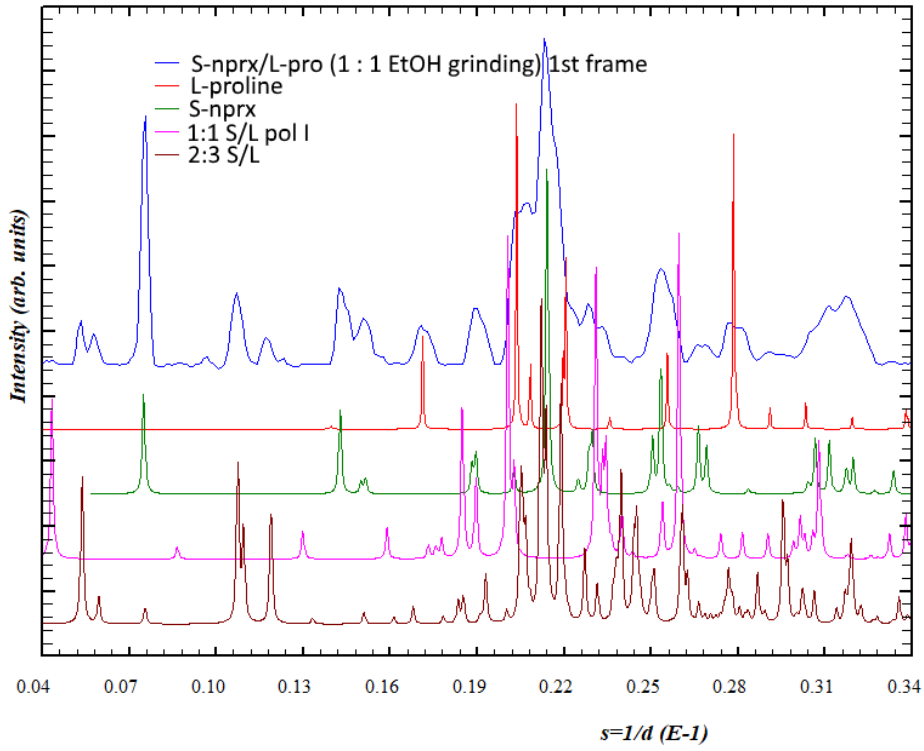

(*a*)

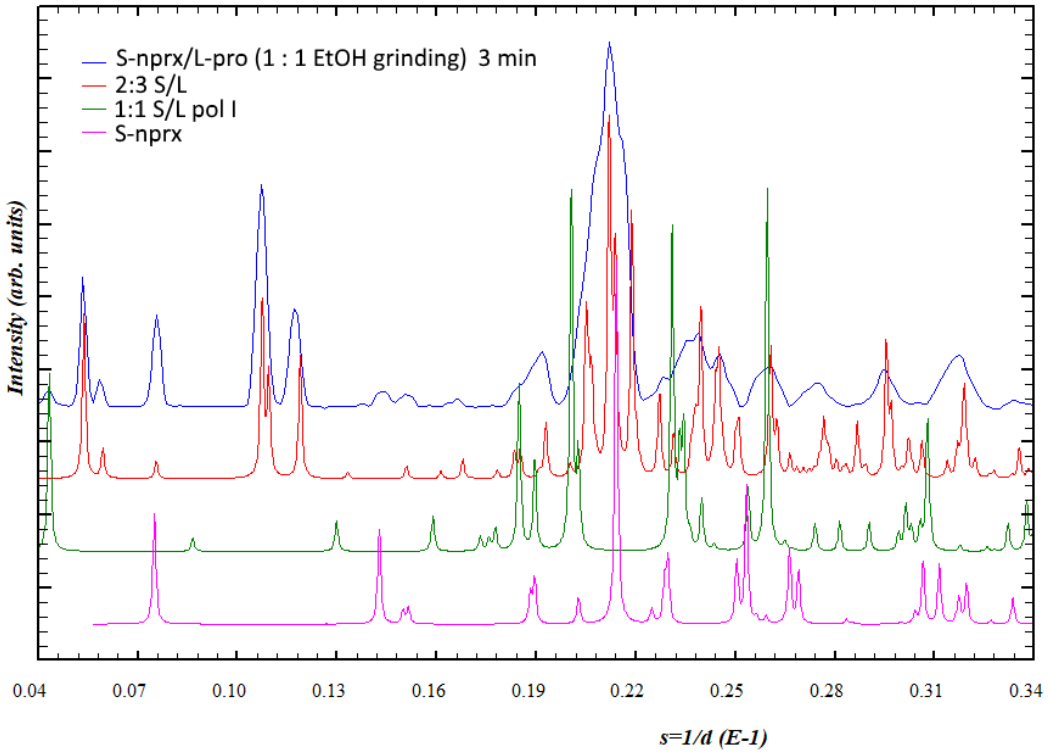
S-nprx/L-pro (1 : 1 EtOH grinding) 3 min
2:3 S/L
1:1 S/L pol I
S-nprx
Intensity (arb. units)
0.04
0.07
0.10
0.13
0.16
0.19
0.22
0.25
0.28
0.31
0.34
s=1/d (E-1)

(*b*)

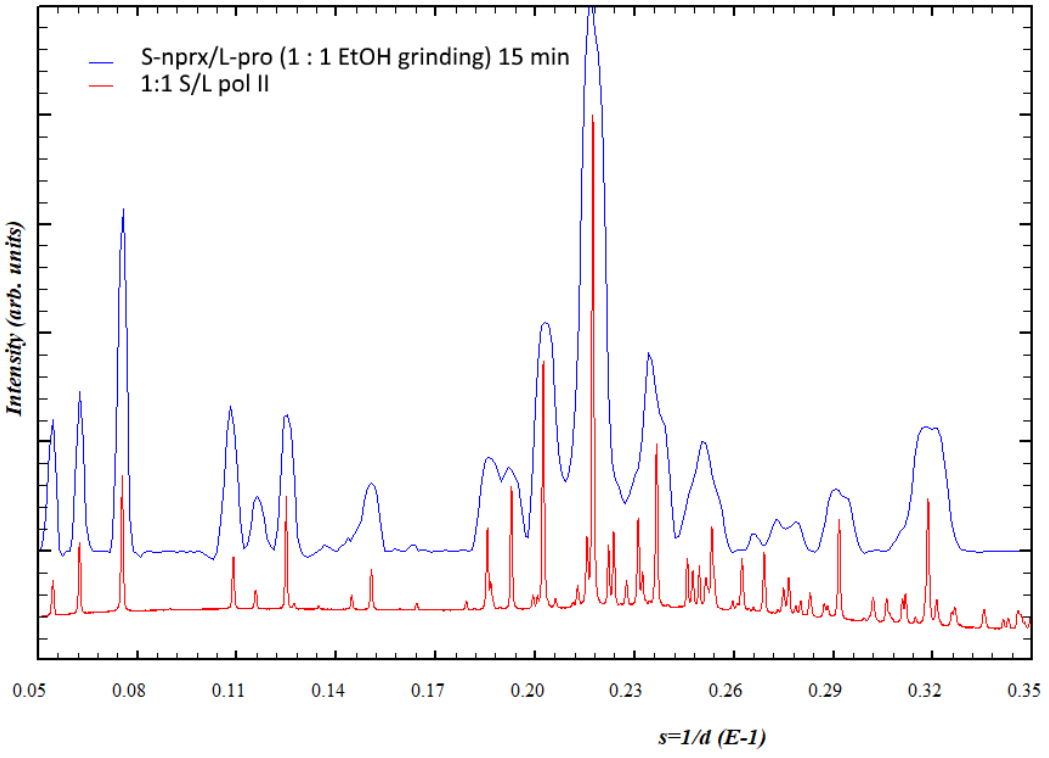
S-nprx/L-pro (1 : 1 EtOH grinding) 15 min
1:1 S/L pol II
Intensity (arb. units)
0.05
0.08
0.11
0.14
0.17
0.20
0.23
0.26
0.29
0.32
0.35
s=1/d (E-1)

(*c*)

Figure S3.1.3. Selected diffraction patterns from the *in-situ* ball-milling experiment for the **S/L** sample, 1 : 1 ISPN-LAG (sample *3* in Table S3.1); the diffraction patterns of the pure phases were simulated from the structures, except the PXRD pattern **1:1 S/L pol II** was taken as measured (sample *13* in Table S4.1). (*a*) –first frame measured within 30 seconds as reaction started; (*b*) – at the 3^{d} minute of reaction; (*c*) – at the 15th minute of reaction; the most visible peaks of the **unknown phase I** are indicated with arrows

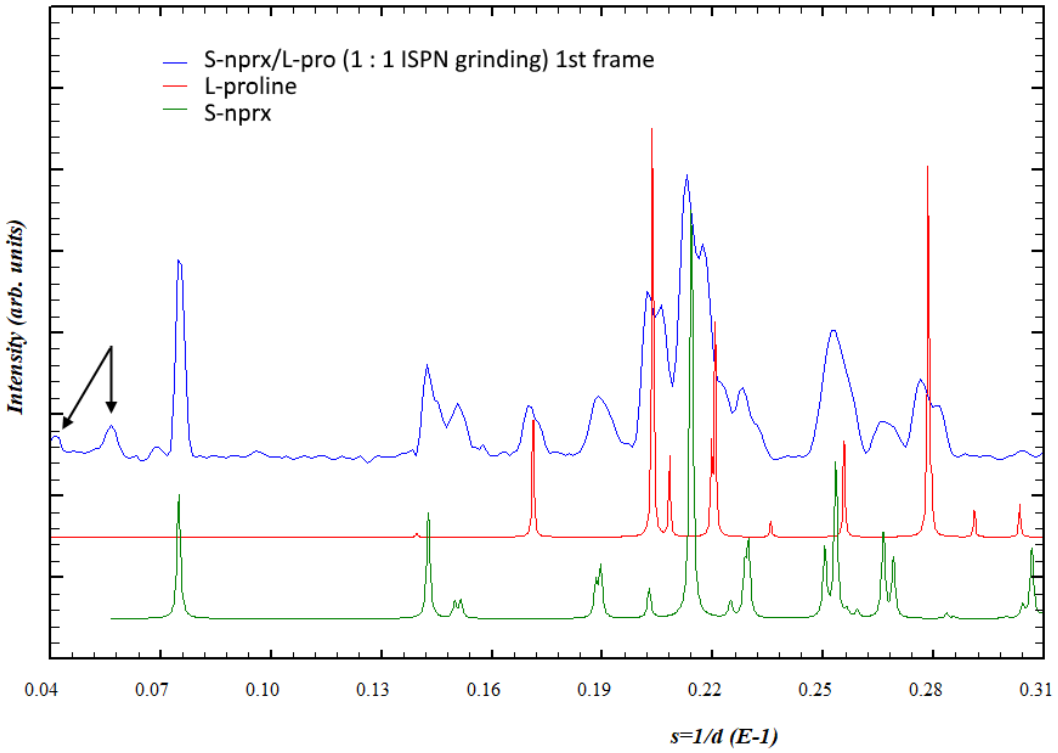

(*a*)

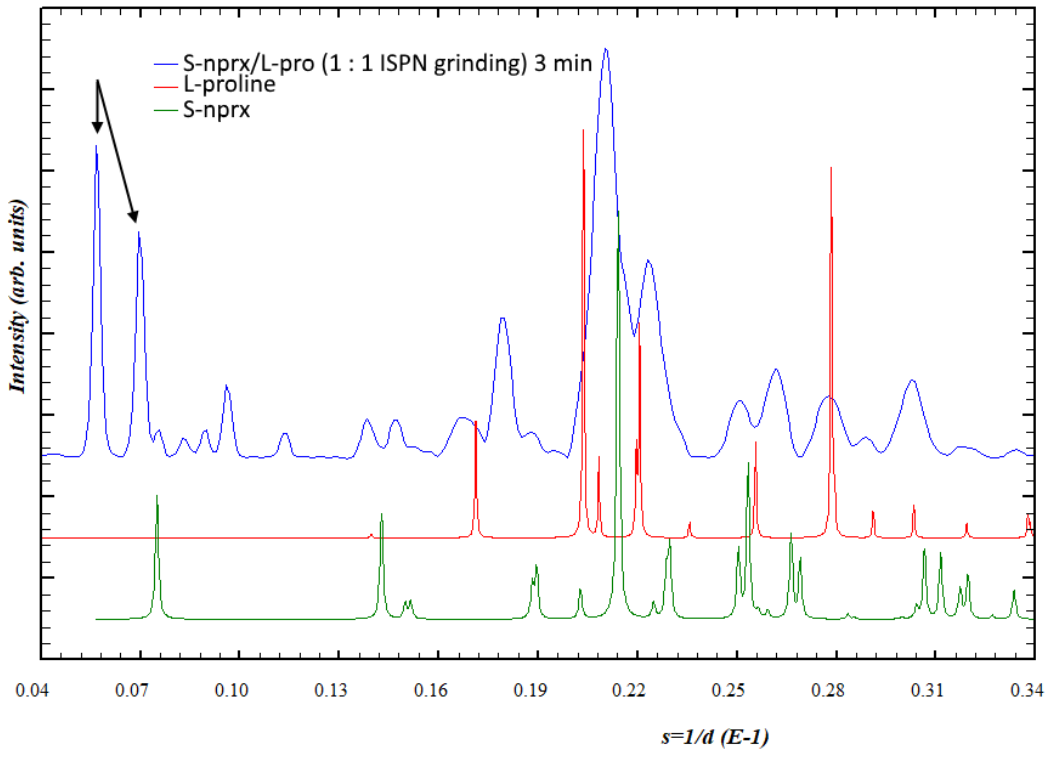

(*b*)

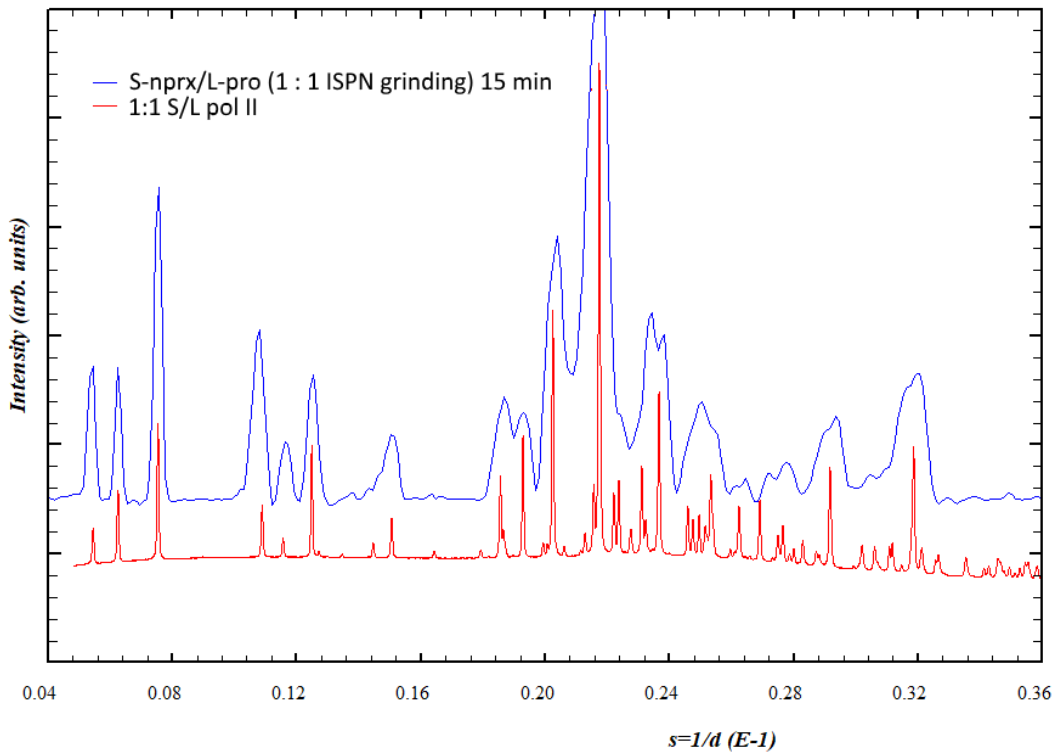

(*c*)

Figure S3.1.4. Selected diffraction patterns from the *in-situ* ball-milling experiment for the **S/L** sample, 1 : 1 ACN-LAG (sample *4* in Table S3.1); the diffraction patterns of the pure phases were simulated from the structures, except the PXRD pattern **1:1 S/L pol II** was taken as measured (sample *13* in Table S4.1). (*a*) – first frame measured within 30 seconds as reaction started; (*b*) – at the 1st minute of reaction; (*c*) – at the 15th minute of reaction; the most visible peaks of the **unknown phase I** are indicated with arrows

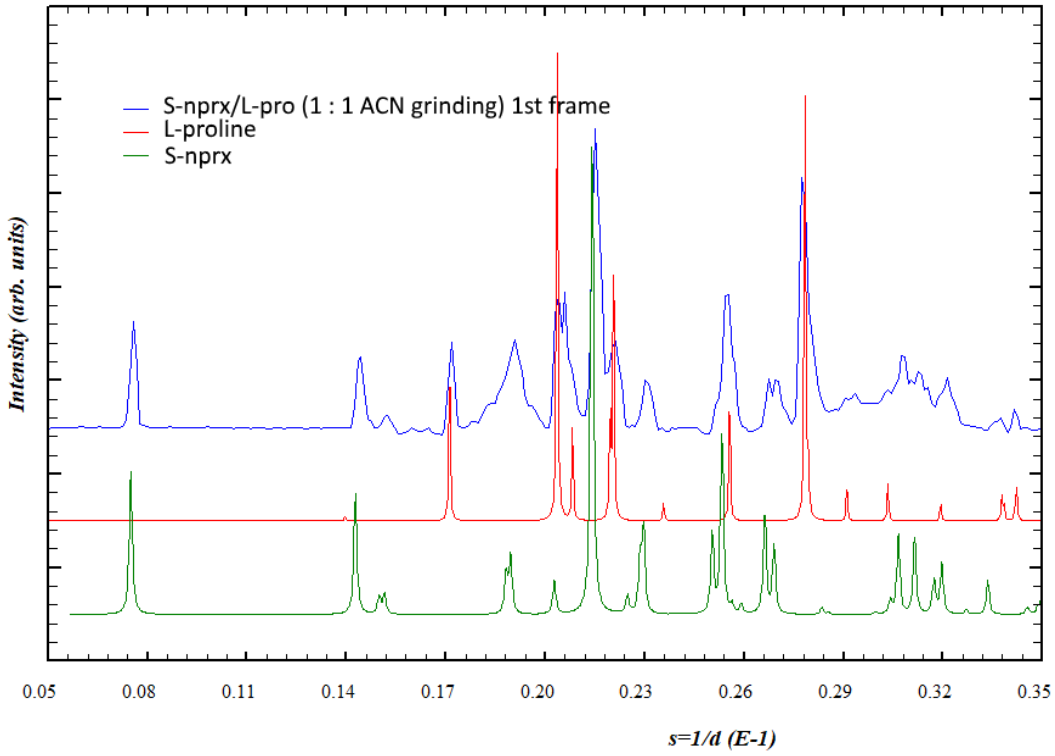

(*a*)

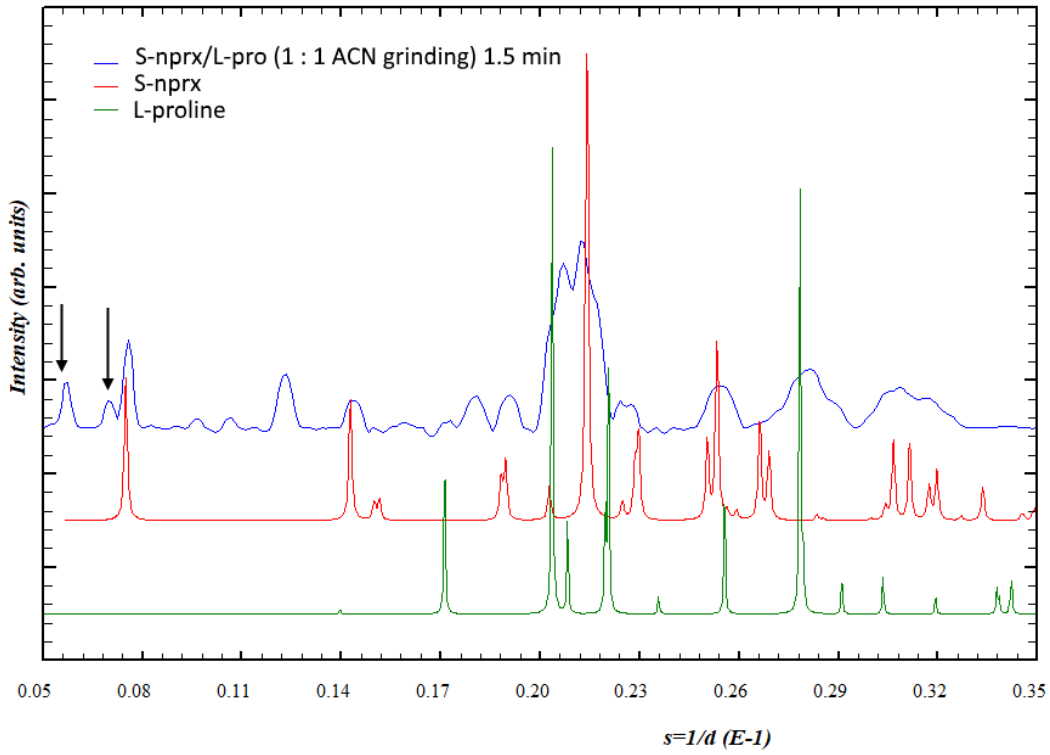
S-nprx/L-pro (1 : 1 ACN grinding) 1.5 min
S-nprx
L-proline
Intensity (arb. units)
0.05
0.08
0.11
0.14
0.17
0.20
0.23
0.26
0.29
0.32
0.35
s=1/d (E-1)

(*b*)

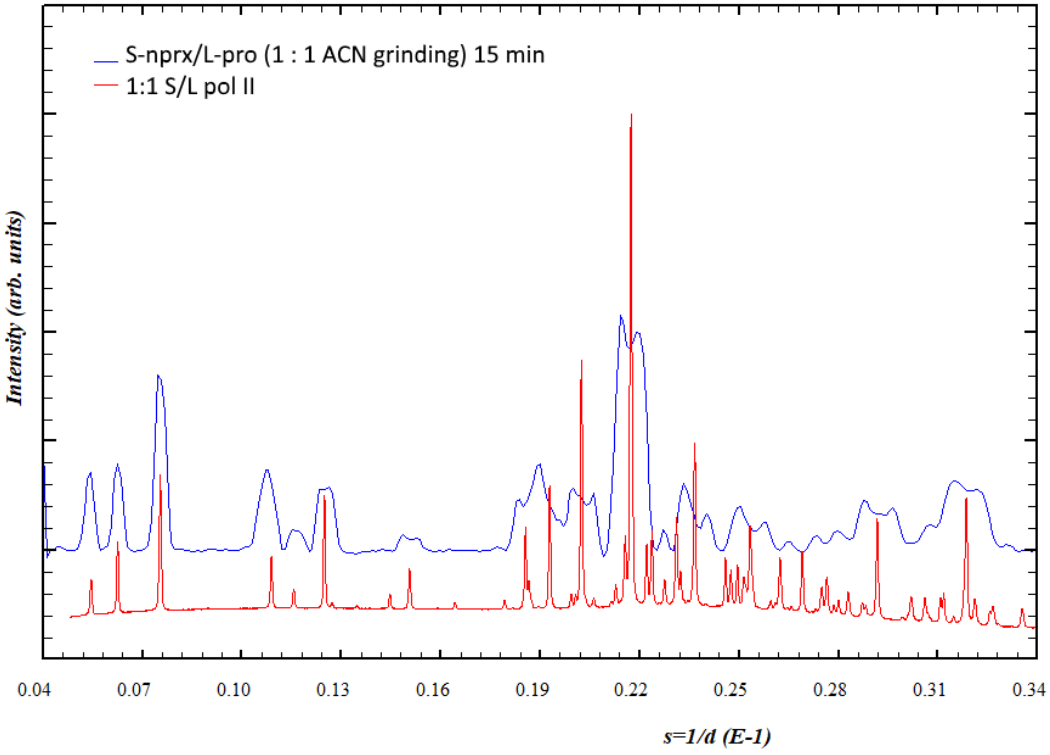
S-nprx/L-pro (1 : 1 ACN grinding) 15 min
1:1 S/L pol II
Intensity (arb. units)
0.04
0.07
0.10
0.13
0.16
0.19
0.22
0.25
0.28
0.31
0.34
s=1/d (E-1)

(*c*)

Figure S3.1.5. Selected diffraction patterns from the *in-situ* ball-milling experiment for the **RS/L** sample, 1 : 1 MeOH-LAG (sample *9* in Table S3.1); the diffraction patterns of the pure phases were simulated from the structures, except the PXRD pattern of **1:1 RS/L pol II** was taken as measured (sample *17* in Table S7.1).

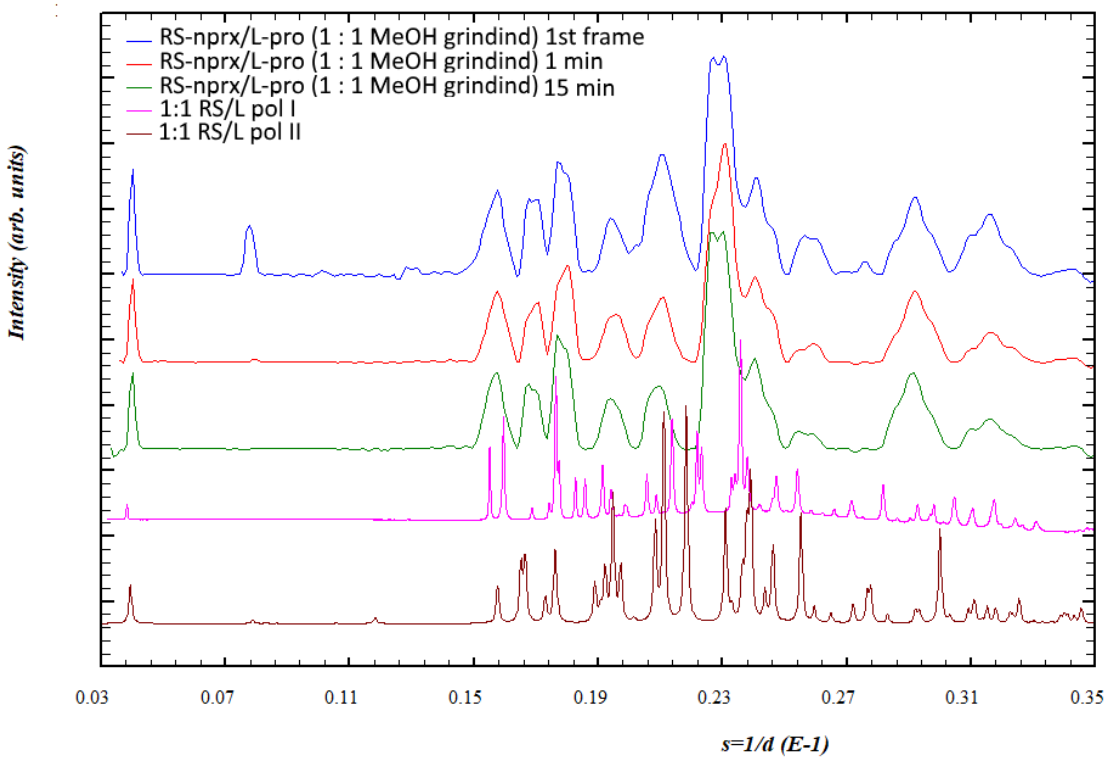

Figure S3.1.6. Selected diffraction patterns from the *in-situ* ball-milling experiment for the **RS/L** sample, 1 : 1 EtOH-LAG (sample *10* in Table S3.1); the diffraction patterns of the pure phases were simulated from the structures, except the PXRD patterns of **1:1 RS/L pol II** and **1:2 RS/L** were taken as measured (samples *17* and *10* and in Table S7.1). (*a*) –first frame measured within 30 seconds as reaction started; (*b*) – at the 15th minute of reaction

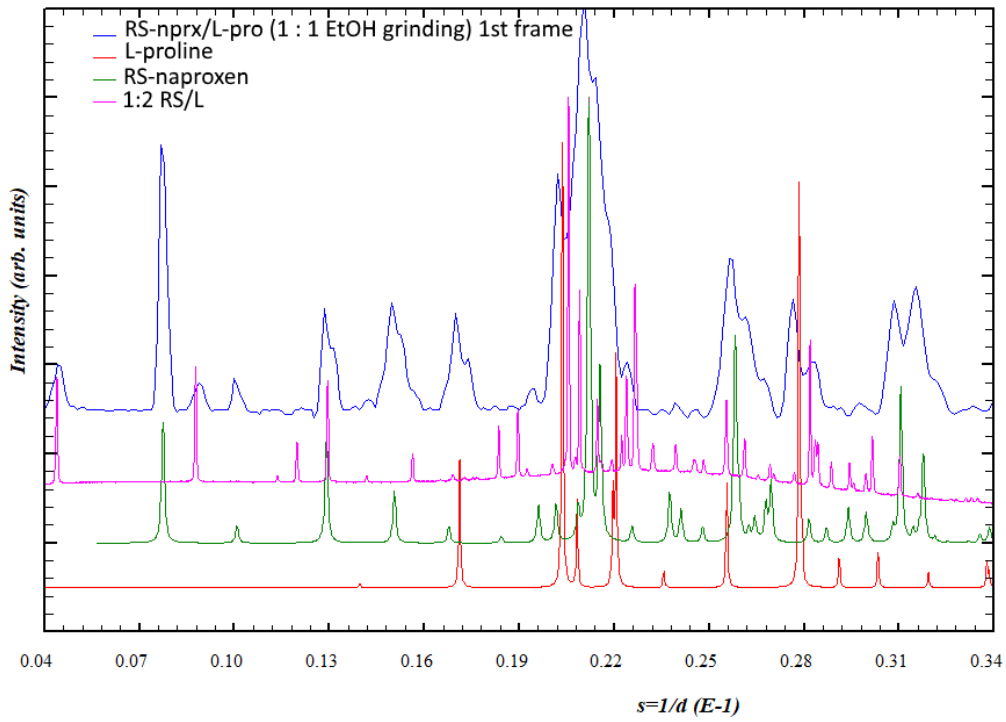

(*a*)

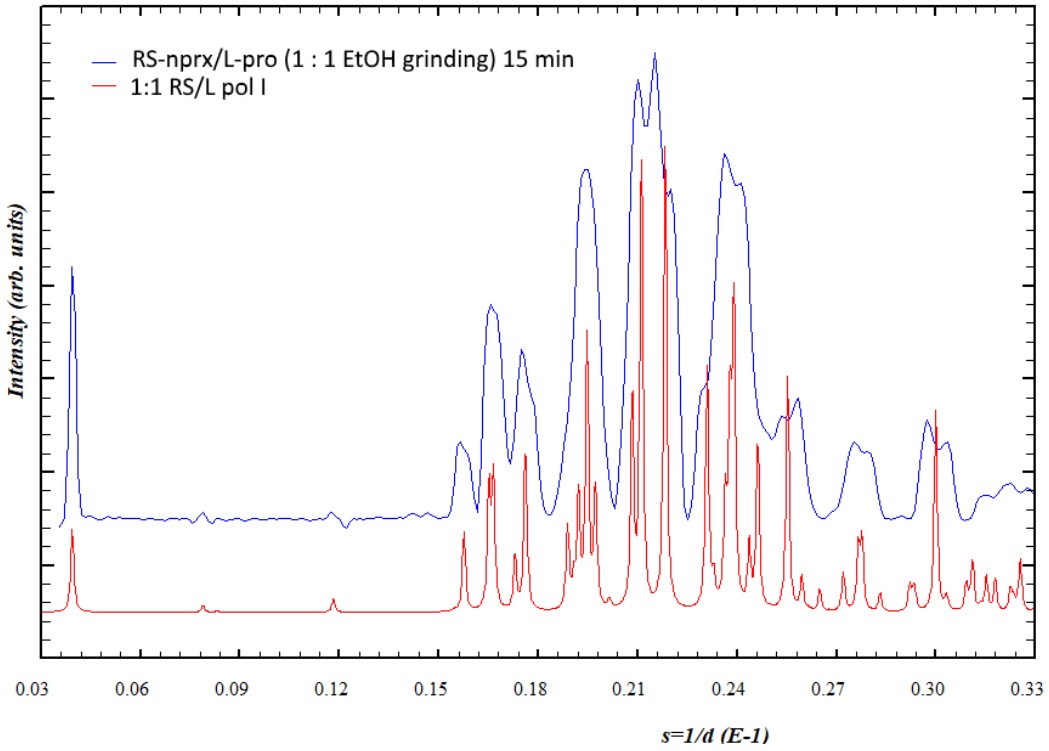

(*b*)

Figure S3.1.7. Selected diffraction patterns from the *in-situ* ball-milling experiment for the **RS/L** sample, 1 : 1 ISPN-LAG (sample *11* in Table S3.1); the diffraction patterns of the pure phases were simulated from the structures, except the PXRD pattern of **1:1 RS/L pol II** was taken as measured (samples *17* in Table S7.1). (*a*) –first frame measured within 30 seconds as reaction started; (*b*) – at the 15th minute of reaction

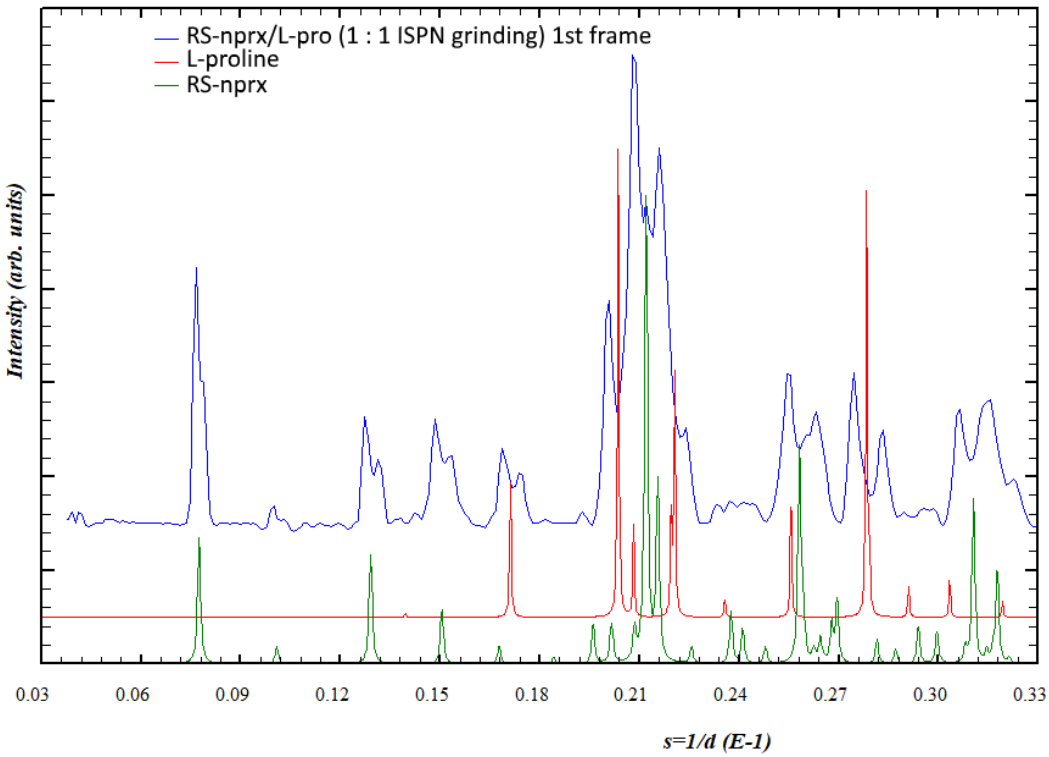

(*a*)

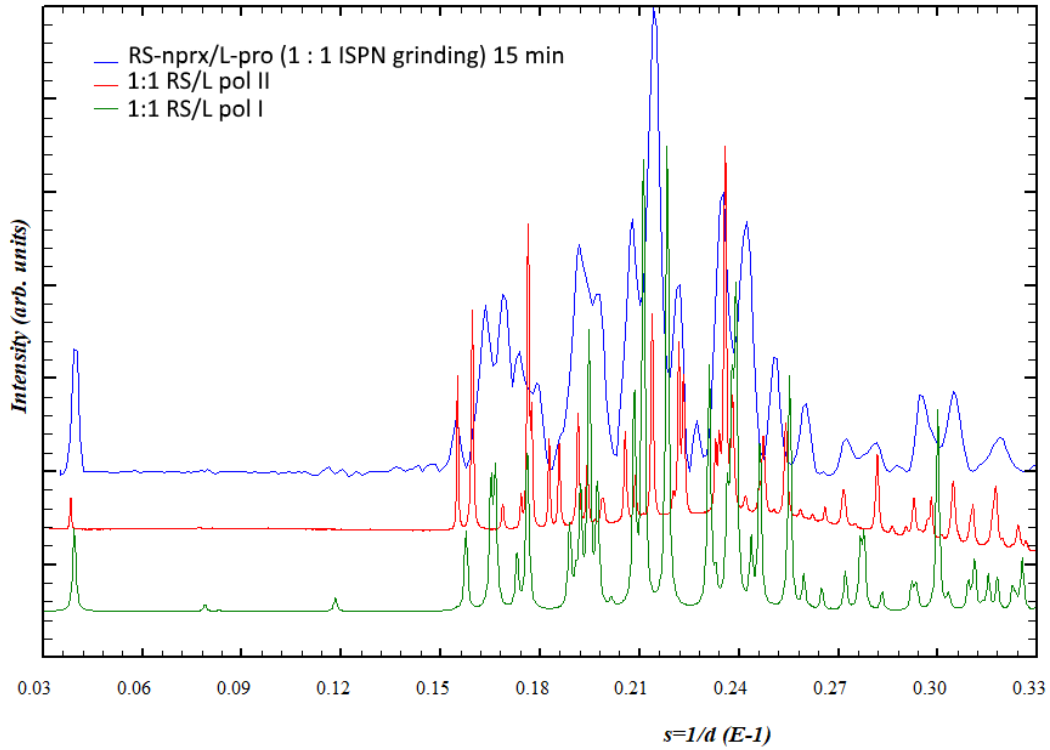

(*b*)

Figure S3.1.8. Selected diffraction patterns from the *in-situ* ball-milling experiment for the **RS/L** sample, 1 : 1 ACN-LAG (sample *12* in Table S3.1); the diffraction patterns of the pure phases were simulated from the structures, except the PXRD pattern of **1:1 RS/L pol II** was taken as measured (samples *17* in Table S7.1). (*a*) –first frame measured within 30 seconds as reaction started; (*b*) – at the 4th minute of reaction; (*c*) – at the 15th minute of reaction; the most visible peaks of the **unknown phase III** are indicated with arrows

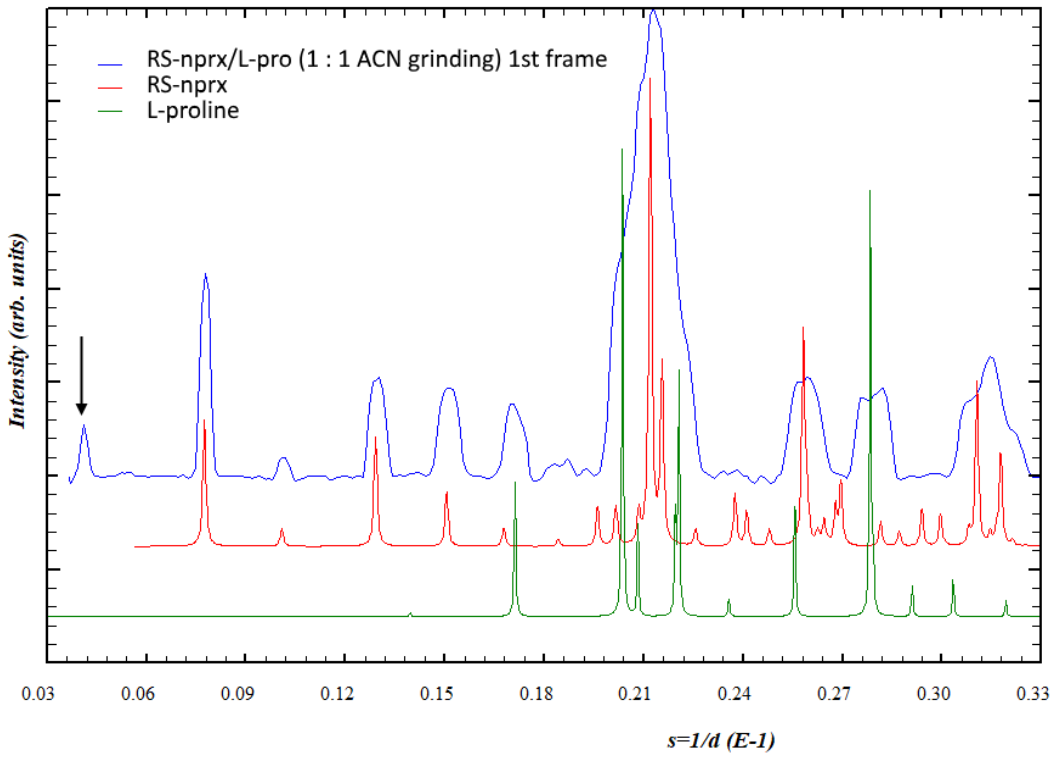

(*a*)

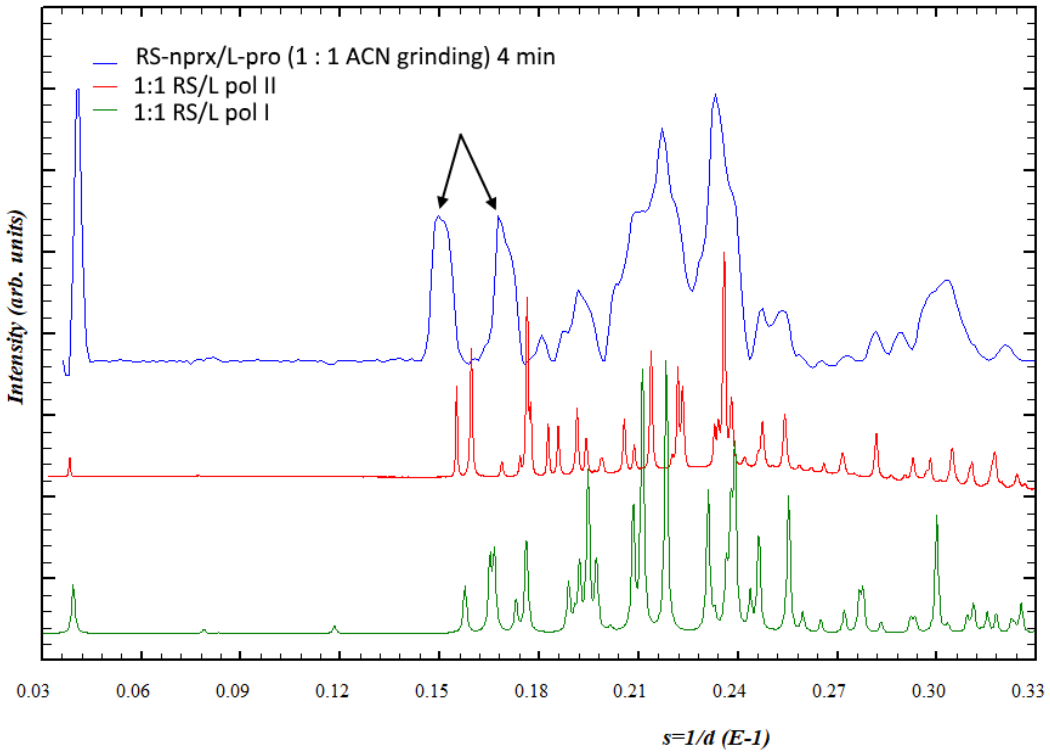
RS-nprx/L-pro (1 : 1 ACN grinding) 4 min
1:1 RS/L pol II
1:1 RS/L pol I
Intensity (arb. units)
0.03
0.06
0.09
0.12
0.15
0.18
0.21
0.24
0.27
0.30
0.33
s=1/d (E-1)

(*b*)

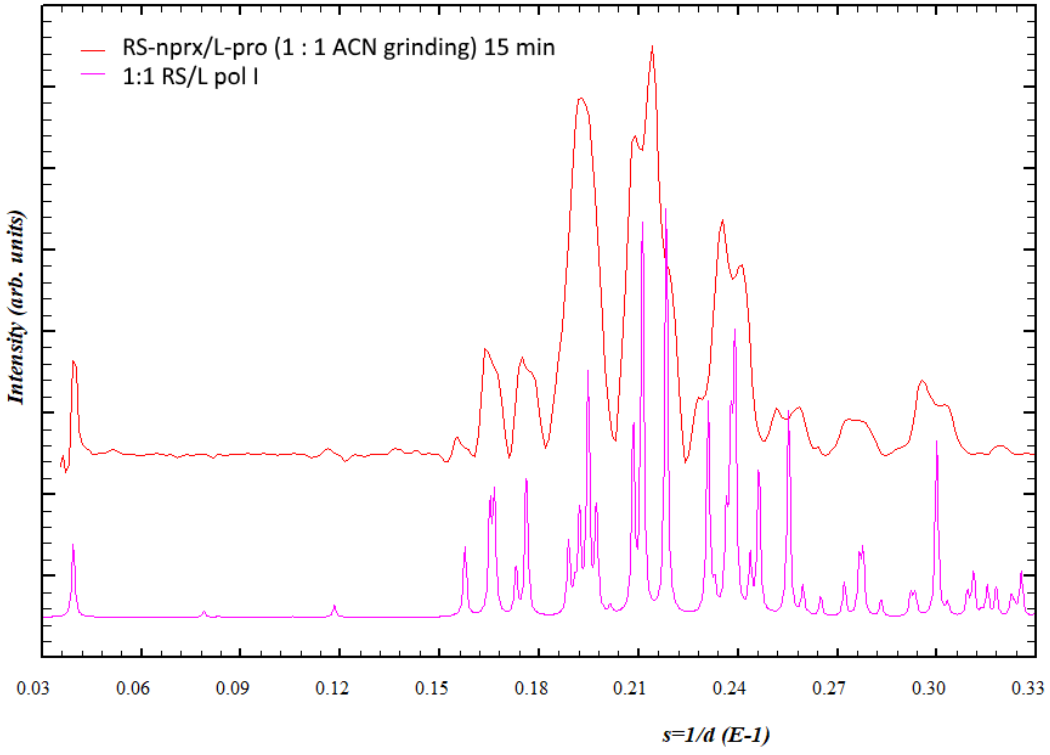
RS-nprx/L-pro (1 : 1 ACN grinding) 15 min
1:1 RS/L pol I
Intensity (arb. units)
0.03
0.06
0.09
0.12
0.15
0.18
0.21
0.24
0.27
0.30
0.33
s=1/d (E-1)

(*c*)

Figure S3.1.9. Selected diffraction patterns from the *in-situ* ball-milling experiment for the **RS/L** sample, 1 : 2 ISPN-LAG (sample *13* in Table S3.1); the diffraction patterns of the pure phases were simulated from the structures, except the PXRD pattern of **1:1 RS/L pol II** was taken as measured (samples *17* in Table S7.1). (*a*) –first frame measured within 30 seconds as reaction started; (*b*) – at the 4th minute of reaction; (*c*) – at the 11th minute of reaction; (*d*) – PXRD pattern of the resultant powder measured at a laboratory diffractometer (Cu*K*α radiation)

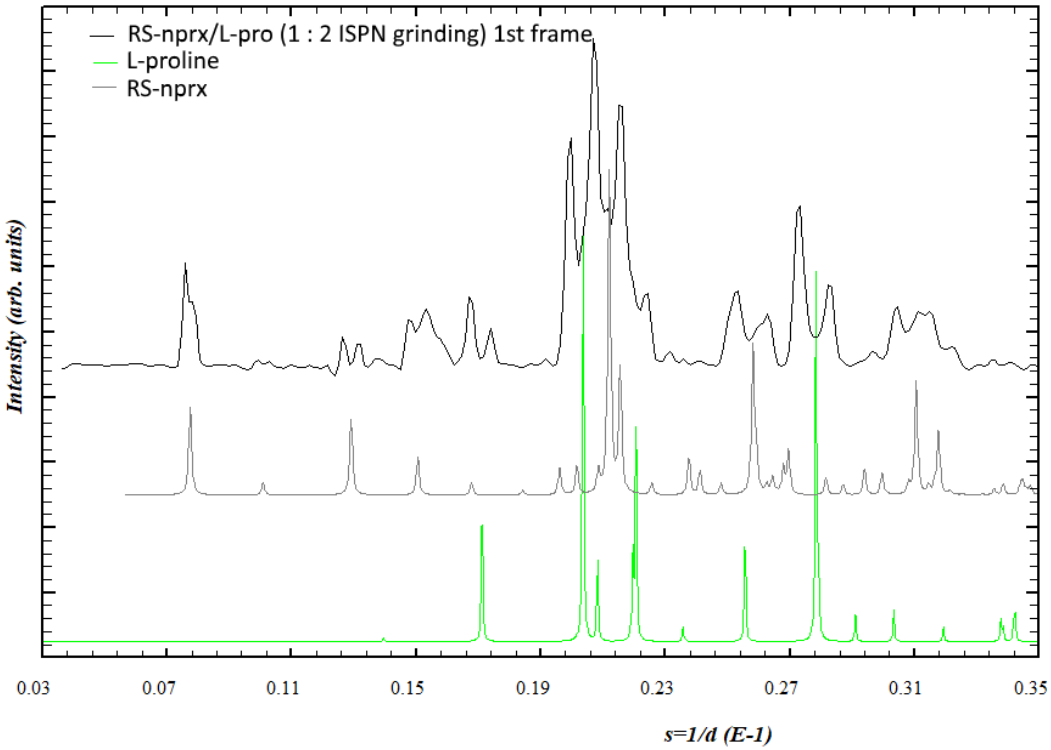

(*a*)

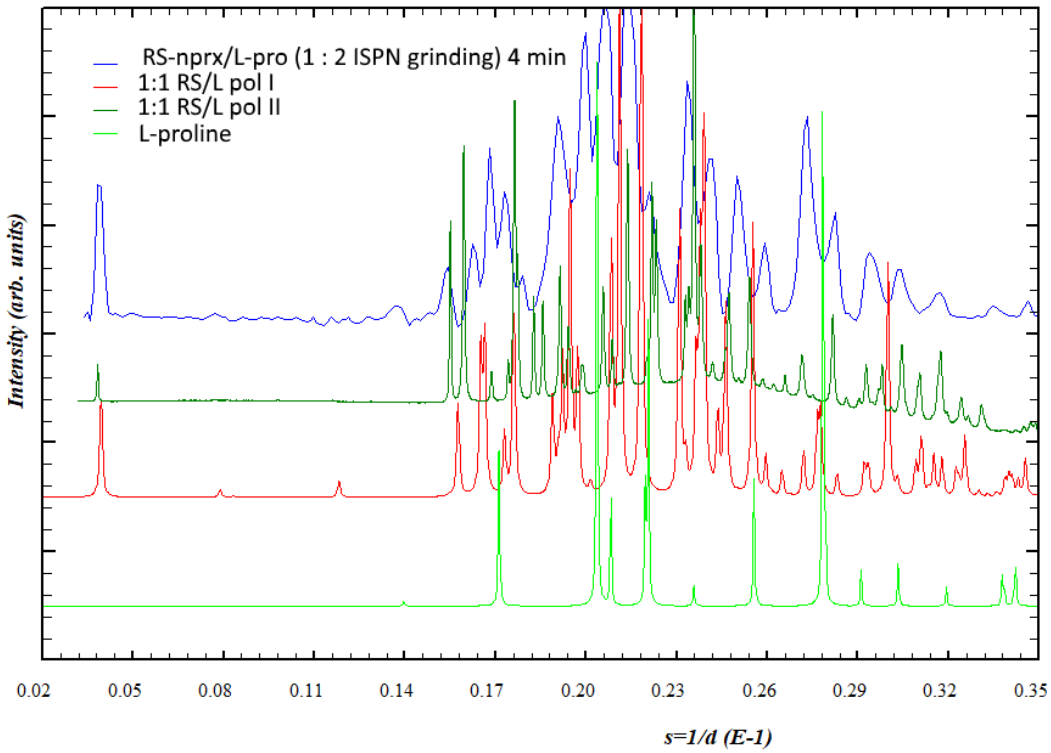

(*b*)

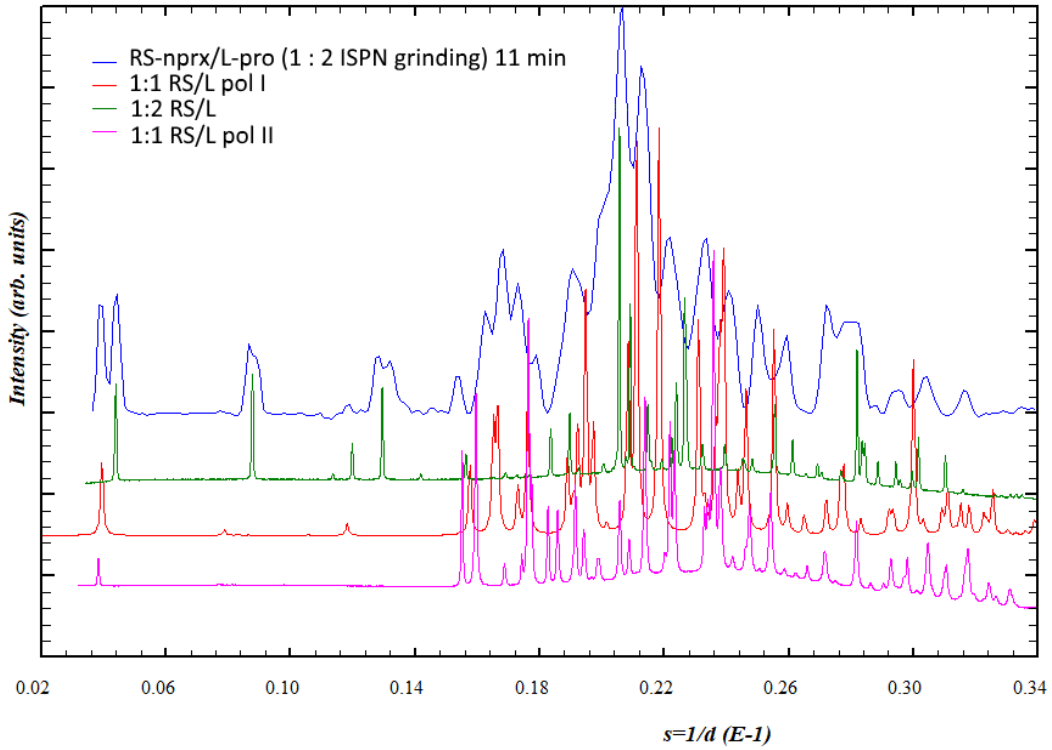
RS-nprx/L-pro (1 : 2 ISPN grinding) 11 min
1:1 RS/L pol I
1:2 RS/L
1:1 RS/L pol II
Intensity (arb. units)
0.02
0.06
0.10
0.14
0.18
0.22
0.26
0.30
0.34
s=1/d (E-1)

(*c*)

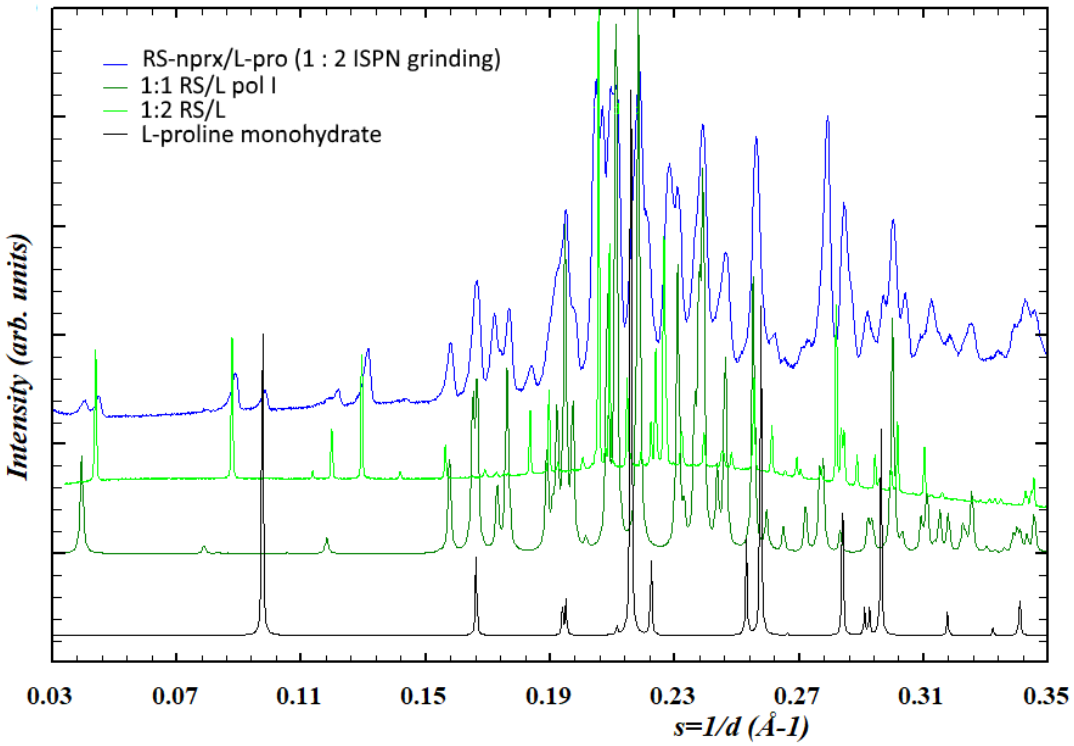
RS-nprx/L-pro (1 : 2 ISPN grinding)
1:1 RS/L pol I
1:2 RS/L
L-proline monohydrate
Intensity (arb. units)
0.03
0.07
0.11
0.15
0.19
0.23
0.27
0.31
0.35
s=1/d (Å-1)

(*d*)

Figure S3.1.10. Diffraction pattern measured for the final powder obtained in the *in-situ* ball-milling experiment for the **RS/L** sample, 1 : 2 MeOH-LAG (sample *14* in Table S3.1); the diffraction patterns of the pure phases were simulated from the structures

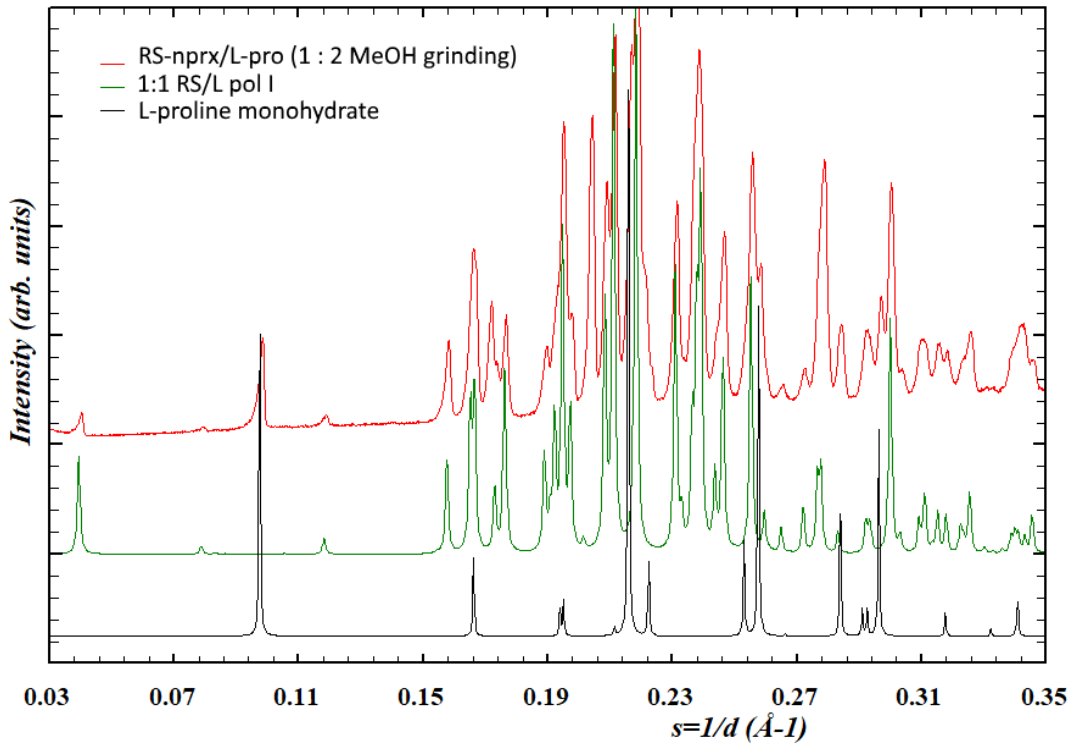

Figure S3.1.11. Diffraction patterns measured for the final powders obtained in the *in-situ* ball-milling experiments for the **RS/L** system, 1 : 1 MeOH-, EtOH-, ISPN, and ACN-LAG (sample *9-12* in Table S3.1); the diffraction patterns of the pure phases were simulated from the structures

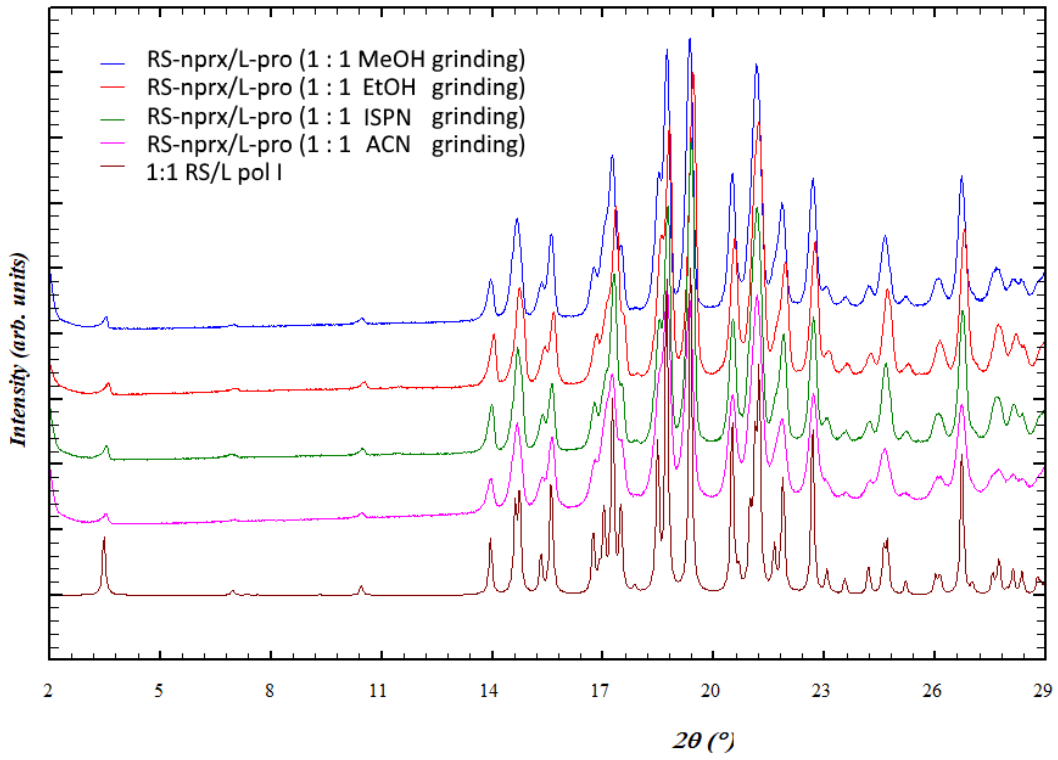

Figure S3.1.12. Selected diffraction patterns from the *in-situ* ball-milling experiment for the **RS/DL** sample, 1 : 1 MeOH-LAG (sample *15* in Table S3.1); the diffraction patterns of the pure phases were simulated from the structures. First frame measured within 30 seconds as reaction started.

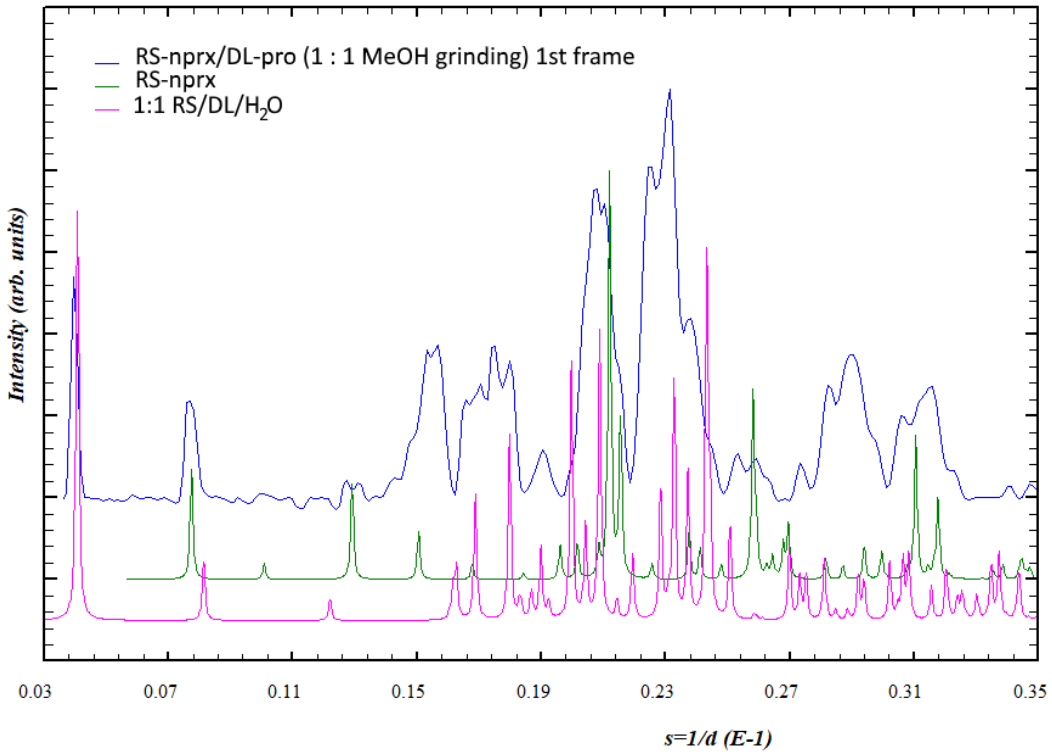

Figure S3.1.13. Selected diffraction patterns from the *in-situ* ball-milling experiment for the **RS/DL** sample, 1 : 2 MeOH-LAG (sample *17* in Table S3.1); the diffraction patterns of the pure phases were simulated from the structures. (*a*) –first frame measured within 30 seconds as reaction started; (*b*) – at the 1st minute of reaction; (*c*) – at the 15th minute of reaction

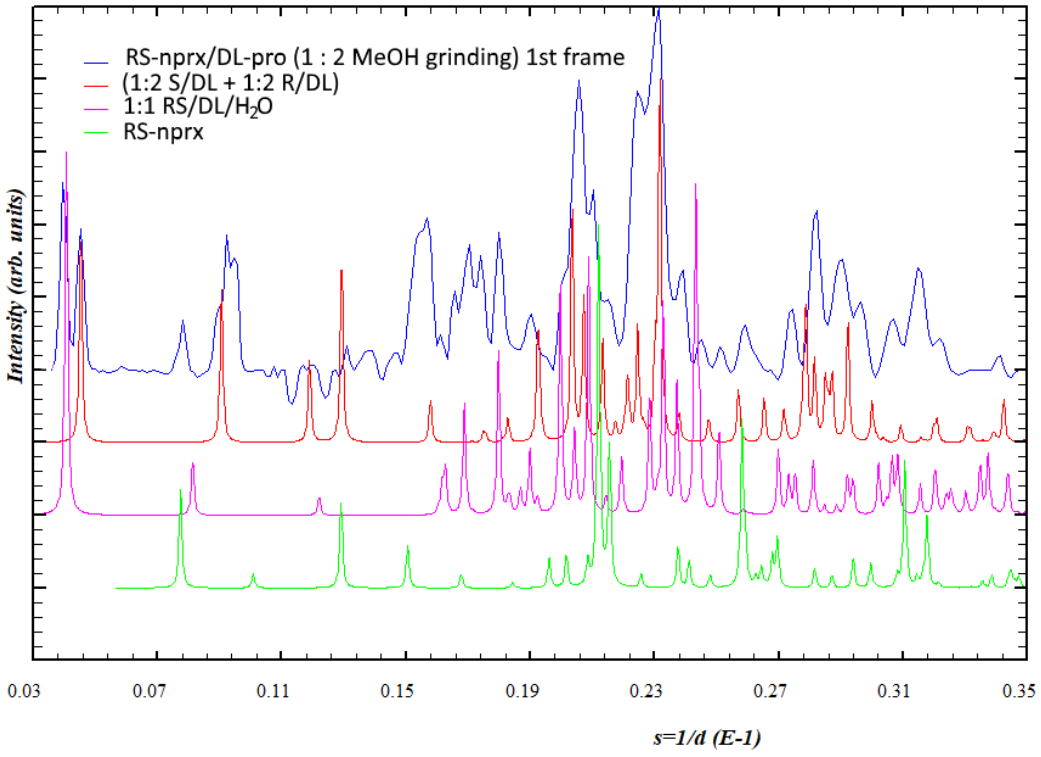

(*a*)

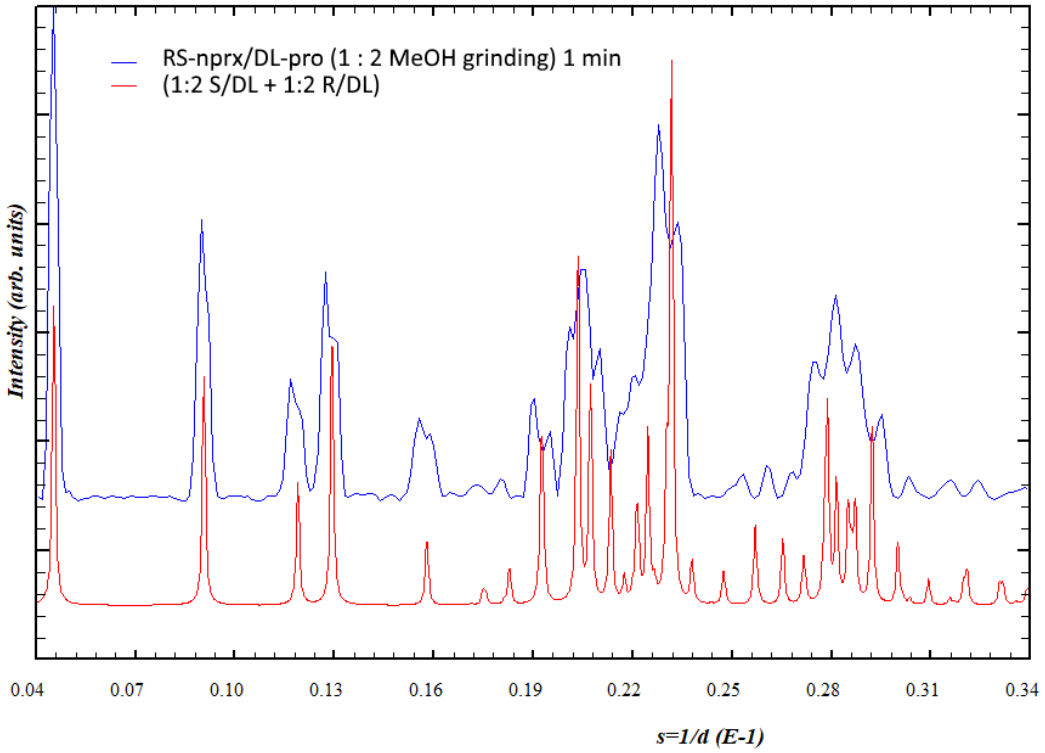
RS-nprx/DL-pro (1 : 2 MeOH grinding) 1 min
(1:2 S/DL + 1:2 R/DL)
Intensity (arb. units)
0.04
0.07
0.10
0.13
0.16
0.19
0.22
0.25
0.28
0.31
0.34
s=1/d (E-1)

(*b*)

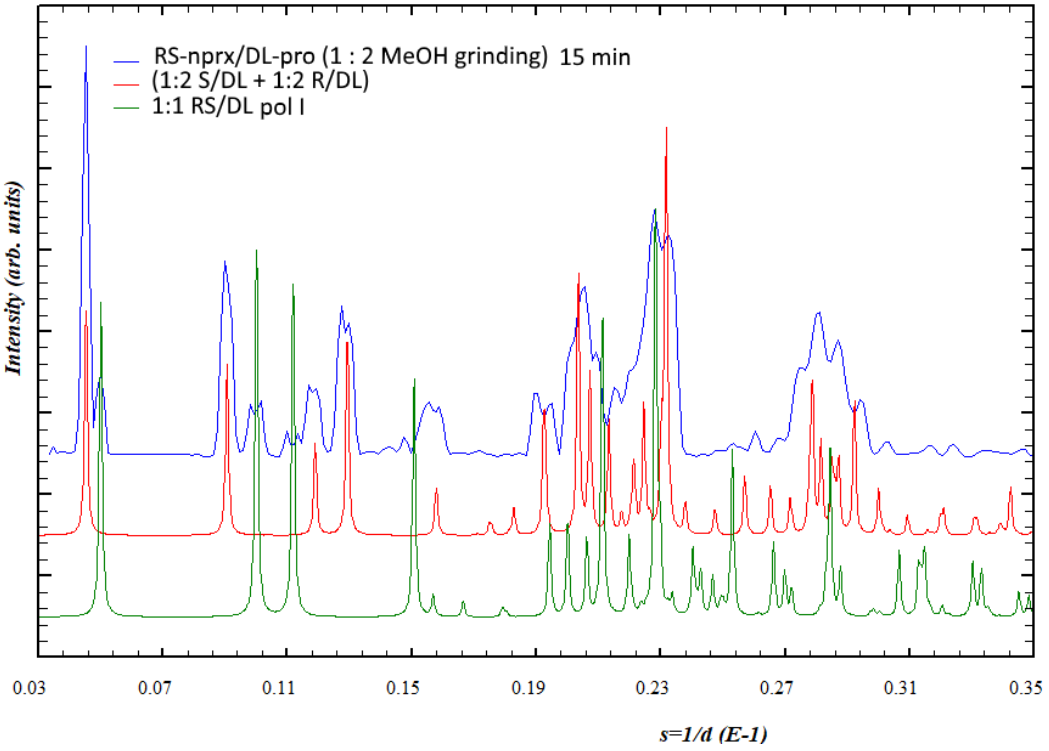
RS-nprx/DL-pro (1 : 2 MeOH grinding) 15 min
(1:2 S/DL + 1:2 R/DL)
1:1 RS/DL pol I
Intensity (arb. units)
0.03
0.07
0.11
0.15
0.19
0.23
0.27
0.31
0.35
s=1/d (E-1)

(*c*)

Figure S3.1.14. Selected diffraction patterns from the *in-situ* ball-milling experiment for the **RS/DL** sample, 1 : 2 ISPN-LAG (sample *18* in Table S3.1); the diffraction patterns of the pure phases were simulated from the structures. (*a*) –first frame measured within 30 seconds as reaction started; (*b*) – at the 1st minute of reaction; (*c*) – at the 15th minute of reaction; (*d*) – PXRD pattern of the resultant powder measured at a laboratory diffractometer (Cu*K*α radiation)

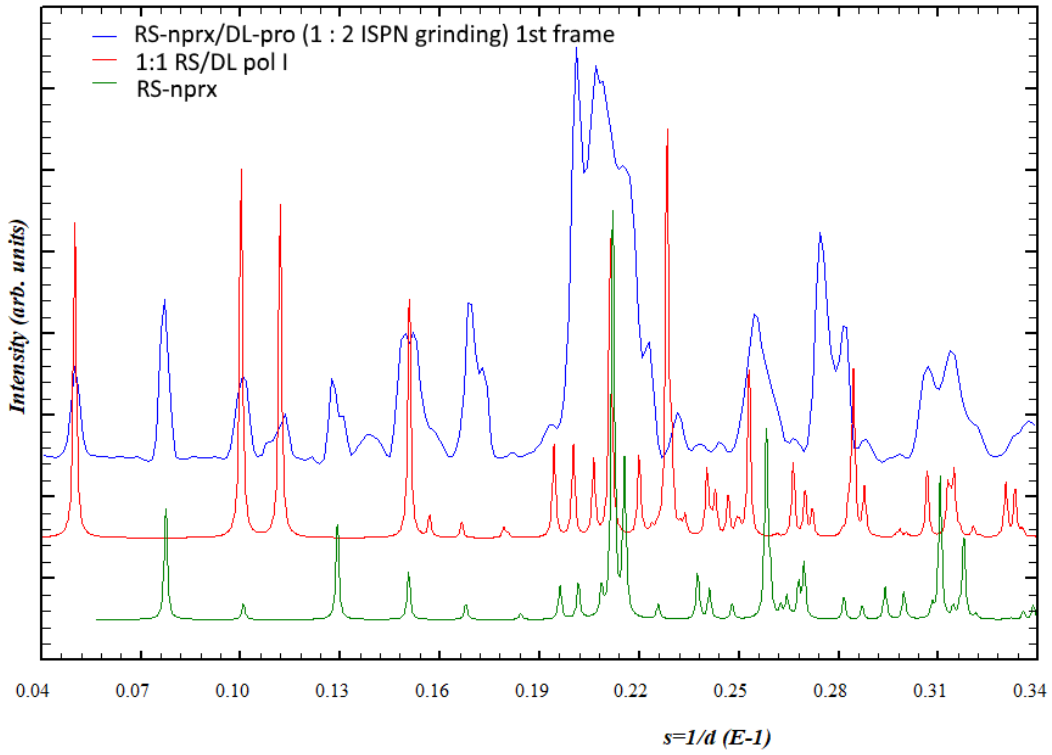

(*a*)

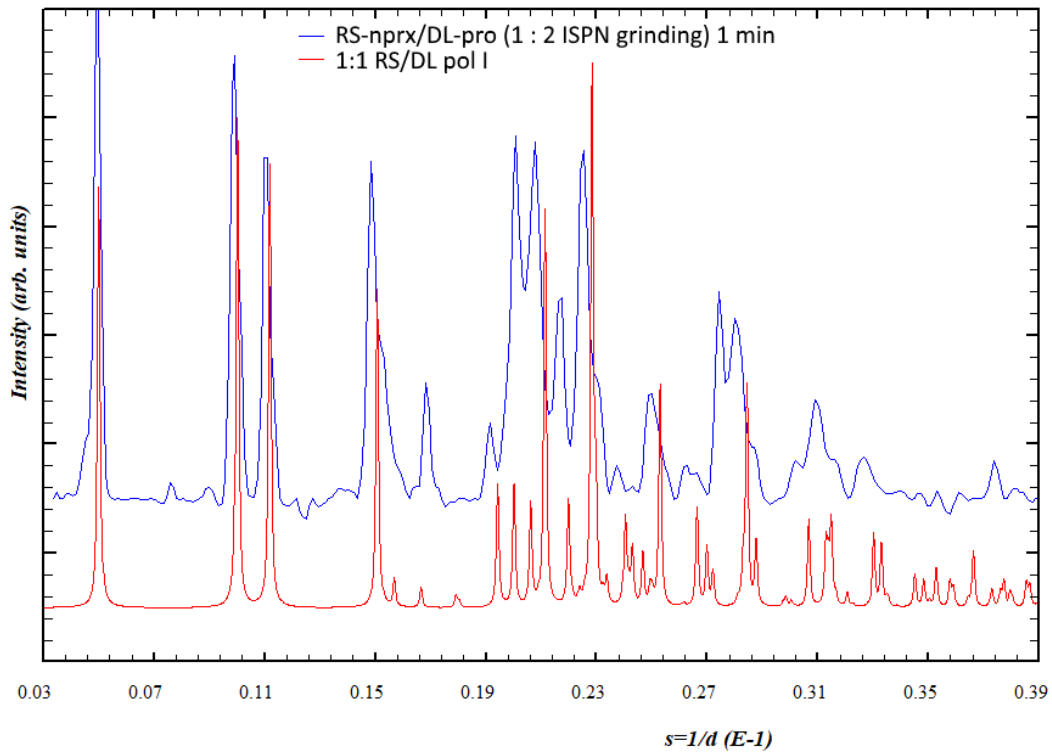

(*b*)

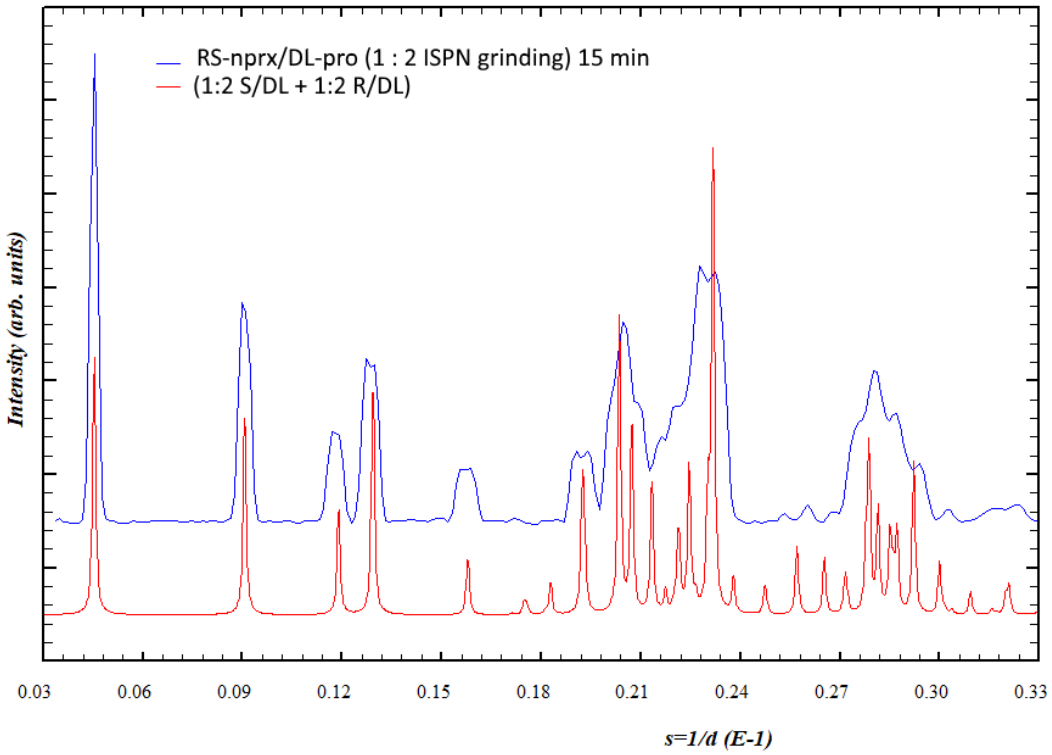
RS-nprx/DL-pro (1 : 2 ISPN grinding) 15 min
(1:2 S/DL + 1:2 R/DL)
Intensity (arb. units)
0.03
0.06
0.09
0.12
0.15
0.18
0.21
0.24
0.27
0.30
0.33
s=1/d (E-1)

(*c*)

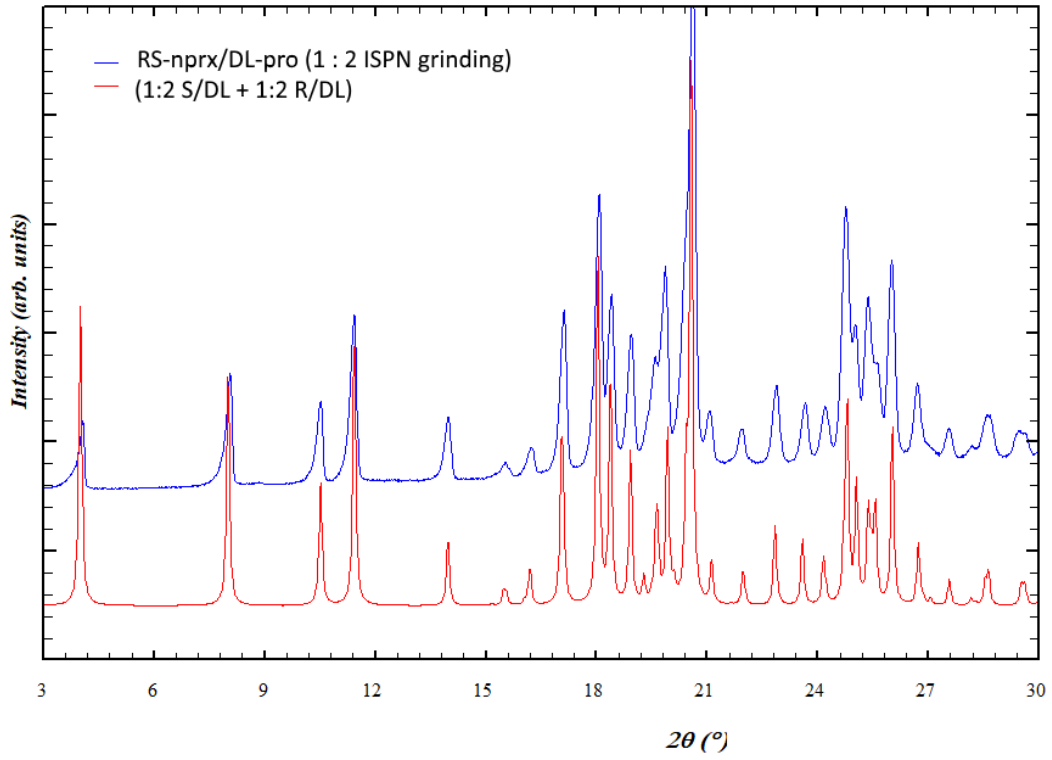
RS-nprx/DL-pro (1 : 2 ISPN grinding)
(1:2 S/DL + 1:2 R/DL)
Intensity (arb. units)
3
6
9
12
15
18
21
24
27
30
2θ (°)

(*d*)

Figure S3.1.15. Selected diffraction patterns from the *in-situ* ball-milling experiment for the **S/DL** sample, 1 : 1 MeOH-LAG (sample 5 in Table S3.1); the diffraction patterns of the pure phases were simulated from the structures. (*a*) –first frame measured within 30 seconds as reaction started; (*b*) – at the 15th minute of reaction

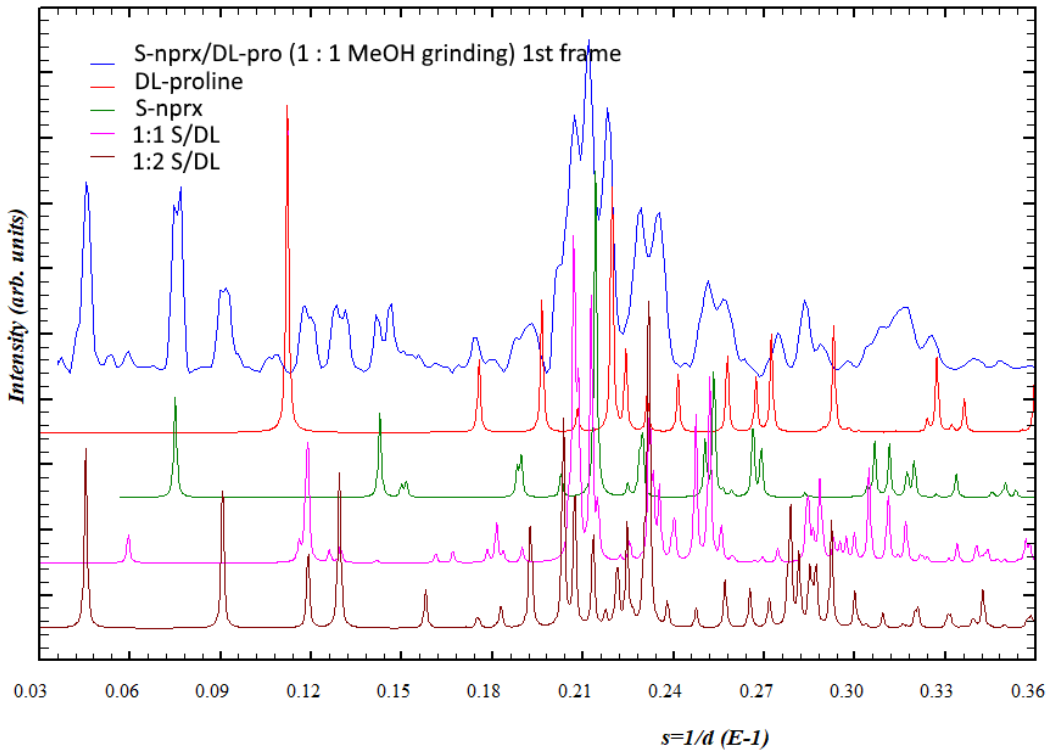

(*a*)

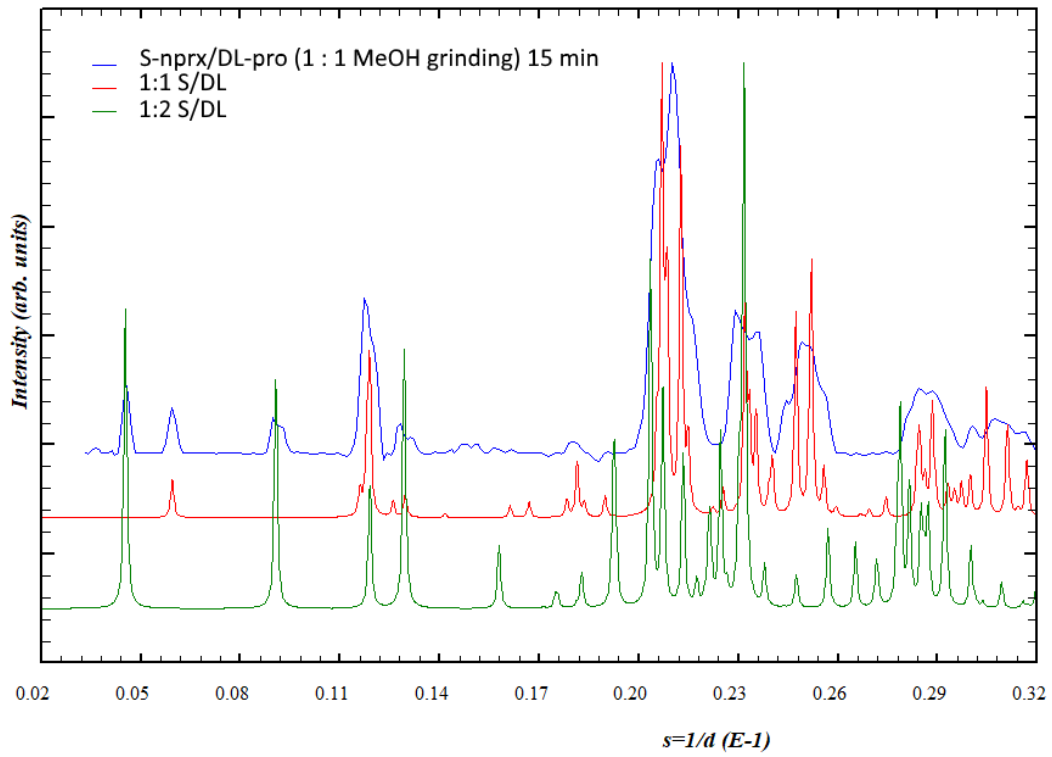

(*b*)

Figure S3.1.16. Selected diffraction patterns from the *in-situ* ball-milling experiment for the **S/DL** sample, 1 : 1 EtOH-LAG (sample *6* in Table S3.1); the diffraction patterns of the pure phases were simulated from the structures. (*a*) –first frame measured within 30 seconds as reaction started; (*b*) – at the 1st minute of reaction; (*c*) – at the 15th minute of reaction

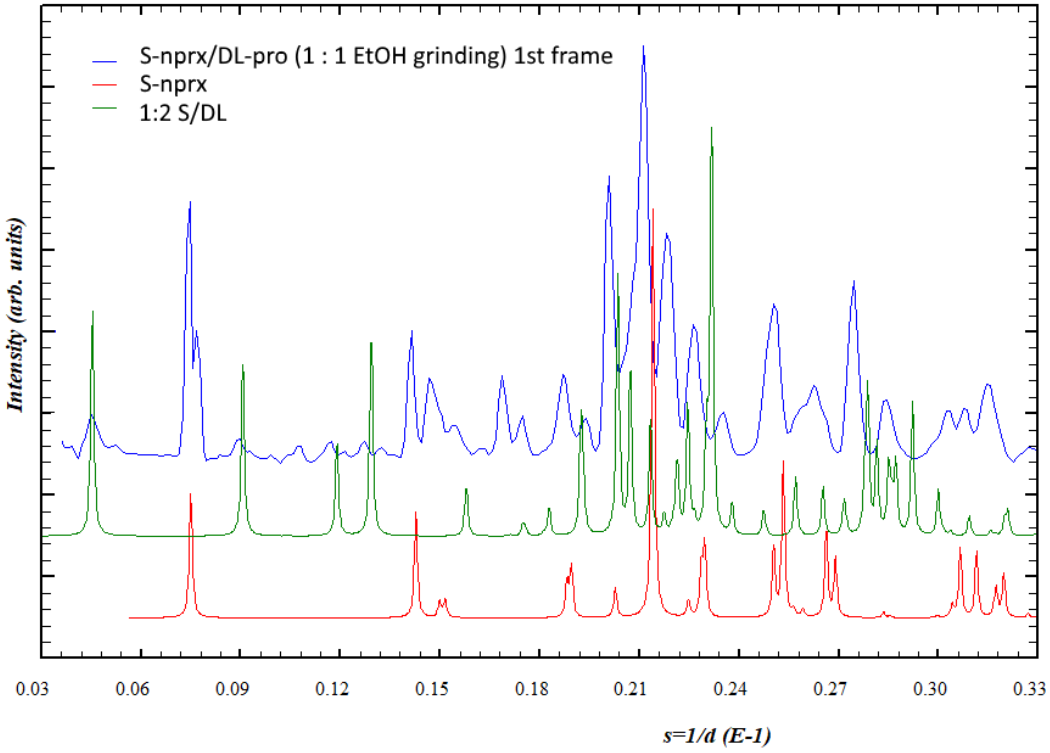

(*a*)

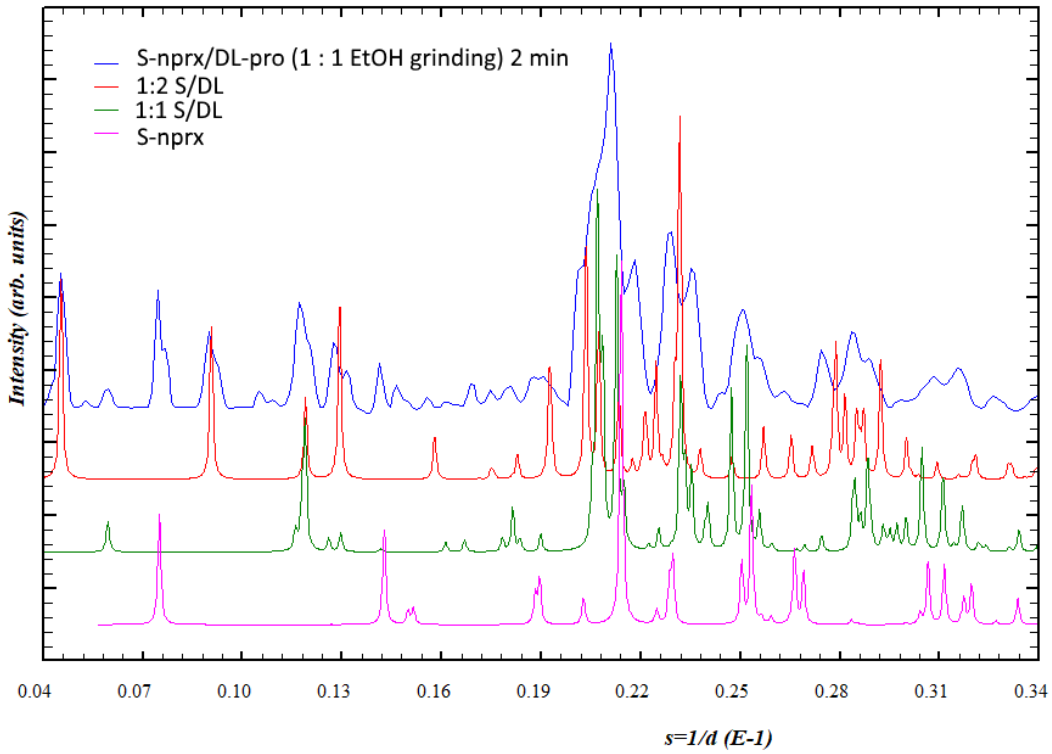

(*b*)

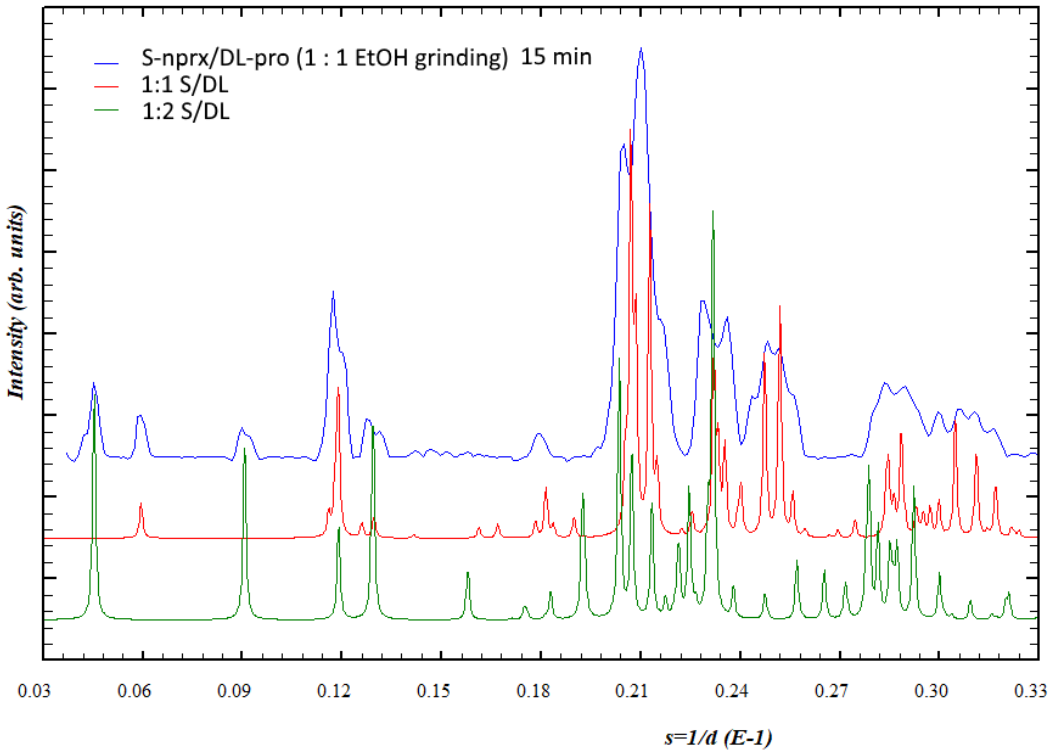

(*c*)

Figure S3.1.17. Diffraction patterns measured for the final powders obtained in the *in-situ* ball-milling experiments for the **S/DL** system, 1 : 1 MeOH-, EtOH-, ISPN, and ACN-LAG (sample *5-8* in Table S3.1); the diffraction patterns of the pure phases were simulated from the structures

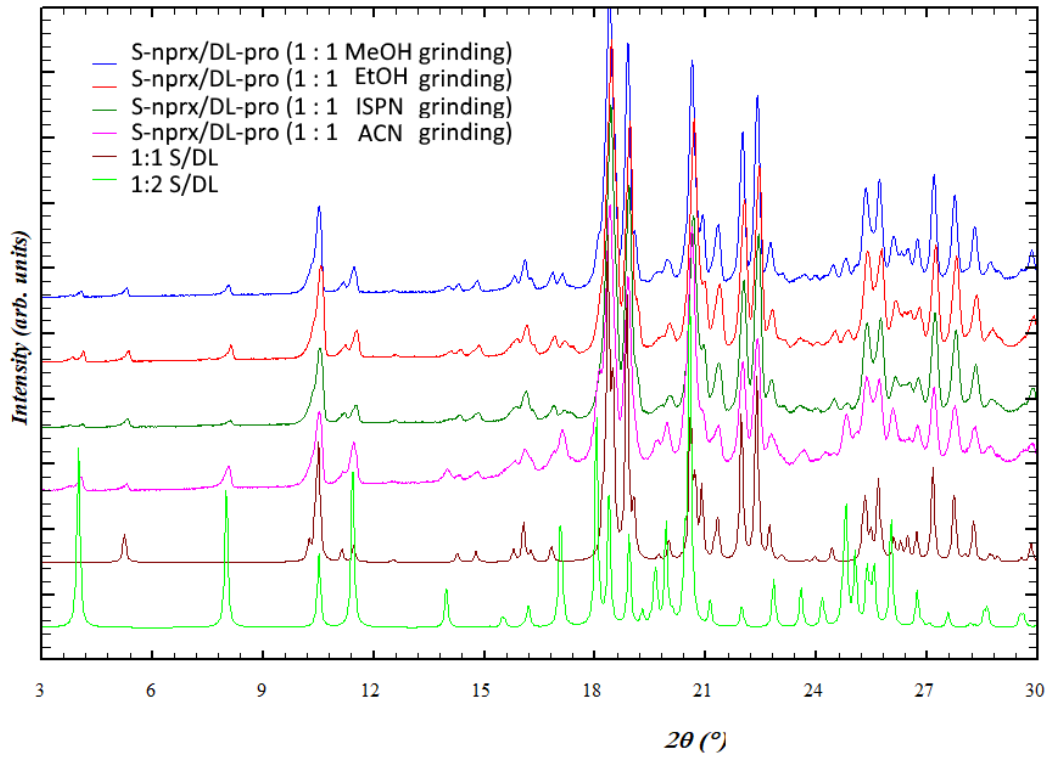

Figure S3.1.18. *In-situ* ball-milling X-ray diffraction patterns for the **RS/L** system, λ = 1 Å, 1:2 ratio, ISPN-LAG. Colored bands on the right side of each image represent the presence of phases and are shown only for illustrative purpose

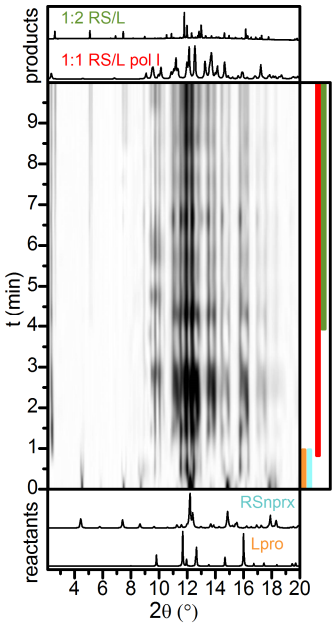

4. Details of LAG experiments and sample analysis for the S/L system (Table S4.1)

Table S4.1 Experimental details for laboratory liquid-assisted grinding and further analysis of obtained S-naproxen/L-proline cocrystals; lab XRD was performed at Cu*K*α radiation

	Molar ratio S-Nprx/L-Pro	Grinding conditions	PXRD analysis	Result	Structures determined from PXRD	Other analysis
1	1 : 1	60 min, 30 Hz, 2 μL MeOH	Synchrotron (λ = 0.708 Å) under variable temperature	Initial sample contained a mixture of 1:1 S/L pol I and 1:1 S/L pol II Upon heating 1:1 S/L pol I disappears first, then the disappearance of the 1:1 S/L pol II is followed by the emergence of 2:3 S/L **(Fig. S4.1.1)**		DSC (**Fig. S4.3.1**)
2	1 : 2	60 min, 30 Hz, 10 μL MeOH	Lab XRD	2:3 S/L **(Fig. S4.2.2)**		
3	2 : 1	60 min, 30 Hz, 2 μL MeOH	Lab XRD	1:1 S/L pol I + S-nprx **(Fig. S4.2.3)**		
4	2 : 3	60 min, 30 Hz, 10 μL MeOH	Lab XRD	2:3 S/L + L-proline monohydrate **(Fig. S4.2.4)**		
5	1 : 1	60 min, 30 Hz, 10 μL EtOH	Synchrotron (λ = 0.62127 Å) under variable temperature	Initial sample contained 1:1 S/L pol I Upon heating 1:1 S/L pol disappears, Followed by the emergence of a mixture of 2:3 S/L and unknown phase II, Upon further heating unknown phase II disappears and only 2:3 S/L is left **(Fig. 3** in the main text)		DSC (**Fig. S4.3.2**)
6	1 : 2	60 min, 30 Hz, 10 μL EtOH	Lab XRD	2:3 S/L **(Fig. S4.2.2)**		
7	2 : 1	60 min, 30 Hz, 10 μL EtOH	Lab XRD	1:1 S/L pol I + 1:1 S/L pol II + S-nprx **(Fig. S4.2.5)**		
8	2 : 3	60 min, 30 Hz, 10 μL EtOH	Lab XRD	2:3 S/L + 1:1 S/L pol I **(Fig. S4.2.6)**		
9	1 : 1	60 min, 30 Hz, 10 μL ISPN	Synchrotron (λ = 0.62127 Å)	1:1 S/L pol II + 1:1 S/L pol I **(Fig. S4.2.7)**		DSC (**Fig. S4.3.3**)

10	1 : 2	60 min, 30 Hz, 10 μL ISPN	Synchrotron (λ = 0.62127 Å)	2:3 S/L **(Fig. S4.2.1)**		DSC (determined the melting point of the **2:3 S/L** phase, T_m **= 181(1)°C**) (**Fig. S4.3.4**)
11	2 : 1	60 min, 30 Hz, 10 μL ISPN	Lab XRD	1:1 S/L pol II + S-nprx **(Fig. S4.2.8)**		
12	2 : 3	60 min, 30 Hz, 10 μL ISPN	Synchrotron (λ = 0.708 Å)	2:3 S/L + 1:1 S/L pol II + 1:1 S/L pol I + 1:2 S/L L-proline **(Fig. S4.2.9)**		
13	1 : 1	60 min, 30 Hz, 2 μL ACN	Synchrotron (λ = 0.708 Å) under variable temperature	Initial sample contained a mixture of 1:1 S/L pol I and 1 : 1 S/L pol II Upon heating 1:1 S/L pol I melts first, then 1:1 S/L pol II disappears as well followed by the emergence of 2:3 S/L (**Fig. 2** in the main text)	1:1 S/L pol II (for Rietveld refinement see **Fig. S2.1**)	DSC (**Fig. S4.3.5**)
14	1 : 2	60 min, 30 Hz, 10 μL ACN	Lab XRD	2:3 S/L **(Fig. S4.2.1)**		
15	2 : 1	60 min, 30 Hz, 2 μL ACN	Lab XRD	1:1 S/L pol II + S-nprx **(Fig. S4.2.10)**		
16	2 : 3	60 min, 30 Hz, 10 μL ACN	Lab XRD	2:3 S/L + 1:1 S/L pol II **(Fig. S4.2.11)**		
17	1 : 1	60 min, 30 Hz, 2 μL H_2O	Lab XRD	1:1 S/L pol II **(Fig. S4.2.12)**		
18	1 : 2	60 min, 30 Hz, 10 μL H_2O	Lab XRD	1:2 S/L + 2:3 S/L + L-proline + S-nprx **(Fig. S4.2.13)**		
19	2 : 3	60 min, 30 Hz, 10 μL H_2O	Lab XRD	1:1 S/L pol I + 1:1 S/L pol II + S-nprx **(Fig. S4.2.14)**		

4.1 PXRD upon varied temperature for the S/L system (Fig. S4.1.1)

Figure S4.1.1 PXRD patterns measured *in situ* upon heating (from 38 to 166 °C, 2 °C/min) for the **S/L** sample prepared by 1:1 MeOH-LAG (sample *1* in Table S4.1), λ = 0.708 Å: (left) film representation; (right) XRD patterns at selected temperatures: *T* = 38 °C – **1:1 S/L pol I** (marked as '*') and **1:1 S/L pol II**; *T* = 117 °C – **1:1 S/L pol II**; and *T* = 140 °C – **2:3 S/L**.

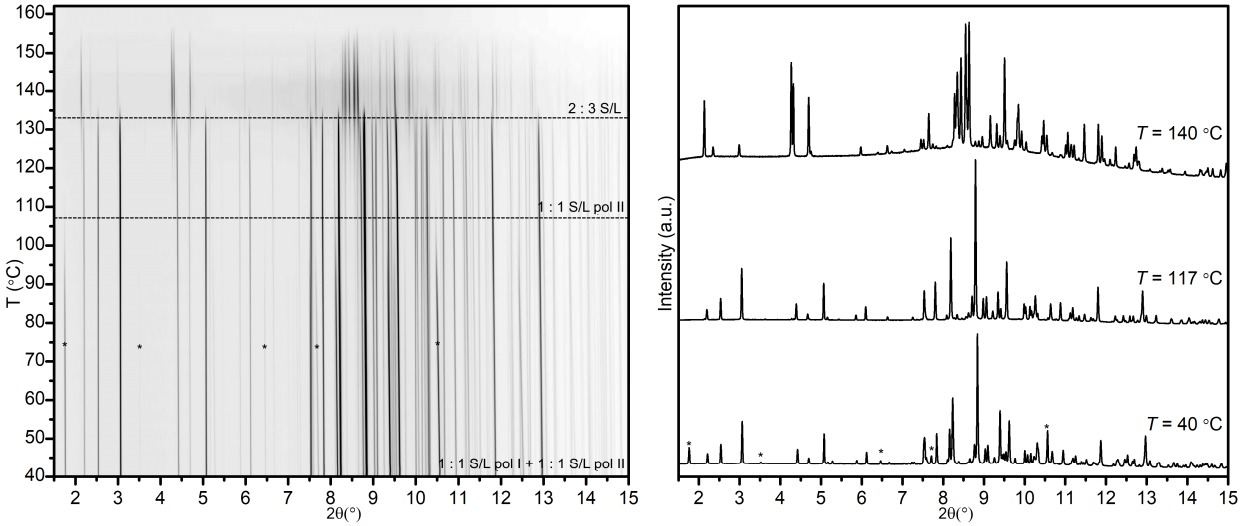

4.2 PXRD analysis of the S/L samples (Figs. S4.2.1-S4.2.14)

Figure S4.2.1 Rietveld refinement plot for the **S/L** sample obtained by 1 : 2 ISPN-LAG (sample *10* in Table S4.1); percentages are given in wt %; red and blue patterns represent calculated and experimental data, respectively; grey line corresponds to the difference profile; and blue and black marks below represent Bragg positions for **2:3 S/L** and **L-proline**, respectively; unit cell, profile parameters, zero point and positions of molecules were refined

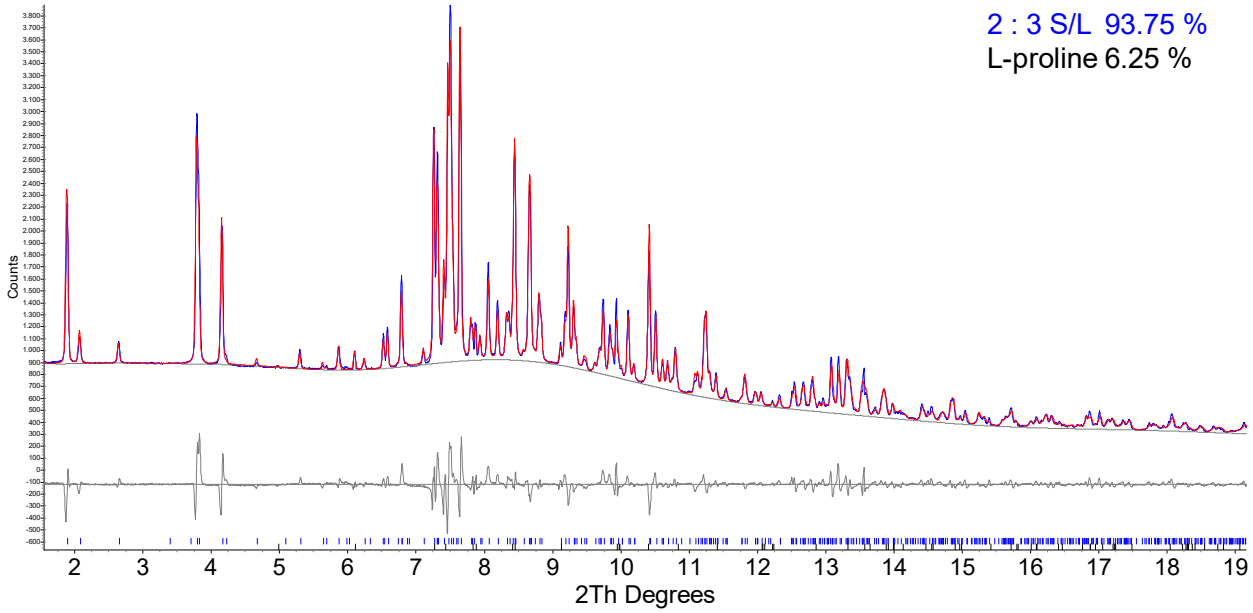

Figure S4.2.2. Diffraction patterns for the **S/L** samples prepared by 1 : 2 MeOH-, EtOH-, ACN-, and ISPN-LAG (samples *2*, *6*, *10*, and *14* in Table S4.1); the diffraction pattern for **2:3 S/L** cocrystal was simulated from the structure

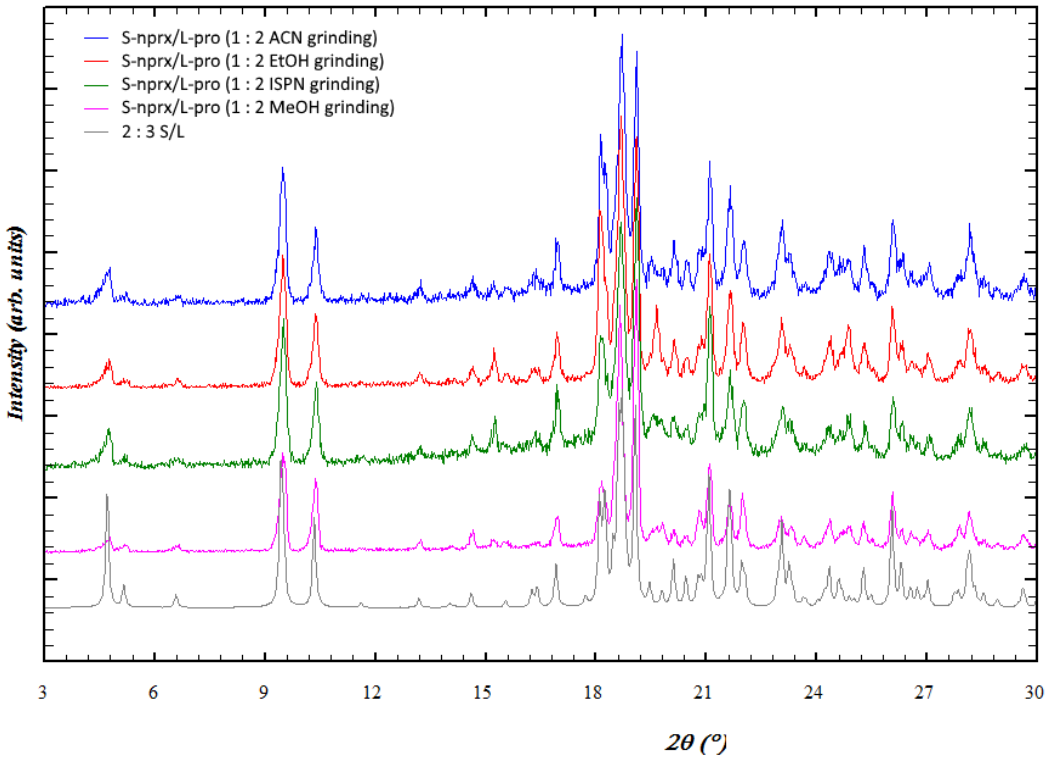

Figure S4.2.3. Diffraction pattern for the **S/L** sample prepared by 2 : 1 MeOH-LAG (sample *3* in Table); the diffraction patterns of the pure phases were simulated from the structures

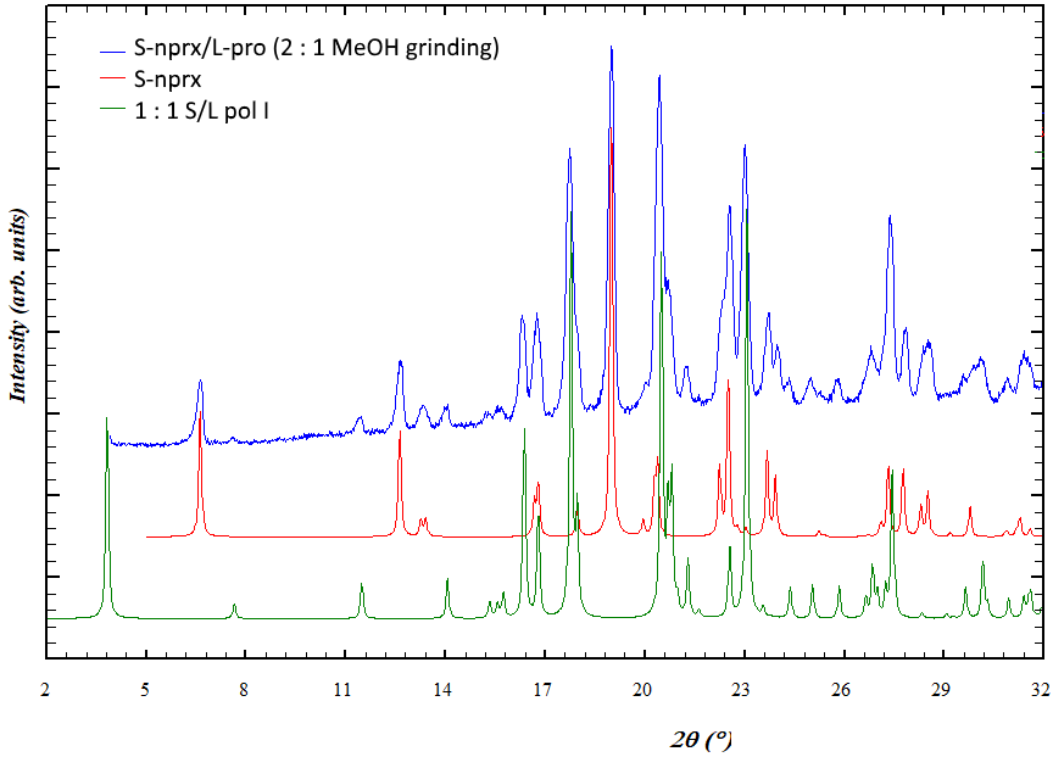

Figure S4.2.4. Diffraction pattern for the **S/L** sample prepared by 2 : 3 MeOH-LAG (sample *4* in Table S4.1); the diffraction patterns of the pure phases were simulated from the structures

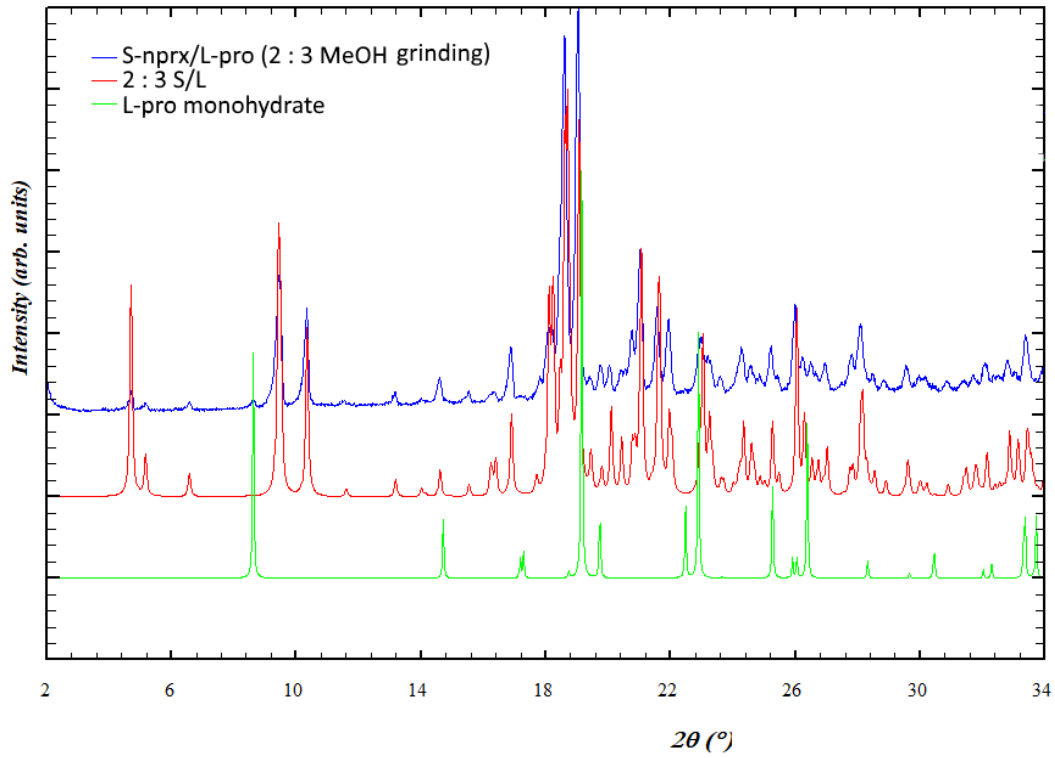

Figure S4.2.5. Diffraction pattern for the **S/L** sample prepared by 2 : 1 EtOH-LAG (sample *7* in Table S4.1); the diffraction pattern of pure **1:1 S/L pol I** and **S-nprx** were simulated from the structures and the diffraction pattern of pure **1:1 S/L pol II** corresponds to the synchrotron data measured for sample *13* (Table S4.1)

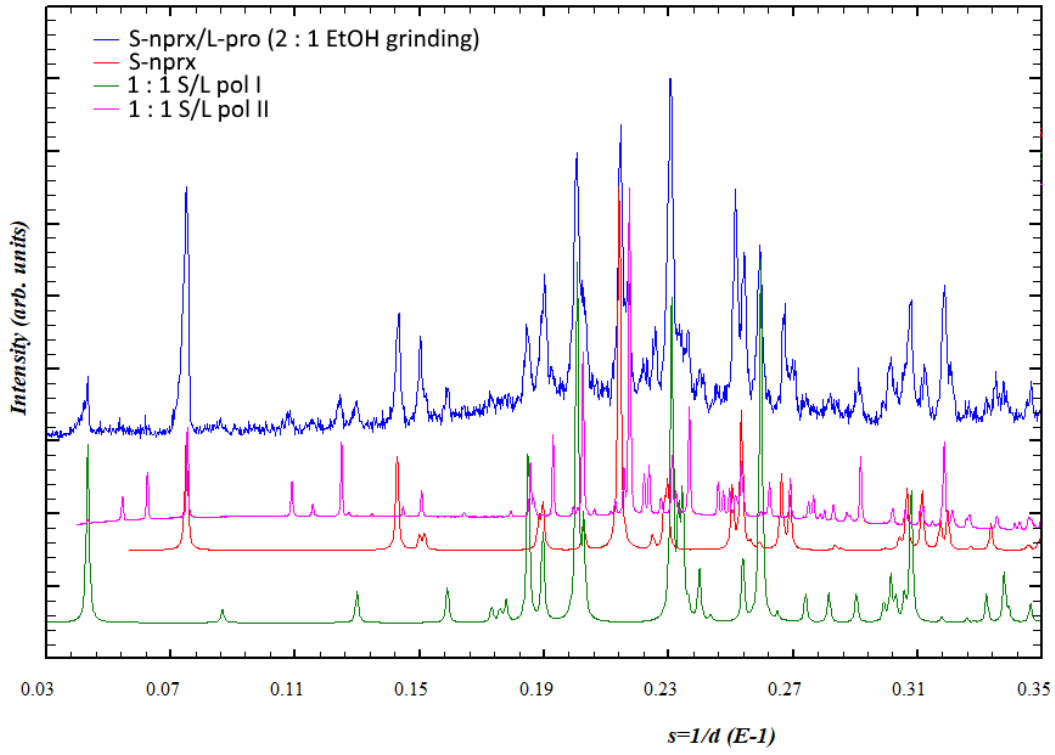

Figure S4.2.6. Diffraction pattern for the **S/L** sample prepared by 2 : 3 EtOH-LAG (sample *8* in Table S4.1); the diffraction patterns of pure **2:3 S/L** phase was simulated from the structure and the diffraction pattern of pure **1:1 S/L pol II** corresponds to the synchrotron data measured for sample *13* (Table S4.1)

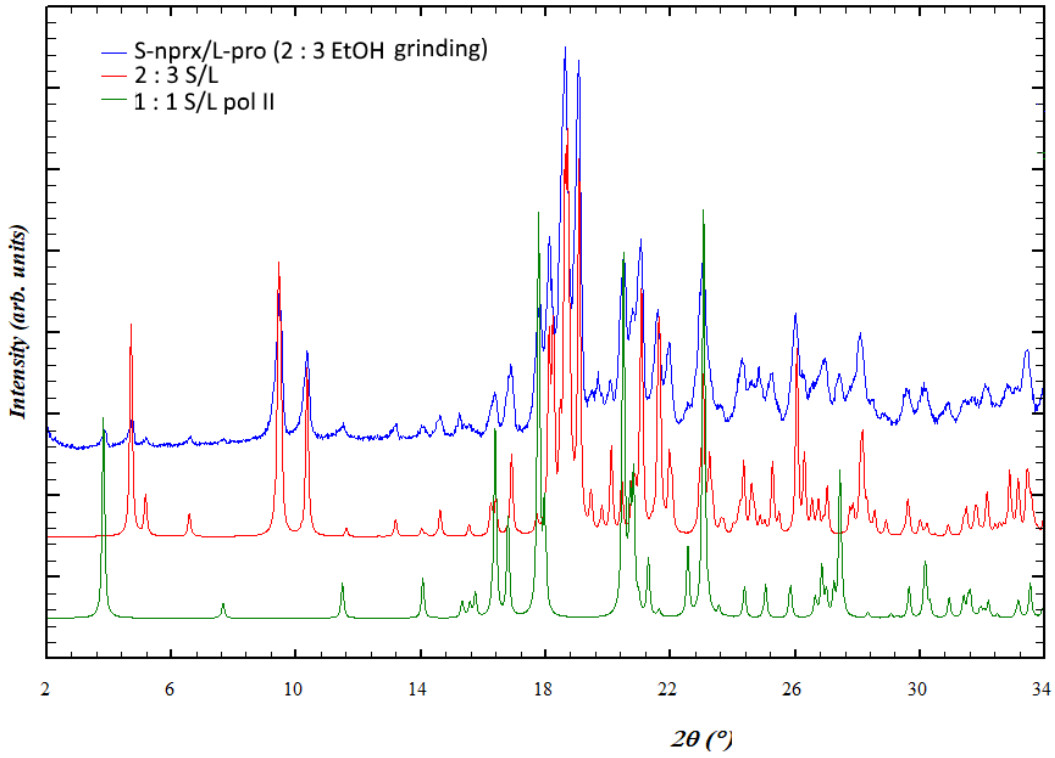

Figure S4.2.7. Diffraction pattern for the **S/L** sample prepared by 1 : 1 ISPN-LAG (sample *9* in Table S4.1); the diffraction patterns of pure **1:1 S/L pol I** phase was simulated from the structure and the diffraction pattern of pure **1:1 S/L pol II** corresponds to the synchrotron data measured for sample *13* (Table S4.1)

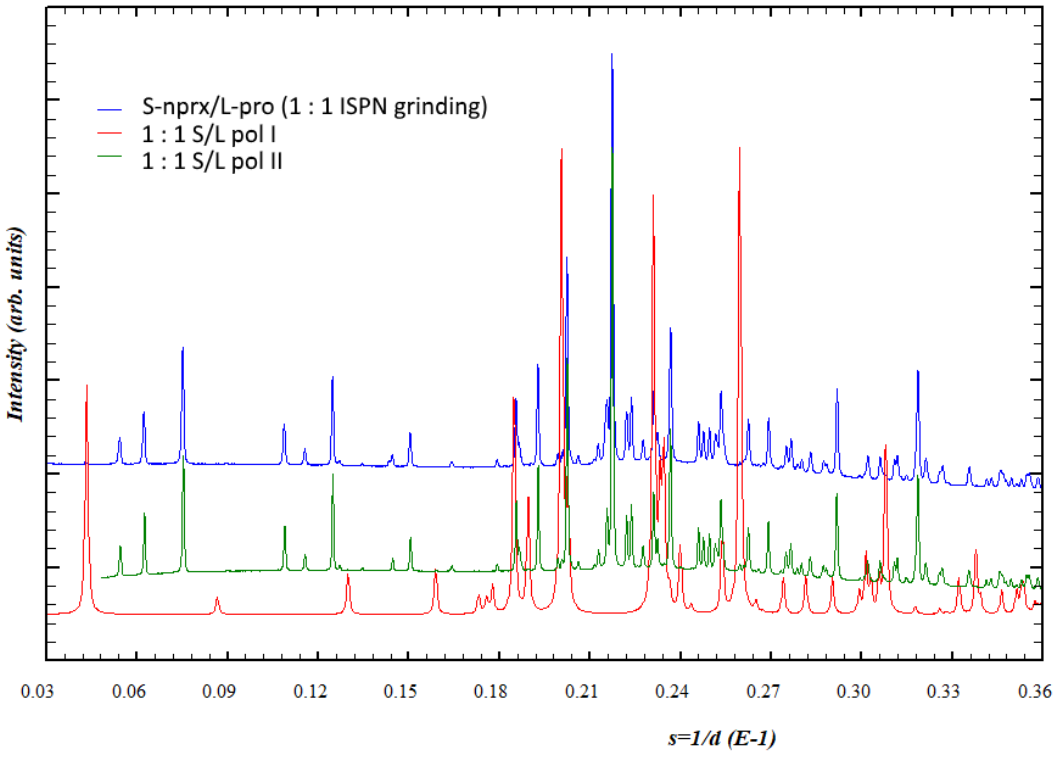

Figure S4.2.8. Diffraction pattern for the **S/L** sample prepared by 2 : 1 ISPN-LAG (samples *11* in Table S4.1); the diffraction patterns of pure **S-nprx** was simulated from the structure and the diffraction pattern of pure **1:1 S/L pol II** corresponds to the synchrotron data measured for sample *13* (Table S4.1)

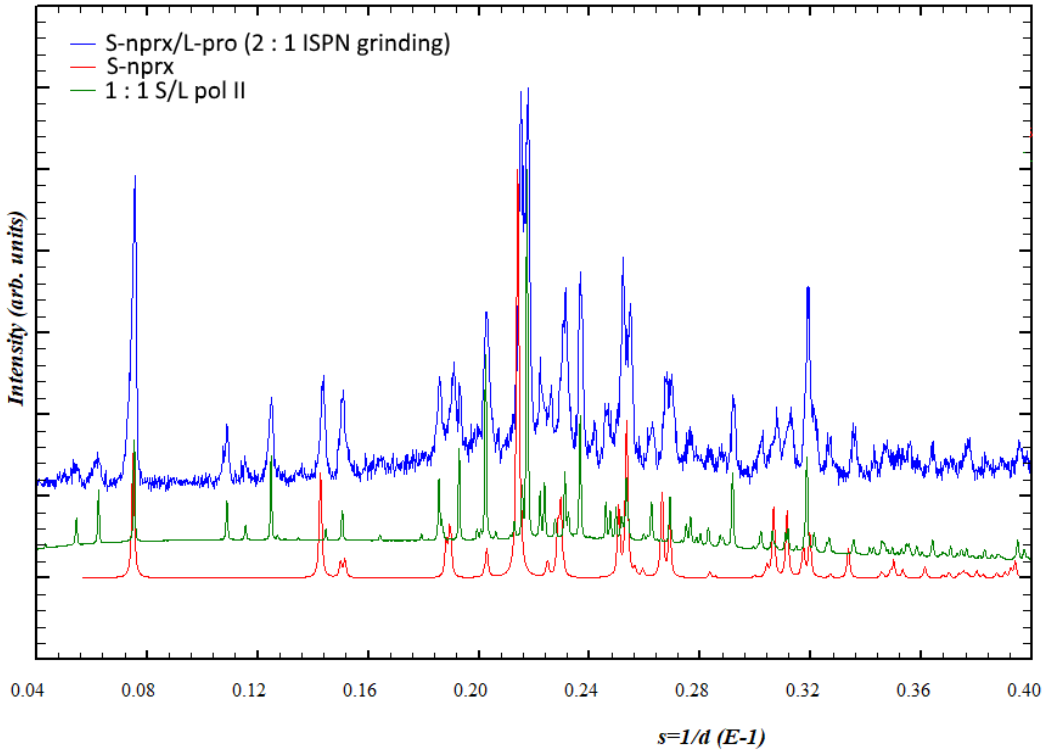

Figure S4.2.9. Diffraction pattern for the **S/L** sample prepared by 2:3 ISPN-LAG (samples *12* in Table S4.1); the diffraction patterns of the pure phases were simulated from the structures, except that the diffraction pattern of pure **1:1 S/L pol II** corresponds to the synchrotron data measured for sample *13* (Table S4.1)

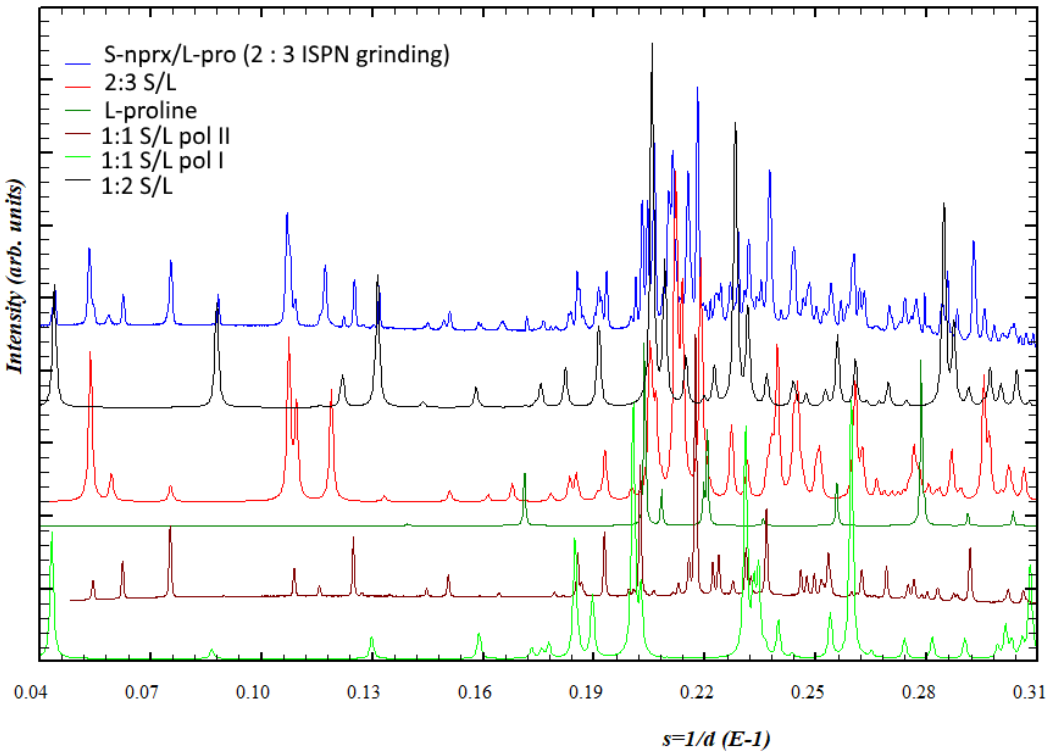

Figure S4.2.10. Diffraction pattern for the **S/L** sample prepared by 2 : 1 ACN-LAG (sample *15* in Table S4.1); the diffraction patterns of the pure phases were simulated from the structures

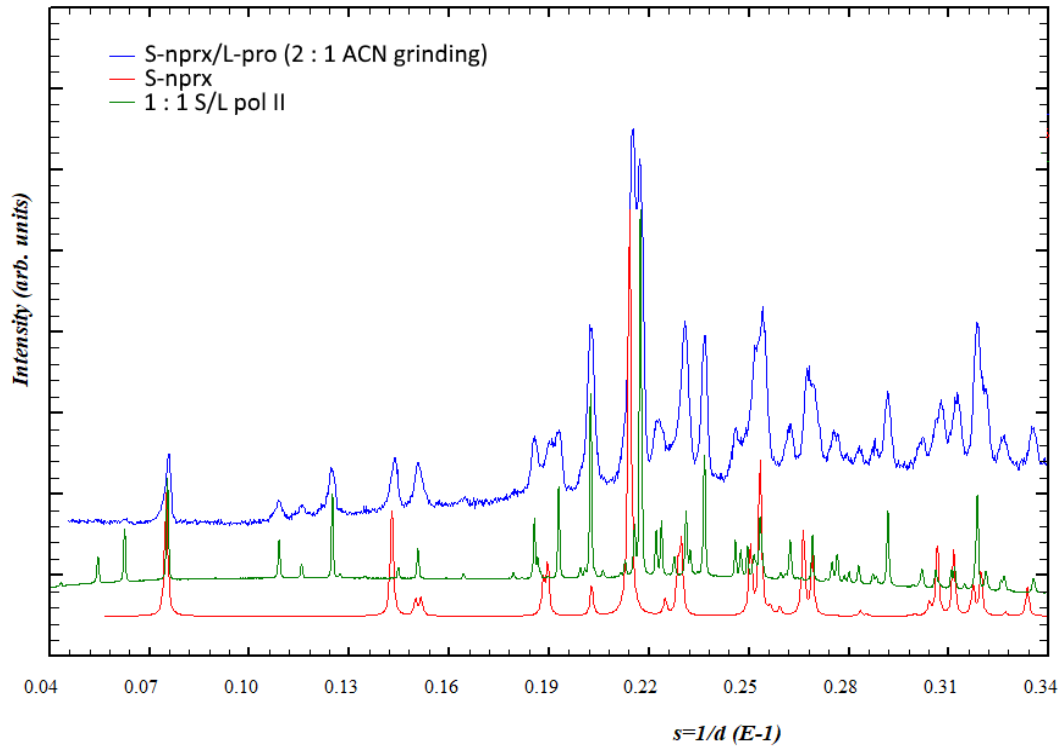

Figure S4.2.11. Diffraction pattern for the **S/L** sample prepared by 2 : 3 ACN-LAG (sample *16* in Table S4.1); the diffraction patterns of pure **2:3 S/L** phase was simulated from the structure and the diffraction pattern of pure **1:1 S/L pol II** corresponds to the synchrotron data measured for sample *13* (Table S4.1)

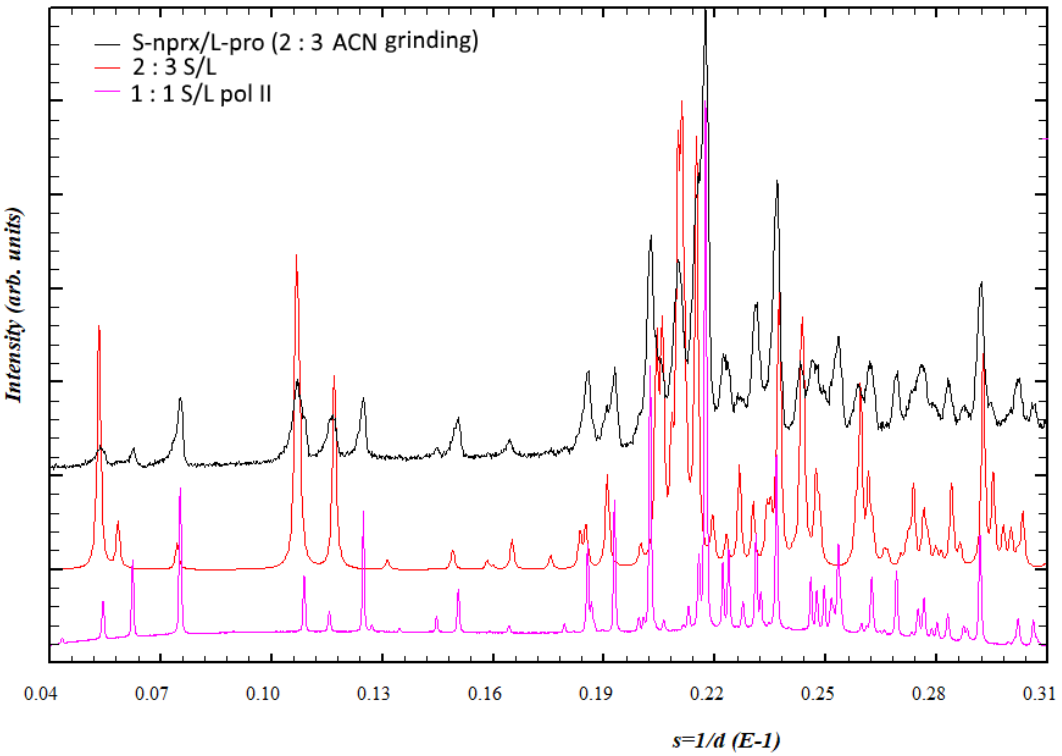

Figure S4.2.12. Diffraction pattern for the **S/L** sample prepared by 1 : 1 water-LAG (sample *17* in Table S4.1); the diffraction pattern of pure **1:1 S/L pol II** corresponds to the synchrotron data measured for sample *13* (Table S4.1)

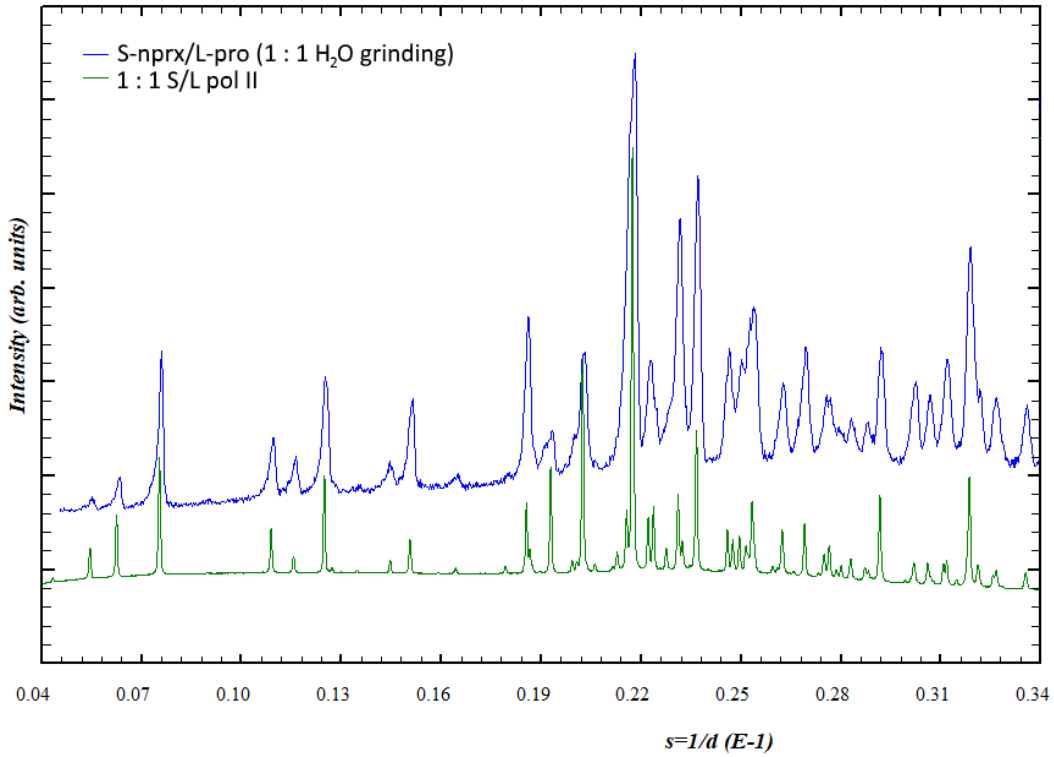

Figure S4.2.13. Diffraction pattern for the **S/L** sample prepared by 1 : 2 water-LAG (sample *18* in Table S4.1); the diffraction patterns of the pure phases were simulated from the structures

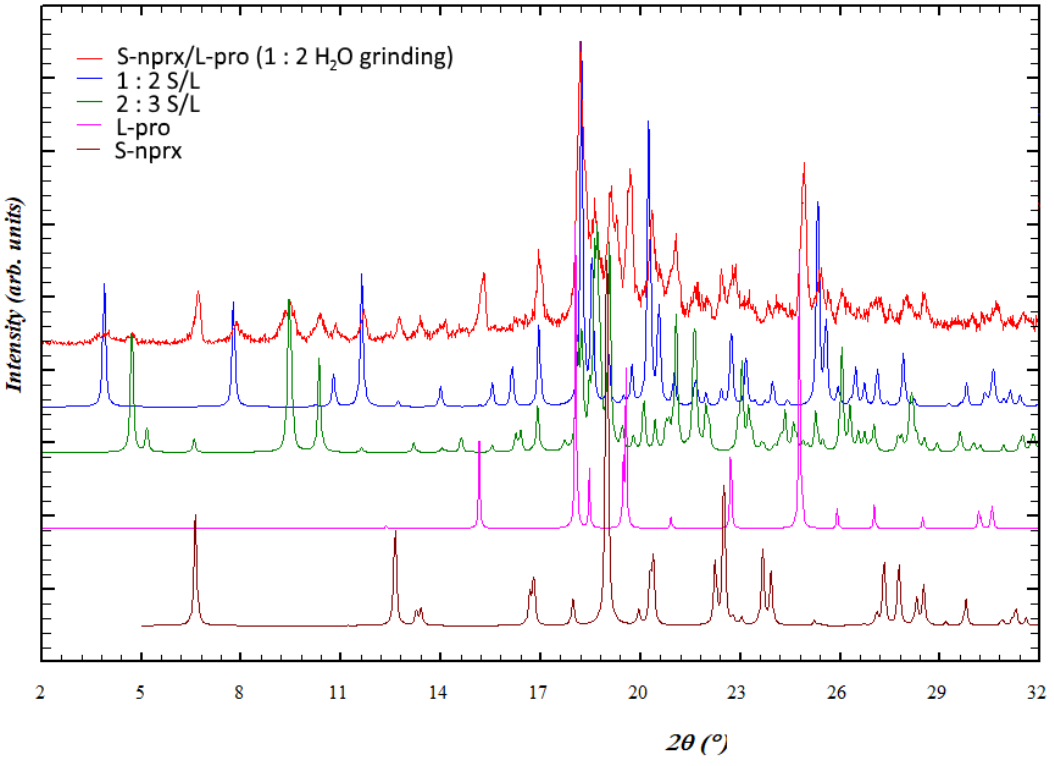

Figure S4.2.14. Diffraction pattern for the **S/L** sample prepared by 2 : 3 water-LAG (samples *19* in Table S4.1); the diffraction pattern of pure **1:1 S/L pol I** and **S-nprx** were simulated from the structures and the diffraction pattern of pure **1:1 S/L pol II** corresponds to the synchrotron data measured for sample *13* (Table S4.1)

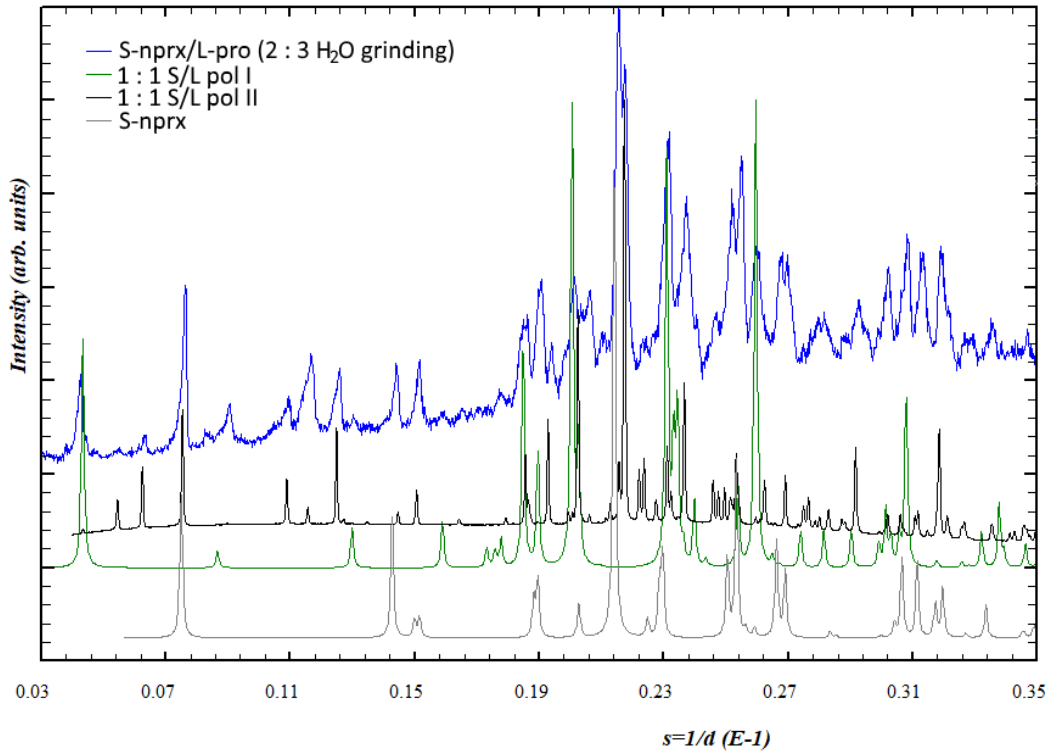

4.3 DSC data measured for selected S/L samples (Figs. S4.3.1-S4.3.5)

Figure S4.3.1. DSC curve measured for the **S/L** sample prepared by 1:1 MeOH-LAG (sample *1* in Table S4.1). The curve has multiple peaks, suggesting the presence of multiple phases.

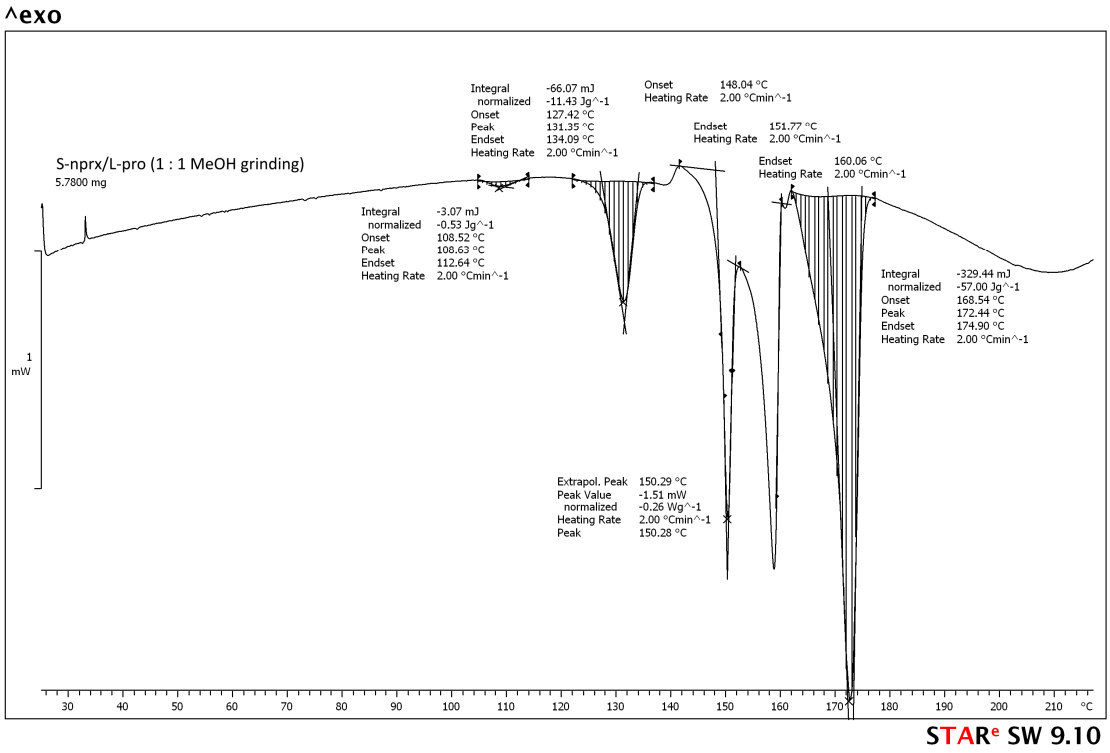

Figure S4.3.2. DSC curve measured for the **S/L** sample prepared by 1:1 EtOH-LAG (sample *5* in Table S4.1). The curve has multiple peaks, suggesting the presence of multiple phases.

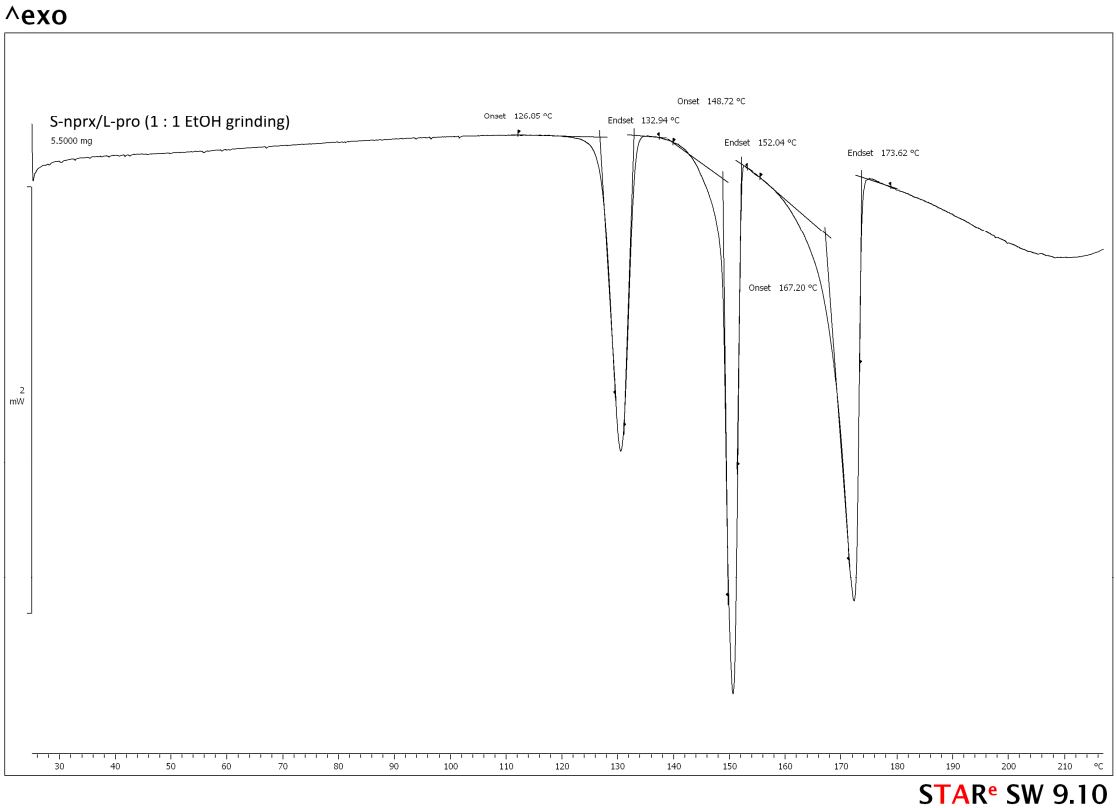

Figure S4.3.3. DSC curve measured for the **S/L** sample prepared by 1:1 ISPN-LAG (sample *9* in Table S4.1). The curve has multiple peaks, suggesting the presence of multiple phases.

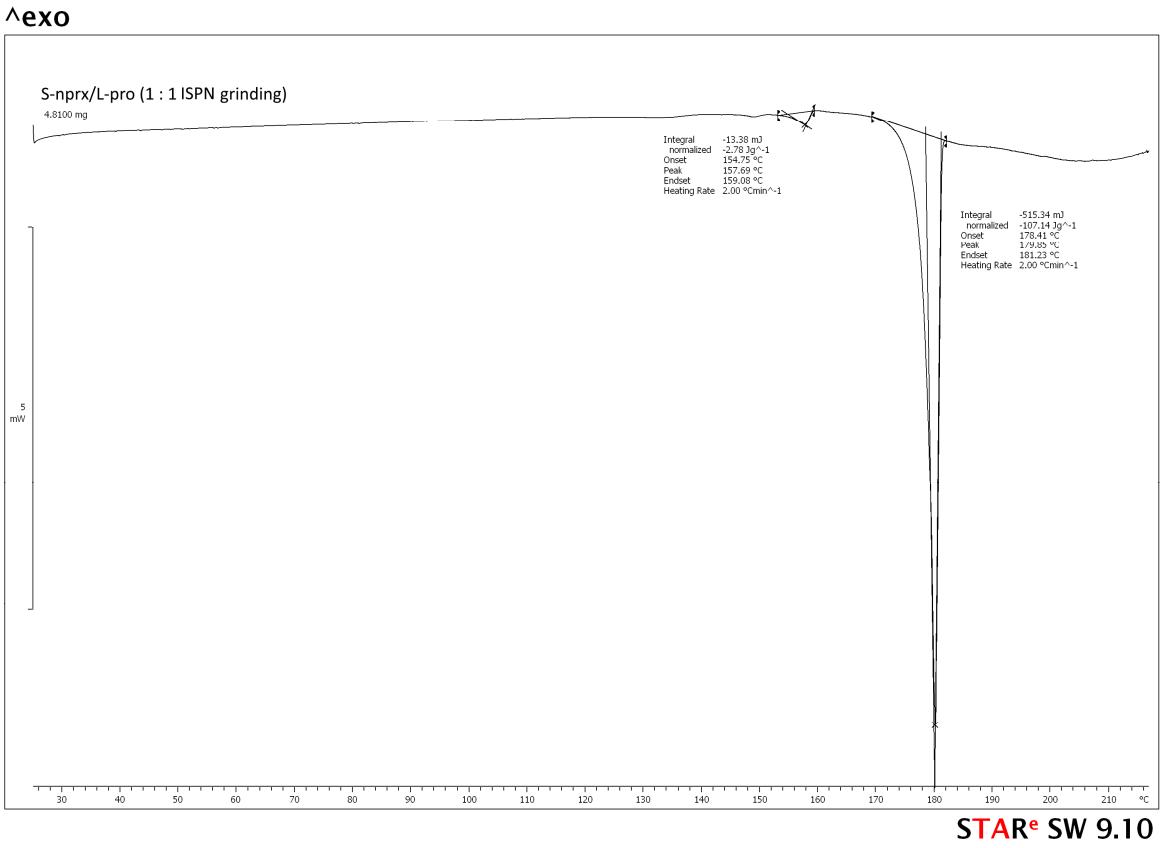

Figure S4.3.4. DSC curve measured for the **S/L** sample prepared by 1:2 ISPN-LAG (sample *10* in Table S4.1). The curve has only one peak, which corresponds to the melting point of the **2:3 S/L** phase.

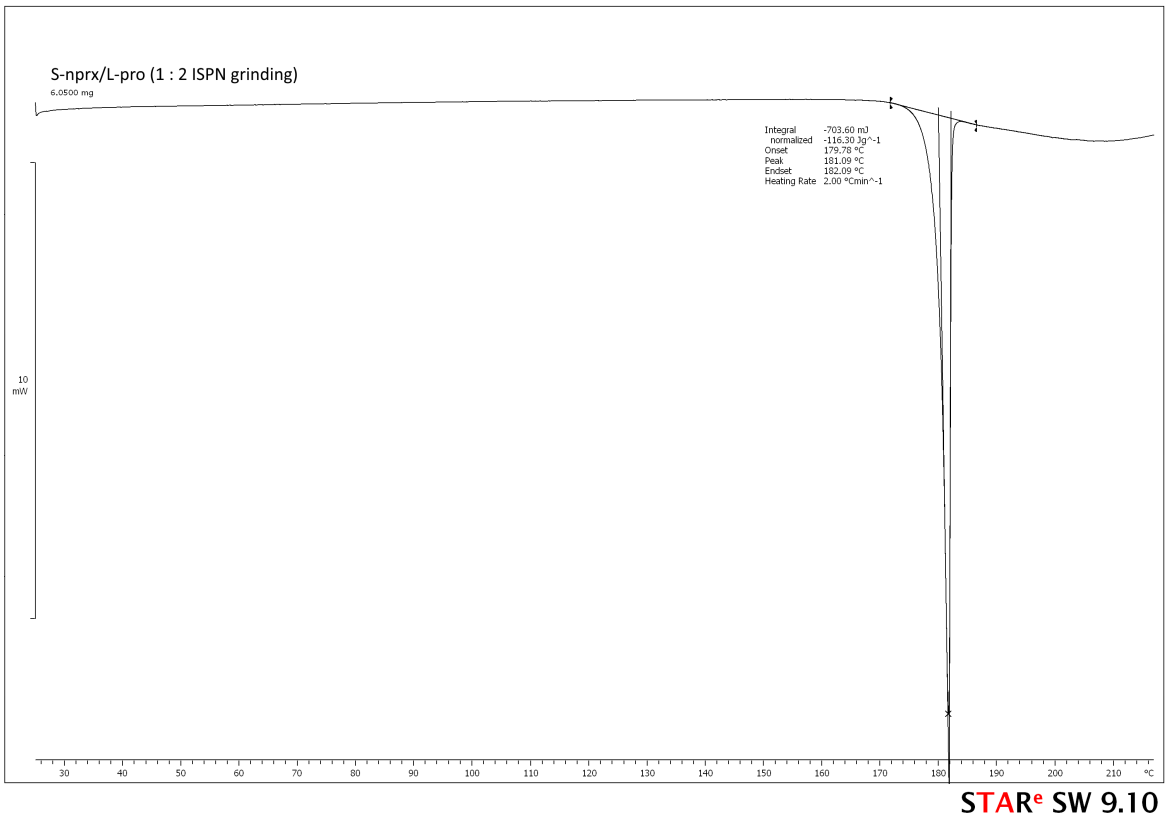

Figure S4.3.5. DSC curve measured for the **S/L** sample prepared by 1:1 ACN-LAG (sample *13* in Table S4.1). The curve has multiple peaks, suggesting the presence of multiple phases.

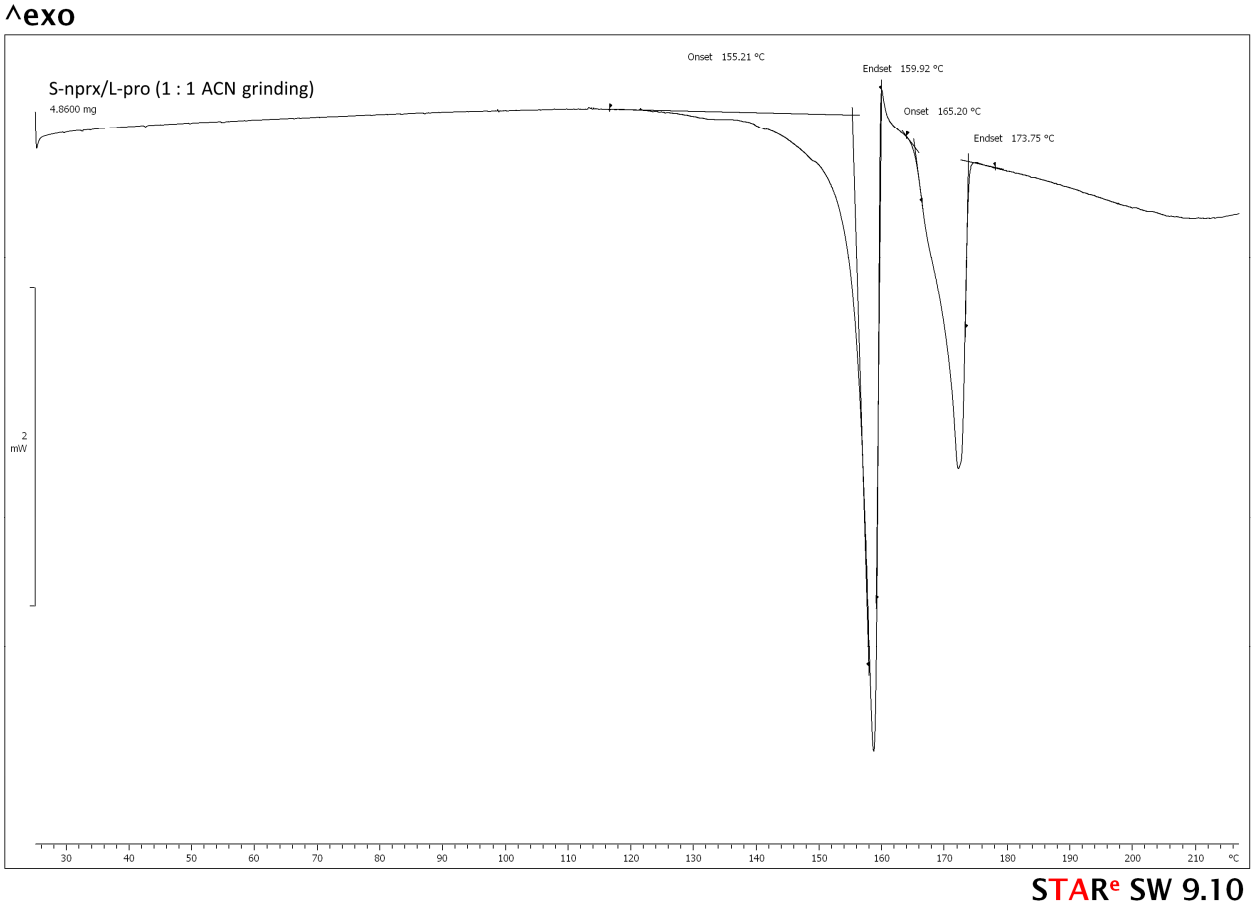

5. Details of LAG experiments and sample analysis for the S/D system (Table S5.1)

Table S5.1 Experimental details for laboratory liquid-assisted grinding and further analysis of obtained S-naproxen/D-proline cocrystals; lab XRD was performed at Cu*K*α radiation

	Molar ratio S-Nprx/D-Pro	Grinding conditions	PXRD analysis	Result	Other analysis
1	1 : 1	60 min, 30 Hz, 2 μL MeOH	Lab XRD	1:1 S/D **(Fig. S5.1.1)**	DSC (determined the melting point of the **1:1 S/D** phase, T_m **= 155(1)°C**) (**Fig. S5.2.1**)
2	1 : 2	60 min, 30 Hz, 10 μL MeOH	Lab XRD	1:1 S/D + D-proline **(Fig. S5.1.2)**	
3	2 : 1	60 min, 30 Hz, 2 μL MeOH	Lab XRD	1:1 S/D + S-naproxen **(Fig. S5.1.3)**	
4	2 : 3	60 min, 30 Hz, 10 μL MeOH	Lab XRD	1:1 S/D + D-proline + D-proline monohydrate **(Fig. S5.1.4)**	
5	1 : 1	60 min, 30 Hz, 10 μL EtOH	Lab XRD	1:1 S/D **(Fig. S5.1.1)**	
6	1 : 2	60 min, 30 Hz, 10 μL EtOH	Lab XRD	1:1 S/D + D-proline **(Fig. S5.1.2)**	
7	2 : 1	60 min, 30 Hz, 10 μL EtOH	Lab XRD	1:1 S/D + S-naproxen **(Fig. S5.1.3)**	
8	2 : 3	60 min, 30 Hz, 10 μL EtOH	Lab XRD	1:1 S/D + D-proline **(Fig. S5.1.4)**	
9	1 : 1	60 min, 30 Hz, 2 μL ISPN	Lab XRD	1:1 S/D **(Fig. S5.1.1)**	
10	1 : 2	60 min, 30 Hz, 10 μL ISPN	Lab XRD	1:1 S/D + D-proline **(Fig. S5.1.2)**	
11	2 : 1	60 min, 30 Hz, 10 μL ISPN	Lab XRD	1:1 S/D + S-naproxen **(Fig. S5.1.3)**	
12	2 : 3	60 min, 30 Hz, 10 μL ISPN	Lab XRD	1:1 S/D + D-proline **(Fig. S5.1.4)**	
13	1 : 1	60 min, 30 Hz, 2 μL ACN	Lab XRD	1:1 S/D **(Fig. S5.1.1)**	
14	1 : 2	60 min, 30 Hz, 10 μL ACN	Lab XRD	1:1 S/D + D-proline **(Fig. S5.1.2)**	
15	2 : 1	60 min, 30 Hz, 2 μL ACN	Lab XRD	1:1 S/D + S-naproxen **(Fig. S5.1.3)**	
16	2 : 3	60 min, 30 Hz, 10 μL ACN	Lab XRD	1:1 S/D + D-proline **(Fig. S5.1.4)**	
17	1 : 1	60 min, 30 Hz, 2 μL H_2O	Lab XRD	1:1 S/D + + D-proline monohydrate + S-nprx **(Fig. S5.1.5)**	

18	2 : 1	60 min, 30 Hz, 10 μL H_2O	Lab XRD	1:1 S/D + S-nprx **(Fig. S5.1.5)**
19	2 : 3	60 min, 30 Hz, 10 μL H_2O	Lab XRD	1:1 S/D + S-nprx **(Fig. S5.1.5)**

5.1 PXRD analysis of the S/D samples (Figs. S5.1.1-S5.1.5)

Figure S5.1.1. Diffraction patterns for the **S/D** samples prepared by 1 : 1 MeOH-, EtOH-, ACN-, and ISPN-LAG (samples *1*, *5*, *9*, and *13* in Table S5.1); the diffraction pattern of the **1:1 R/D** cocrystal was simulated from the structure

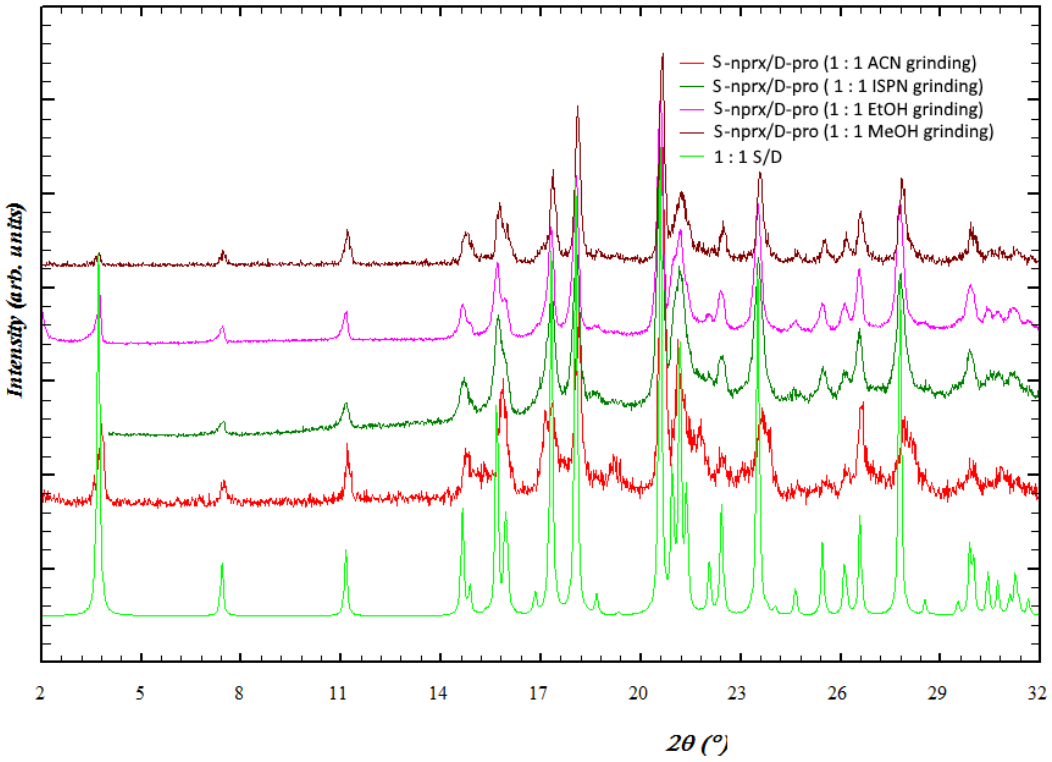

Figure S5.1.2. Diffraction patterns for the **S/D** samples prepared by 1 : 2 MeOH-, EtOH-, ACN-, and ISPN-LAG (samples *2*, *6*, *10*, and *14* in Table S5.1); the diffraction patterns of the **1:1 R/D** cocrystal and **D-proline** were simulated from the structures

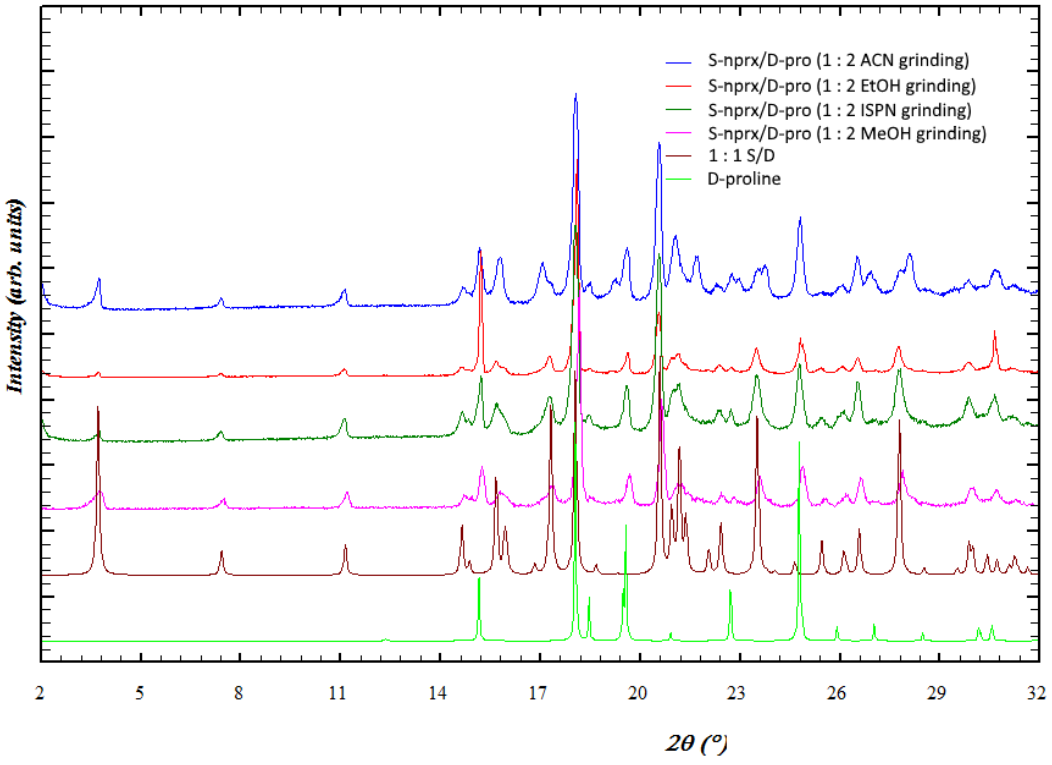

Figure S5.1.3. Diffraction patterns for the **S/D** samples prepared by 2 : 1 MeOH-, EtOH-, ACN-, and ISPN-LAG (samples *3*, *7*, *11*, and *15* in Table S5.1); the diffraction patterns of the **1:1 R/D** cocrystal and **S-naproxen** were simulated from the structures

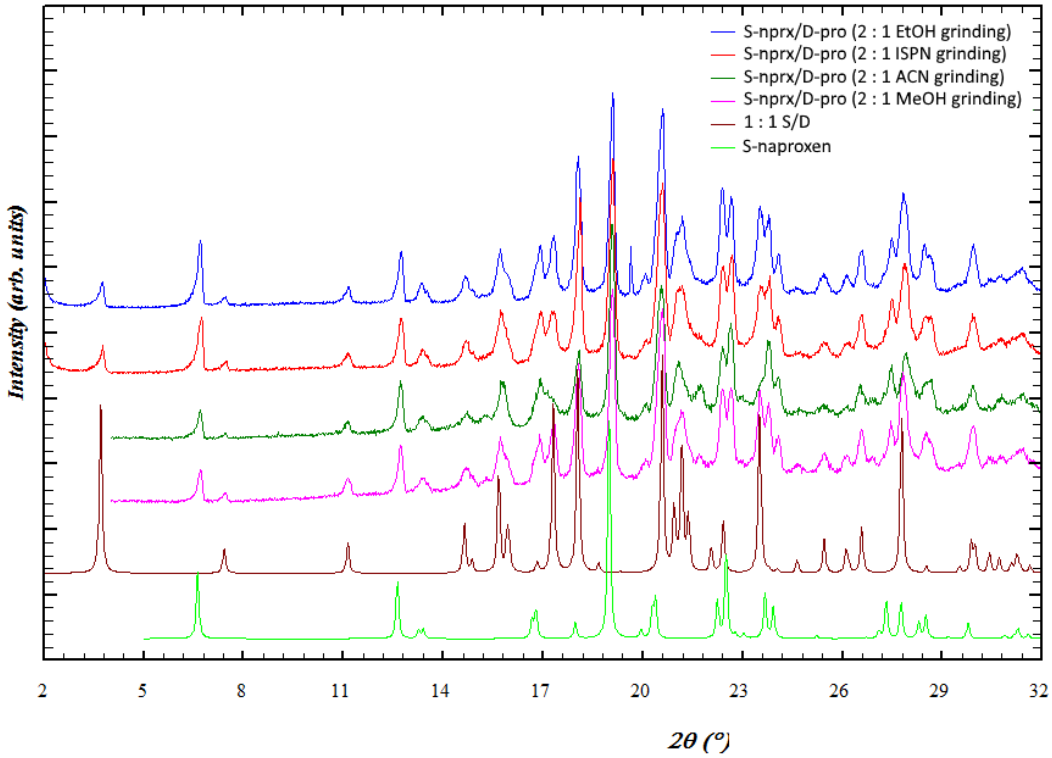

Figure S5.1.4. Diffraction patterns for the **S/D** samples prepared by 2 : 3 MeOH-, EtOH-, ACN-, and ISPN-LAG (samples *4*, *8*, *12*, and *16* in Table S5.1); the diffraction patterns of the **1:1 R/D** cocrystal, **D-proline**, and **D-proline monohydrate** were simulated from the structures

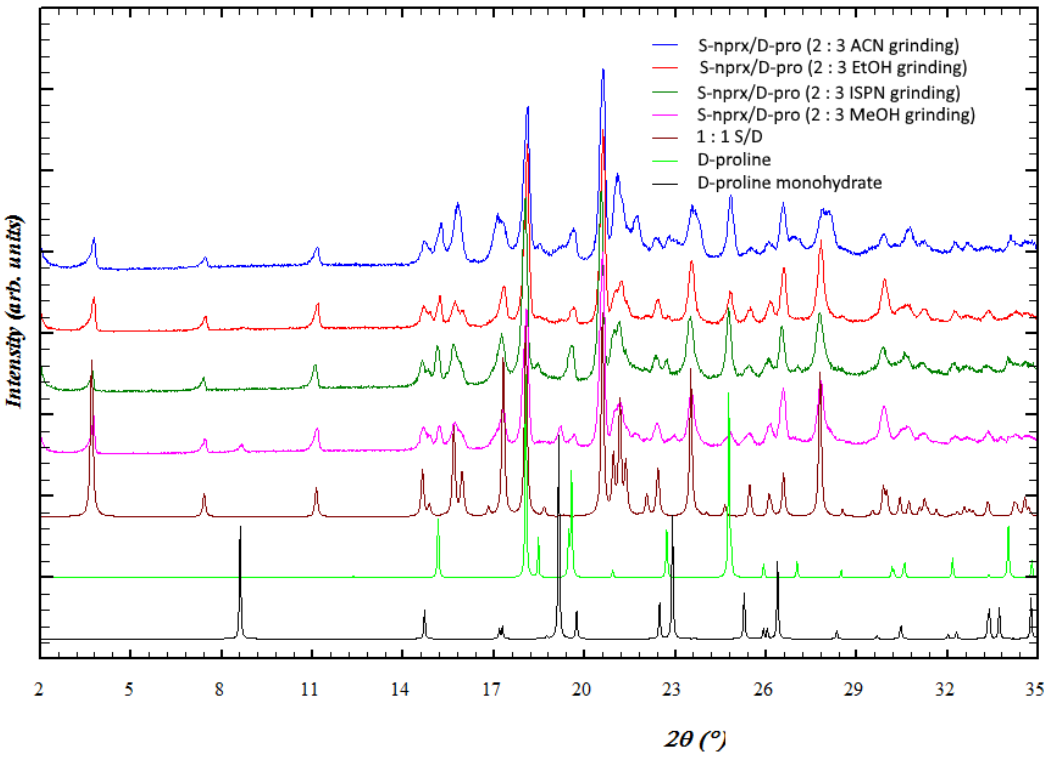

Figure S5.1.5. Diffraction patterns for the **S/D** samples prepared by water-assisted grinding in 1 : 1, 2 : 1, and 2 : 3 ratios (samples *17-19* in Table S5.1); the diffraction patterns of the **1:1 R/D** cocrystal and **S-naproxen** were simulated from the structures

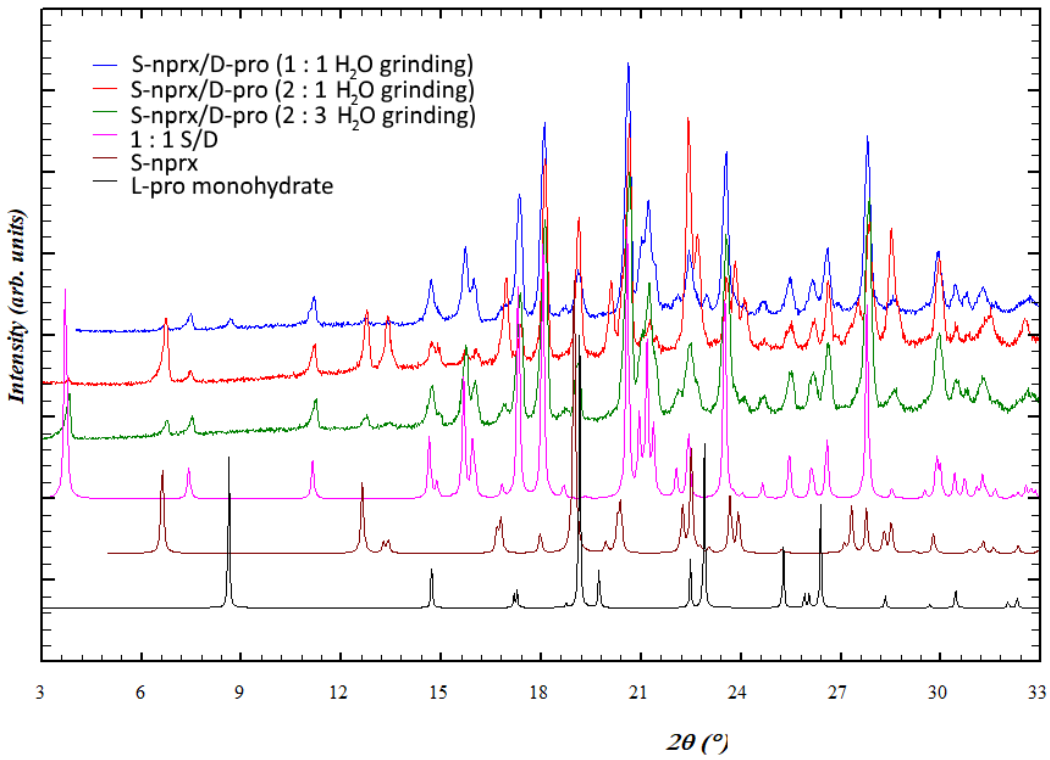

5.2 DSC data measured for a selected S/D sample (Fig. S5.2.1)

Figure S5.2.1. DSC curve measured for the S/D sample prepared by 1:1 MeOH-LAG

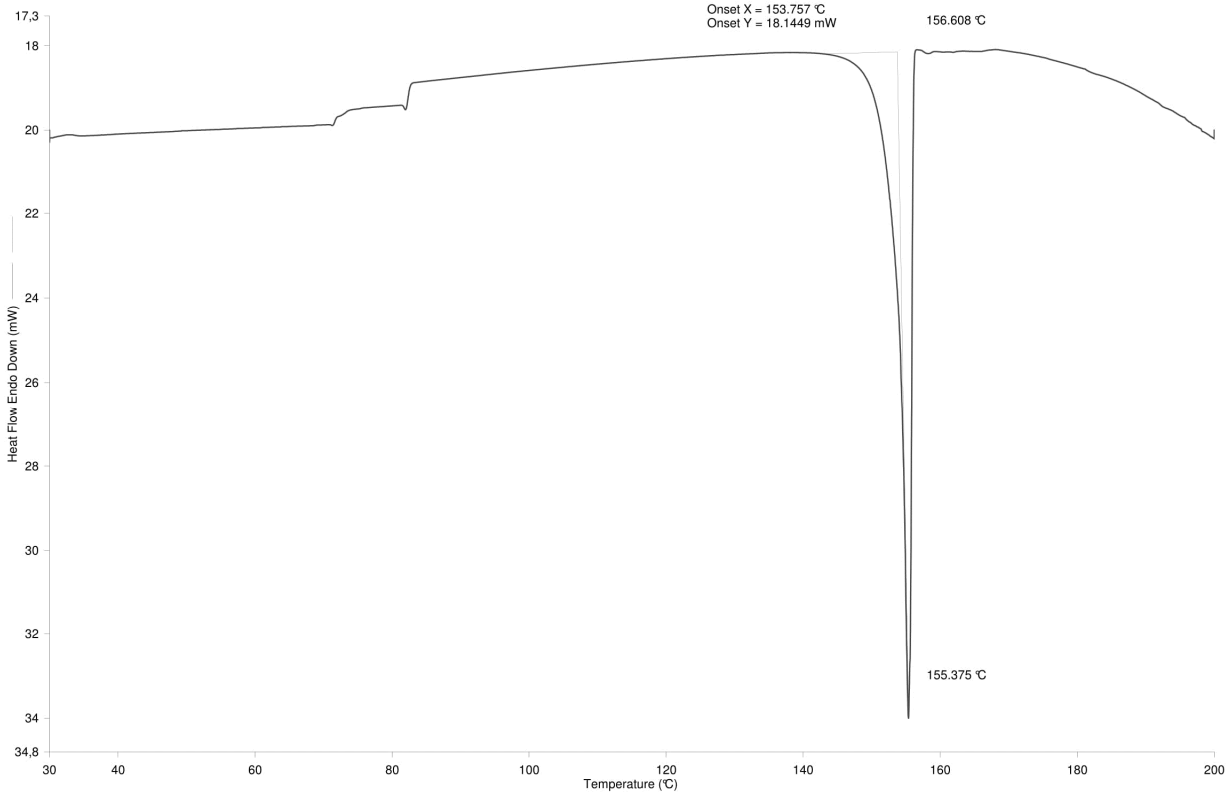

6. Details of LAG experiments and sample analysis for the RS/D system (Table S6.1)

Table S6.1 Experimental details for laboratory liquid-assisted grinding and further analysis of obtained RS-naproxen/D-proline cocrystals; lab XRD was performed at Cu*K*α radiation

	Molar ratio RS-Nprx/D-Pro	Grinding conditions	PXRD analysis	Result	Structures determined from PXRD	Other analysis
1	1 : 1	60 min, 30 Hz, 2 μL MeOH	Synchrotron (λ = 0.776188 Å)	1:1 RS/D pol I (**Fig. S6.1.1**)		DSC (determined the melting point of the **1:1 RS/D pol I** phase, T_m **= 162(1)°C**) (**Fig. S6.2.1**)
2	1 : 2	60 min, 30 Hz, 10 μL MeOH	Lab XRD	1:1 RS/D pol I + D-proline (**Fig. S6.1.2**)		
3	2 : 1	60 min, 30 Hz, 2 μL MeOH	Lab XRD	1:1 RS/D pol I + RS-naproxen (**Fig. S6.1.3**)		
4	2 : 3	60 min, 30 Hz, 10 μL MeOH	Lab XRD	1:1 RS/D pol I + D-proline (**Fig. S6.1.4**)		
5	1 : 1	60 min, 30 Hz, 10 μL EtOH	Lab XRD	1:1 RS/D pol I (**Fig. S6.1.5**)		
6	1 : 2	60 min, 30 Hz, 10 μL EtOH	Lab XRD	1:1 RS/D pol I + 1:2 RS/D (**Fig. S6.1.6**)		DSC (determined the melting point of the **1:2 RS/D** phase, T_m **= 171(1)°C**) (**Fig. S6.2.3**)
7	2 : 1	60 min, 30 Hz, 10 μL EtOH	Lab XRD	1:1 RS/D pol I + RS-naproxen (**Fig. S6.1.3**)		
8	2 : 3	60 min, 30 Hz, 10 μL EtOH	Lab XRD	1:1 RS/D pol I + 1:2 RS/D+ D-proline (**Fig. S6.1.7**)		
9	1 : 1	60 min, 30 Hz, 2 μL ISPN	Lab XRD	1:1 RS/D pol I (**Fig. S6.1.5**)		
10	1 : 2	60 min, 30 Hz, 10 μL ISPN	Lab XRD	1:1 RS/D pol I + 1:2 RS/D (**Fig. S6.1.6**)		
11	2 : 1	60 min, 30 Hz, 10 μL ISPN	Lab XRD	1:1 RS/D pol I + RS-naproxen (**Fig. S6.1.3**)		
12	2 : 3	60 min, 30 Hz, 10 μL ISPN	Lab XRD	1:1 RS/D pol I + 1:2 RS/D + D-proline (**Fig. S6.1.7**)		

13	1 : 1	60 min, 30 Hz, 2 µL ACN	Synchrotron (λ = 1.0007 Å)	1:1 RS/D pol II	1:1 RS/D pol II (for Rietveld refinement see **Fig. S2.2**)	DSC (determined the melting point of the **1:1 RS/D pol II** phase, T_m **= 159(1)°C**) (**Fig. S6.2.2**)
14	1 : 2	60 min, 30 Hz, 10 µL ACN	Lab XRD	1:1 RS/D pol II + D-proline (**Fig. S6.1.8**)		
15	2 : 1	60 min, 30 Hz, 2 µL ACN	Lab XRD	1:1 RS/D pol II + RS-naproxen (**Fig. S6.1.3**)		
16	2 : 3	60 min, 30 Hz, 10 µL ACN	Lab XRD	1:1 RS/D pol II + D-proline (**Fig. S6.1.9**)		
17	1 : 1	60 min, 30 Hz, 2 µL H_2O	Lab XRD	1:1 RS/D/H_2O + RS-nprx (**Fig. S6.1.10**)		
18	1 : 2	60 min, 30 Hz, 10 µL H_2O	Lab XRD	1:1 RS/D/H_2O + D-pro monohydrate + D-pro (**Fig. S6.1.11**)		
19	2 : 3	60 min, 30 Hz, 10 µL H_2O	Lab XRD	1:1 RS/D/H_2O + RS-nprx (**Fig. S6.1.12**)		

6.1 PXRD analysis of the RS/D samples (Figs. S6.1.2-S6.1.12)

Figure S6.1.2. Diffraction pattern for the **RS/D sample** prepared by 1 : 1 MeOH-LAG (samples *1* in Table S6.1); the diffraction pattern of the **1:1 RS/D pol I** cocrystal was simulated from the structure

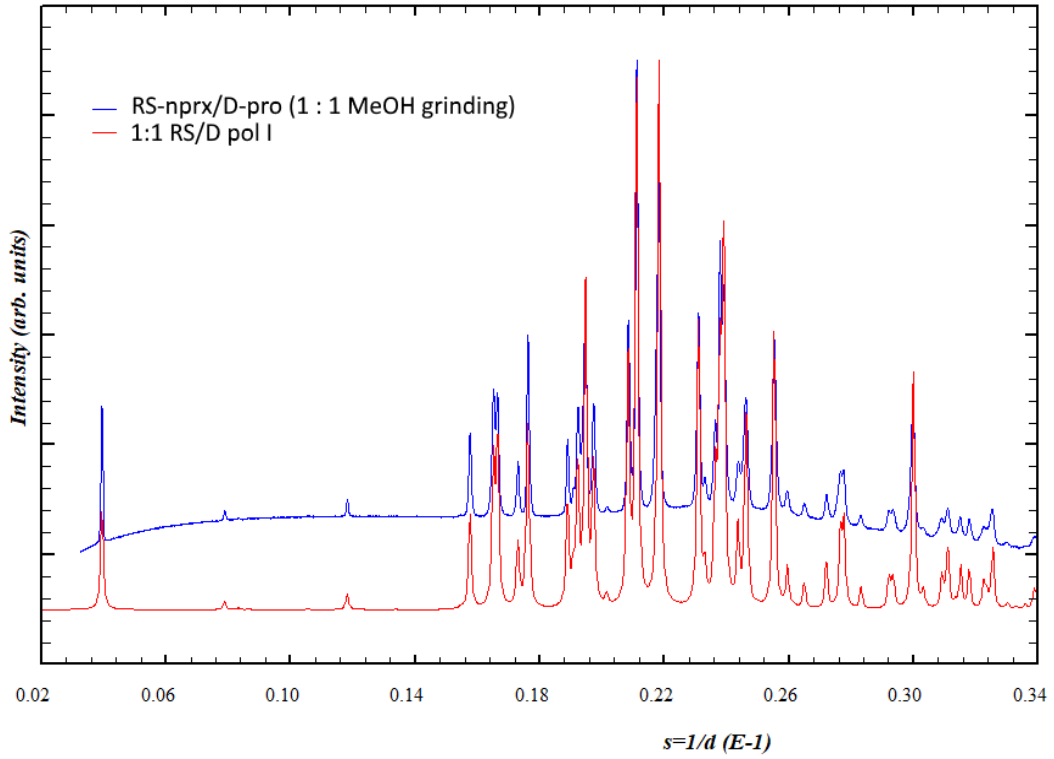

Figure S6.1.2. Diffraction pattern for the **RS/D sample** prepared by 1 : 2 MeOH-LAG (samples *2* in Table S6.1); the diffraction patterns of **1:1 RS/D pol I** and **D-proline** were simulated from the structures

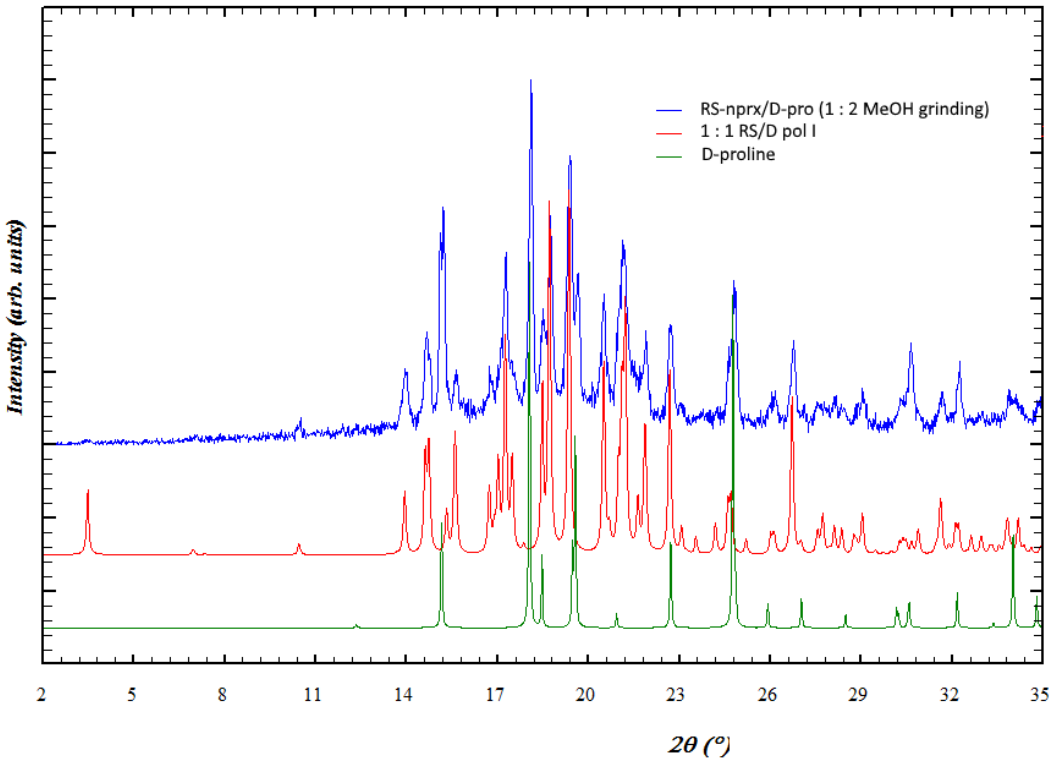

Figure S6.1.3. Diffraction patterns for the **RS/D** samples prepared by 2 : 1 MeOH-, EtOH, ACN-, and ISPN-LAG (samples *3*, *7*, *11*, and *15* in Table S6.1); the diffraction patterns of the pure phases were simulated from the structure, except **1:1 RS/D pol II** was taken as measured at synchrotron (sample *13* in Table S6.1)

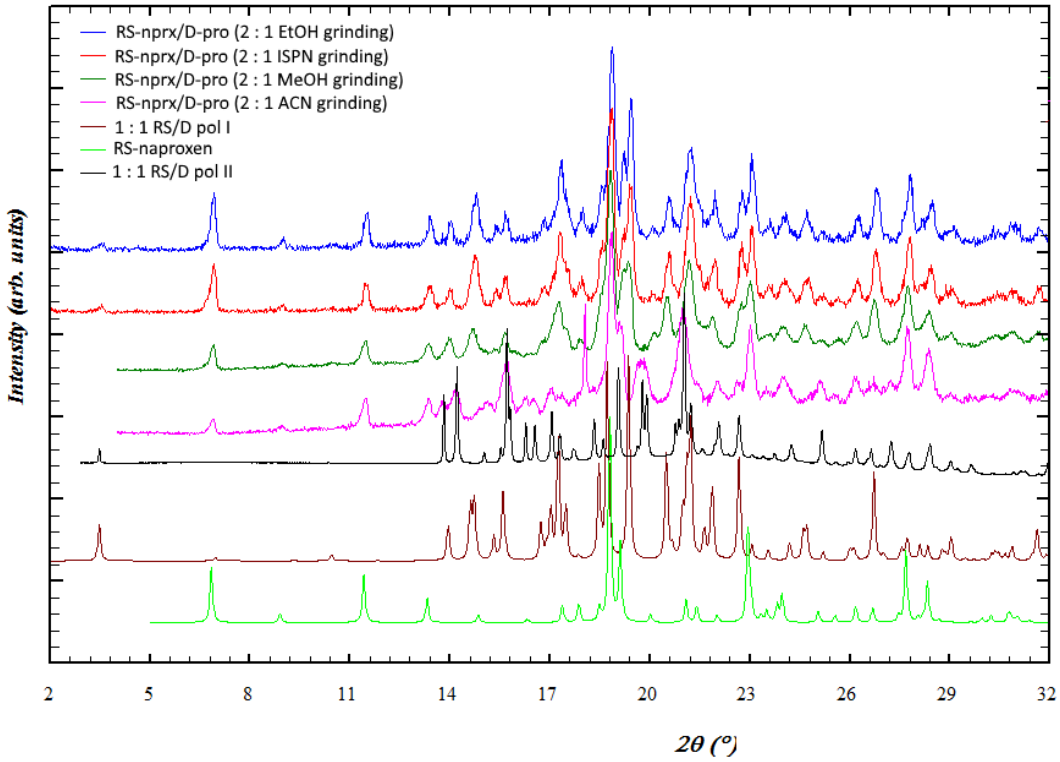

Figure S6.1.4. Diffraction pattern for the **RS/D** sample prepared by 2 : 3 MeOH-LAG (samples *4* in Table S6.1); the diffraction patterns of **1:1 RS/D pol I** and **D-proline** were simulated from the structures

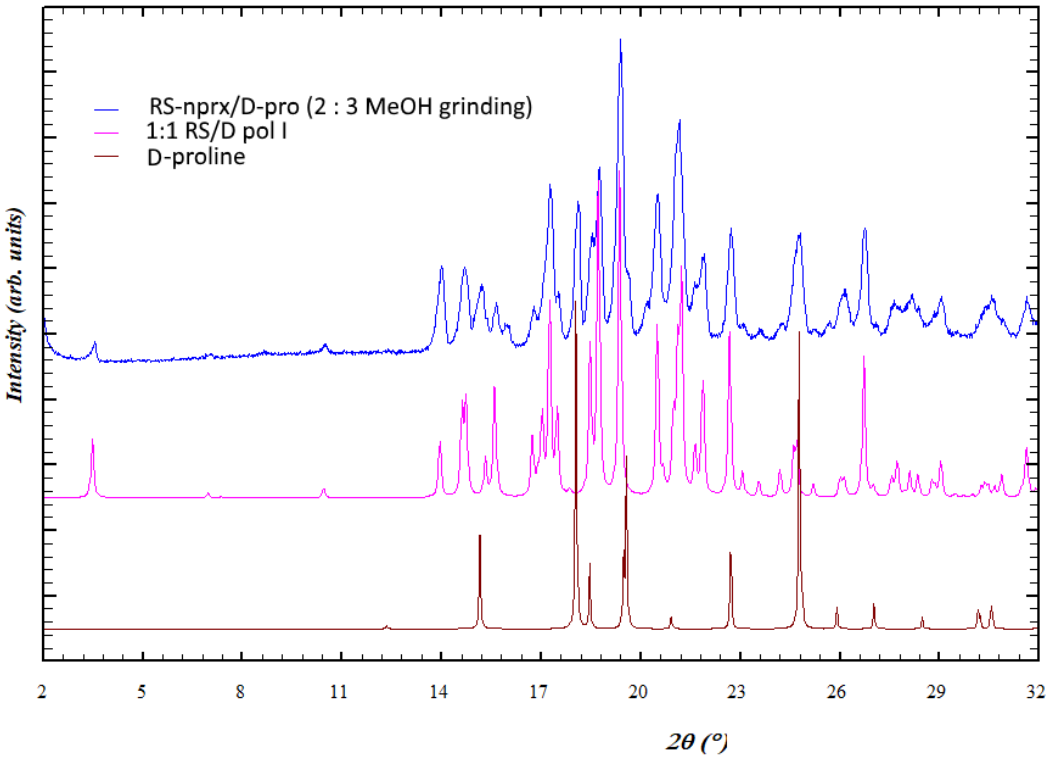

Figure S6.1.5. Diffraction patterns for the **RS/D** samples prepared by 1 : 1 EtOH- and ISPN-LAG (samples *5* and *9* in Table S6.1); the diffraction pattern of the **1:1 RS/D pol I** cocrystal was simulated from the structure

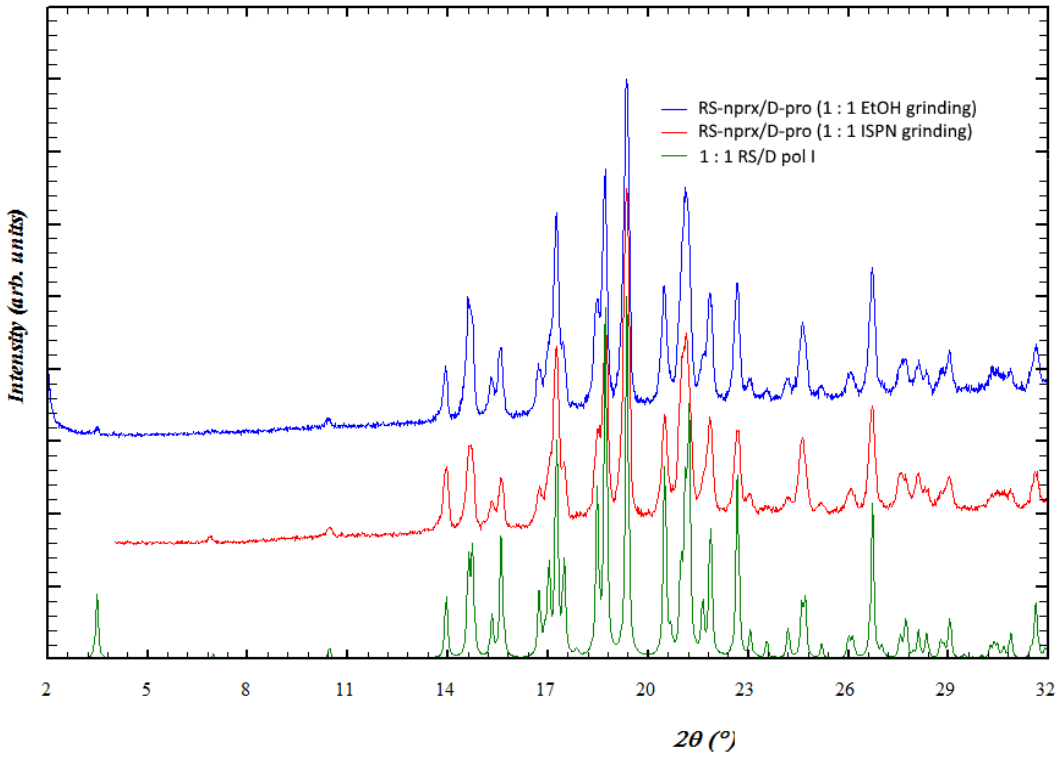

Figure S6.1.6. Diffraction patterns for the **RS/D** samples prepared by 1 : 2 EtOH- and ISPN-LAG (samples *6* and *10* in Table S6.1); the diffraction pattern of pure **1:1 RS/D pol I** was simulated from the structure and that of the pure **1:2 RS/D** was taken as measured at synchrotron (sample *10* in Table S7.1 as the pattern of 1:2 RS/L is the same as 1:2 RS/D)

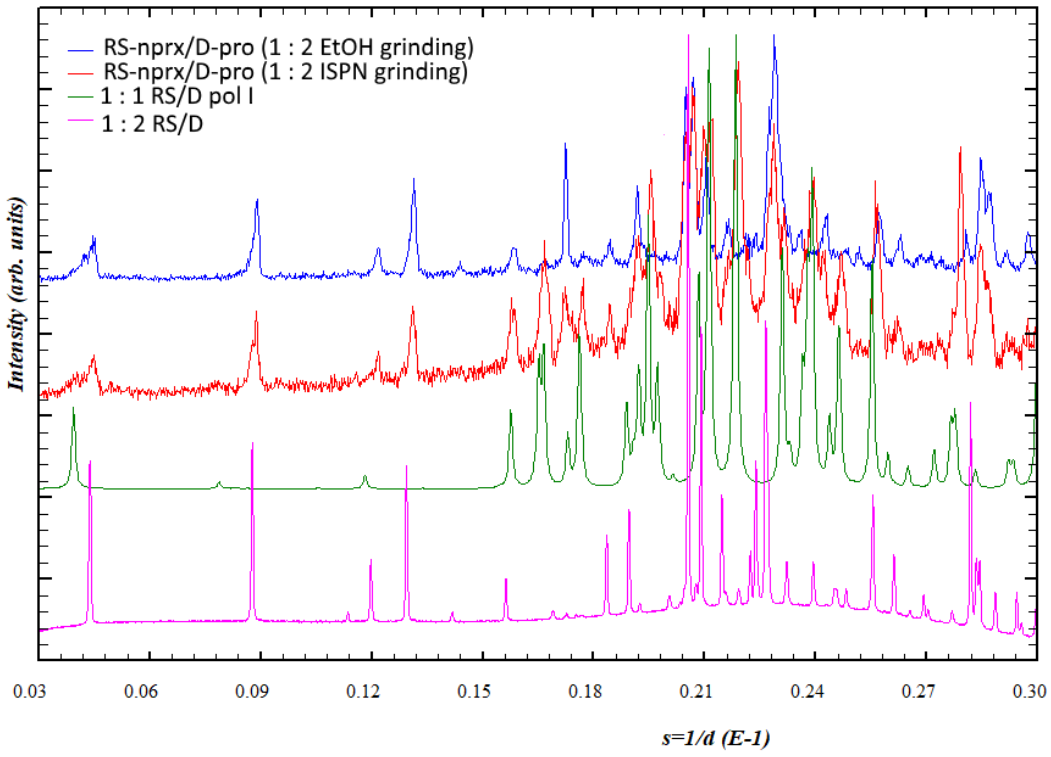

Figure S6.1.7. Diffraction patterns for the **RS/D** samples prepared by 2 : 3 EtOH- and ISPN-LAG (samples *8* and *12* in Table S6.1); the diffraction patterns of pure **1:1 RS/D pol I** and **D-proline** were simulated from the structure and that of the pure **1:2 RS/D** was taken as measured at synchrotron (sample *10* in Table S7.1 as the pattern of 1:2 RS/L is the same as 1:2 RS/D)

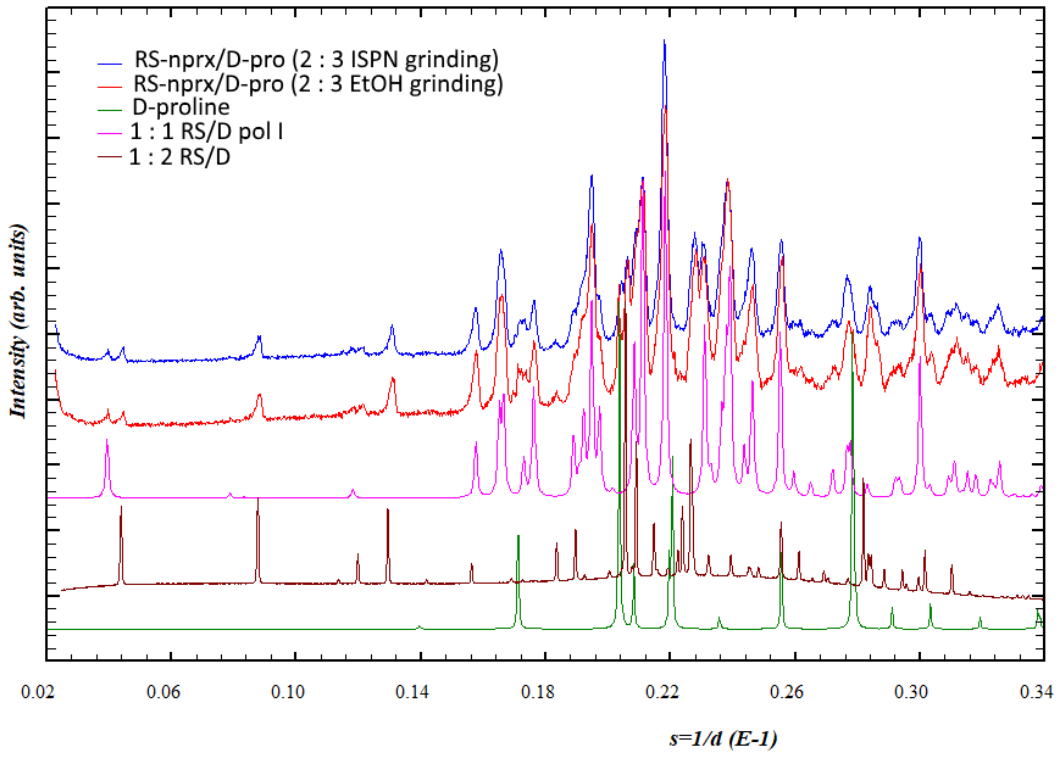

Figure S6.1.8. Diffraction pattern for the **RS/D** sample prepared by 1 : 2 ACN-LAG (samples *14* in Table S6.1); the diffraction pattern of **1:1 RS/D pol** was taken as measured at synchrotron (sample *13* in Table S6.1), and pure **D-proline** was simulated from the structure

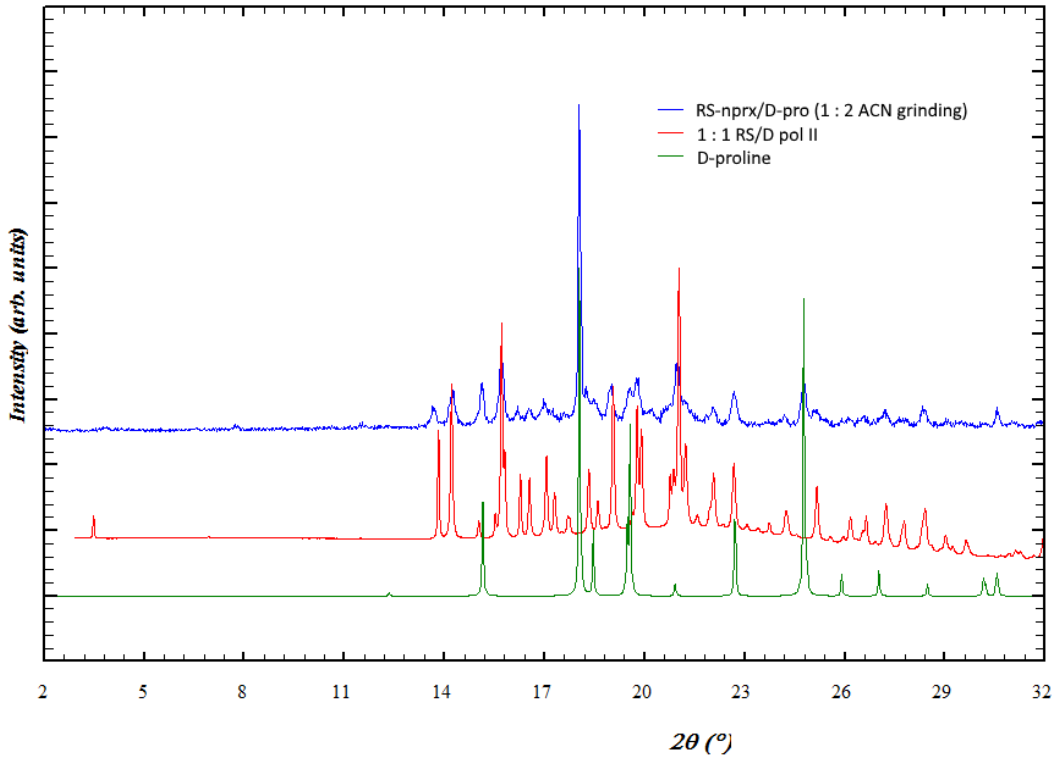

Figure S6.1.9. Diffraction pattern for the **RS/D** sample prepared by 2 : 3 ACN-LAG (samples *16* in Table S6.1); the diffraction pattern of **1:1 RS/D pol** was taken as measured at synchrotron (sample *13* in Table S6.1), and pure **D-proline** was simulated from the structure

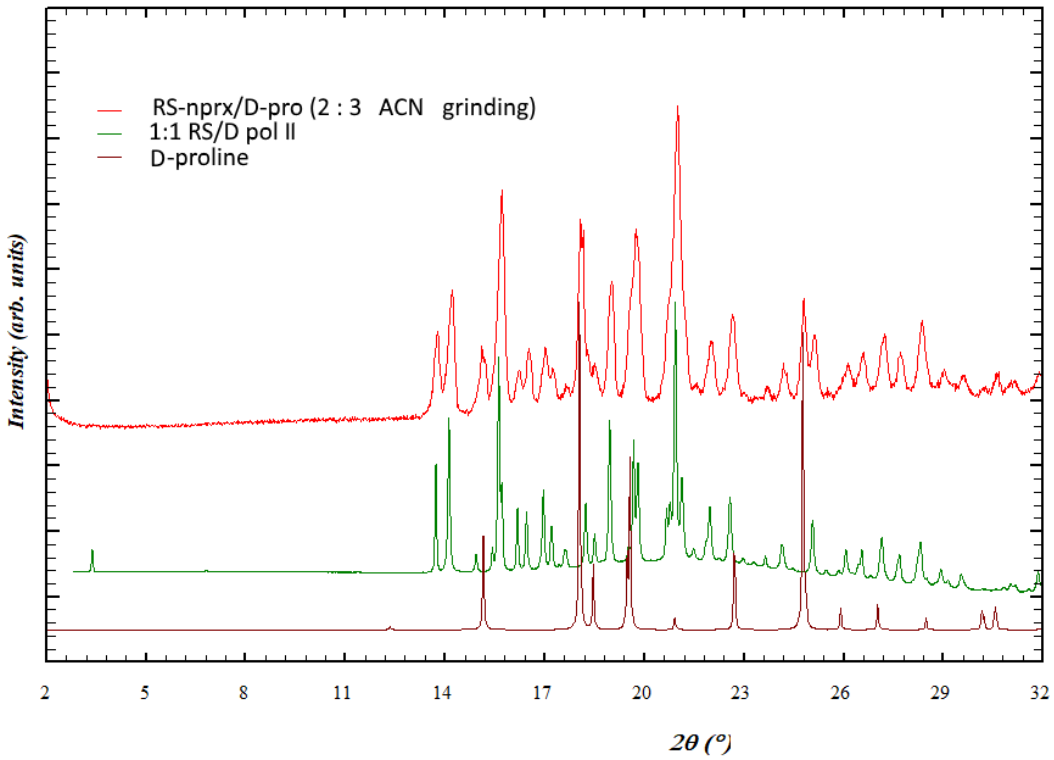

Figure S6.1.10. Diffraction pattern for the **RS/D** sample prepared by water-assisted grinding in 1 : 1 ratio (sample *17* in Table S6.1); the diffraction patterns of the pure phases were simulated from the structures

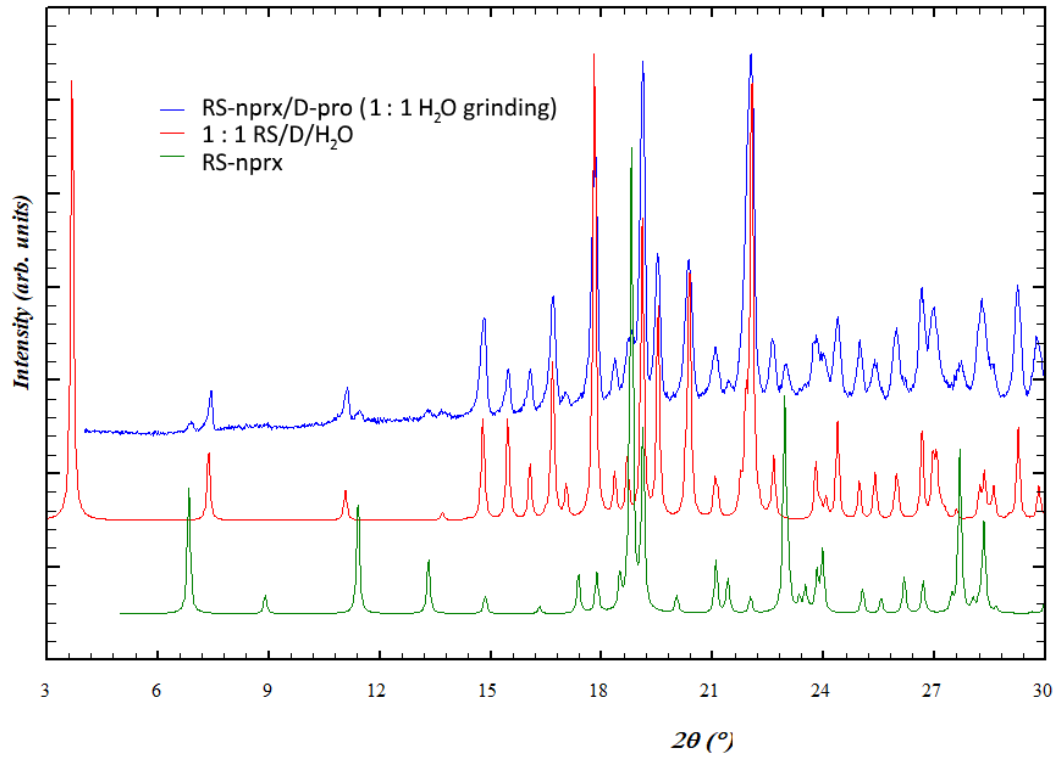

Figure S6.1.11. Diffraction pattern for the **RS/D** sample prepared by water-assisted grinding in 1 : 2 ratio (samples *18* in Table); the diffraction patterns of the pure phases were simulated from the structures

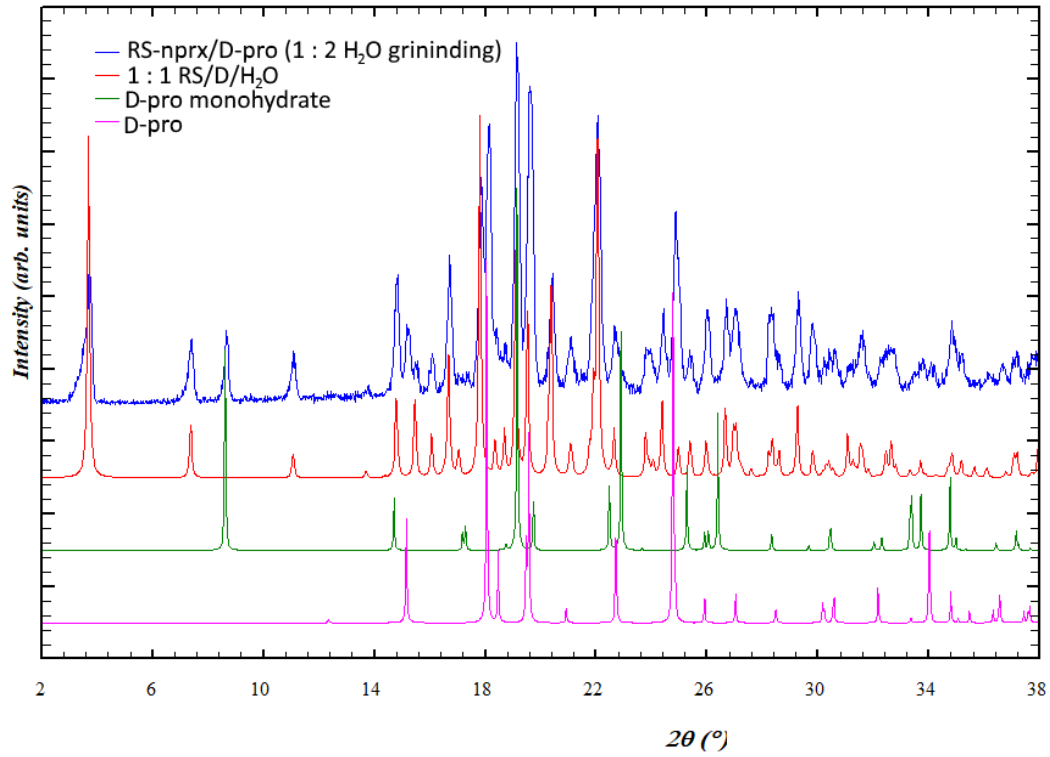

Figure S6.1.12. Diffraction pattern for the **RS/D** sample prepared by water-assisted grinding in 2 : 3 ratio (samples *19* in Table S6.1); the diffraction patterns of the pure phases were simulated from the structures

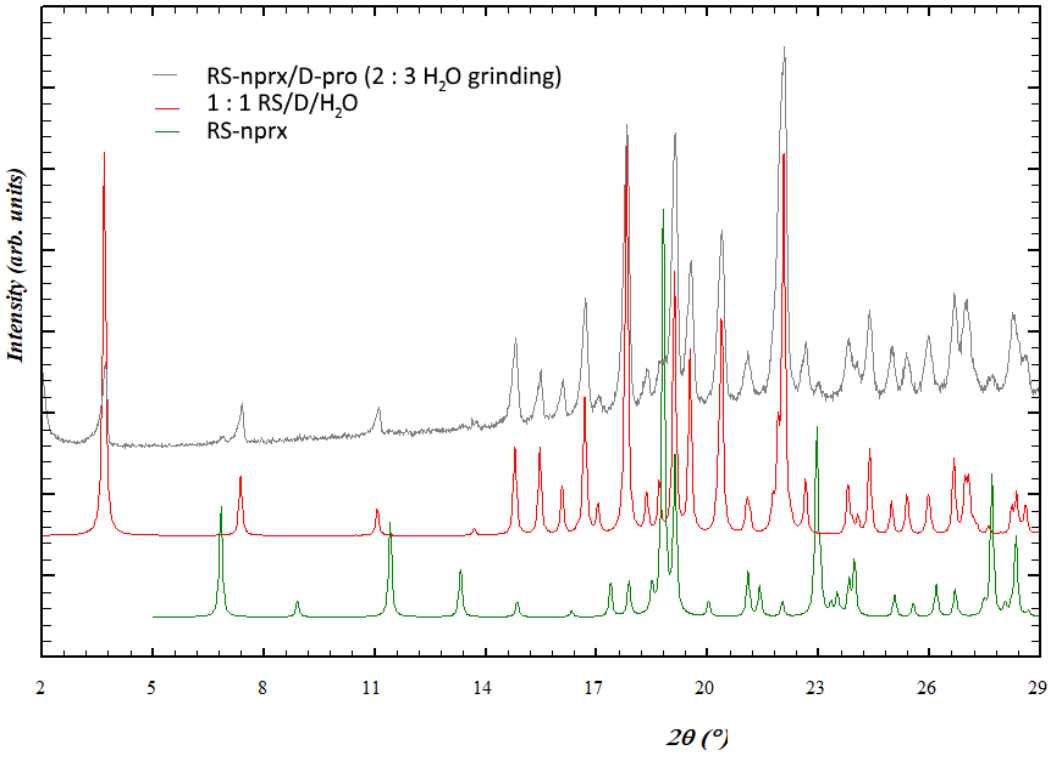

6.2 DSC data measured for selected RS/D samples (Figs. S6.2.1 S6.2.3)

Figure S6.2.1. DSC curve measured for the **RS/D** sample prepared by 1 : 1 MeOH-LAG (sample *1* in Table S6.1). The curve has only one peak, which corresponds to the melting point of the **1:1 RS/D pol I** phase.

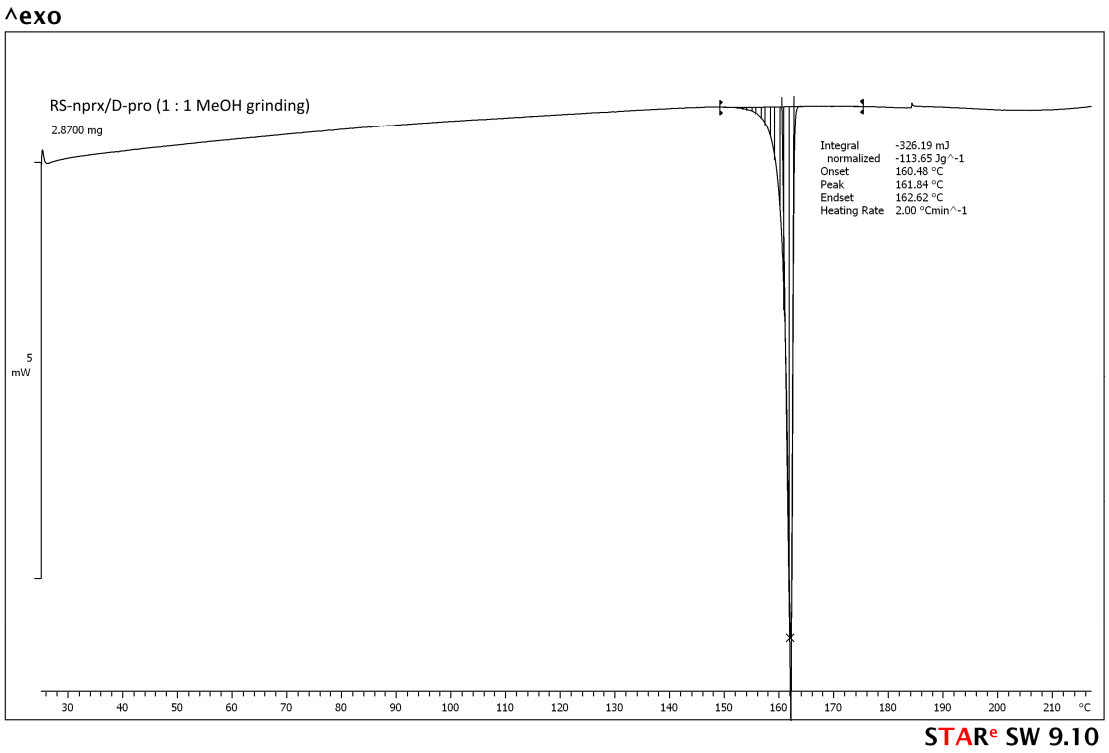

Figure S6.2.2. DSC curve measured for the **RS/D** sample prepared by 1 : 1 ACN-LAG (sample *13* in Table S6.1). The curve has only one peak, which corresponds to the melting point of the **1:1 RS/D pol II** phase.

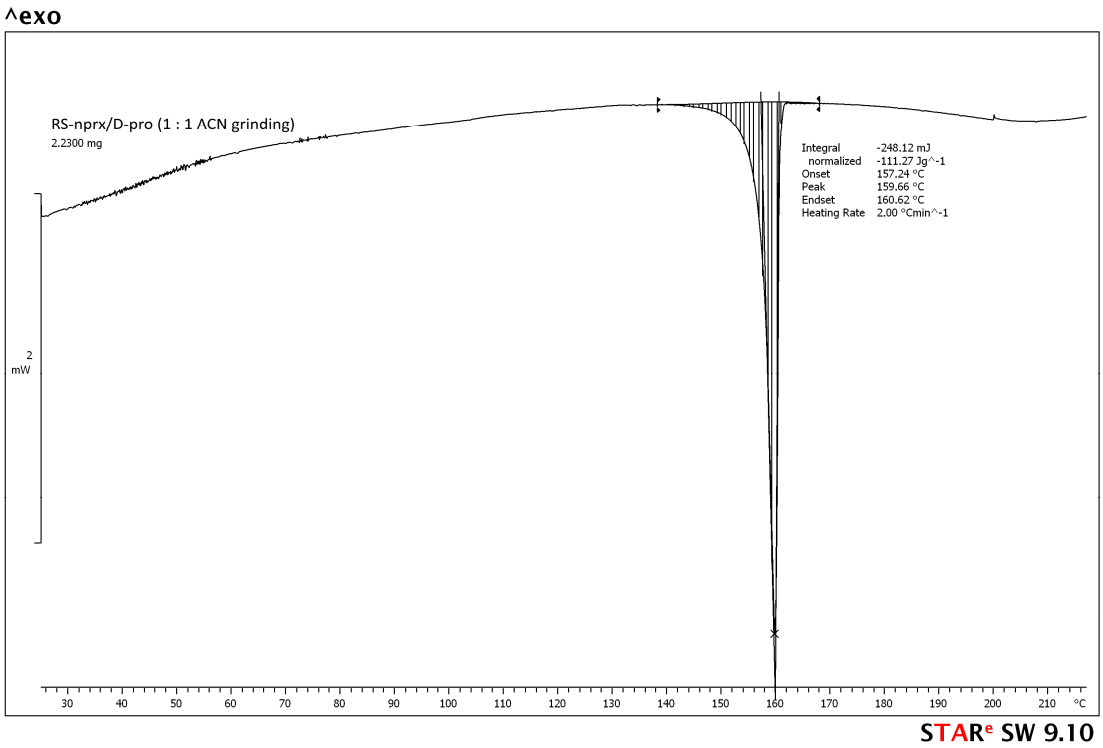

Figure S6.2.3. DSC curve measured for the **RS/D** sample prepared by 1 : 2 EtOH-LAG (sample *6* in Table S6.1). The curve has one big peak, which corresponds to the melting point of the **1:2 RS/D** phase and one small peak that corresponds to the melting of the **1:1 RS/D pol I** phase. Since the amount of the latter is small, we are very close to the melting of pure **1:2 RS/D** and, thus we take the value of 171(1)°C for the melting point of the **1:2 RS/D**.

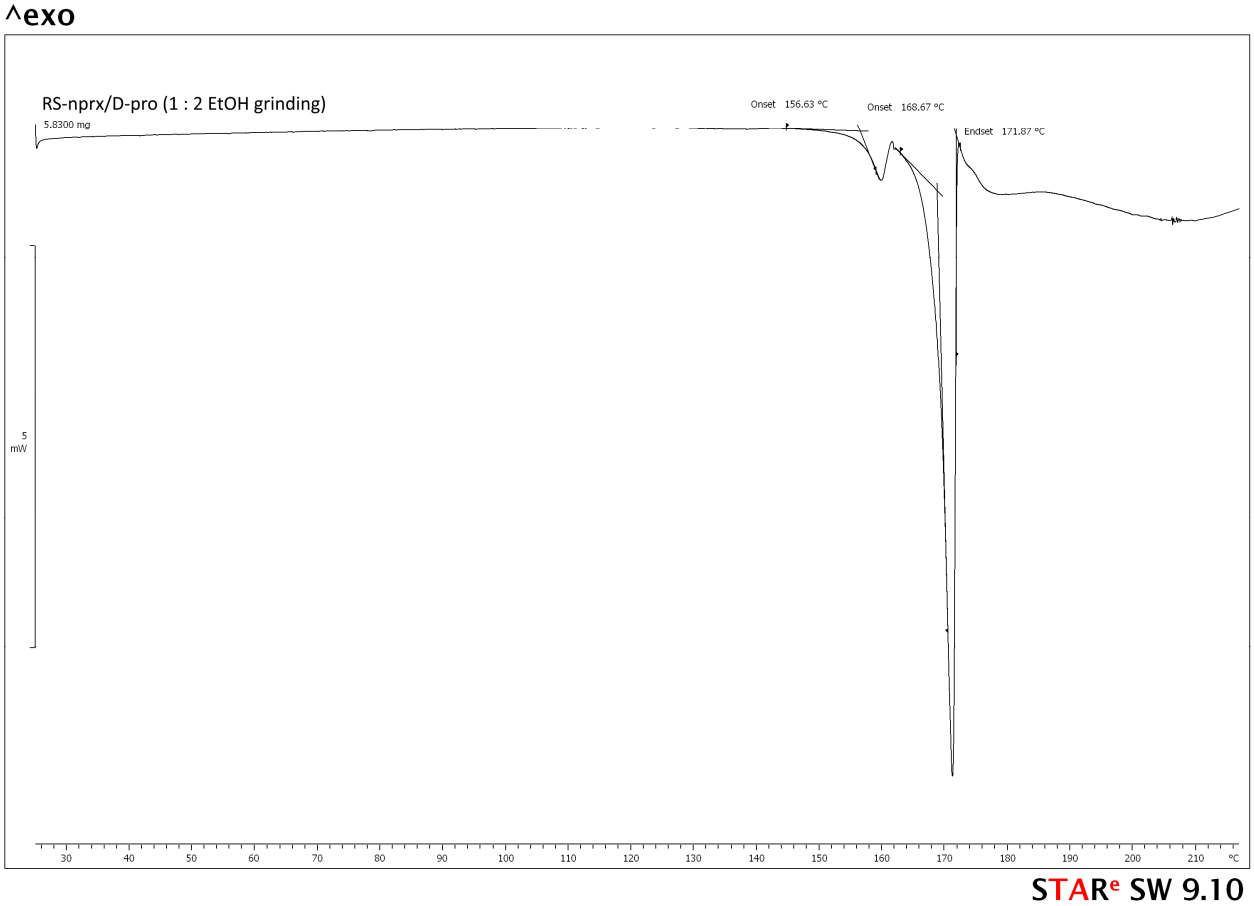

7. Details of LAG experiments and sample analysis for the RS/L system (Table S7.1)

Table S7.1 Experimental details for laboratory liquid-assisted grinding and further analysis of obtained RS-naproxen/L-proline cocrystals; lab XRD was performed at Cu*K*α radiation

	Molar ratio RS-Nprx/L-Pro	Grinding conditions	PXRD analysis	Result	Structures determined from PXRD	Other analysis
1	1 : 1	60 min, 30 Hz, 2 μL MeOH	Lab XRD	1:1 RS/L pol I (**Fig. S7.1.1**)		
2	1 : 2	60 min, 30 Hz, 10 μL MeOH	Lab XRD	1:1 RS/L pol I + L-proline (**Fig. S7.1.2**)		
3	2 : 1	60 min, 30 Hz, 2 μL MeOH	Lab XRD	1:1 RS/L pol I + RS-naproxen (**Fig. S7.1.3**)		
4	2 : 3	60 min, 30 Hz, 10 μL MeOH	Lab XRD	1:1 RS/L pol I + L-proline + L-proline monohydrate (**Fig. S7.1.2**)		
5	1 : 1	60 min, 30 Hz, 10 μL EtOH	Lab XRD	1:1 RS/L pol I (**Fig. S7.1.1**)		
6	1 : 2	60 min, 30 Hz, 10 μL EtOH	Synchrotron (λ = 0.62127 Å)	1:1 RS/L pol I + 1:2 RS/L + 1:1 RS/L/H_2O + L-proline(**Fig. S7.1.4**)		
7	2 : 1	60 min, 30 Hz, 10 μL EtOH		1:1 RS/L pol I + RS-naproxen (**Fig. S7.1.3**)		
8	2 : 3	60 min, 30 Hz, 10 μL EtOH	Synchrotron (λ = 0.708 Å)	1:1 RS/L pol I + 1:2 RS/L + 1:1 RS/L/H_2O + L-proline (**Fig. S7.1.5**)		
9	1 : 1	60 min, 30 Hz, 2 μL ISPN	Lab XRD	1:1 RS/L pol I (**Fig. S7.1.1**)		
10	1 : 2	60 min, 30 Hz, 10 μL ISPN	Synchrotron (λ = 0.708 Å) under variable temperature	Initially, the sample contained a mixture of L-pro, 1:1 RS/L pol I, and 1:2 RS/L; Upon heating 1:1 RS/L pol I disappears, and only 1:2 RS/L and a negligible amount of L-pro are left; Further heating leads to a disappearance of 1:2 RS/L; and, finally L-pro melts as well (**Fig. 8** in the main text)	1:2 RS/L (for Rietveld refinement see **Fig. S2.3**)	DSC (**Fig. S7.2.1**)
11	2 : 1	60 min, 30 Hz, 10 μL ISPN	Lab XRD	1:1 RS/L pol I + RS-naproxen (**Fig. S7.1.3**)		
12	2 : 3	60 min, 30 Hz, 10 μL ISPN	Lab XRD	1:1 RS/L pol I + 1:2 RS/L (**Fig. S7.1.6**)		
13	1 : 1	60 min, 30 Hz, 2 μL ACN	Lab XRD	1:1 RS/L pol II + RS-naproxen (**Fig. S7.1.7**)		
14	1 : 2	60 min, 30 Hz, 10 μL ACN	Lab XRD	1:1 RS/L pol II + L-pro (**Fig. S7.1.8**)		
15	2 : 1	60 min, 30 Hz, 2 μL ACN	Lab XRD	1:1 RS/L pol II + RS-naproxen (**Fig. S7.1.9**)		
16	2 : 3	60 min, 30 Hz, 10 μL ACN	Lab XRD	1:1 RS/L pol II + 1:2 RS/L (**Fig. S7.1.10**)		

17	1 : 1	60 min, 30 Hz, 2 μL H_2O	Synchrotron (λ = 0.78487 Å) under variable temperature	The initial sample contained 1:1 RS/L/H_2O and RS-nprx; Upon heating and water evaporation, both 1:1 RS/L/H_2O and RS-nprx disappear and a new 1:1 RS/L pol III cocrystal emerges; upon further heating, 1:1 RS/L pol III disappears, and 1:1 RS/L pol I emerges, which finally melts (**Fig. 9** in the main text)	1:1 RS/L pol III (for Rietveld refinement see **Fig. S2.4**)
18	1 : 2	60 min, 30 Hz, 10 μL H_2O	Lab XRD	1:1 RS/L/H_2O + L-pro monohydrate (**Fig. S7.1.11**)	
19	2 : 3	60 min, 30 Hz, 10 μL H_2O	Lab XRD	1:1 RS/L/H_2O + L-pro monohydrate (**Fig. S7.1.12**)	

7.1 PXRD analysis of the RS/L samples (Figs. S7.1.1-S7.1.12)

Figure S7.1.1. Diffraction patterns for the **RS/L** samples prepared by 1 : 1 MeOH-, EtOH-, and ISPN-LAG (samples *1*, *5*, *9* in Table S7.1); the diffraction pattern of the **1:1 RS/D pol I** cocrystal was simulated from the structure

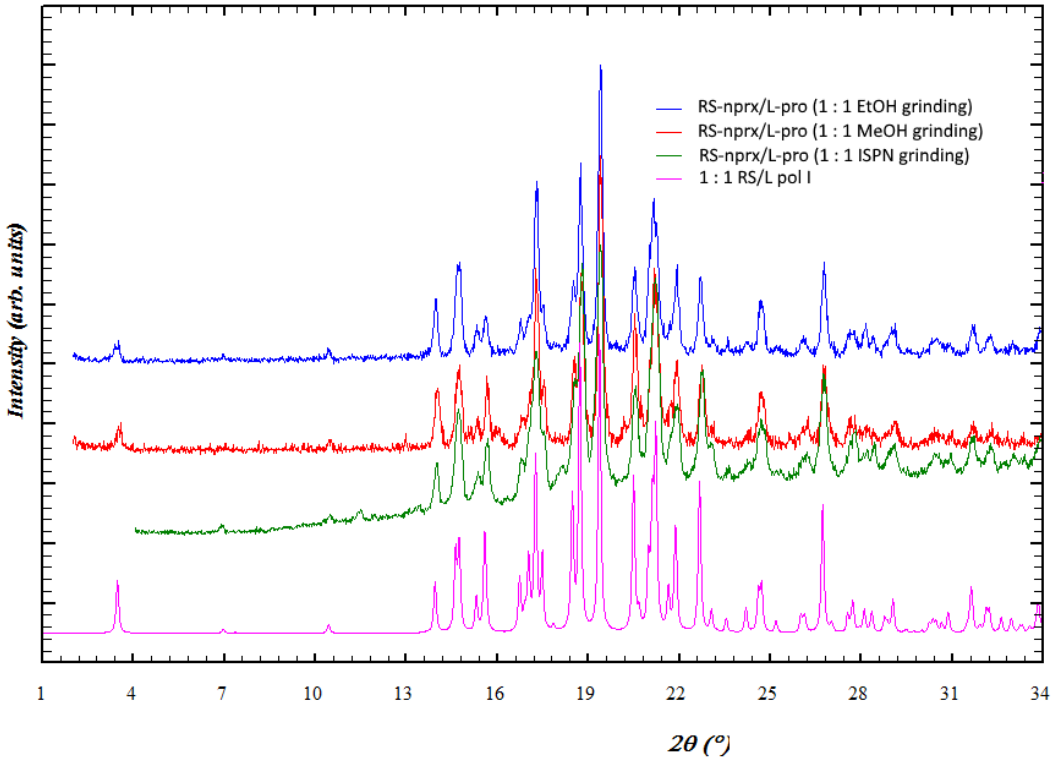

Figure S7.1.2. Diffraction patterns for the **RS/L** samples prepared by 1 : 2 and 2 : 3 MeOH-LAG (samples *2* and *4* in Table S7.1); the diffraction patterns of the pure phases were simulated from the structures

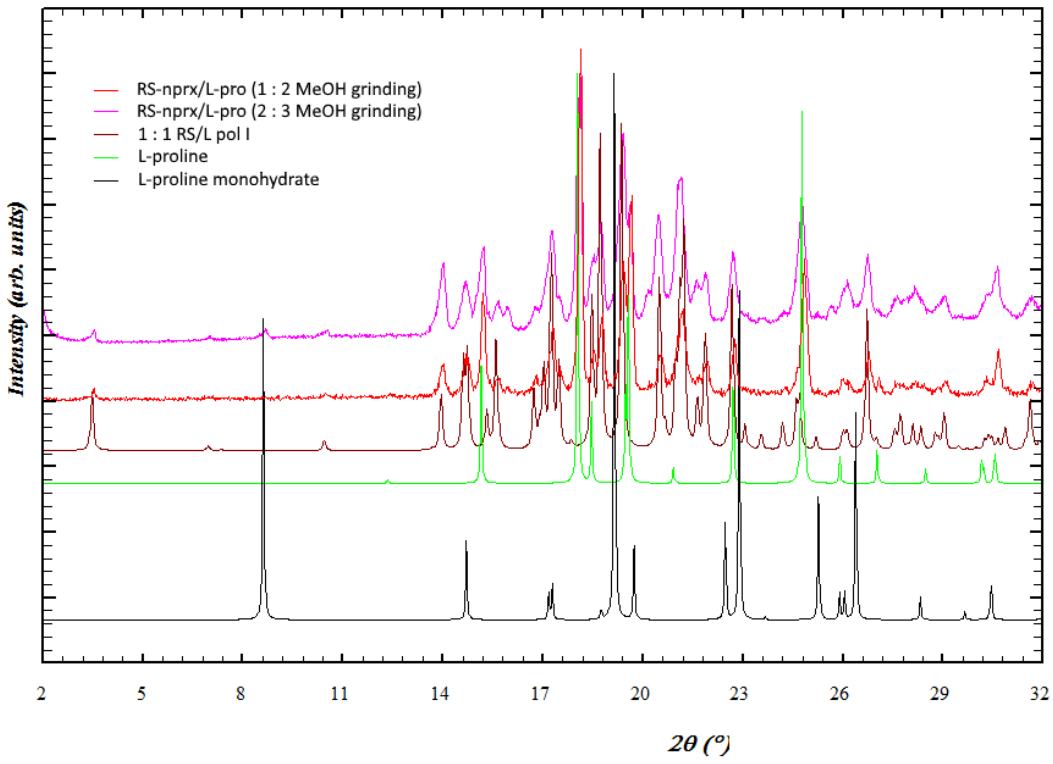

Figure S7.1.3. Diffraction patterns for the **RS/L** samples prepared by 2 : 1 MeOH-, EtOH-, and ISPN-LAG (samples *3*, *7*, and *11* in Table S7.1); the diffraction patterns of the pure phases were simulated from the structures

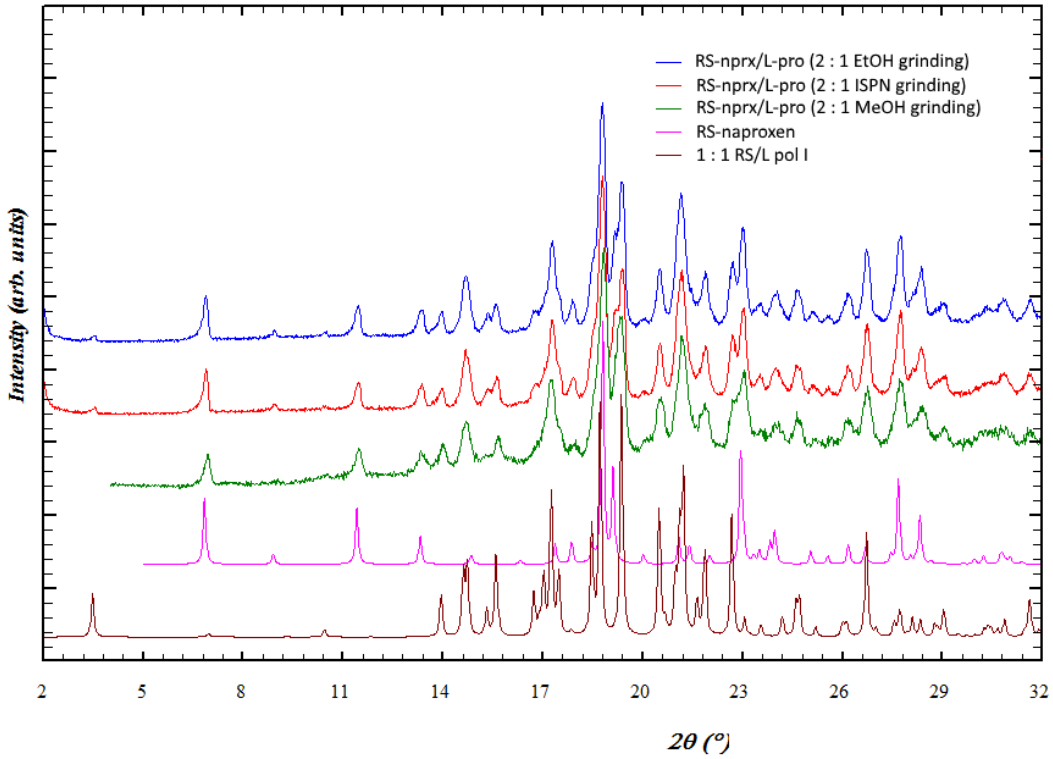

Figure S7.1.4. Diffraction pattern for the **RS/L** sample prepared by 1 : 2 EtOH-LAG (samples *6* in Table S7.1); the diffraction patterns of the pure phases were simulated from the structures, except that of pure **1:2 RS/D**, which was taken as measured at synchrotron (sample *10* in Table S7.1)

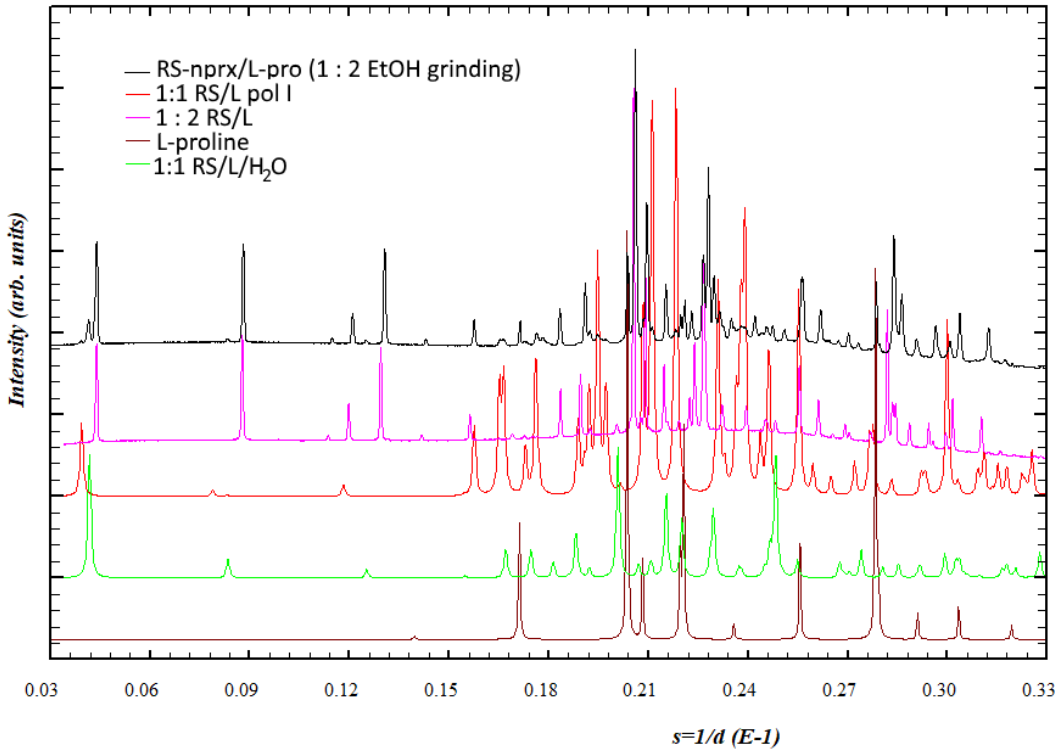

Figure S7.1.5. Diffraction pattern for the **RS/L** sample prepared by 2 : 3 EtOH-LAG (sample *8* in Table S7.1); the diffraction patterns of the pure phases were simulated from the structures, except that of pure **1:2 RS/D**, which was taken as measured at synchrotron (sample *10* in Table S7.1)

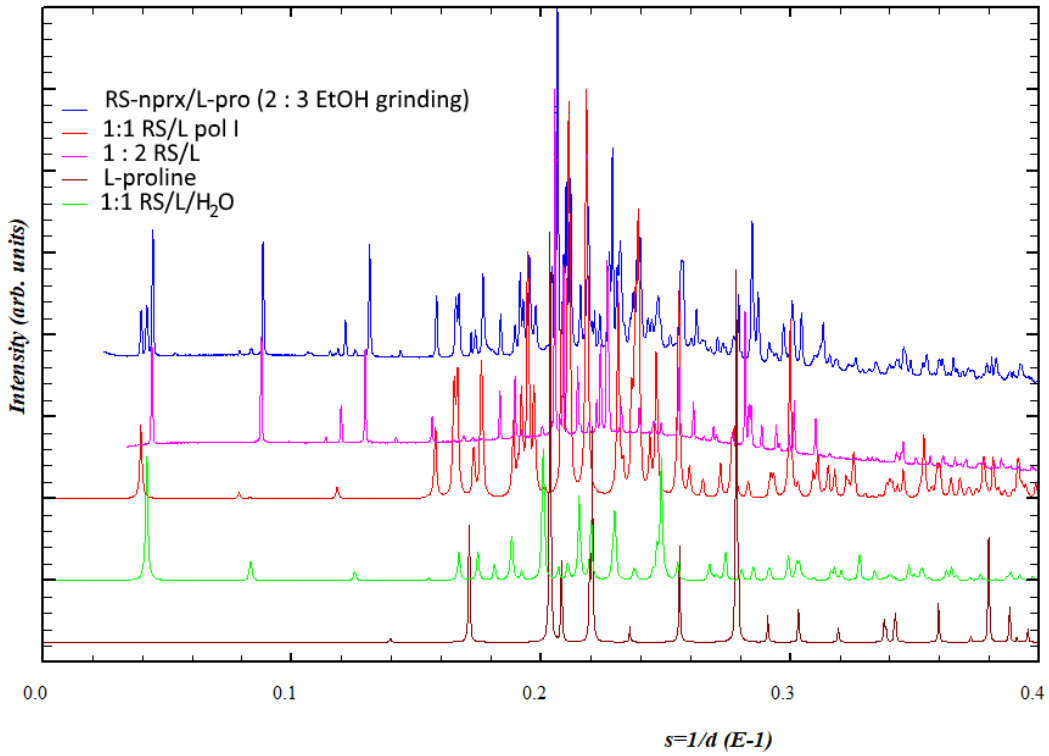

Figure S7.1.6. Diffraction pattern for the **RS/L** sample prepared by 2 : 3 ISPN-LAG (sample *12* in Table S7.1); the diffraction patterns of the pure phases were simulated from the structures, except that of pure **1:2 RS/D**, which was taken as measured at synchrotron (sample *10* in Table S7.1)

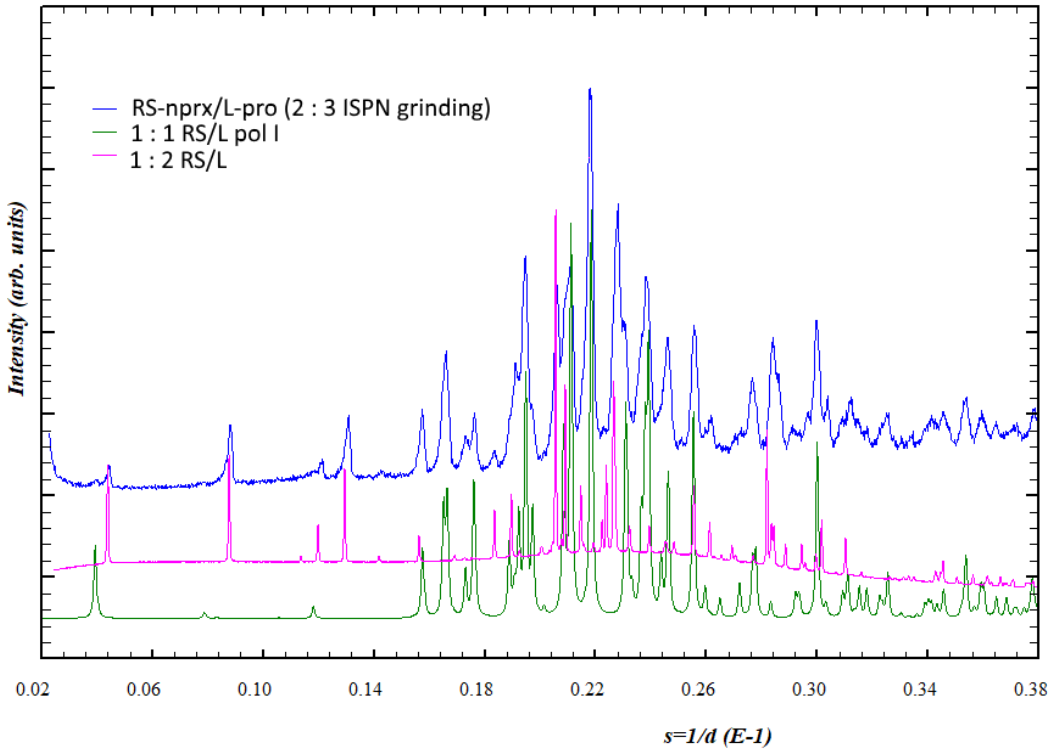

Figure S7.1.7. Diffraction pattern for the **RS/L** sample prepared by 1 : 1 ACN-LAG (sample *13* in Table S7.1); the diffraction patterns of the pure phases were simulated from the structures; the diffraction pattern of **1:1 RS/D pol II** was taken as measured at synchrotron (sample *13* in Table S6.1)

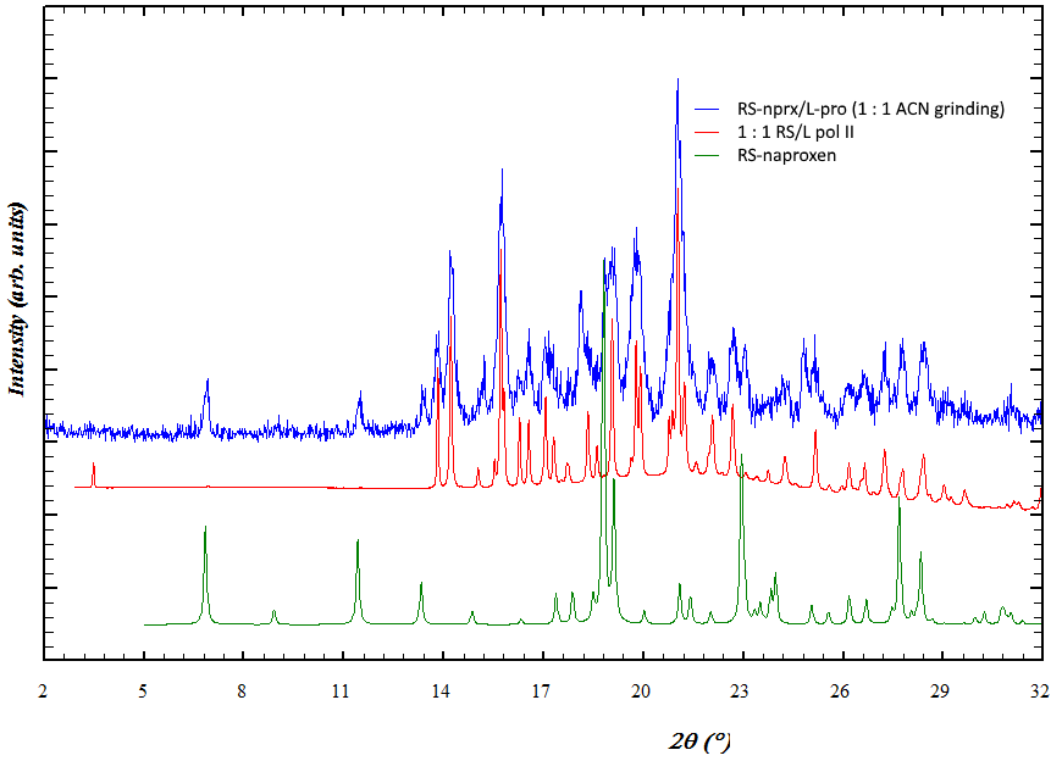

Figure S7.1.8. Diffraction pattern for the **RS/L** sample prepared by 1 : 2 ACN-LAG (samples *14* in Table S7.1); the diffraction patterns of the pure phases were simulated from the structures; the diffraction pattern of **1:1 RS/D pol II** was taken as measured at synchrotron (sample *13* in Table S6.1)

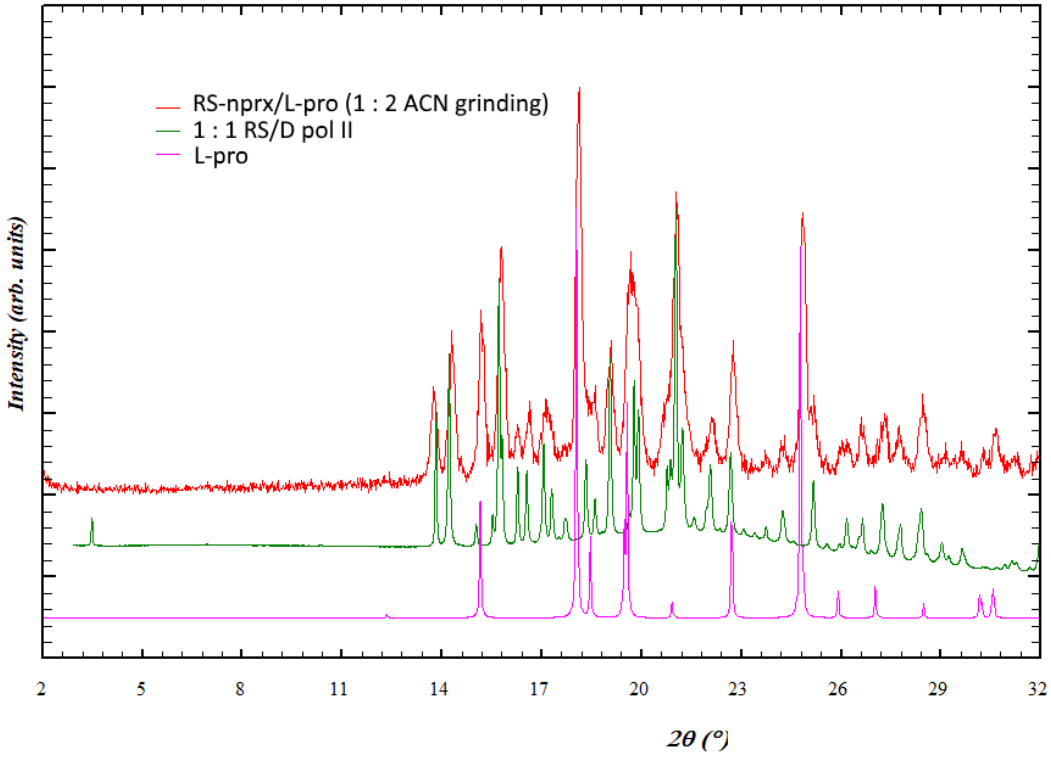

Figure S7.1.9. Diffraction pattern for the **RS/L** sample prepared by 2 : 1 ACN-LAG (sample *15* in Table S7.1); the diffraction patterns of the pure phases were simulated from the structures; the diffraction pattern of **1:1 RS/D pol II** was taken as measured at synchrotron (sample *13* in Table S6.1)

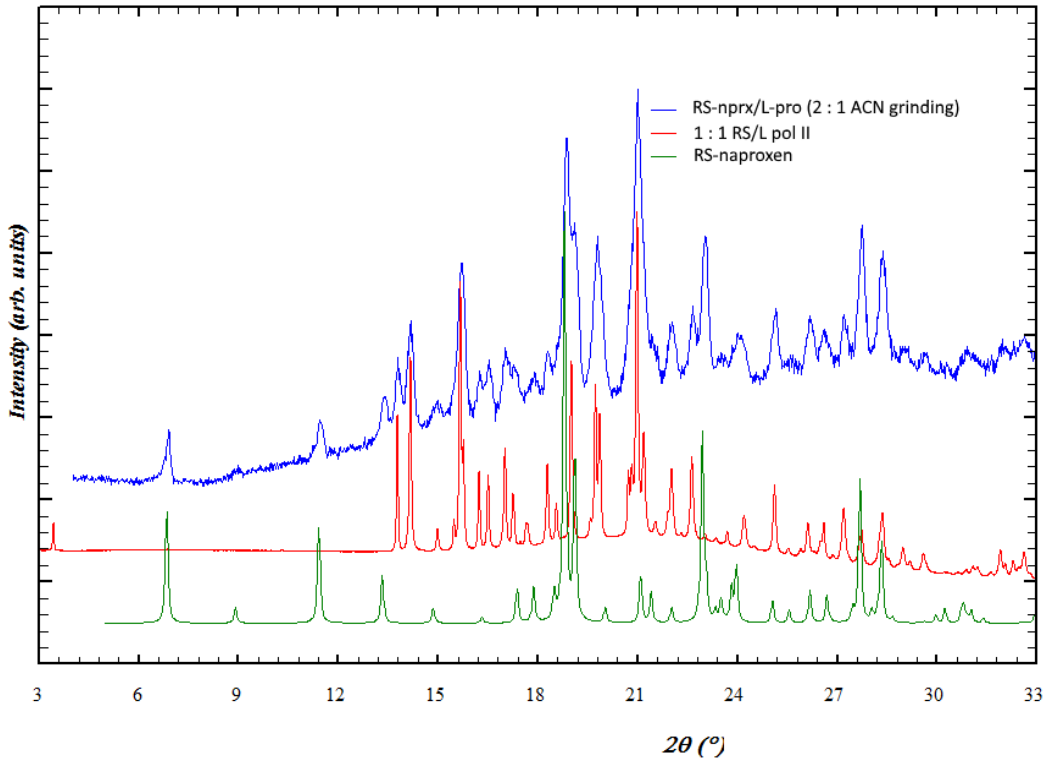

Figure S7.1.10. Diffraction pattern for the **RS/L** sample prepared by 2 : 3 ACN-LAG (sample *16* in Table S7.1); the diffraction pattern of **1:2 RS/D** was taken as measured at synchrotron (sample *10* in Table S7.1) and the diffraction pattern of **1:1 RS/D pol II** was taken as measured at synchrotron (sample *13* in Table S6.1)

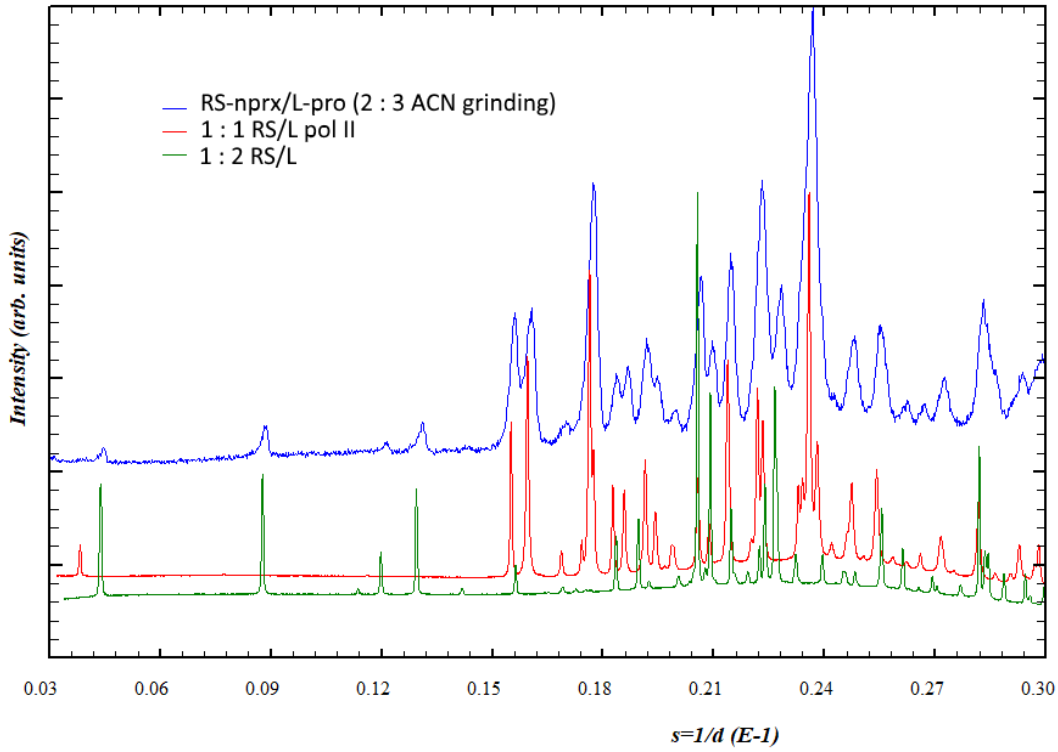

Figure S7.1.11. Diffraction pattern for the **RS/L** sample prepared by 1 : 2 water-assisted grinding (samples *18* in Table S7.1); the diffraction patterns of the pure phases were simulated from the structures

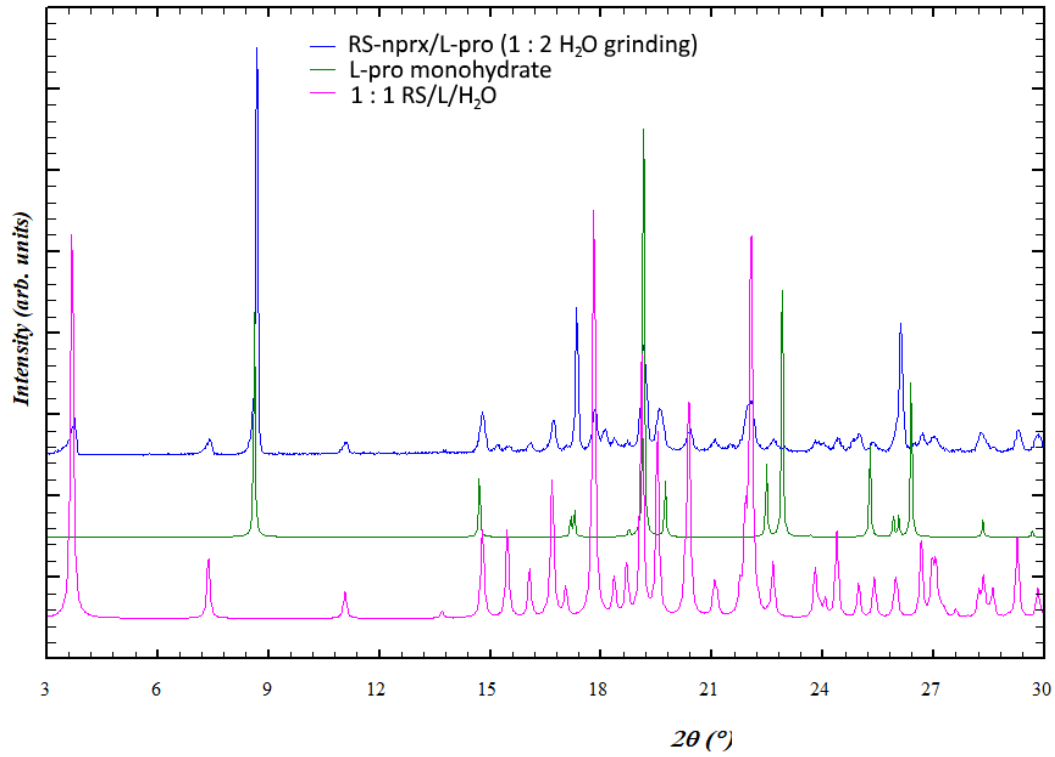

Figure S7.1.12. Diffraction pattern for the **RS/L** sample prepared by 2 : 3 water-assisted grinding (samples *19* in Table S7.1); the diffraction patterns of the pure phases were simulated from the structures

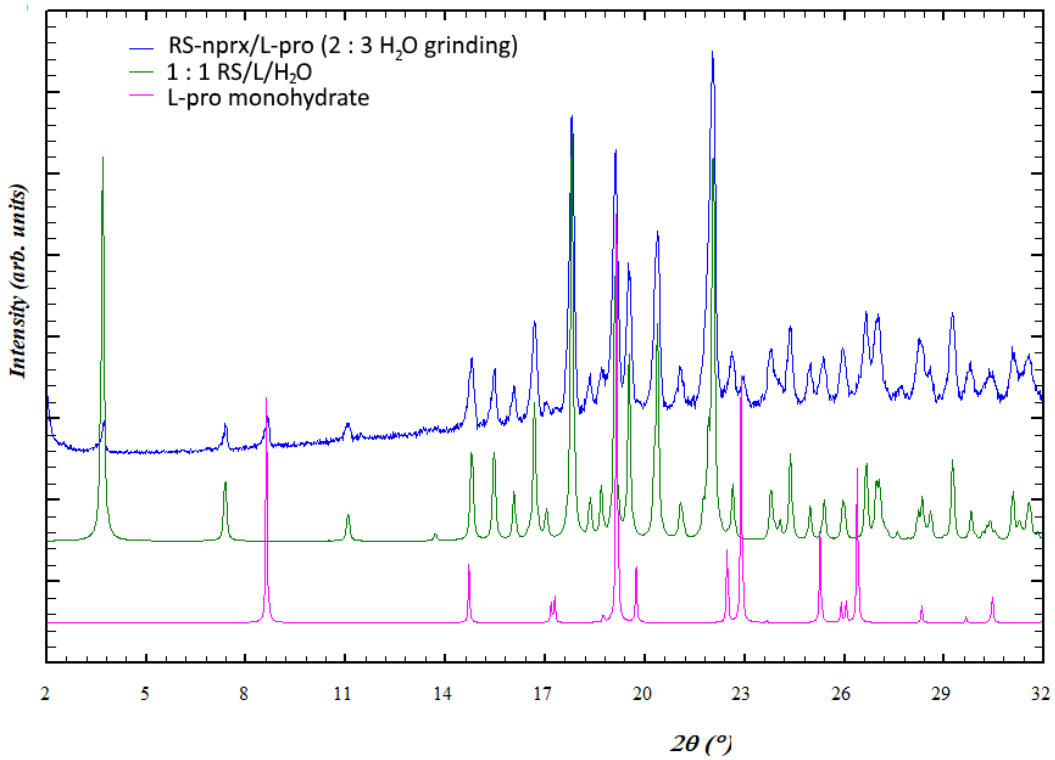

7.2 DSC data measured for a selected RS/L sample (Fig. S7.2.1)

Figure S7.2.1. DSC curve measured for the **RS/L** sample prepared by 1 : 2 ISPN-LAG (sample *10* in Table S7.1). The curve has two peaks, which, as follows from the *in-situ* PXRD data, corresponds to the melting point of the **1:1 RS/D pol I** phase and **1:1 RS/D**, respectively.

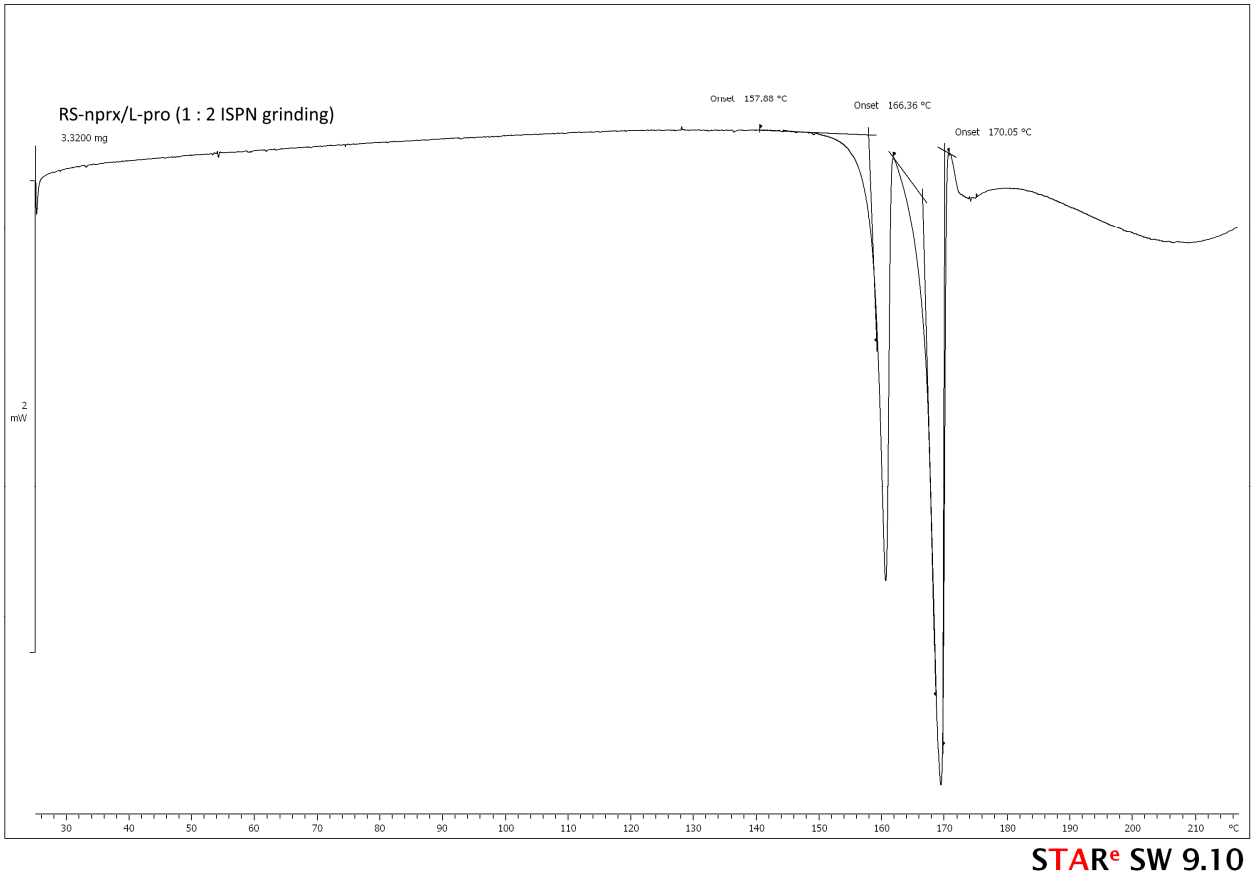

8. Details of LAG experiments and sample analysis for the RS/DL system (Table S8.1)

Table S8.1. Experimental details for laboratory liquid-assisted grinding and further analysis of obtained RS-naproxen/DL-proline cocrystals; lab XRD was performed at Cu*K*α radiation

	Molar ratio RS-Nprx/DL-Pro	Grinding conditions	PXRD analysis	Result	Structures determined from PXRD	Other analysis
1	1 : 1	60 min, 30 Hz, 2 μL MeOH	Synchrotron (λ = 0.776188 Å)	1:1 RS/DL pol I (**Fig. S8.1.1**)		DSC (determined the melting point of the **1:1 RS/DL pol I** phase, T_m **= 152(1)°C**) (**Fig. S8.2.1**)
2	1 : 2	60 min, 30 Hz, 10 μL MeOH	Synchrotron (λ = 0.708 Å) under variable temperature	Initially, the sample contained a mixture of 1:1 RS/DL, (1:2 S/DL + 1:2 R/DL), and DL-pro monohydrate; Upon heating DL-pro monohydrate transforms into DL-pro; then 1:1 RS/DL disappears and only the (1:2 S/DL + 1:2 R/DL) conglomerate is left. (**Fig. 10** in the main text)		
3	2 : 1	60 min, 30 Hz, 2 μL MeOH	Lab XRD	1:1 RS/DL pol I + RS-naproxen (**Fig. S8.1.2**)		
4	2 : 3	60 min, 30 Hz, 10 μL MeOH	Lab XRD	1:1 RS/DL pol I + (1:2 S/DL + 1:2 R/DL) (**Fig. S8.1.3**)		
5	1 : 1	60 min, 30 Hz, 10 μL EtOH	Lab XRD	1:1 RS/DL pol I (**Fig. S8.1.4**)		
6	1 : 2	60 min, 30 Hz, 10 μL EtOH	Lab XRD	1:1 RS/DL pol I + (1:2 S/DL+1:2 R/DL) (**Fig. S8.1.5**)		
7	2 : 1	60 min, 30 Hz, 10 μL EtOH	Lab XRD	1:1 RS/DL pol I + RS-naproxen (**Fig. S8.1.2**)		
8	2 : 3	60 min, 30 Hz, 10 μL EtOH	Lab XRD	1:1 RS/DL pol I + (1:2 S/DL + 1:2 R/DL) + RS-naproxen (**Fig. S8.1.3**)		
9	1 : 1	60 min, 30 Hz, 2 μL ISPN	Lab XRD	1:1 RS/DL pol I + (1:2 S/DL + 1:2 R/DL) + RS-naproxen (**Fig. S8.1.4**)		
10	1 : 2	60 min, 30 Hz, 10 μL ISPN	Lab XRD	1:1 RS/DL pol I + (1:2 S/DL + 1:2 R/DL) (**Fig. S8.1.5**)		
11	2 : 1	60 min, 30 Hz, 10 μL ISPN	Lab XRD	1:1 RS/DL pol I + RS-naproxen (**Fig. S8.1.2**)		

12	2 : 3	60 min, 30 Hz, 10 μL ISPN	Lab XRD	1:1 RS/DL pol I + (1:2 S/DL + 1:2 R/DL) (**Fig. S8.1.3**)		
13	1 : 1	60 min, 30 Hz, 2 μL ACN	Synchrotron (λ = 0.776188 Å)	1:1 RS/DL pol I + RS-nprx (**Fig. S8.1.6**)		
14	1 : 2	60 min, 30 Hz, 10 μL ACN	Lab XRD	(1:2 S/DL + 1:2 R/DL) (**Fig. S8.1.5**)		DSC (determined the eutectic point of the **(1:2 S/DL + 1:2 R/DL)** conglomerate phase, T_{et} = **168(1)°C**) (**Fig. S8.2.2**)
15	2 : 1	60 min, 30 Hz, 2 μL ACN	Lab XRD	1:1 RS/DL pol I + RS-naproxen (**Fig. S8.1.2**)		
16	2 : 3	60 min, 30 Hz, 10 μL ACN	Lab XRD	1:1 RS/DL pol I + (1:2 S/DL + 1:2 R/DL) (**Fig. S8.1.3**)		
17	1 : 1	60 min, 30 Hz, 2 μL H_2O	Synchrotron (λ = 0.78487 Å) under variable temperature	Initially the sample contained 1:1 RS/DL/H_2O, RS-nprx, and DL-pro monohydrate; upon heating, first 1:1 RS/DL/H_2O and DL-pro monohydrate disappear and 1:1 RS/DL pol II emerges; upon further heating RS-nprx disappears, and finally 1:1 RS/DL pol II melts (**Fig. 12** in the main text)	1:1 RS/DL pol II (for Rietveld refinement see **Fig. S2.5**)	
18	2 : 1	60 min, 30 Hz, 10 μL H_2O	Lab XRD	1:1 RS/DL/H_2O + RS-nprx + DL-pro monohydrate (**Fig. S8.1.7**)		
19	2 : 3	60 min, 30 Hz, 10 μL H_2O	Lab XRD	1:1 RS/DL/H_2O + RS-nprx + DL-pro monohydrate (**Fig. S8.1.7**)		

8.1 PXRD analysis of the RS/DL samples (Figs. S8.1.1-S8.1.7)

Figure S8.1.1. Diffraction pattern for the **RS/DL** sample prepared by 1 : 1 MeOH-LAG (samples *1* in Table S8.1); the diffraction patterns of the pure phases were simulated from the structures

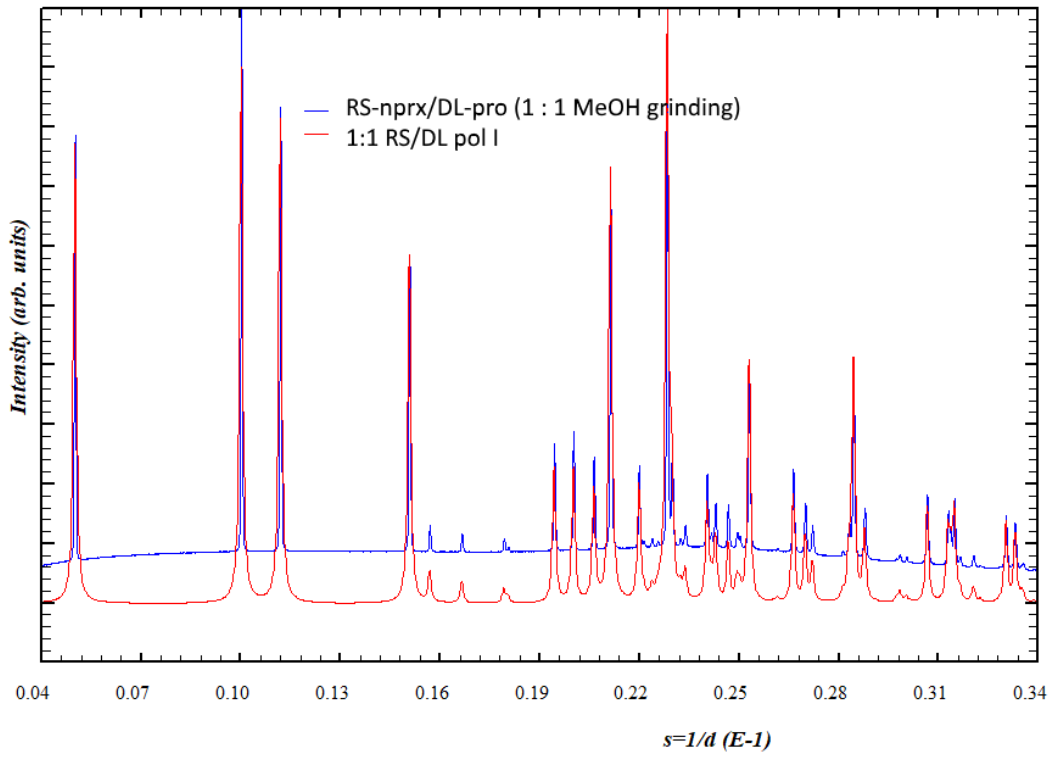

Figure S8.1.2. Diffraction patterns for the **RS/DL** samples prepared by 2 : 1 MeOH-, EtOH-, ACN,-and ISPN-LAG (samples *3*, *7*, *11* and *15* in Table S8.1); the diffraction patterns of the pure phases were simulated from the structures

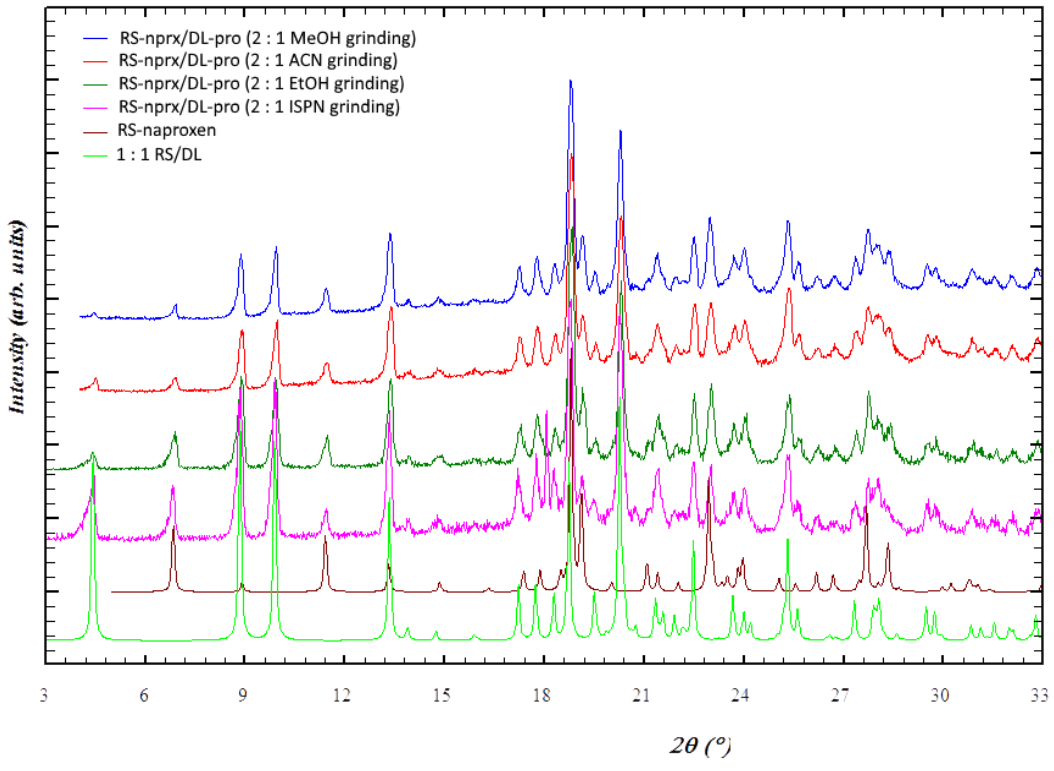

Figure S8.1.3. Diffraction patterns for the **RS/DL** samples prepared by 2 : 3 MeOH-, EtOH-, ACN,-and ISPN-LAG (samples *4*, *8*, *12* and *16* in Table S8.1); the diffraction patterns of the pure phases were simulated from the structures

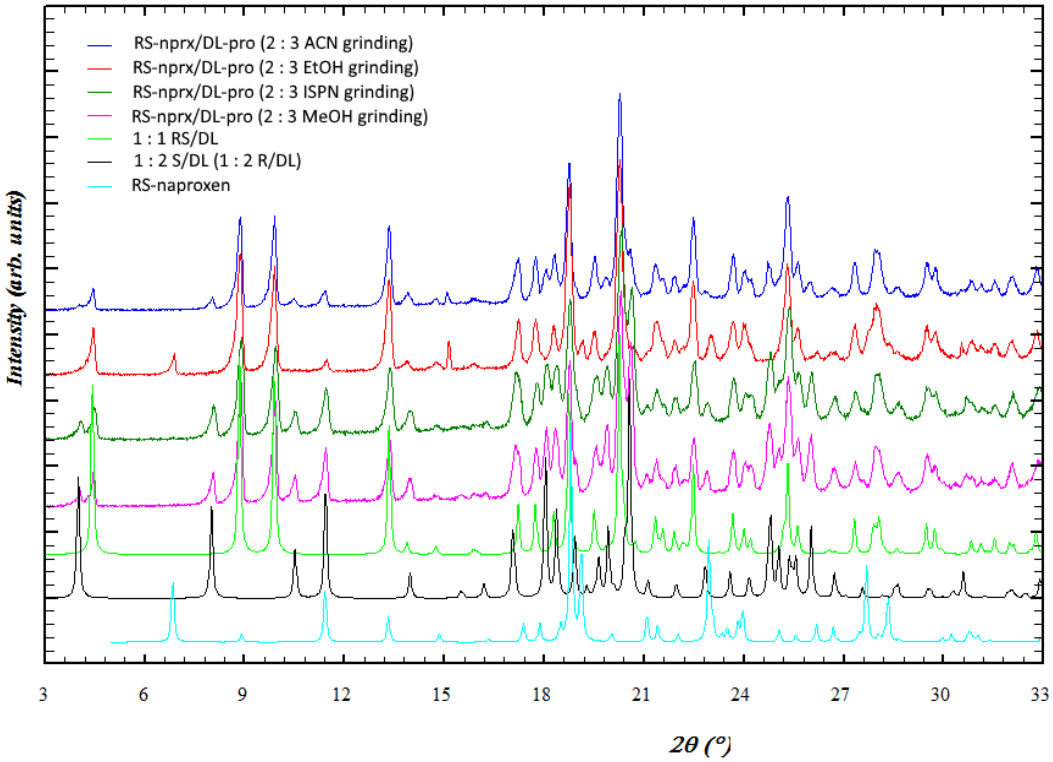

Figure S8.1.4. Diffraction patterns for the **RS/DL** samples prepared by 1 : 1 EtOH- and ISPN-LAG (samples *5* and *9* in Table S8.1); the diffraction patterns of the pure phases were simulated from the structures

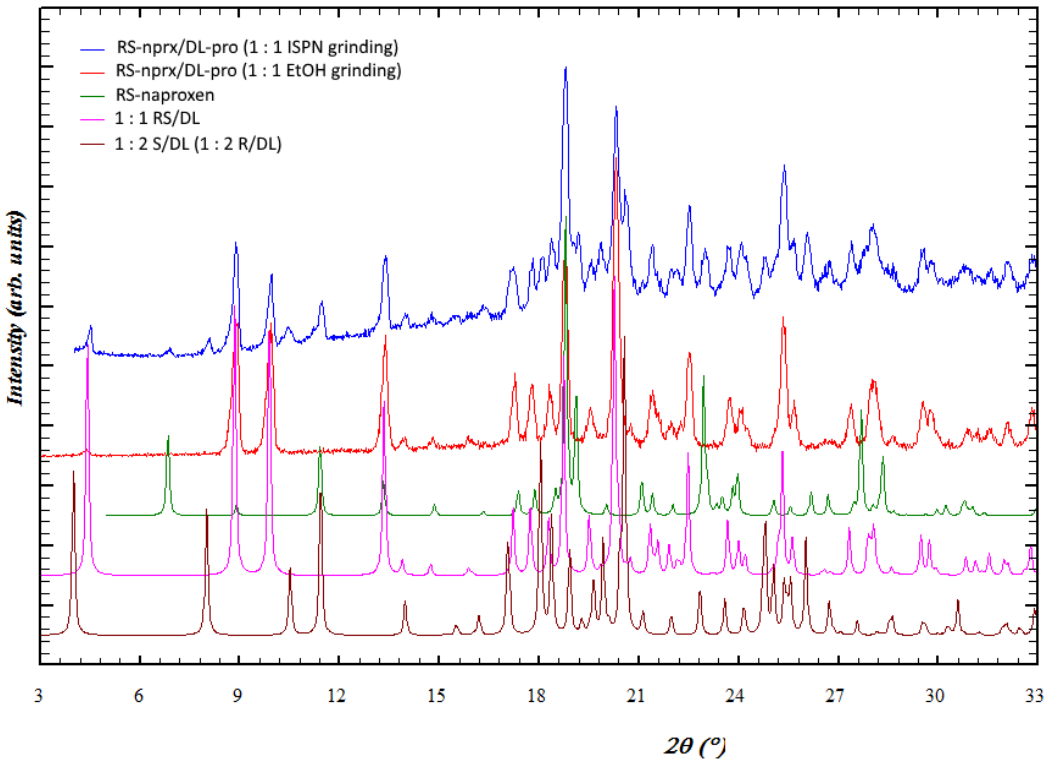

Figure S8.1.5. Diffraction patterns for the **RS/DL** samples prepared by 1 : 2 MeOH-, EtOH-, ACN,-and ISPN-LAG (samples *2*, *6*, *10* and *14* in Table S8.1); the diffraction patterns of the pure phases were simulated from the structures

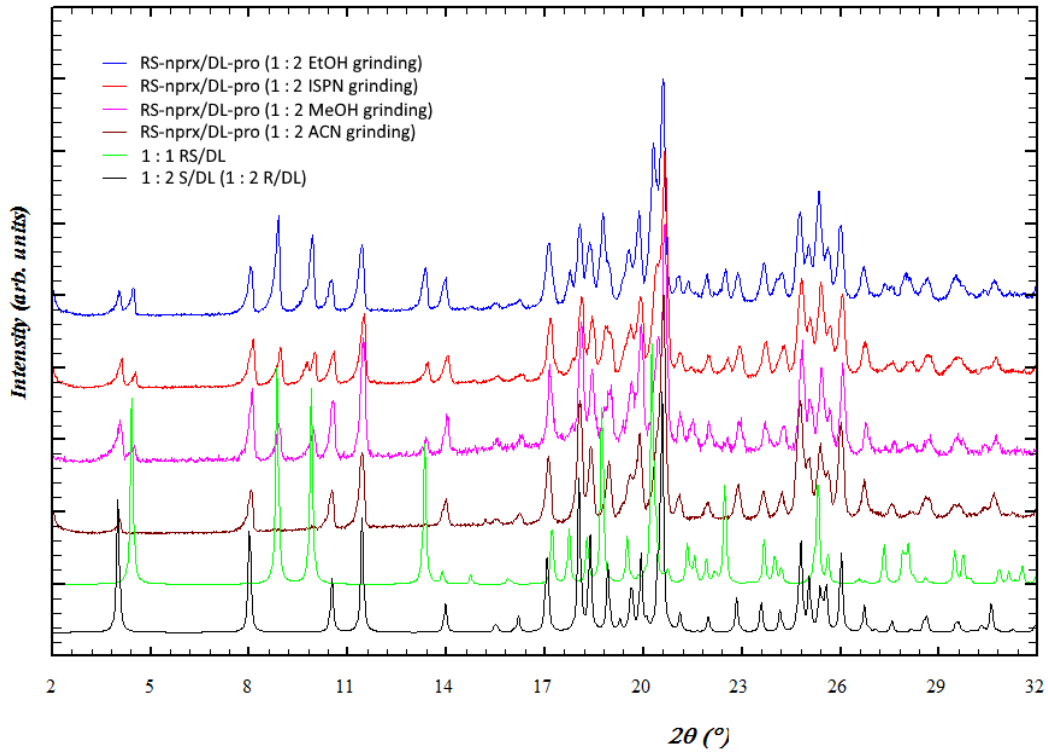

Figure S8.1.6. Diffraction pattern for the **RS/DL** sample prepared by 1 : 1 ACN-LAG (samples *13* in Table S8.1); the diffraction patterns of the pure phases were simulated from the structures

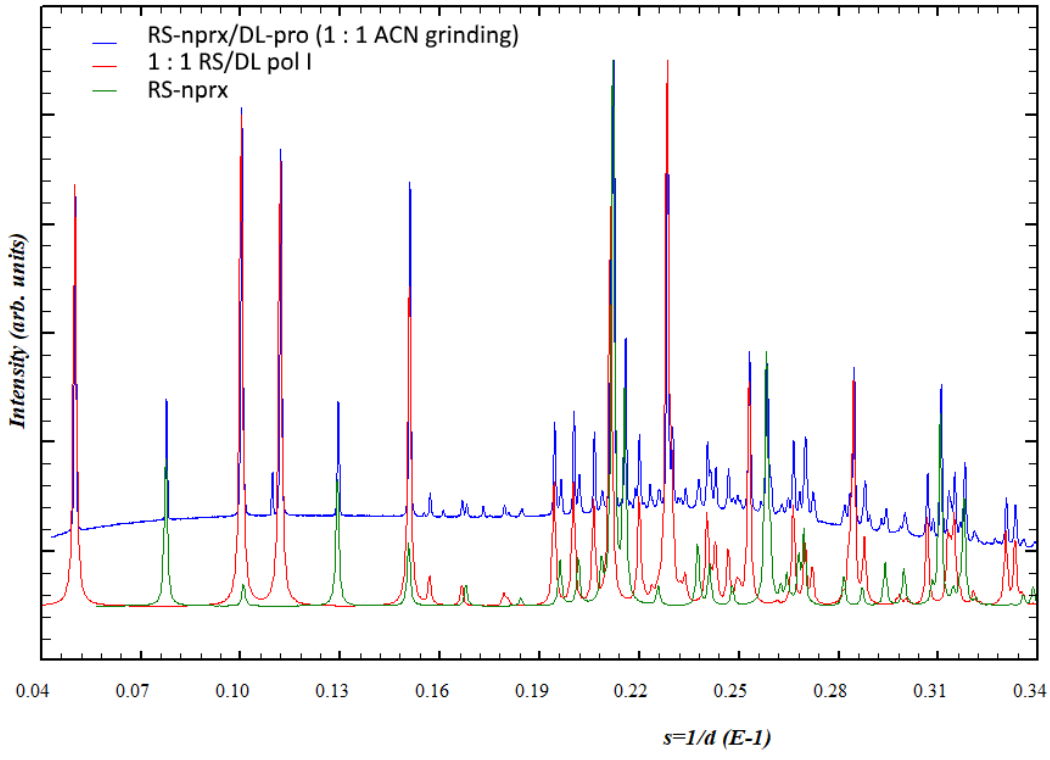

Figure S8.1.7. Diffraction patterns for the **RS/DL** samples prepared by water-assisted grinding in 1 : 1, 1 : 2, and 2 : 3 ratios (samples *17-19* in Table S8.1); the diffraction patterns of the pure phases were simulated from the structures

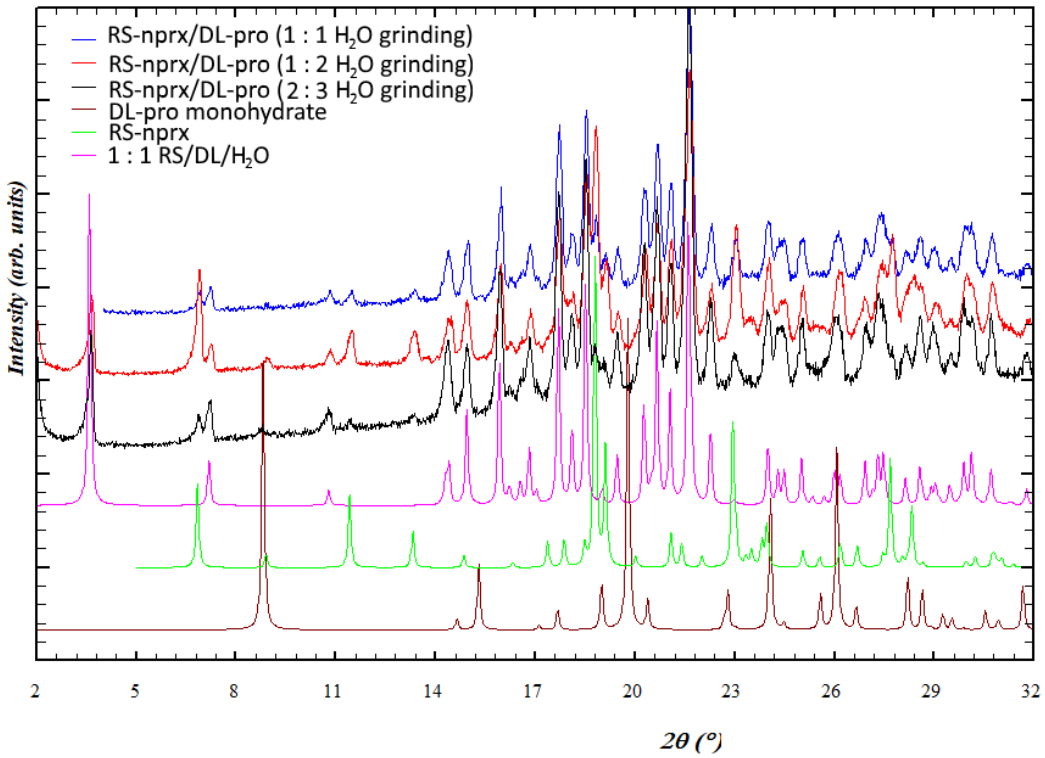

8.2 DSC measured for selected RS/DL samples (Figs. S8.2.1-S8.2.2)

Figure S8.2.1. DSC curve measured for the **RS/DL** sample prepared by 1 : 1 MeOH-LAG (sample *1* in Table S8.1). The curve has only one peak corresponding to the melting point of the **1:1 RS/DL pol I** cocrystal.

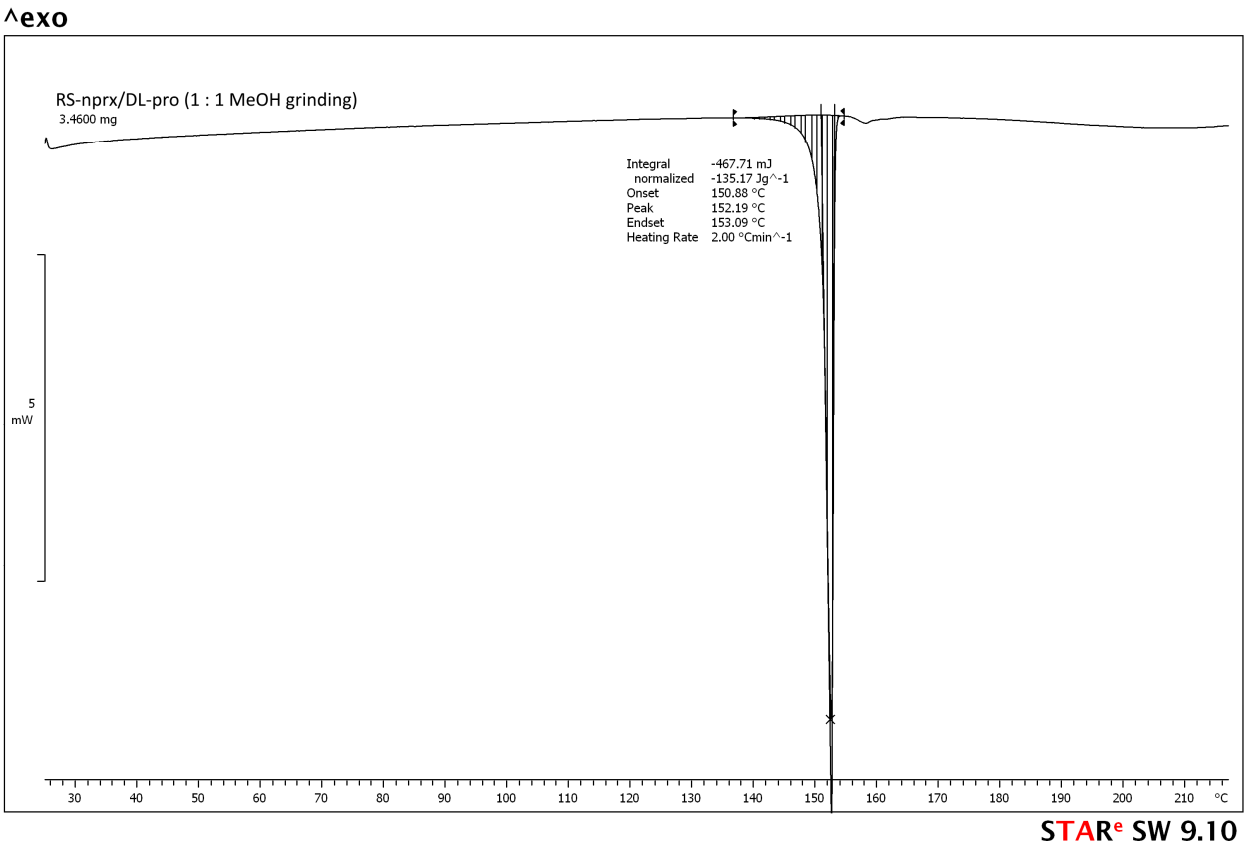

Figure S8.2.2. DSC curve measured for the **RS/DL** sample prepared by 1 : 2 ACN-LAG (sample *14* in Table S8.1). The curve has only one peak corresponding to the eutectic point of the (**1:2 S/DL + 1:2 R/DL**) conglomerate.

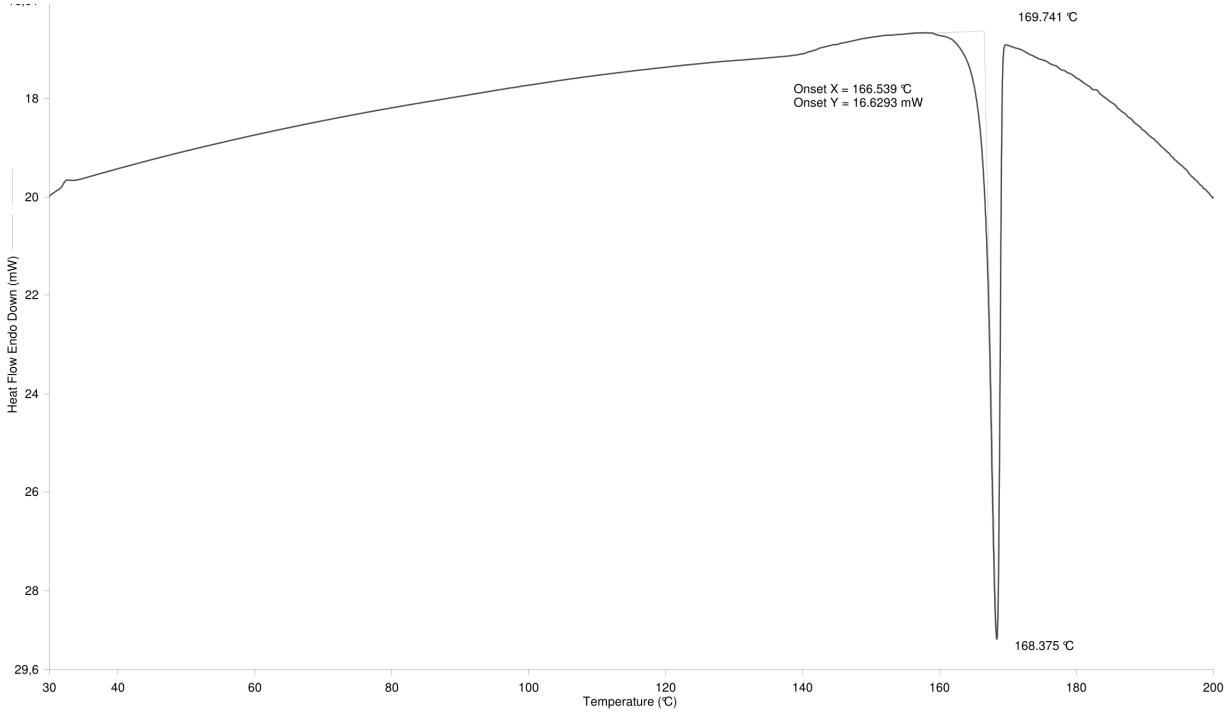

9. Details of LAG experiments and sample analysis for the S/DL system (Table S9.1)

Table S9.1 Experimental details for laboratory liquid-assisted grinding and further analysis of obtained S-naproxen/DL-proline cocrystals; lab XRD was performed at Cu*K*α radiation

	Molar ratio S-Nprx/DL-Pro	Grinding conditions	PXRD analysis	Result	Structures determined from PXRD	Other analysis
1	1 : 1	60 min, 30 Hz, 2 μL MeOH	Synchrotron (λ = 0.77663 Å) under variable temperature	Initially, the sample contained a mixture of 1:1 S/DL, 1:2 S/DL, and 1:1 S/DL/H_2O Upon heating 1:1 S/DL/H_2O disappears first; Further heating leads to the disappearance of 1:1 S/DL, and finally 1:2 S/DL (**Fig. 5** in the main text)		DSC (**Fig. S9.3.1**)
2	1 : 2	60 min, 30 Hz, 10 μL MeOH	Synchrotron (λ = 0.62127 Å)	1:2 S/DL (**Fig. S9.2.1**)		DSC (determined the melting point of the **1:2 S/DL** phase, T_m **= 182(1)°C**) (**Fig. S9.3.2**)
3	2 : 1	60 min, 30 Hz, 10 μL MeOH	Synchrotron (λ = 0.62127 Å)	1:1 S/DL + S-nprx (**Fig. S9.2.3**)		
4	2 : 3	60 min, 30 Hz, 10 μL MeOH	Lab XRD	1:1 S/DL + 1:2 S/DL (**Fig. S9.2.4**)		
5	1 : 1	60 min, 30 Hz, 10 μL EtOH	Lab XRD	1:1 S/DL + S-nprx (**Fig. S9.2.5**)		DSC (**Fig. S9.3.3**)
6	1 : 2	60 min, 30 Hz, 10 μL EtOH	Lab XRD	1:2 S/DL (**Fig. S9.2.2**)		
7	2 : 1	60 min, 30 Hz, 10 μL EtOH	Lab XRD	1:1 S/DL + S-nprx (**Fig. S9.2.3**)		
8	2 : 3	60 min, 30 Hz, 10 μL EtOH	Lab XRD	1:1 S/DL + 1:2 S/DL (**Fig. S9.2.4**)		
9	1 : 1	60 min, 30 Hz, 5 μL ISPN	Synchrotron (λ = 0.77663 Å) under variable temperature	Initially, the sample contained a mixture of 1:1 S/DL, 1:2 S/DL, and 1:1 S/DL/H_2O Upon heating 1:1 S/DL/H_2O disappears first; Further heating leads to the disappearance of 1:1 S/DL, and finally 1:2 S/DL **(Fig. S9.1.1)**		DSC (**Fig. S9.3.4**)
10	1 : 2	60 min, 30 Hz, 10 μL ISPN	Lab XRD	1:2 S/DL (**Fig. S9.2.2**)		
11	2 : 1	60 min, 30 Hz, 10 μL ISPN	Synchrotron (λ = 0.708 Å) under variable	Initially, the sample contained a mixture of 1:1 S/DL, S-nprx, and 1:1 S/DL/H_2O Upon heating 1:1 S/DL/H_2O and S-nprx disappear,		

			temperature	followed by the emergence of 1:2 S/DL **(Fig. S9.1.3)**		
12	2 : 3	60 min, 30 Hz, 10 µL ISPN	Lab XRD	1:1 S/DL + 1:2 S/DL (**Fig. S9.2.4**)		
13	1 : 1	60 min, 30 Hz, 5 µL ACN	Synchrotron (λ = 0.62127 Å) under variable temperature	Initially, the sample contained a mixture of 1:1 S/DL, 1:2 S/DL, S-nprx, and 1:1 S/DL/H_2O Upon heating 1:1 S/DL/H_2O disappears first; Further heating leads to the disappearance of 1:1 S/DL and S-nprx, and, finally, 1:2 S/DL **(Fig. S9.1.2)**		DSC (**Fig. S9.3.5**)
14	1 : 2	60 min, 30 Hz, 10 µL ACN	Lab XRD	1:2 S/DL (**Fig. S9.2.2**)		
15	2 : 1	60 min, 30 Hz, 2 µL ACN	Lab XRD	1:1 S/DL + S-nprx (**Fig. S9.2.3**)		
16	2 : 3	60 min, 30 Hz, 10 µL ACN	Lab XRD	1:1 S/DL + 1:2 S/DL + probably small amount of S-naproxen (**Fig. S9.2.4**)		
17	1 : 1	60 min, 30 Hz, 5 µL H_2O	Synchrotron (λ = 0.798 Å) under variable temperature	1:1 S/DL/H_2O + S-nprx The initial sample contained 1:1S/DL/H_2O and a very small amount of S-nprx; Upon heating 1:1 S/DL/H_2O disappears and a mixture of the 1:1 S/DL and 1:2 S/DL emerges with the amount of S-nprx increased; Further heating leads to the disappearance of the 1:1 S/DL phase, and finally only the 1:2 S/DL phase is left, which later melts as well. (**Fig. 6** in the main text)	1:1 S/DL/H_2O (for Rietveld refinement see **Fig. S2.6**)	TGA **(Fig. S9.3.6)**
18	1 : 2	60 min, 30 Hz, 5 µL H_2O	Lab XRD	1:1 S/DL/H_2O + 1:2 S/DL + S-nprx + DL-proline monohydrate (**Fig. S9.2.6)**		
19	2 : 1	60 min, 30 Hz, 5 µL H_2O	Lab XRD	1:1 S/DL/H_2O + S-nprx (**Fig. S9.2.7)**		
20	2 : 3	60 min, 30 Hz, 5 µL H_2O	Lab XRD	1:1 S/DL/H_2O + S-nprx + DL-proline monohydrate (**Fig. S9.2.8)**		

9.1 PXRD upon varied temperature for the S/DL system (Figs. S9.1.1-S9.1.4)

Figure S9.1.1 PXRD patterns measured *in situ* upon heating (from 31 to 168 °C, 2 °C/min) for the **S/DL** sample prepared by 1 : 1 ISPN-LAG (sample *9* in Table S9.1), λ = 0.77663 Å: (left) film representation; (right) XRD patterns at selected temperatures: *T* = 31 °C – **1:1 S/DL**, **1:2 S/DL**, and **1:1 S/DL/H_2O** (marked as '*'); *T* = 99 °C – **1:1 S/DL** and **1:2 S/DL**; and *T* = 150 °C – **1:2 S/DL**.

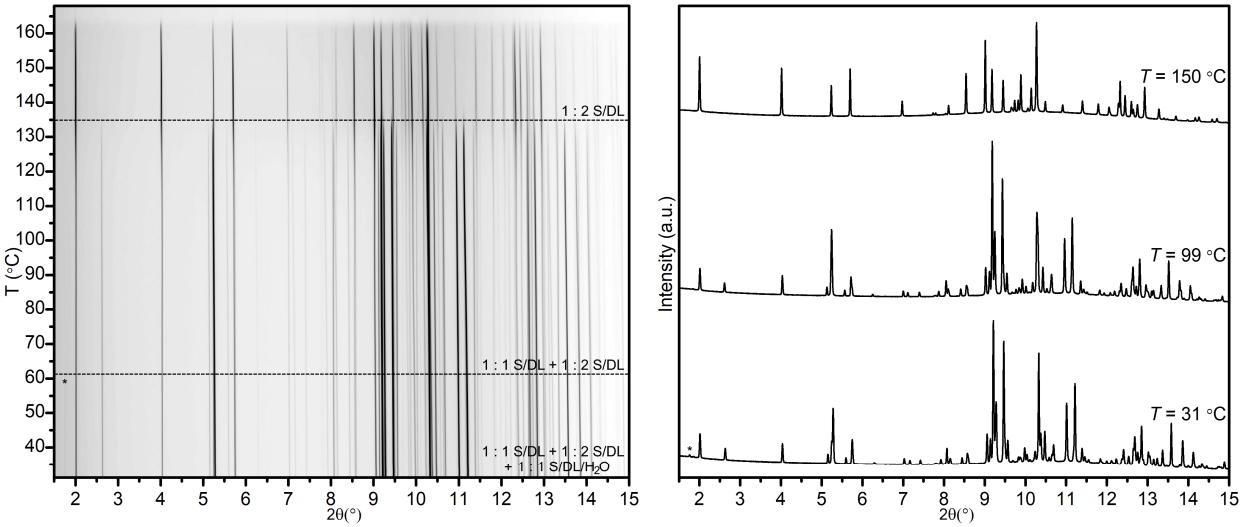

Figure S9.1.2 PXRD patterns measured *in situ* upon heating (from 36 to 173 °C, 2 °C/min) for the **S/DL** sample prepared by 1 : 1 ACN-LAG (sample *13* in Table S9.1), λ = 0.62127 Å: (left) film representation; (right) XRD patterns at selected temperatures: *T* = 31 °C – **1:1 S/DL**, **1:2 S/DL**, **S-nprx** (marked as '†'), and **1:1 S/DL/H_2O** (marked as '*'); *T* = 109 °C – **1:1 S/DL**, **1:2 S/DL**, and **S-nprx**; and *T* = 148 °C – **1:2 S/DL**.

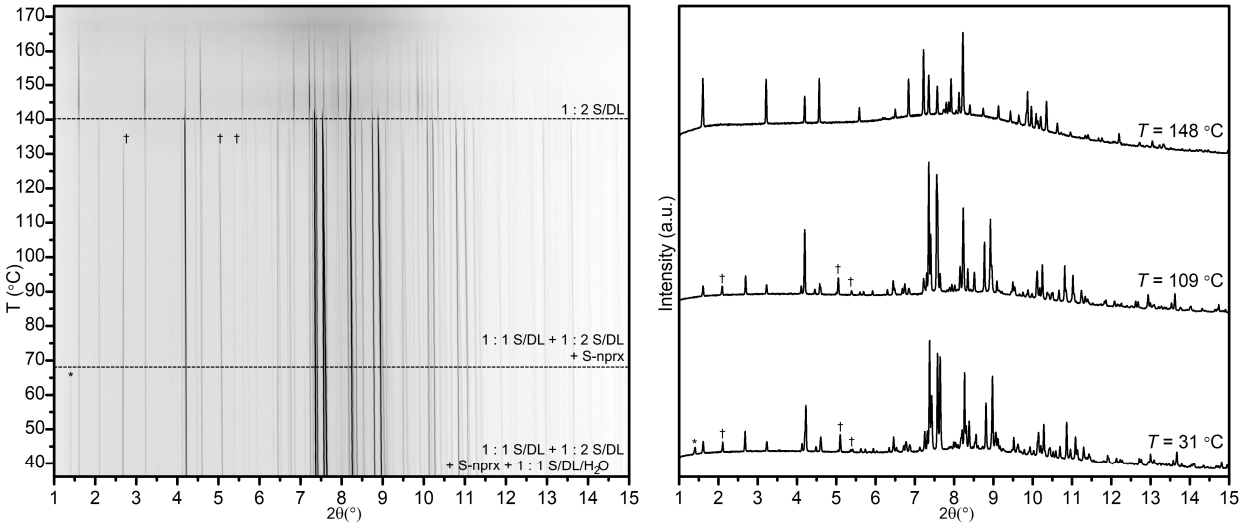

Figure S9.1.3 PXRD patterns measured *in situ* upon heating (from 39 to 145 °C, 2 °C/min) for the **S/DL** sample prepared by 2 : 1 ISPN-LAG (sample *11* in Table S9.1), λ = 0.708 Å: (left) film representation; (right) XRD patterns at selected temperatures: *T* = 39 °C – **1:1 S/DL**, **S-nprx** (marked as '†'), and **1:1 S/DL/H_2O** (marked as '*'); *T* = 138 °C – **1:2 S/DL**.

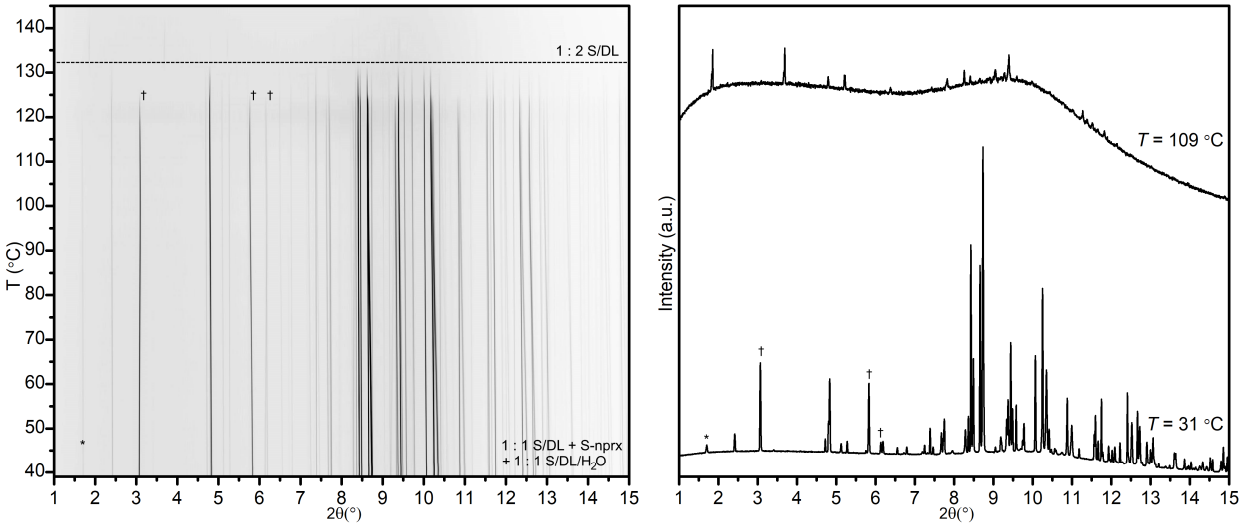

Figure S9.1.4 Comparison of the PXRD patterns measured *in situ* at *T* = 31 °C for the samples prepared by 1 : 1 MeOH- and water-LAG (samples *1* and *17* in Table S9.1). The figure confirms that both samples contain the same phase: **1:1 S/DL/H_2O**.

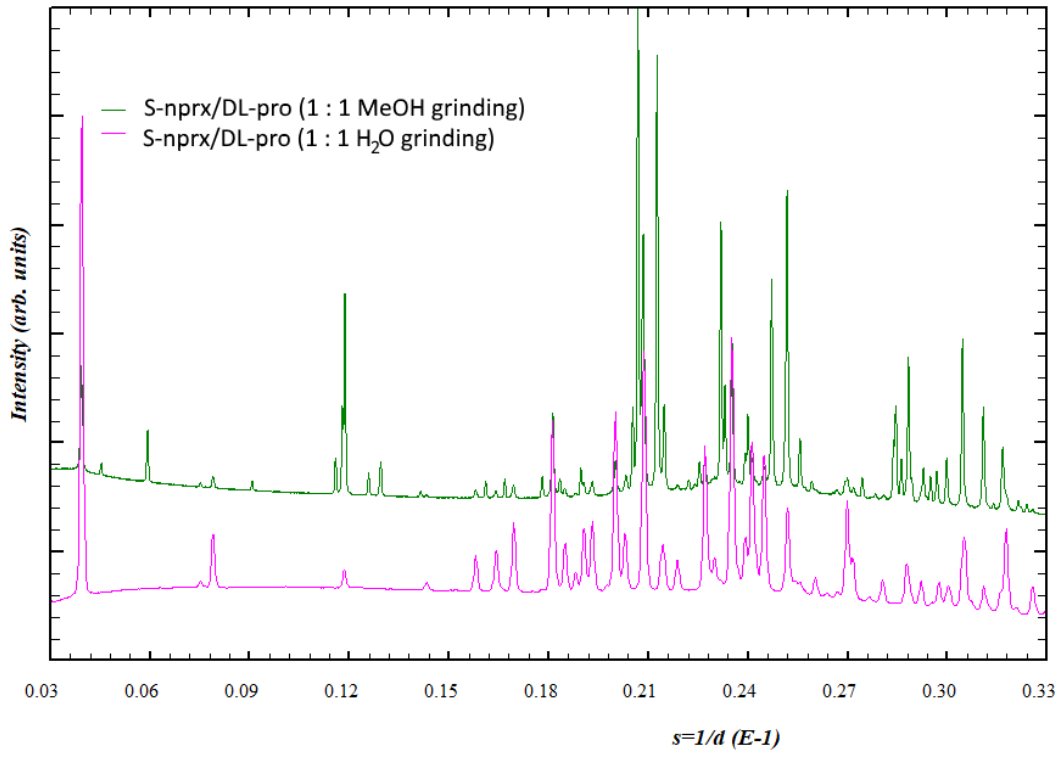

9.2 PXRD analysis of the S/DL samples (Figs. S9.2.1-S9.2.8)

Figure S9.2.1. Rietveld refinement plot for the **S/DL** sample obtained by 1 : 2 MeOH-LAG (sample *2* in Table S9.1); percentages are given in wt %; red and blue lines represent calculated and experimental data, respectively; grey line corresponds to the difference profile; and blue marks below represent Bragg positions for **1:2 S/DL**; unit cell, profile parameters, and zero point were refined.

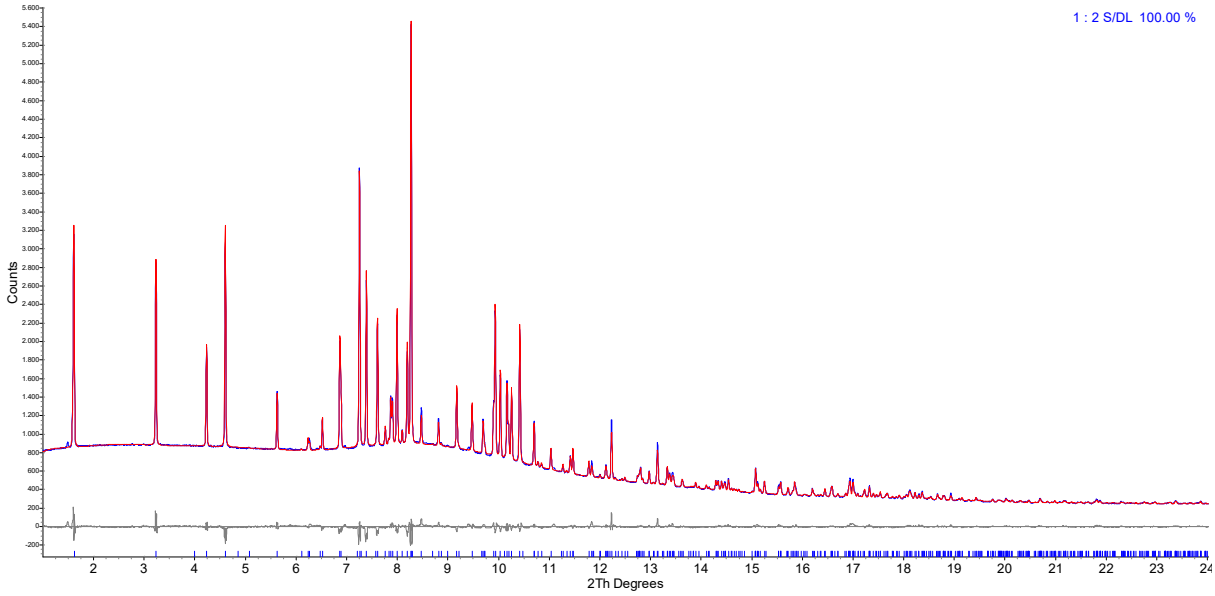

Figure S9.2.2. Diffraction patterns for the **S/DL** samples prepared by 1 : 2 MeOH-, EtOH-, ACN-, and ISPN-LAG (samples *2*, *6*, *10* and *14* in Table S9.1); the diffraction pattern of the **1:2 S/DL** cocrystal was simulated from the structure

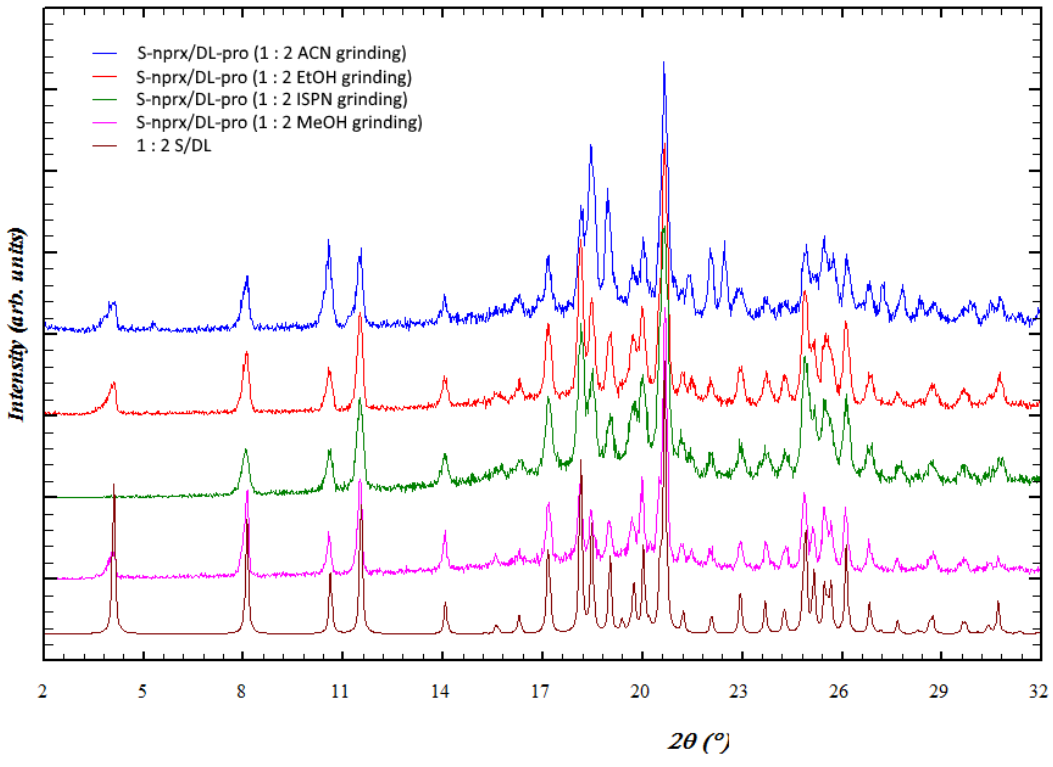

Figure S9.2.3. Diffraction patterns for the **S/DL** samples prepared by 2 : 1 MeOH-, EtOH-, ACN-, and ISPN-LAG (samples *3*, *7*, *11* and *15* in Table S9.1); the diffraction patterns of the pure phases were simulated from the structure

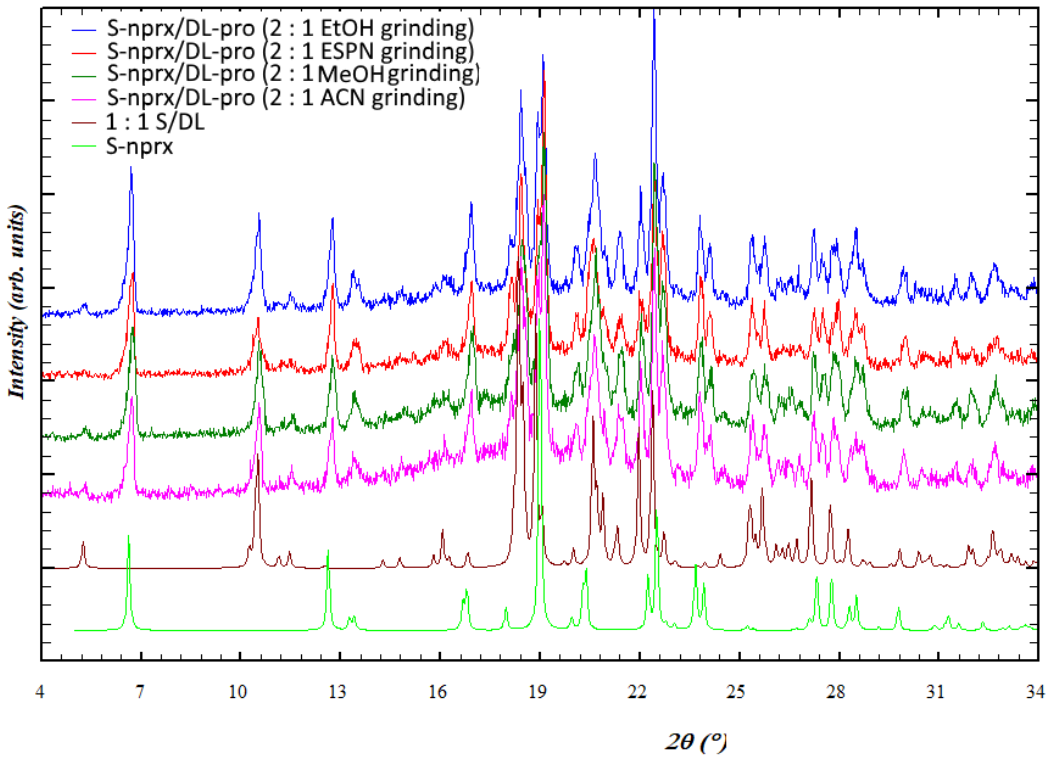

Figure S9.2.4. Diffraction patterns for the **S/DL** samples prepared by 2 : 3 MeOH-, EtOH-, ACN-, and ISPN-LAG (samples *4*, *8*, *12* and *16* in Table S9.1); the diffraction patterns of the pure phases were simulated from the structure

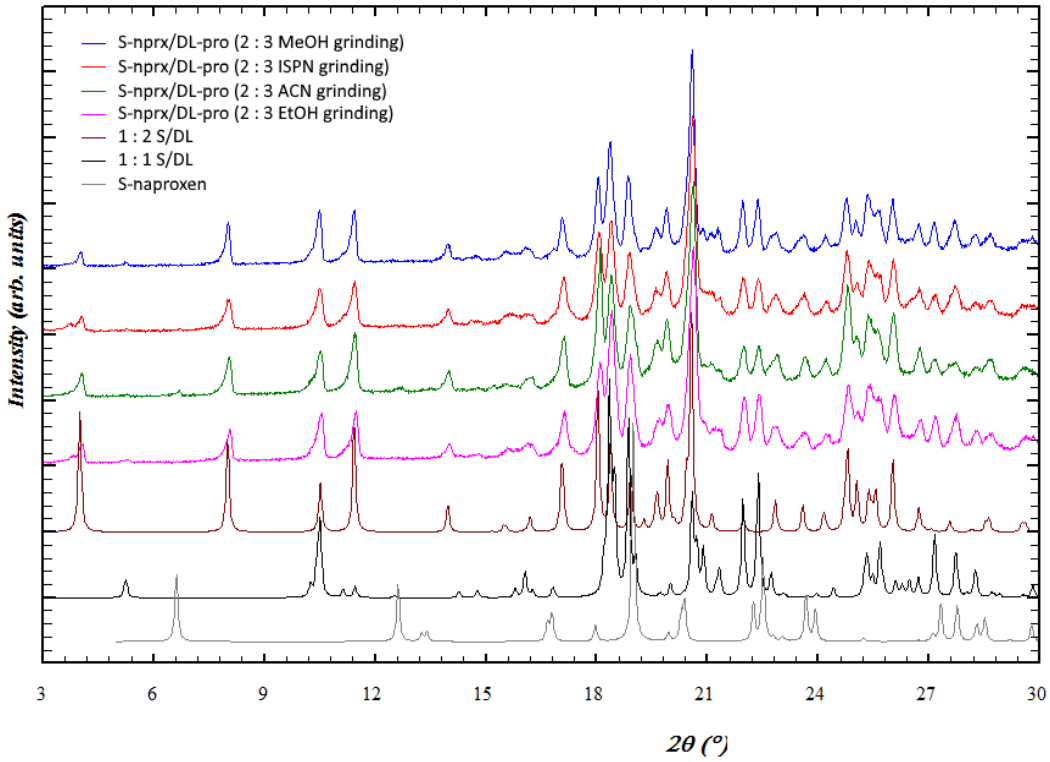

Figure S9.2.5. Diffraction pattern for the **S/DL** sample prepared by 1 : 1 EtOH-LAG (samples *5* in Table S9.1); the diffraction patterns of the pure phases were simulated from the structure

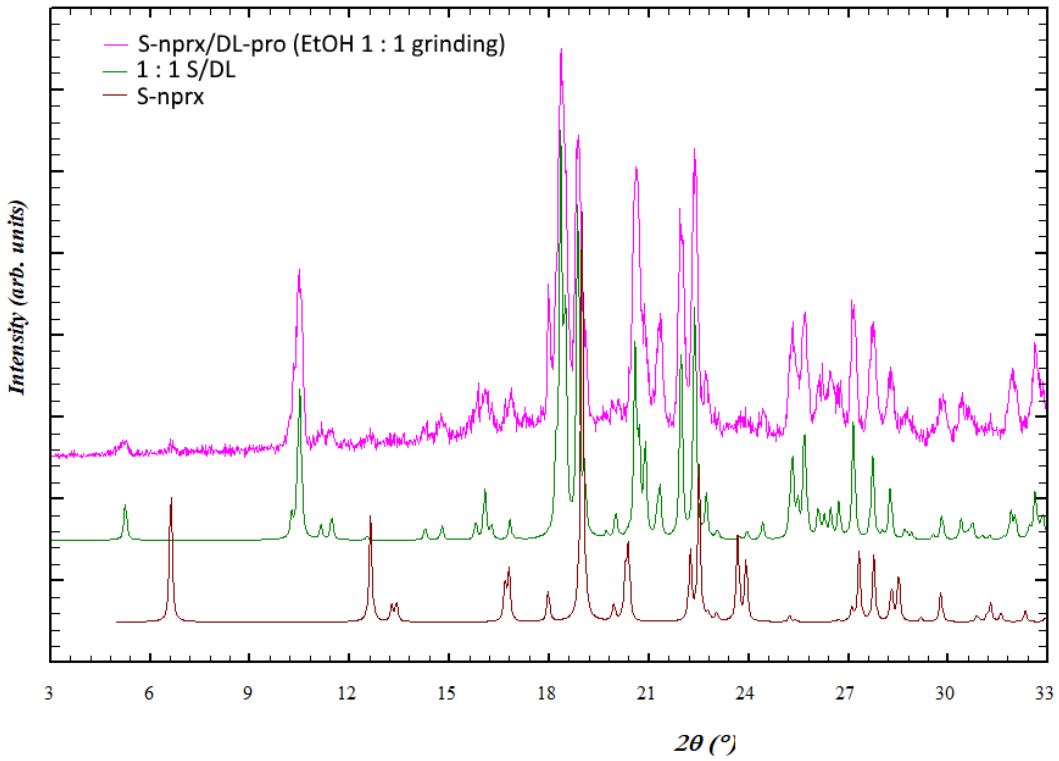

Figure S9.2.6. Diffraction pattern for the **S/DL** sample prepared by 1 : 2 water-LAG (samples *18* in Table S9.1); the diffraction patterns of the pure phases were simulated from the structure, except that of **1:1 S/DL/H_2O** which was taken as measured at synchrotron (sample *17* in Table S9.1)

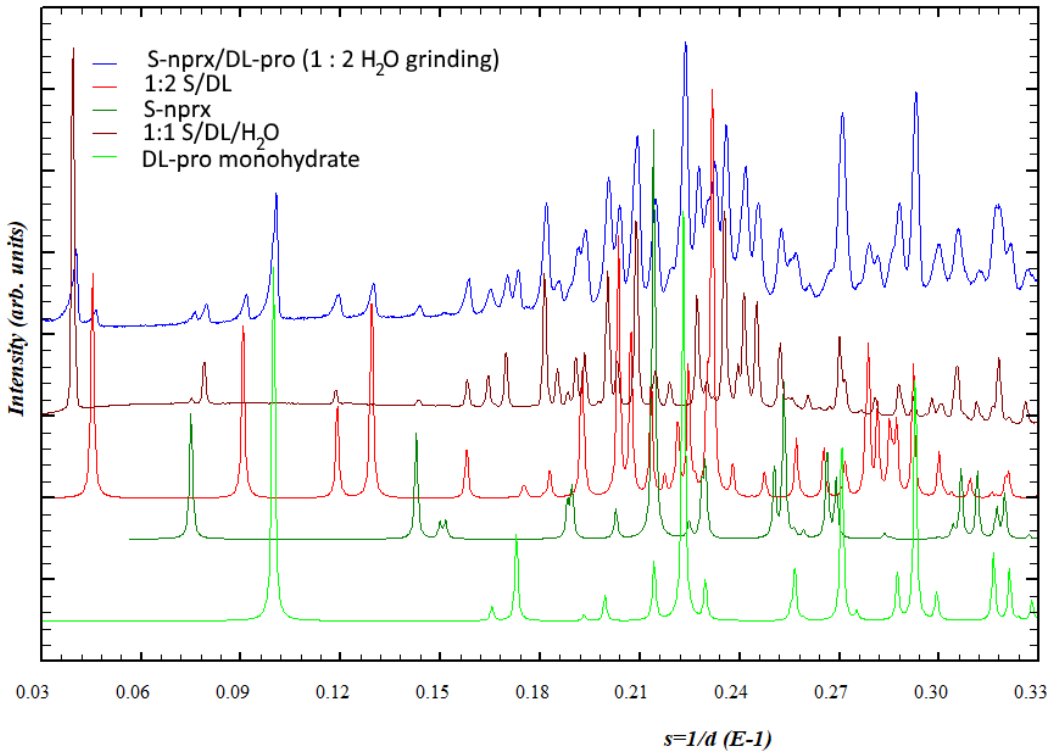

Figure S9.2.7. Diffraction pattern for the **S/DL** sample prepared by 2 : 1 water-LAG (samples *19* in Table S9.1); the diffraction patterns of the pure phases were simulated from the structure, except that of **1:1 S/DL/H_2O** which was taken as measured at synchrotron (sample *17* in Table S9.1)

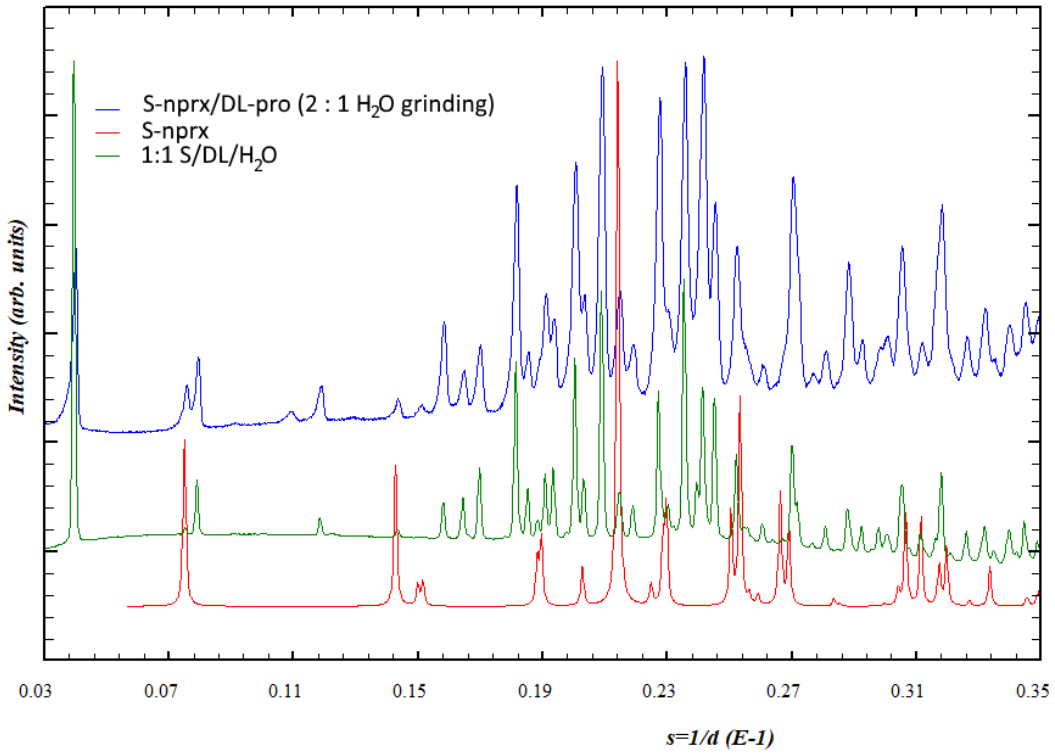

Figure S9.2.8. Diffraction pattern for the **S/DL** sample prepared by 2 : 3 water-LAG (samples *20* in Table S9.1); the diffraction patterns of the pure phases were simulated from the structure, except that of **1:1 S/DL/H_2O** which was taken as measured at synchrotron (sample *17* in Table S9.1)

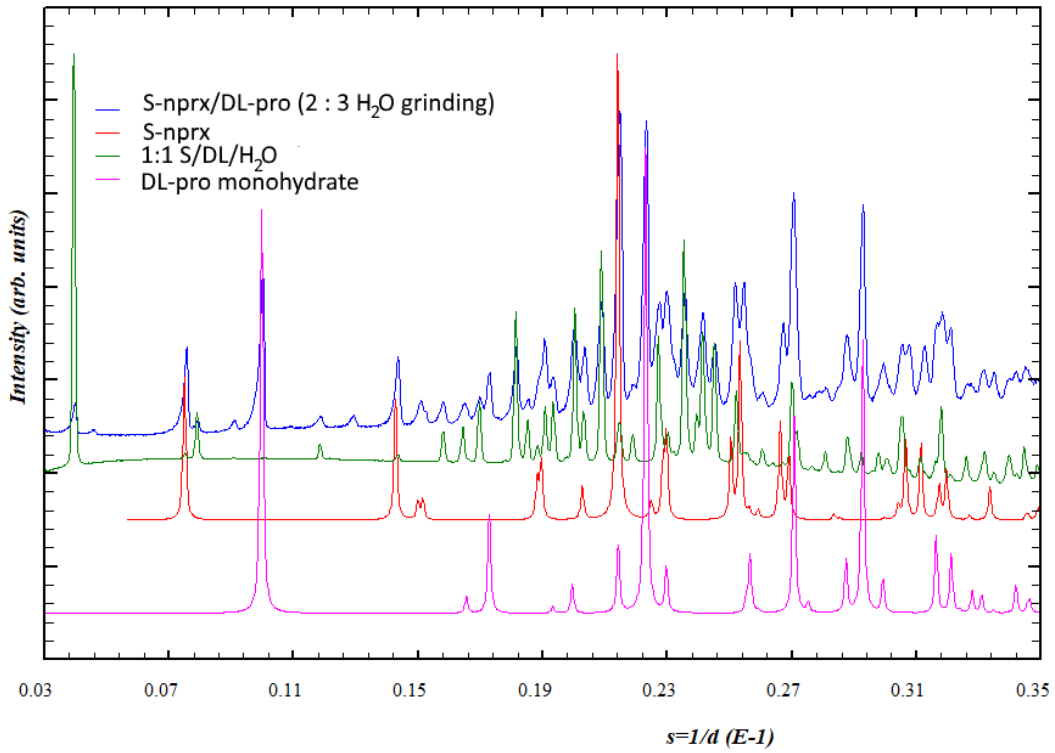

9.3 DSC and TG data measured for selected S/DL sample (Figs. S9.3.1-S8.3.6)

Figure S9.3.1. DSC curve measured for the **S/DL** sample prepared by 1 : 1 MeOH-LAG (sample *1* in Table S9.1). The curve has multiple peaks, indicating the presence of multiple phases in the sample, including one containing a solvent as the first peak occurs at a relatively low temperature and has a wide profile (this peak most corresponds to the evaporation of water from the **1:1 S/DL/H_2O** structure)

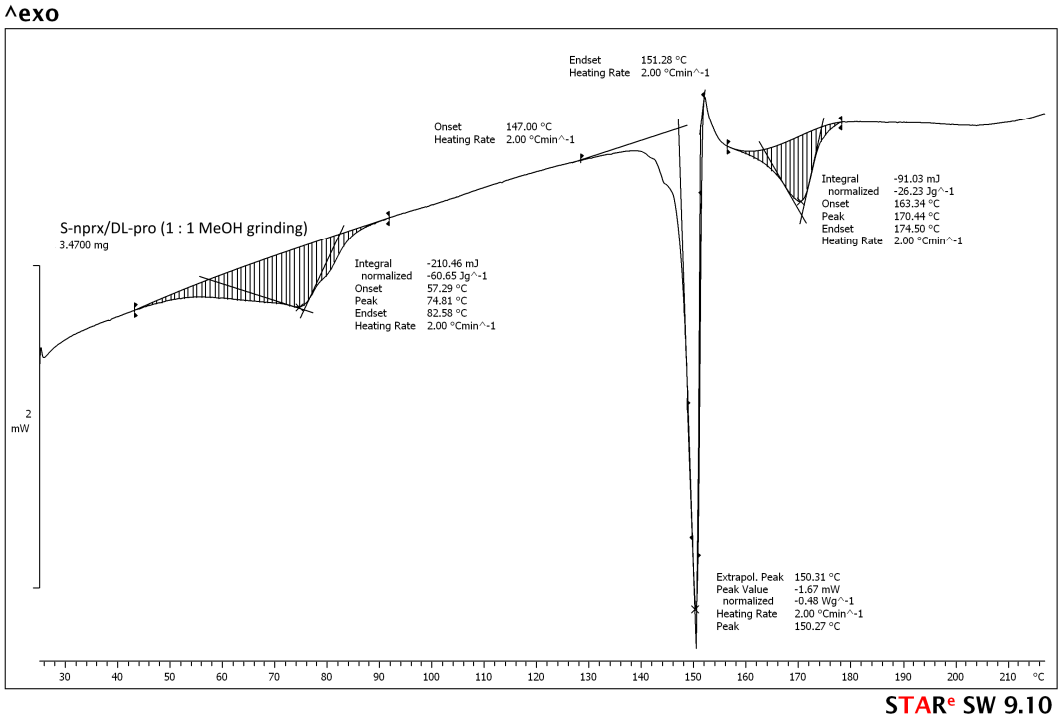

Figure S9.3.2. DSC curve measured for the **S/DL** sample prepared by 1 : 2 MeOH-LAG (sample *2* in Table S9.1). The curve has only one peak corresponding to the melting point of the **1:2 S/DL** cocrystal.

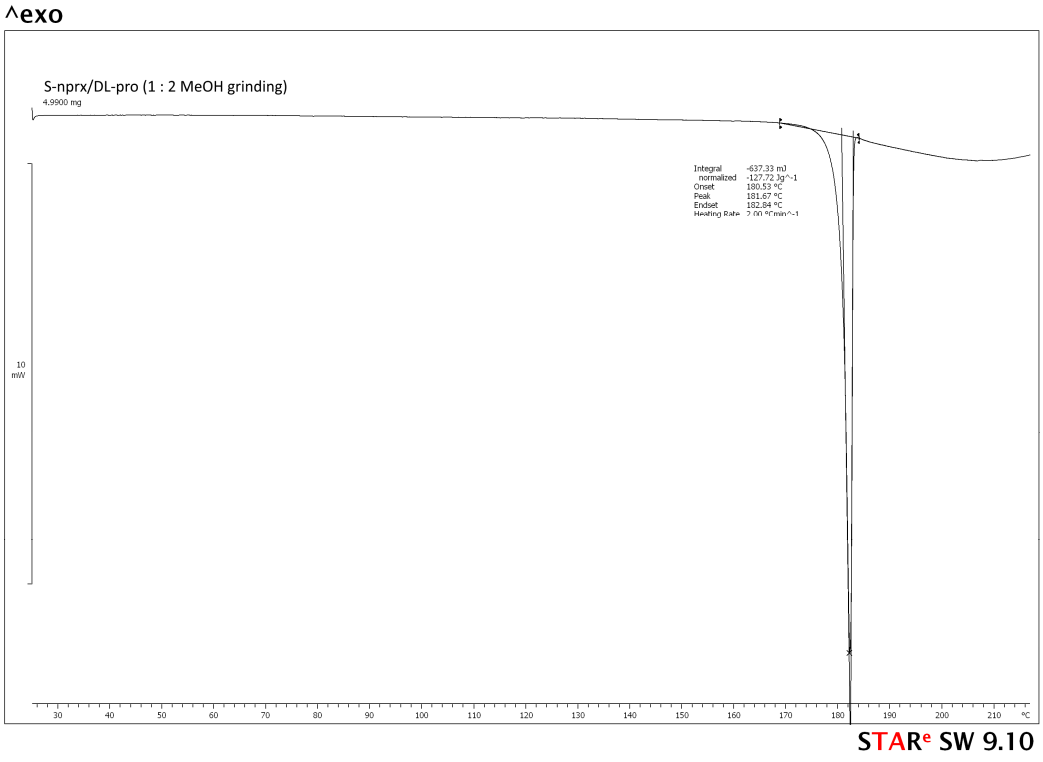

Figure S9.3.3. DSC curve measured for the **S/DL** sample prepared by 1 : 1 EtOH-LAG (sample 5 in Table S9.1). The first peak most likely corresponds to the melting of the **1:1 S/DL** phase followed by crystallization of another phase (probably **1:2 S/DL** as it has the highest melting point and observed as the last phase in the in-situ measurements upon varied temperature)

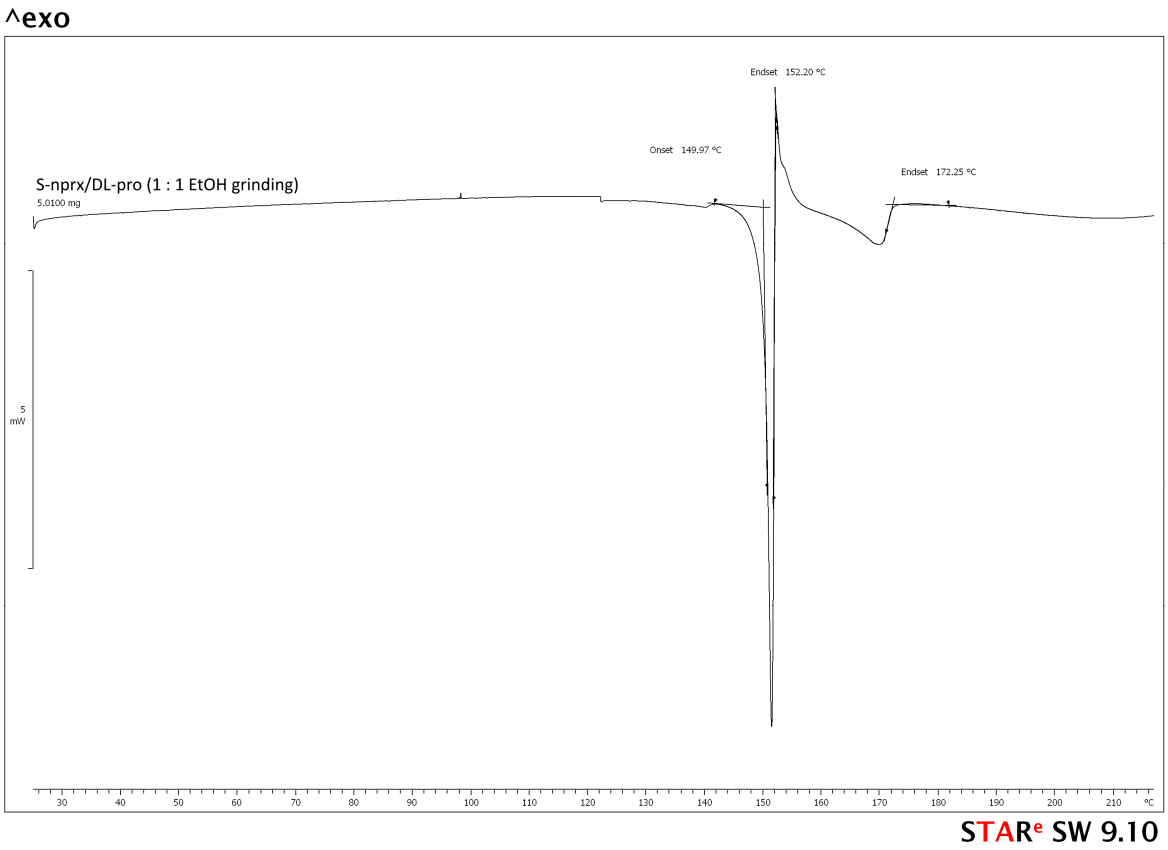

Figure S9.3.4. DSC curve measured for the **S/DL** sample prepared by 1 : 1 ISPN-LAG (sample 9 in Table S9.1). The curve has multiple peaks, suggesting the presence of multiple phases.

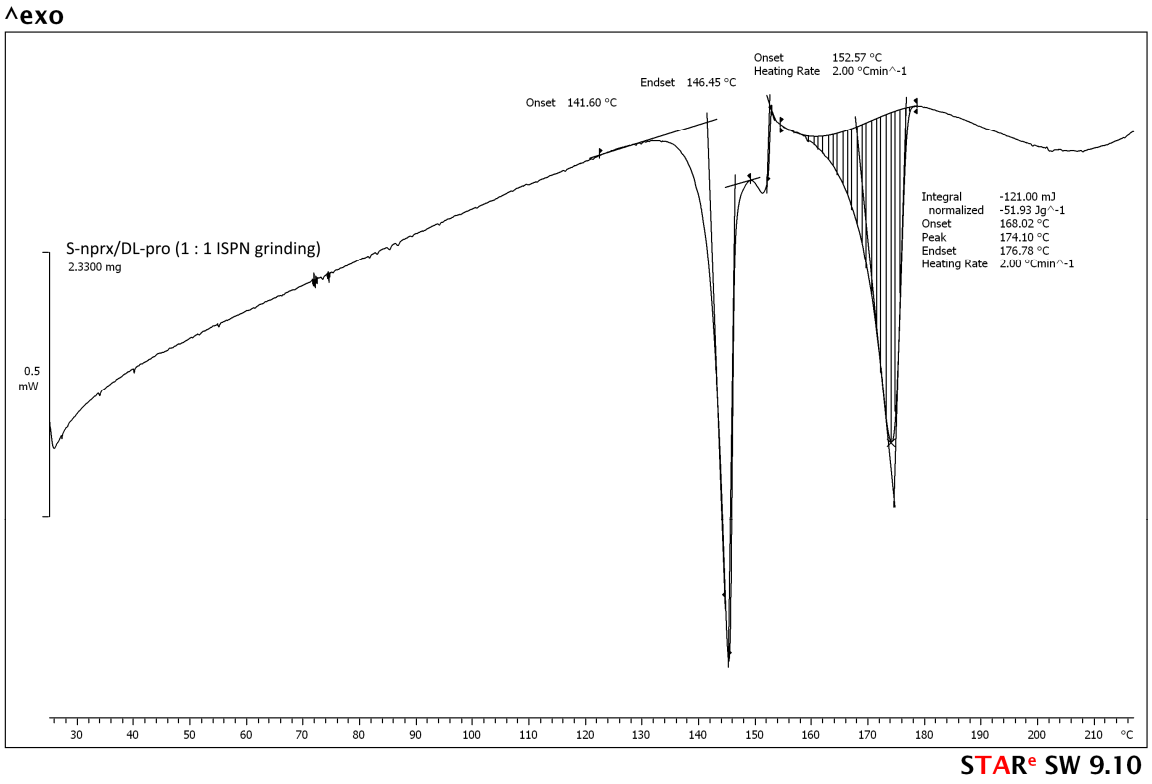

Figure S9.3.5. DSC curve measured for the **S/DL** sample prepared by 1 : 1 ACN-LAG (sample *13* in Table S9.1). The curve has multiple peaks, suggesting the presence of multiple phases.

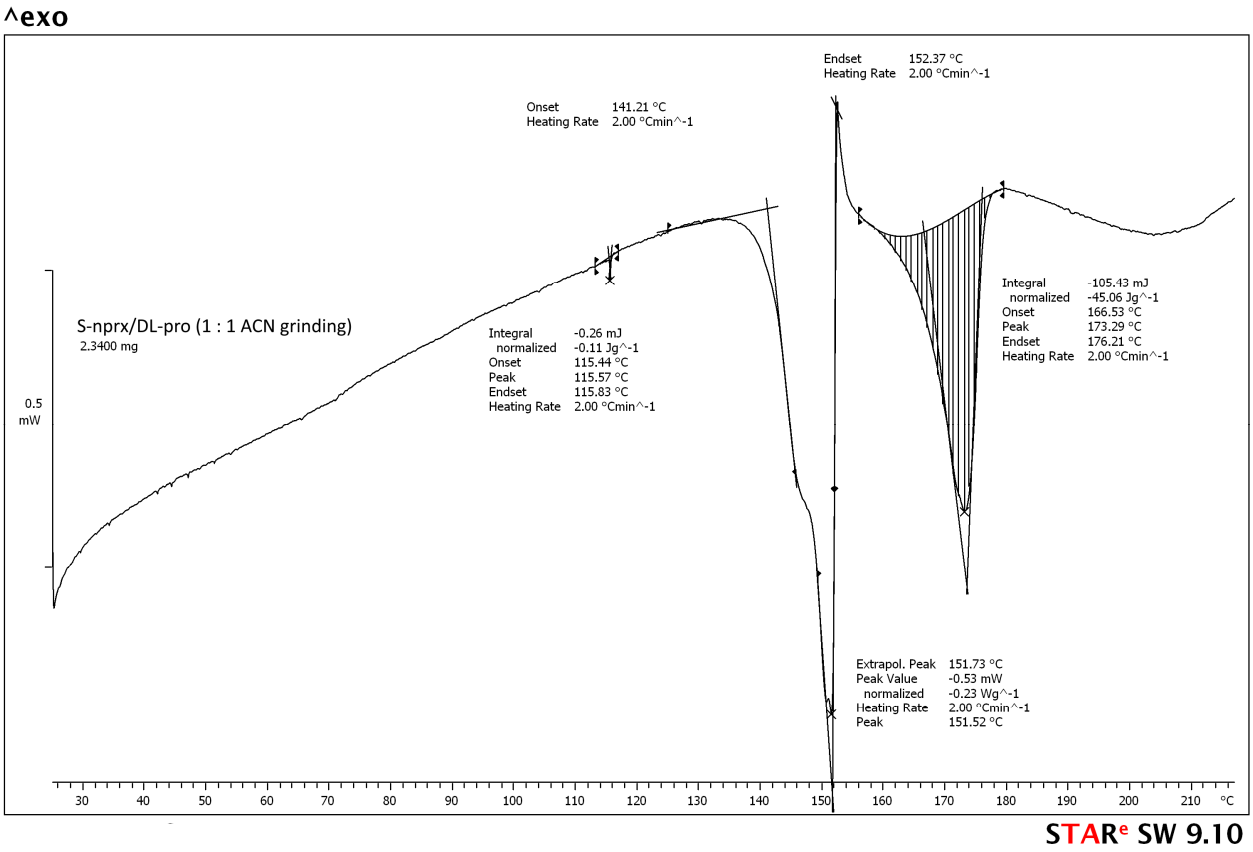

Figure S9.3.6. TGA curve measured for the **S/DL** sample prepared by 1 : 1 water-LAG (sample *17* in Table S9.1). These data were used to determine the number of water molecules in the asymmetric unit cell of the **1:1 S/DL/H_2O** cocrystal phase. The theoretical value for two water molecules per unit cell is 4.95 wt %; the experimental value turned out to be 4.13 wt % (the first step seen on the curve), which is slightly less due to the S-nprx impurity in the sample.

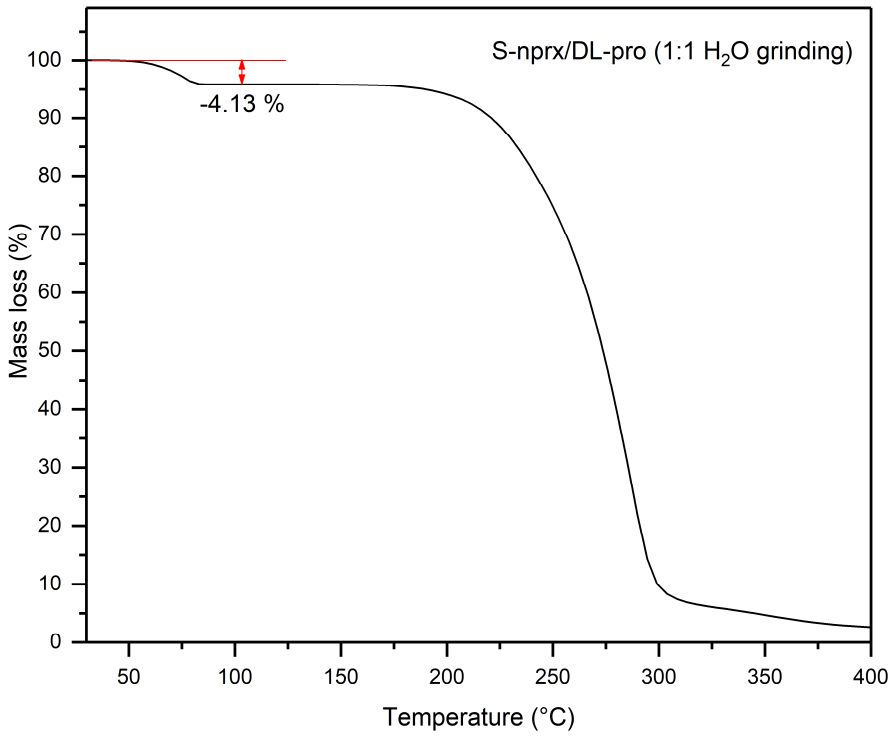

10. Structural Analysis (Figs. S10.1-S10.5)

Figure S10.1. Structure of the **ethanol solvate of S-naproxen**. Ethanol molecules (highlighted with blue circles) are wedged in between naproxen dimers, thus keeping the structure together. This is why the structure is highly unstable and breaks easily when ethanol evaporates

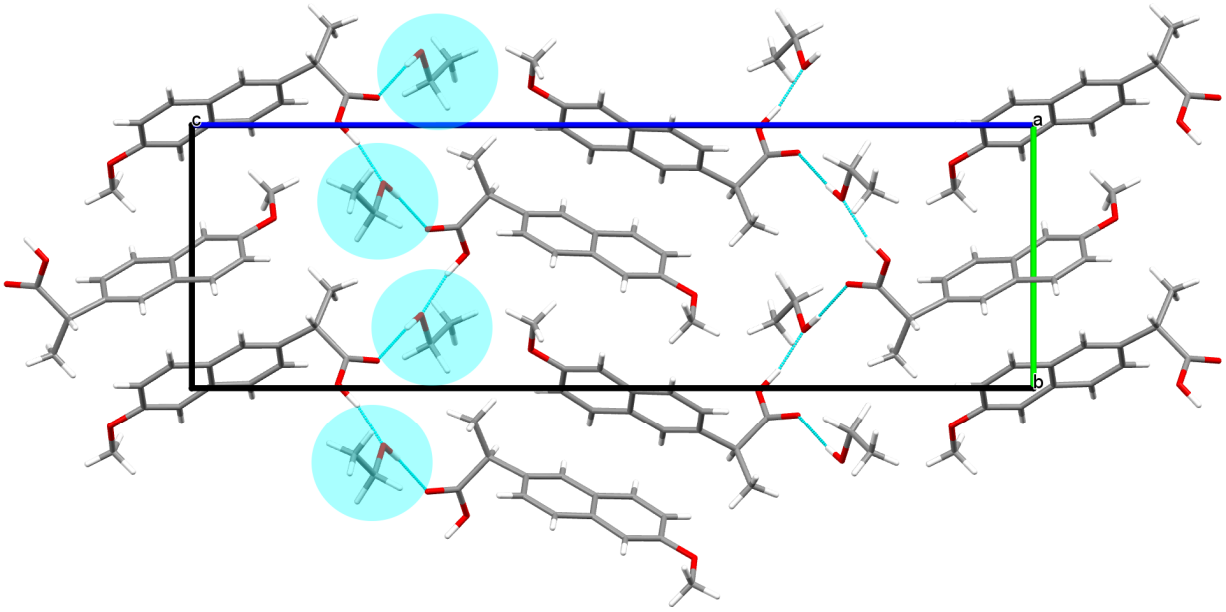

Figure S10.2. Comparison of the structures of the **1:1 RS/L** cocrystals. The **1:1 RS/L pol I, 1:1 RS/L pol II, 1:1 RS/L/MeOH**, and **1:1 RS/L/H_2O** cocrystals exhibit the Type I packing, whereas **1:1 RS/L pol III** crystallizes with the Type II packing. In Type I, each sandwich is highlighted with blue and pink and is comprised of a proline layer with naproxen attached from both sides. In Type II, the layers made of naproxen alternate with those made of proline. (Disordered parts are deleted for clarity)

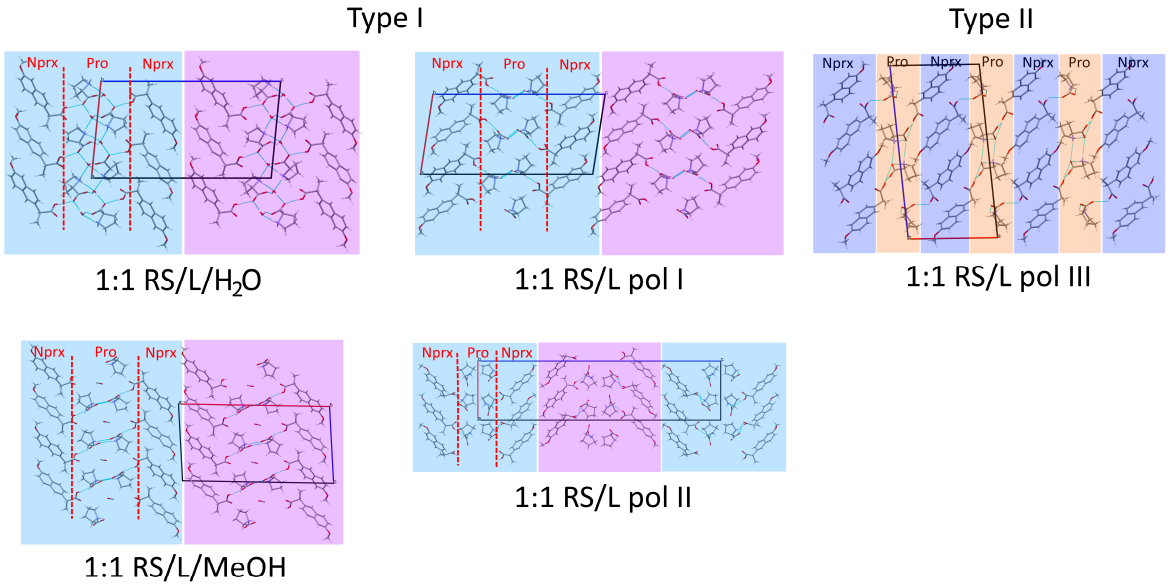

Figure S10.3. Comparison of the structures of the **1:1 RS/DL** cocrystals. The **1:1 RS/DL pol I** and **1:1 RS/DL/H_2O** cocrystals exhibit the Type I packing (sandwich-like), whereas **1:1 RS/DL pol II** crystallizes with the Type II (layered) packing. In Type I, each sandwich is highlighted with blue and pink and is comprised of a proline layer with naproxen attached from both sides. In Type II, the layers made of naproxen alternate with those made of proline. (Disordered parts are deleted for clarity)

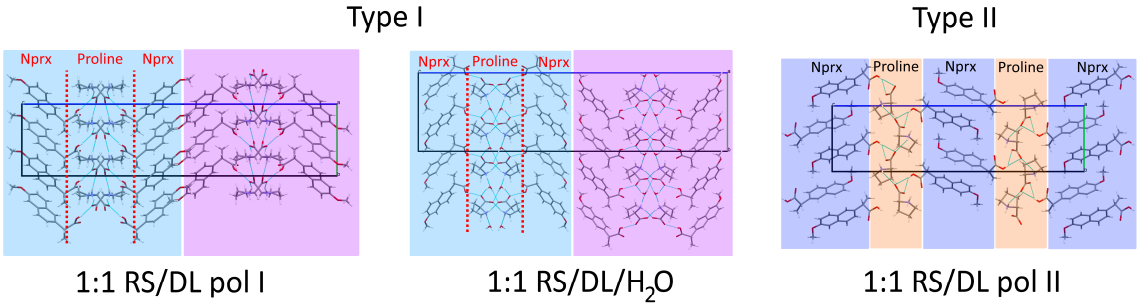

Figure S10.4. Comparison of the structures of the **1:2 R-flurbiprofen/L-proline** and **1:2 S/L** cocrystals. Proline forms two perpendicular head-to-tail chains (one ∥ to the *b* axis, and one ∥ to the *a* axis, highlighted with orange and blue, respectively) in the same manner: only one symmetrically nonequivalent chain is connected to the API (naproxen or flurbiprofen)

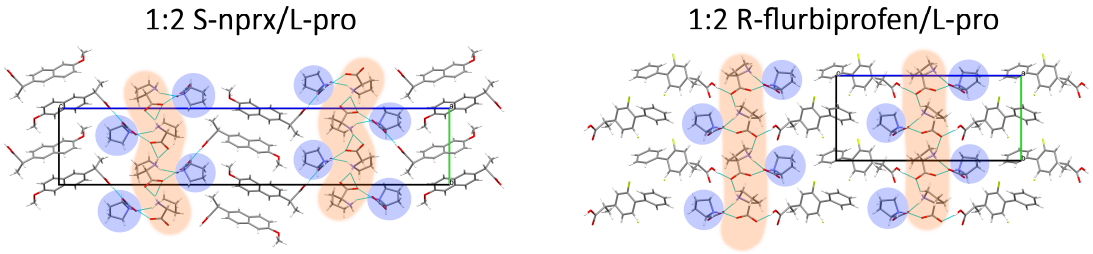

Figure S10.5. Structure of the **2:3 S/L** cocrystals. the **pro** layer is comprised of clusters situated one on top of another and made of three interconnected **pro** chains (indicated with blue); **nprx** is attached to only two chains from the cluster (indicated with red)

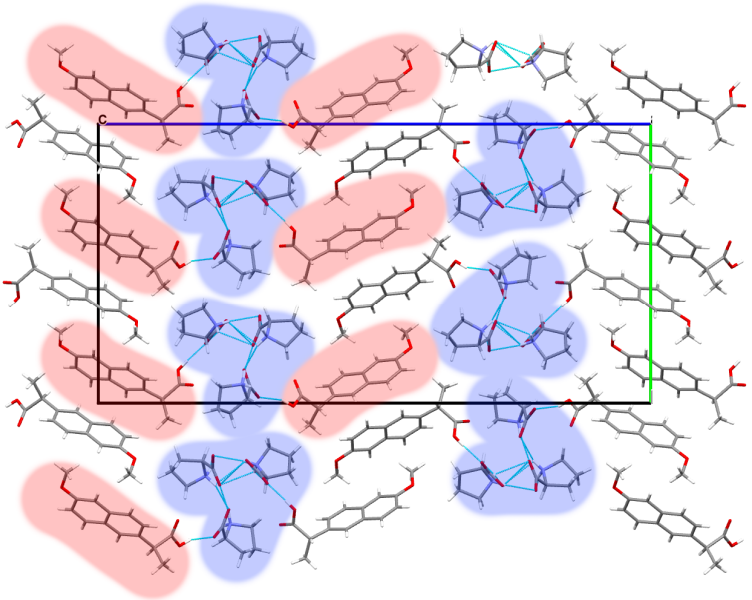

11. DSC data measured for the initial S- and RS-naproxen (Figs. S11.1-S11.2)

Figure S11.1. DSC curve measured for S-naproxen. The peak observed corresponds to the melting point of S-naproxen

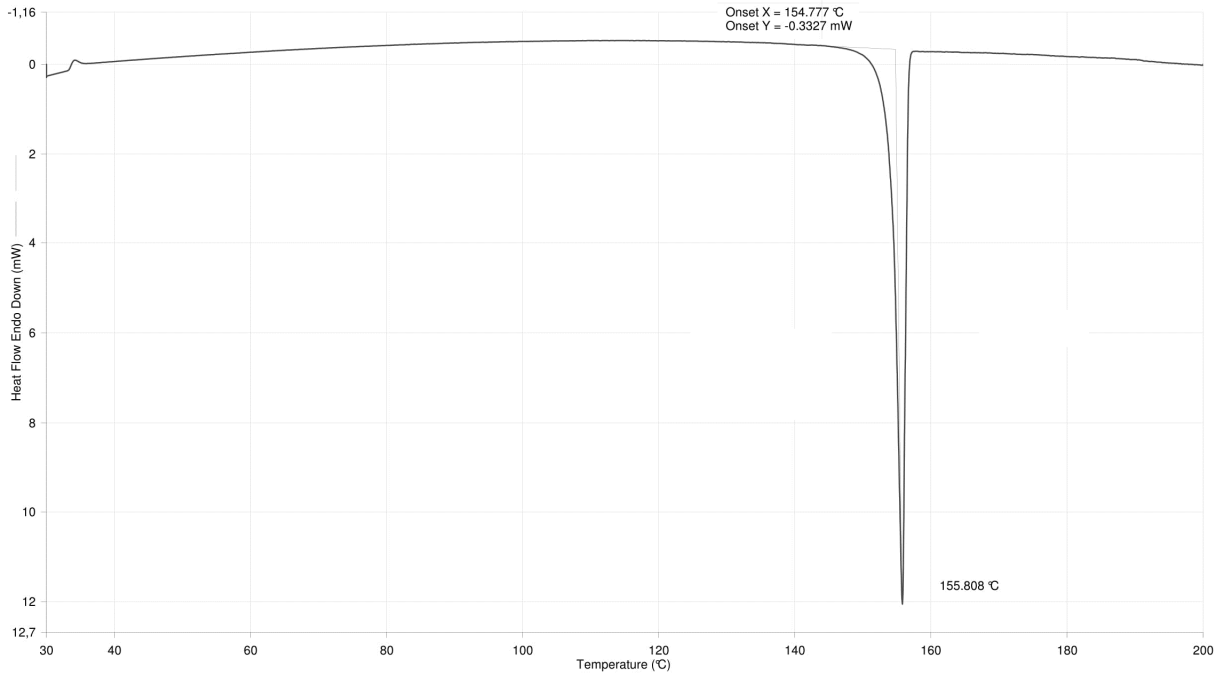

Figure S11.2. DSC curve measured for RS-naproxen. The peak observed corresponds to the melting point of RS-naproxen

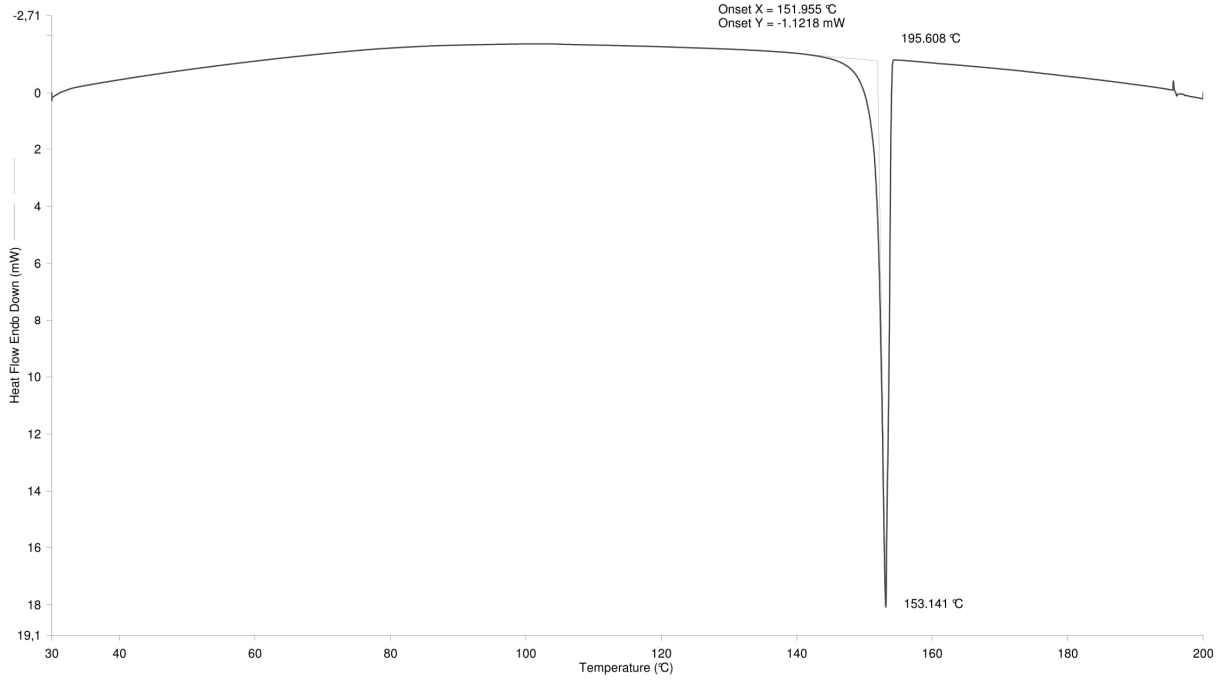

References

1. Agilent Technologies, 2013.
2. G. M. Sheldrick, *Acta Crystallogr. A.*, 2008, **64**, 112–22.
3. G. M. Sheldrick, *Acta Crystallogr. Sect. A Found. Adv.*, 2015, **71**, 3–8.
4. G. M. Sheldrick, *Acta Crystallogr. Sect. C Struct. Chem.*, 2015, **71**, 3–8.
5. C. B. Hübschle, G. M. Sheldrick, and B. Dittrich, *J. Appl. Crystallogr.*, 2011, **44**, 1281–1284.
6. C. F. Macrae, I. J. Bruno, J. A. Chisholm, P. R. Edgington, P. McCabe, E. Pidcock, L. Rodriguez-Monge, R. Taylor, J. van de Streek, and P. A. Wood, *J. Appl. Crystallogr.*, 2008, **41**, 466–470.
7. F. H. Allen, O. Johnson, G. P. Shields, B. R. Smith, and M. Towler, *J. Appl. Crystallogr.*, 2004, **37**, 335–338.
8. M. Chall, K. Knorr, L. Ehm, and W. Depmeier, *High Press. Res.*, 2000, **17**, 315–323.
9. V. Favre-Nicolin and R. Černý, *J. Appl. Crystallogr.*, 2002, **35**, 734–743.
10. A. A. Coelho, 2012.
11. J. S. O. Evans, *Mater. Sci. Forum*, 2010, **651**, 1–9.
12. N. Tumanova, N. Tumanov, K. Robeyns, F. Fischer, L. Fusaro, F. Morelle, V. Ban, G. Hautier, Y. Filinchuk, J. Wouters, T. Leyssens, and F. Emmerling, *Cryst. Growth Des.*, 2018, **18**, 954–961.
13. A. L. Spek, *Acta Crystallogr. D. Biol. Crystallogr.*, 2009, **65**, 148–155.